AD-A036 972 GENERAL DYNAMICS/POMONA CALIF POMONA DIV F/G 17/9
TAGSEA PROGRAM. VOLUME II. PROCEDURES AND OUTPUT FORMS.(U)
AUG 76 N00017-73-C-2244
UNCLASSIFIED NL

1 OF 2
AD A036972

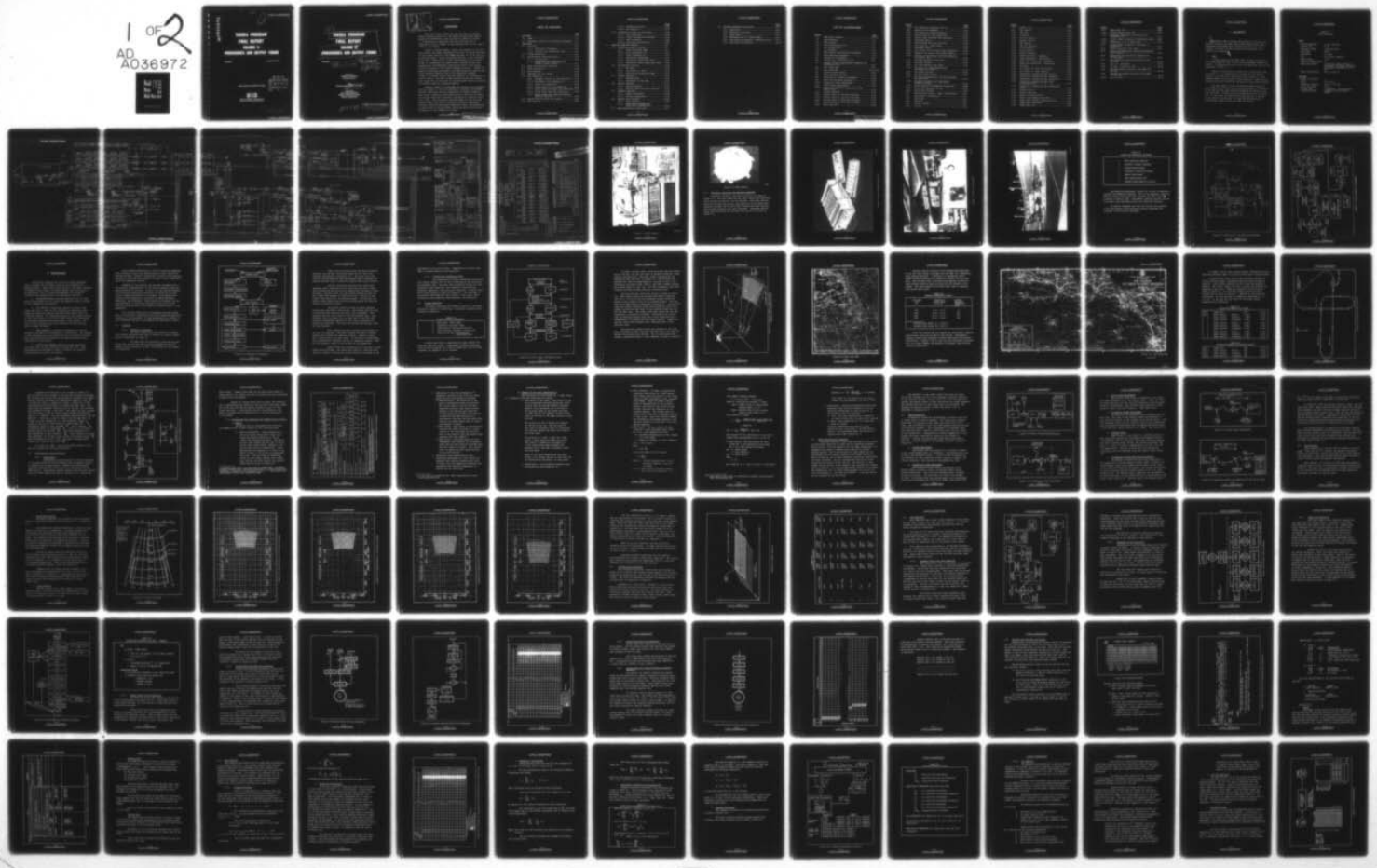

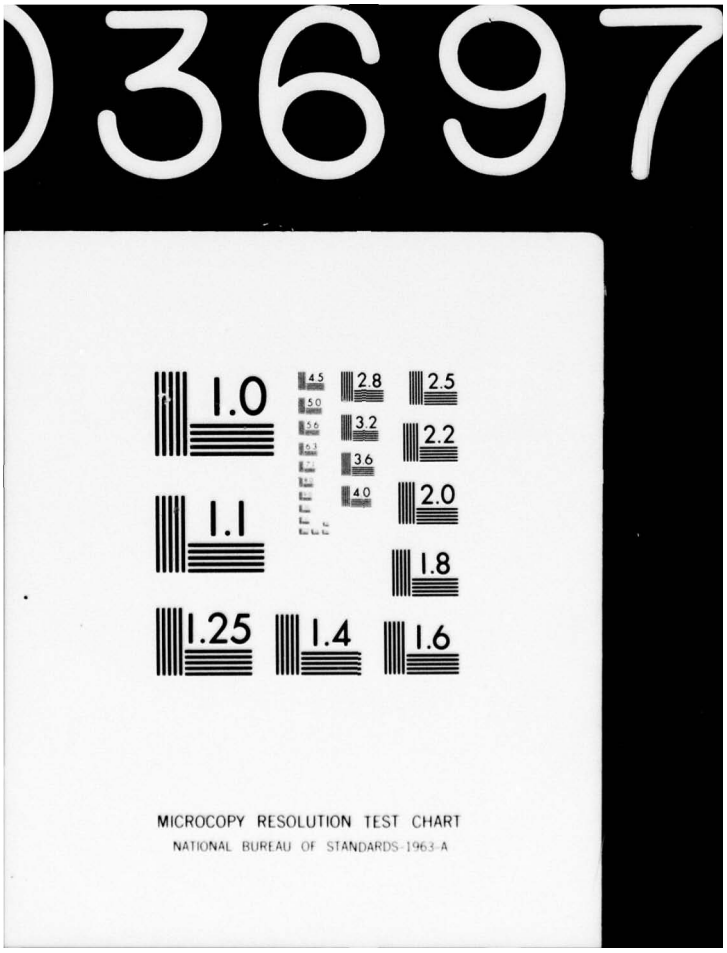
03697
1.0
1.1
1.25
1.4
1.6
1.8
2.0
2.2
2.5
2.8
3.2
3.6
4.0
4.5
5.0
5.6
6.3
MICROCOPY RESOLUTION TEST CHART
NATIONAL BUREAU OF STANDARDS-1963-A

UNCLASSIFIED

TAGSEA PROGRAM
FINAL REPORT
VOLUME II
PROCEDURES AND OUTPUT FORMS

BR-9254-2

27 AUGUST 1976

Prime Contract No. N00017-73-C-2244

RAYTHEON COMPANY
MISSILE SYSTEMS DIVISION

UNCLASSIFIED

(6)

TAGSEA PROGRAM.

FINAL REPORT

VOLUME II.

PROCEDURES AND OUTPUT FORMS.

BR-9254-2

(9) Final rept.

(11) 27 AUGUST 1976

(12) 193 p.

Prepared For
GENERAL DYNAMICS
Pomona, California
DIV.

Under
Prime Contract No. N00017-73-C-2244
(15)

Prepared By
RAYTHEON COMPANY
MISSILE SYSTEMS DIVISION
Bedford, Massachusetts

147850

AB

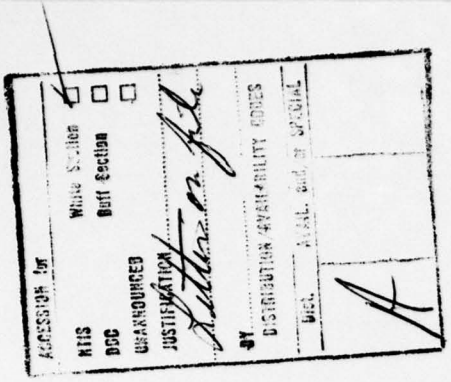

FOREWORD

This final report summarizes the work done by Raytheon Missile Systems Division for the TAGSEA Program under General Dynamics PO #304490-PB, prime contract No. N00017-73-C-2244. It is submitted in compliance with Data Item A015 and is organized into four volumes to ease handling and for the convenience of the readers.

Volume I, Clutter Models, reports the essence of the work and contains the models themselves which were the prime objective of the clutter portion of the TAGSEA program; it can be read on a stand-alone basis. Enough peripheral material is also included to provide a framework for a good understanding of the models. Volume II, Procedures and Output Forms, provides details and explanations on methodology including the form of the outputs and the structures of the clutter simulation effort. Volume III, Supportive Analyses and Outputs, provides analytical back-up and a more complete detailed view of the simulation software. Volume IV, Standard Clutter Analysis Outputs, is a compilation in various forms of the mass of data analyzed during the program. Each volume has its own table of contents which serves to outline the specific material presented therein.

Raytheon wishes to acknowledge the valuable aid and support given by members of the team composed of personnel from NAVSEA, APL/JHU, Technology Service Corporation and General Dynamics. Many helpful suggestions were made during a series of critiques and reviews which most assuredly contributed to a better resultant output. The assistance received ranged all the way from general support and overall guidance to specific supportive analyses, detailed unpublished comparative data, and suggestions of exact forms of clutter models and plots which would be most informative to the community at large.

TABLE OF CONTENTS

LIST OF ILLUSTRATIONS

7. EQUIPMENT

Equipment used in clutter data gathering, reduction and analysis included; the ARTS (Active Radar Test System) radar, associated pod mounted units, recording equipment in the A-3 aircraft, non-real time data reduction test equipment and a computer for analysis.

7.1 ARTS

A block diagram of the ARTS radar is shown in Figure 7-1 with those areas not used in the clutter experiment deleted for clarity. Parameters pertinent to the data gathering function are summarized in Table 7-1.

ARTS is a modification of CMDR and is shown during test in Figure 7-2. Two other portions of ARTS are the antenna, Figure 7-3, and the Data Conditioning Unit, Figure 7-4. The modified seeker and the antenna were mounted in a captive-carry aircraft pod while the DCU was installed in the aircraft proper.

The pod, Figure 7-5 had the modified seeker mounted in the forward section while the antenna was mounted in a radome so as to look out the right side with boresight 90 degrees to the line of flight. The pod is shown mounted on the A-3 in Figure 7-6. In this view the radome can be seen mounted on the pod to the right of the engine. An auxiliary pod containing a surveillance camera was mounted under the cockpit.

TABLE 7-1

ARTS PARAMETERS

Radar	
Antenna Beamwidth	51 deg (one way)
Antenna Gain	11 dB
Microwave Losses	2 dB (each way)
Peak Power	2000W
Pulsewidth	0.2 μsec
PRF	20 K p/sec (nominal)
Noise Figure	8 dB
Number of Range Gates	16
Range Gate Output	16 parallel analog channels, box-carred, filtered, and offset in doppler one-quarter of the PRF
Range Gate settings	4500 to 6100 ft
Recorder	
Number of Channels	7
Speed	60 in./sec
Frequency response	400 Hz - 375 kHz
Record Time/Reel	30 min.
Clutter Data recording method	4 frequency - multiplexed FM channels on each of the 4 tracks

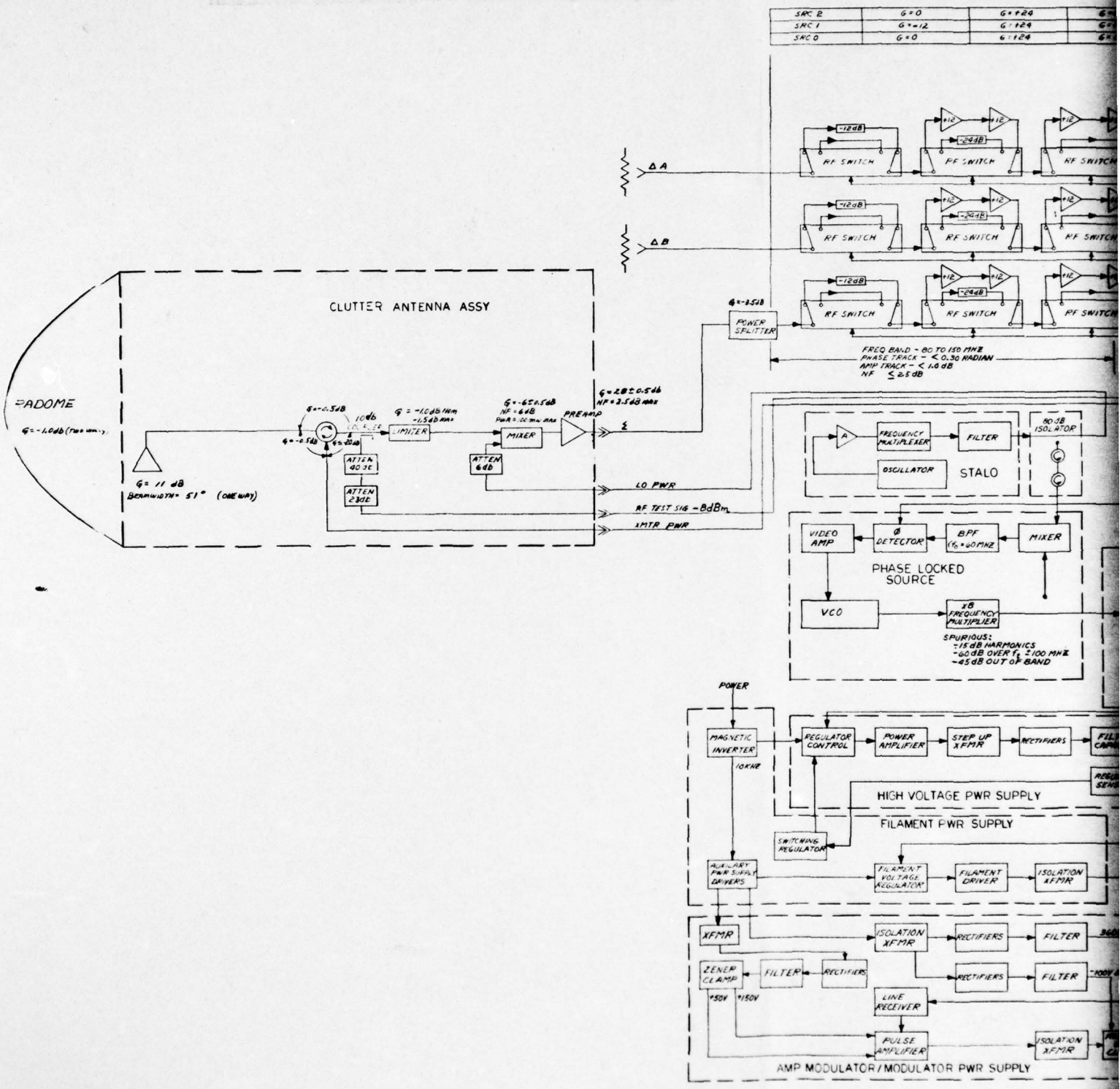

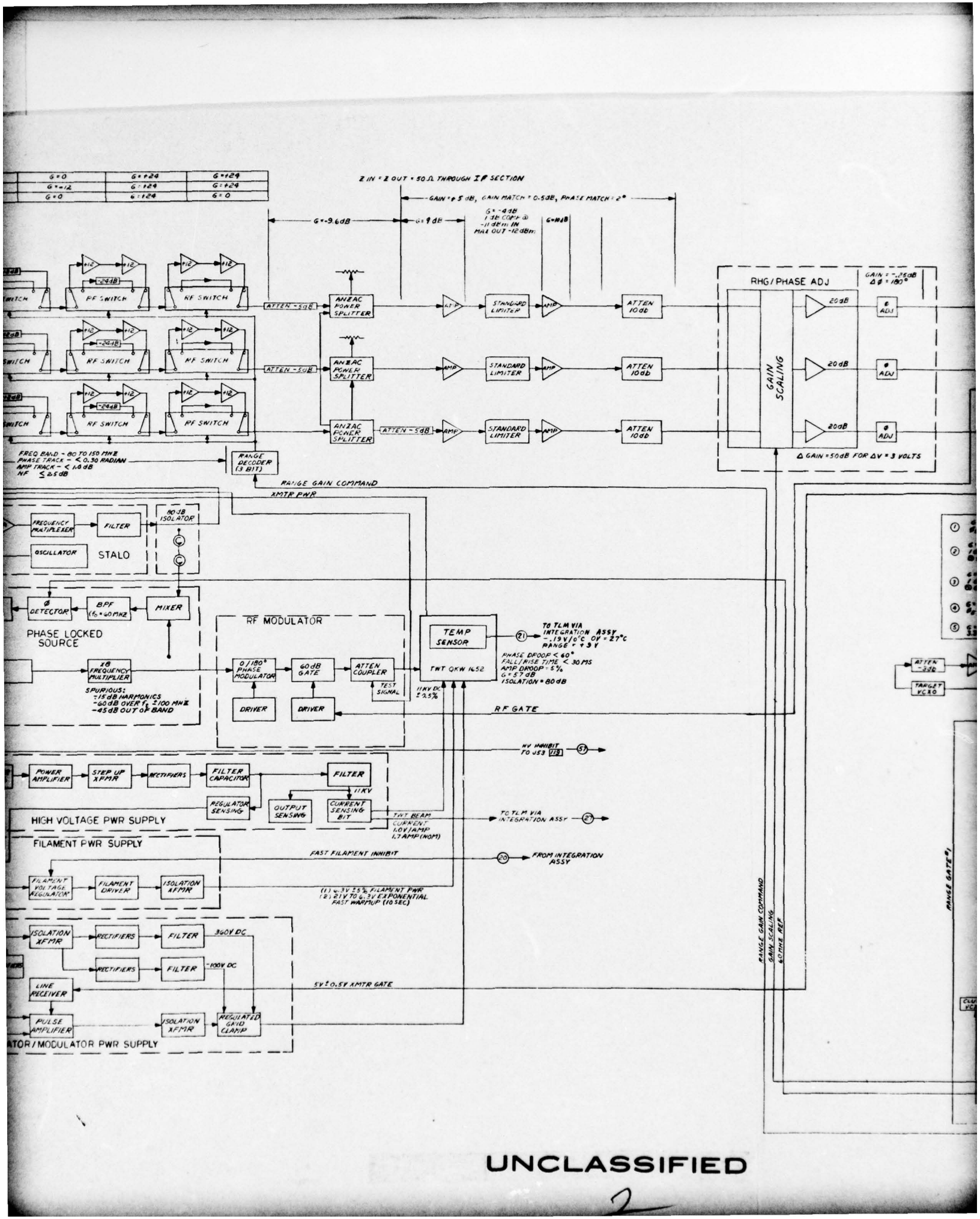

UNCLASSIFIED

2

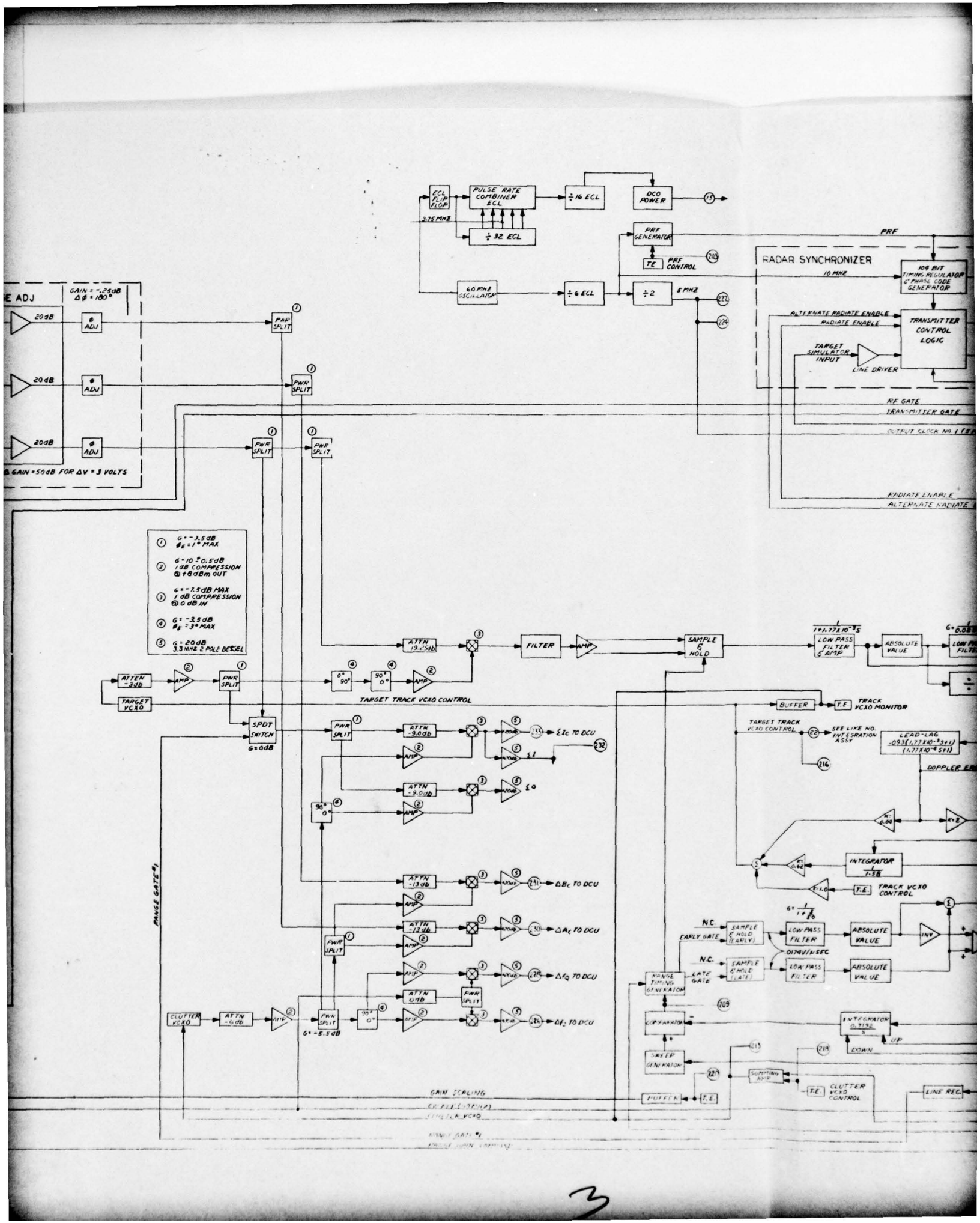
ECL FLIP FLOP
PULSE RATE COMBINER ECL
÷16 ECL
DCO POWER
÷32 ECL
3.75 MHZ
PRF GENERATOR
PRF CONTROL
PRF
RADAR SYNCHRONIZER
10 MHZ
104 BIT TIMING REGULATOR & PHASE CODE GENERATOR
ALTERNATE RADIATE ENABLE
RADIATE ENABLE
TRANSMITTER CONTROL LOGIC
TARGET SIMULATOR INPUT
LINE DRIVER
RF GATE
TRANSMITTER GATE
60 MHZ OSCILLATOR
÷6 ECL
÷2
5 MHZ
GAIN = -25dB Δφ = 180°
20dB
ø ADJ
PWR SPLIT
Δ GAIN = 50dB FOR ΔV = 3 VOLTS
① G = -3.5dB øE = 1° MAX
② G = 10 ± 0.5dB 1dB COMPRESSION @ +8dBm OUT
③ G = -7.5dB MAX 1 dB COMPRESSION @ 0 dB IN
④ G = -3.5dB øE = 3° MAX
⑤ G = 20dB 3.3 MHZ 2 POLE BESSEL
ATTN -3db
AMP
TARGET VCXO
SPDT SWITCH
G = 0dB
RANGE GATE #1
ATTN 19.05db
FILTER
SAMPLE & HOLD
LOW PASS FILTER & AMP
ABSOLUTE VALUE
TARGET TRACK VCXO CONTROL
BUFFER
T.E
TRACK VCXO MONITOR
ATTN -9.0db
ATTN -13db
ATTN -12db
ATTN 0.1db
ΣIc TO DCU
ΣI
ΣQ
ΔBc TO DCU
ΔAc TO DCU
Δfq TO DCU
Δf2 TO DCU
CLUTTER VCXO
ATTN -6db
G = -5.5dB
SEE LIKE NO. INTEGRATION ASSY
LEAD-LAG
DOPPLER ER
INTEGRATOR
TRACK VCXO CONTROL
N.C.
EARLY GATE
LATE GATE
SAMPLE & HOLD (EARLY)
SAMPLE & HOLD (LATE)
LOW PASS FILTER
ABSOLUTE VALUE
INV
0.174V/MSEC
RANGE TIMING GENERATION
UP/DOWN
INTEGRATOR
UP
DOWN
SWEEP GENERATION
SUMMING AMP
CLUTTER VCXO CONTROL
LINE REG.
GAIN SCALING
BUFFER
T.E.

3

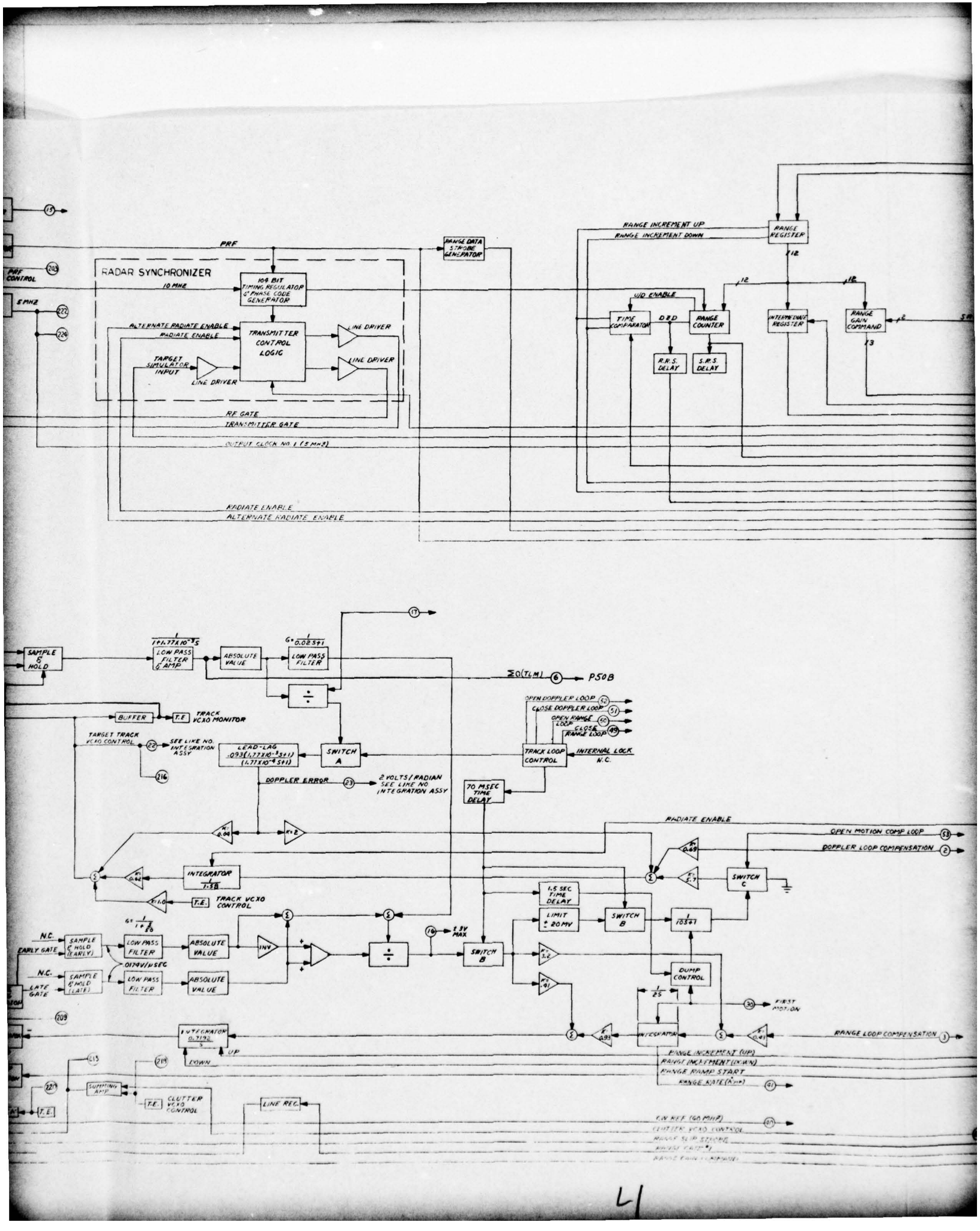
RADAR SYNCHRONIZER
PRF
PRF CONTROL
5 MHZ
10 MHZ
10 BIT TIMING REGULATOR & PHASE CODE GENERATOR
ALTERNATE RADIATE ENABLE
RADIATE ENABLE
TARGET SIMULATOR INPUT
LINE DRIVER
TRANSMITTER CONTROL LOGIC
RF GATE
TRANSMITTER GATE
OUTPUT CLOCK NO. 1 (5 MHZ)
RANGE DATA STROBE GENERATOR
RANGE INCREMENT UP
RANGE INCREMENT DOWN
RANGE REGISTER
U/D ENABLE
TIME COMPARATOR
D & D
RANGE COUNTER
INTERMEDIATE REGISTER
RANGE GAIN COMMAND
R.R.S. DELAY
S.R.S. DELAY
SAMPLE & HOLD
LOW PASS FILTER & AMP
ABSOLUTE VALUE
LOW PASS FILTER
Σ0(T&M)
P50B
BUFFER
T.E.
TRACK VCXO MONITOR
TARGET TRACK VCXO CONTROL
SEE LIKE NO. INTEGRATION ASSY
LEAD-LAG
SWITCH A
OPEN DOPPLER LOOP
CLOSE DOPPLER LOOP
OPEN RANGE LOOP
CLOSE RANGE LOOP
TRACK LOOP CONTROL
INTERNAL LOCK N.C.
DOPPLER ERROR
2 VOLTS/RADIAN SEE LIKE NO INTEGRATION ASSY
70 MSEC TIME DELAY
RADIATE ENABLE
OPEN MOTION COMP LOOP
DOPPLER LOOP COMPENSATION
INTEGRATOR
SWITCH C
TRACK VCXO CONTROL
1.5 SEC TIME DELAY
LIMIT ± 20 MV
SWITCH B
DUMP CONTROL
FIRST MOTION
N.C.
EARLY GATE
SAMPLE & HOLD (EARLY)
LOW PASS FILTER
ABSOLUTE VALUE
INV
.0174V/μSEC
N.C.
LATE GATE
SAMPLE & HOLD (LATE)
LOW PASS FILTER
ABSOLUTE VALUE
4.8V MAX
SWITCH B
INTEGRATOR
RANGE LOOP COMPENSATION
RANGE INCREMENT (UP)
RANGE INCREMENT (DOWN)
RANGE RAMP START
RANGE RATE (K/μs)
UP
DOWN
SUMMING AMP
T.E.
CLUTTER VCXO CONTROL
LINE REG.
CW REF (60 MHZ)
CLUTTER VCXO CONTROL
RANGE SLOP STROBE
RANGE GATE
RANGE RAMP (K/μs)

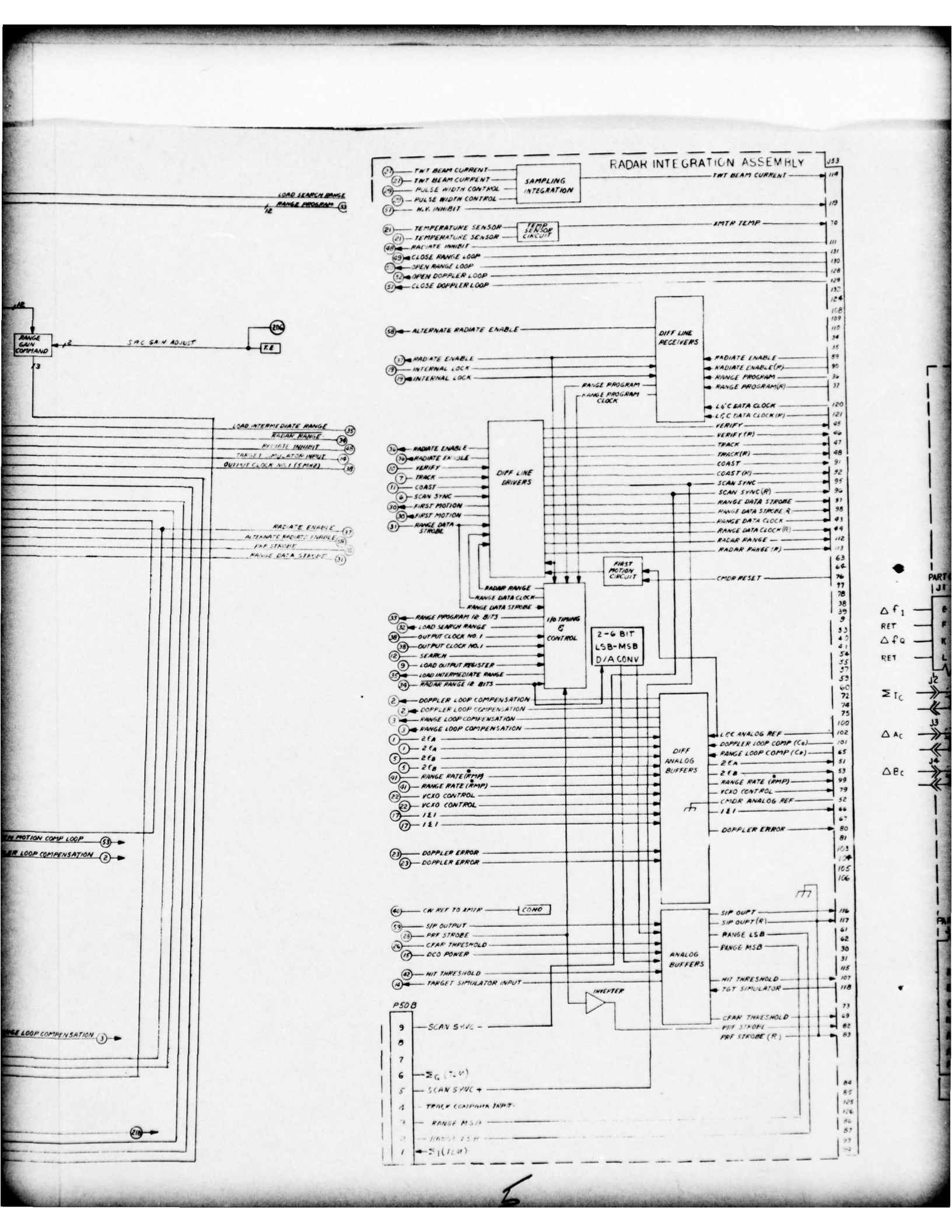
RADAR INTEGRATION ASSEMBLY
J33
SAMPLING INTEGRATION
TEMP SENSOR CIRCUIT
DIFF LINE RECEIVERS
DIFF LINE DRIVERS
I/O TIMING & CONTROL
FIRST MOTION CIRCUIT
2-6 BIT LSB-MSB D/A CONV
DIFF ANALOG BUFFERS
ANALOG BUFFERS
INVERTER
P508
RANGE GAIN COMMAND
T.E
TWT BEAM CURRENT
PULSE WIDTH CONTROL
M.V. INHIBIT
TEMPERATURE SENSOR
RADIATE INHIBIT
CLOSE RANGE LOOP
OPEN RANGE LOOP
OPEN DOPPLER LOOP
CLOSE DOPPLER LOOP
ALTERNATE RADIATE ENABLE
RADIATE ENABLE
INTERNAL LOCK
RANGE PROGRAM
RANGE PROGRAM CLOCK
VERIFY
TRACK
COAST
SCAN SYNC
FIRST MOTION
RANGE DATA STROBE
RADAR RANGE
RANGE DATA CLOCK
RANGE PROGRAM 12 BITS
LOAD SEARCH RANGE
OUTPUT CLOCK NO. 1
SEARCH
LOAD OUTPUT REGISTER
LOAD INTERMEDIATE RANGE
RADAR RANGE 12 BITS
DOPPLER LOOP COMPENSATION
RANGE LOOP COMPENSATION
2εA
2εB
RANGE RATE (RMP)
VCXO CONTROL
1&1
DOPPLER ERROR
CW REF TO XMTR
COHO
S/P OUTPUT
PRF STROBE
CFAR THRESHOLD
DCO POWER
HIT THRESHOLD
TARGET SIMULATOR INPUT
AMTR TEMP
L&C DATA CLOCK
VERIFY (R)
TRACK (R)
COAST (R)
SCAN SYNC (R)
RANGE DATA STROBE R
RANGE DATA CLOCK (R)
RADAR RANGE (R)
CMDR RESET
L&C ANALOG REF
DOPPLER LOOP COMP (Ca)
RANGE LOOP COMP (Ca)
CMDR ANALOG REF
S/P OUPT
S/P OUPT (R)
RANGE LSB
RANGE MSB
TGT SIMULATOR
CFAR THRESHOLD
PRF STROBE
PRF STROBE (R)
SCAN SYNC -
SCAN SYNC +
RANGE MSB
LOAD INTERMEDIATE RANGE
RADAR RANGE
OUTPUT CLOCK NO.1 (5 MHz)
RADIATE ENABLE
ALTERNATE RADIATE ENABLE
PRF STROBE
RANGE DATA STROBE
LOAD SEARCH RANGE
RANGE PROGRAM
SYNC GAIN ADJUST
Δf1
RET
Δfq
RET
ΣIC
ΔAC
ΔBC

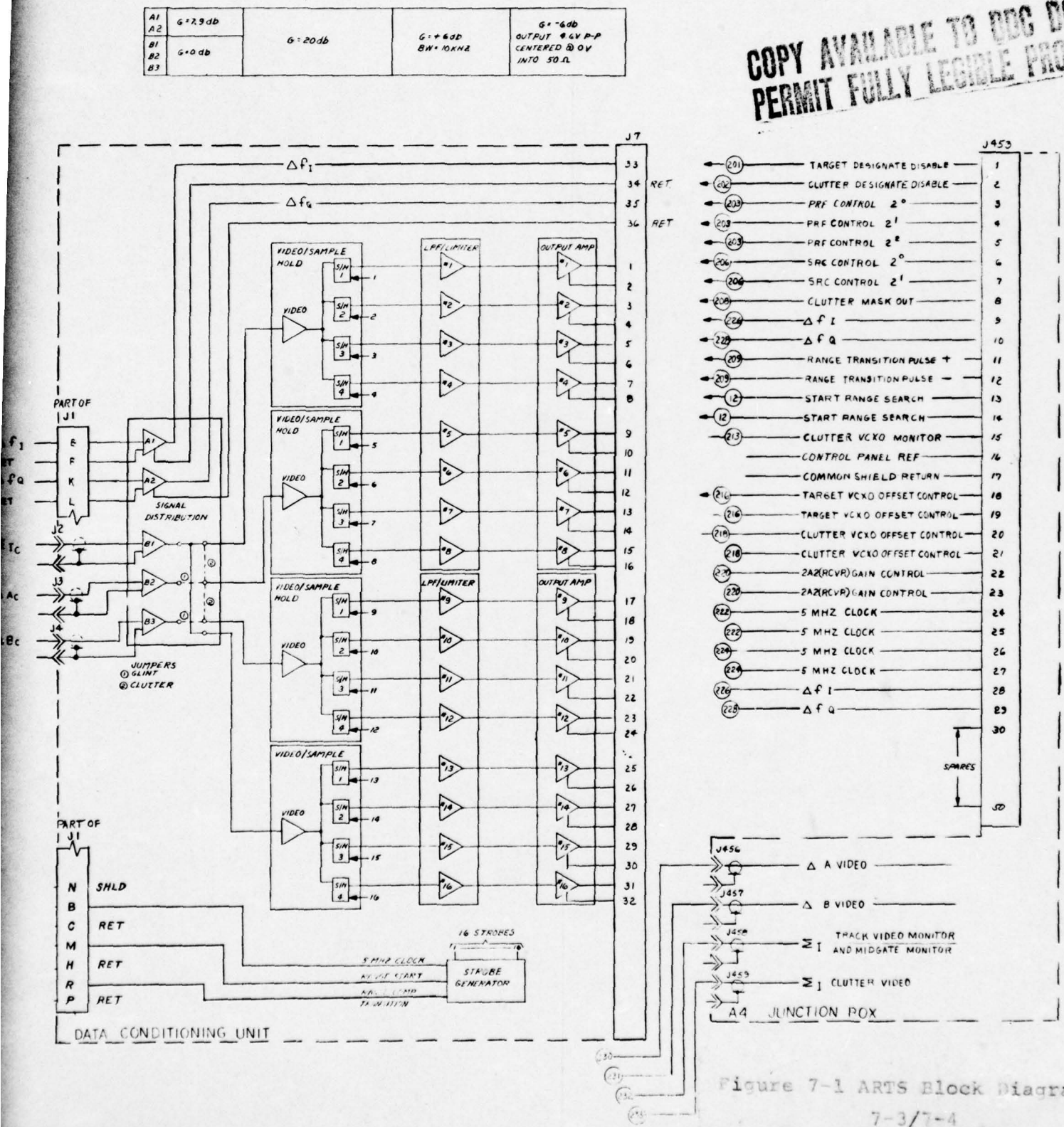

Figure 7-1 ARTS Block Diagram

7-3/7-4

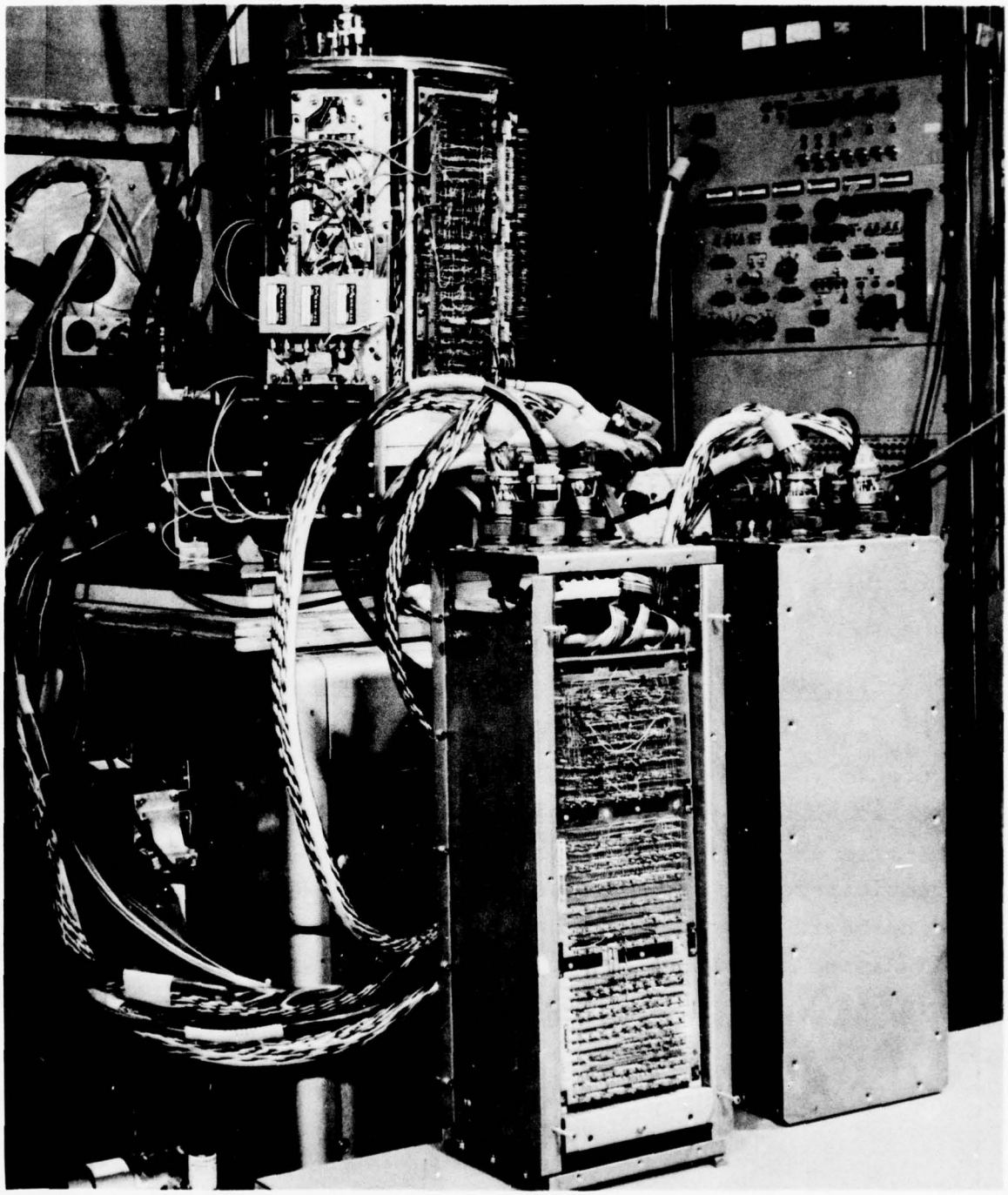

CN-6-3410

Figure 7-2 ARTS Hardware

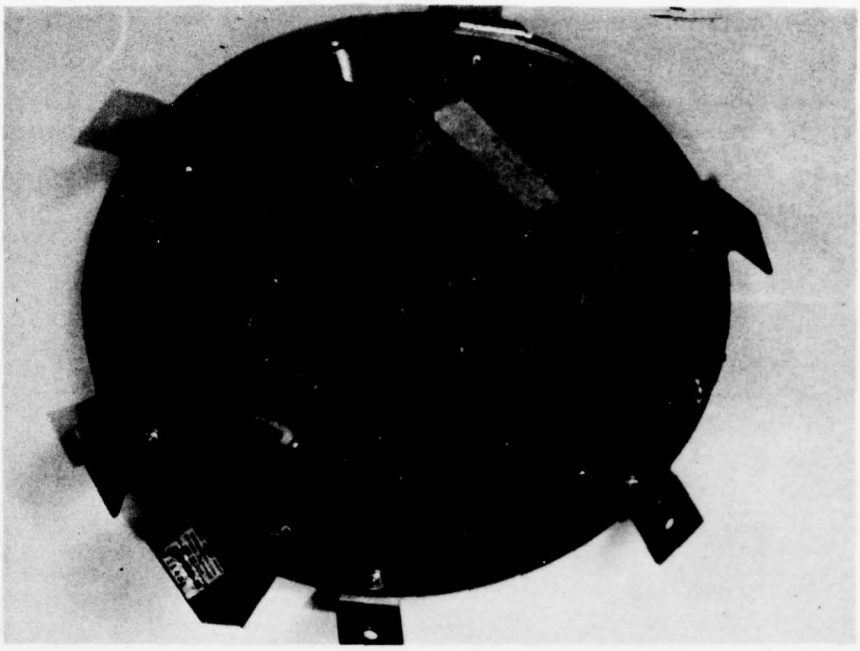

5-3579

Figure 7-3 ARTS Antenna

7.2 Recording, Reduction and Analysis Equipment

Equipment mounted in the cabin of the A-3 is shown in Figure 7-7. The units shown are the radar control and monitoring units located at station 2 of the aircraft. Two other stations were also included for control and operation of the camera and magnetic recorder and for the flight director who also controls the on-board telemetry and chart recorders. Equipment specifically associated with the recording and control is listed in Table 7-2.

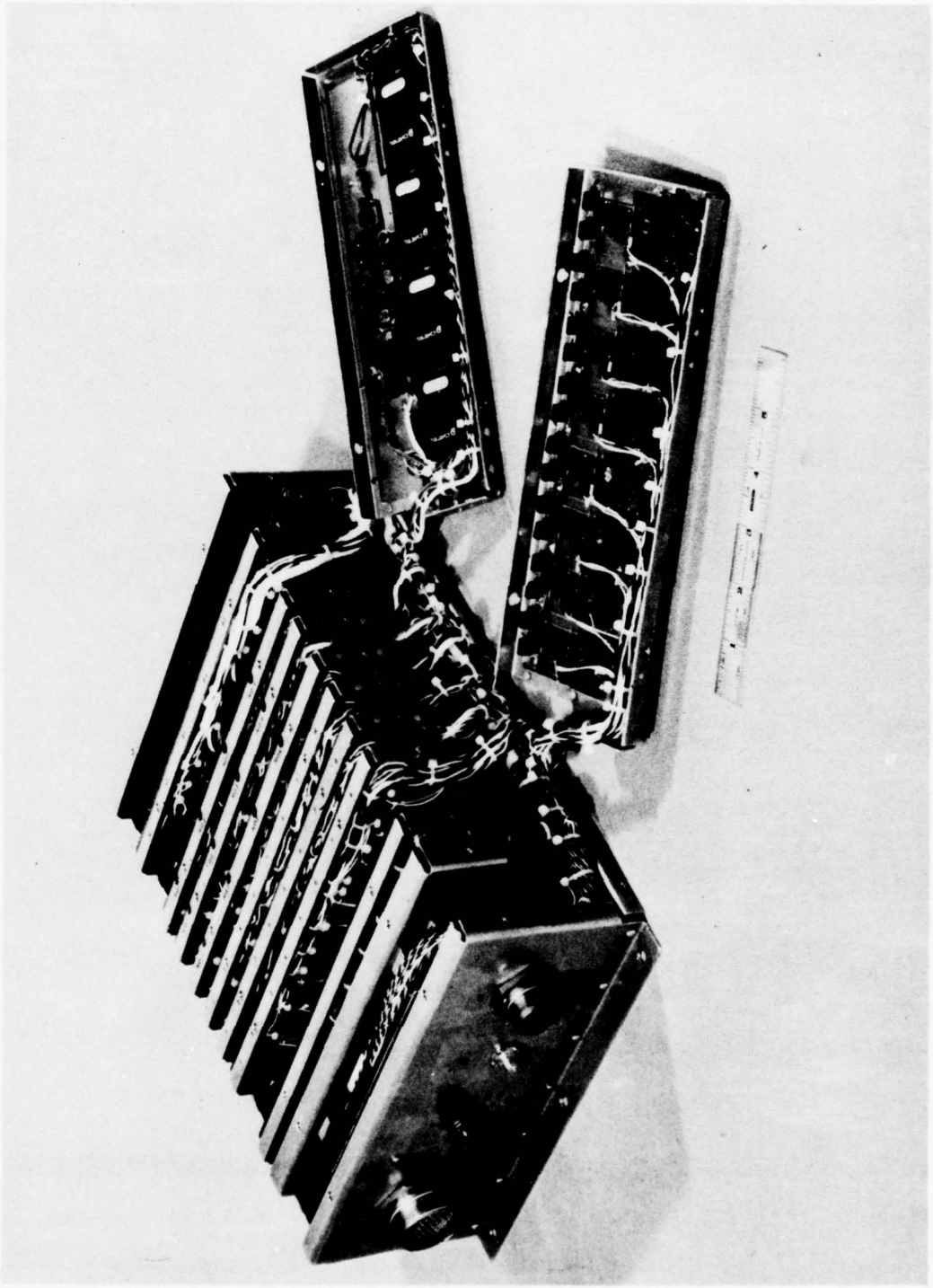

CN-6-3352

Figure 7-4 Data Conditioning Unit

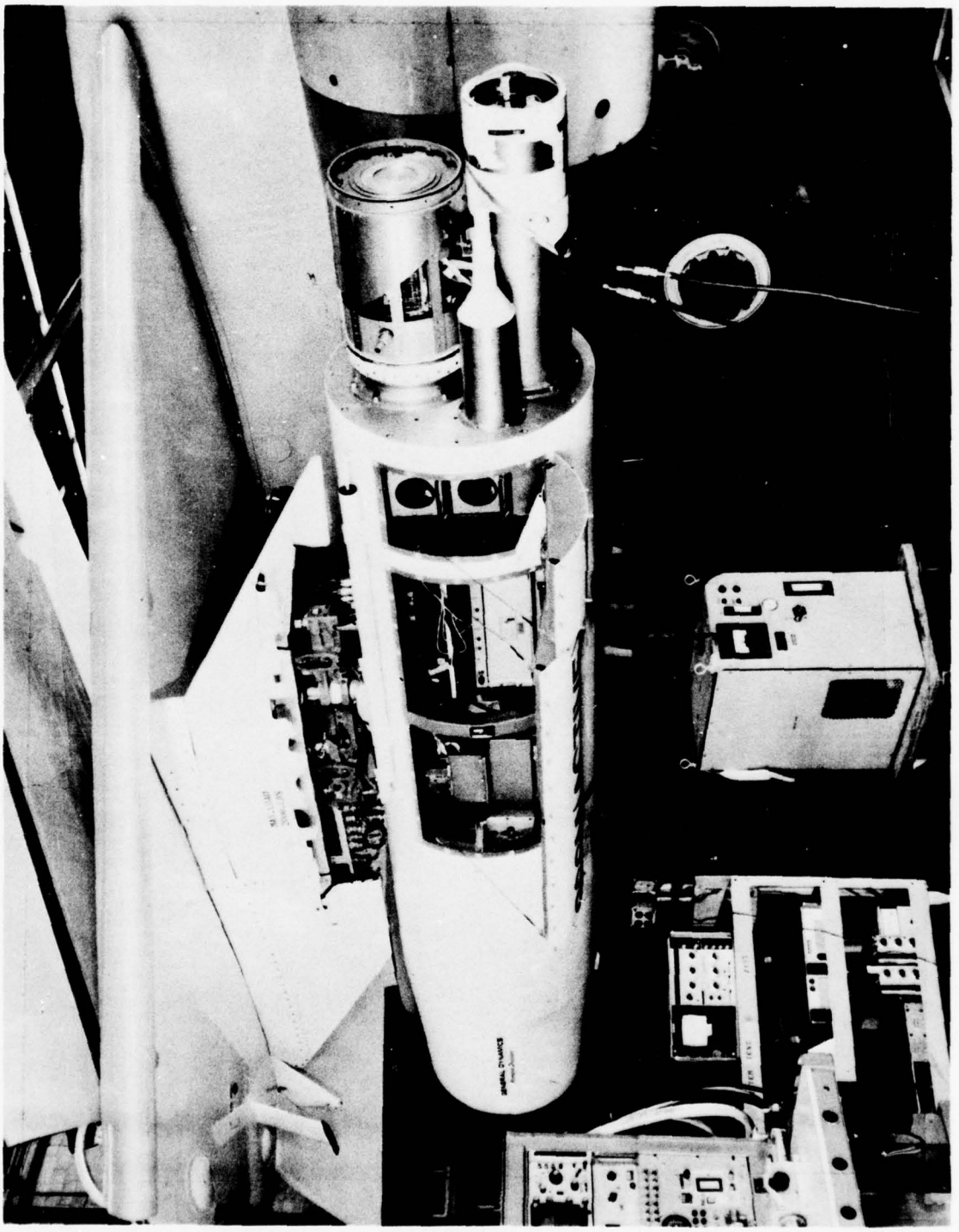

CN-2-2154

Figure 7-5 Pod Configuration

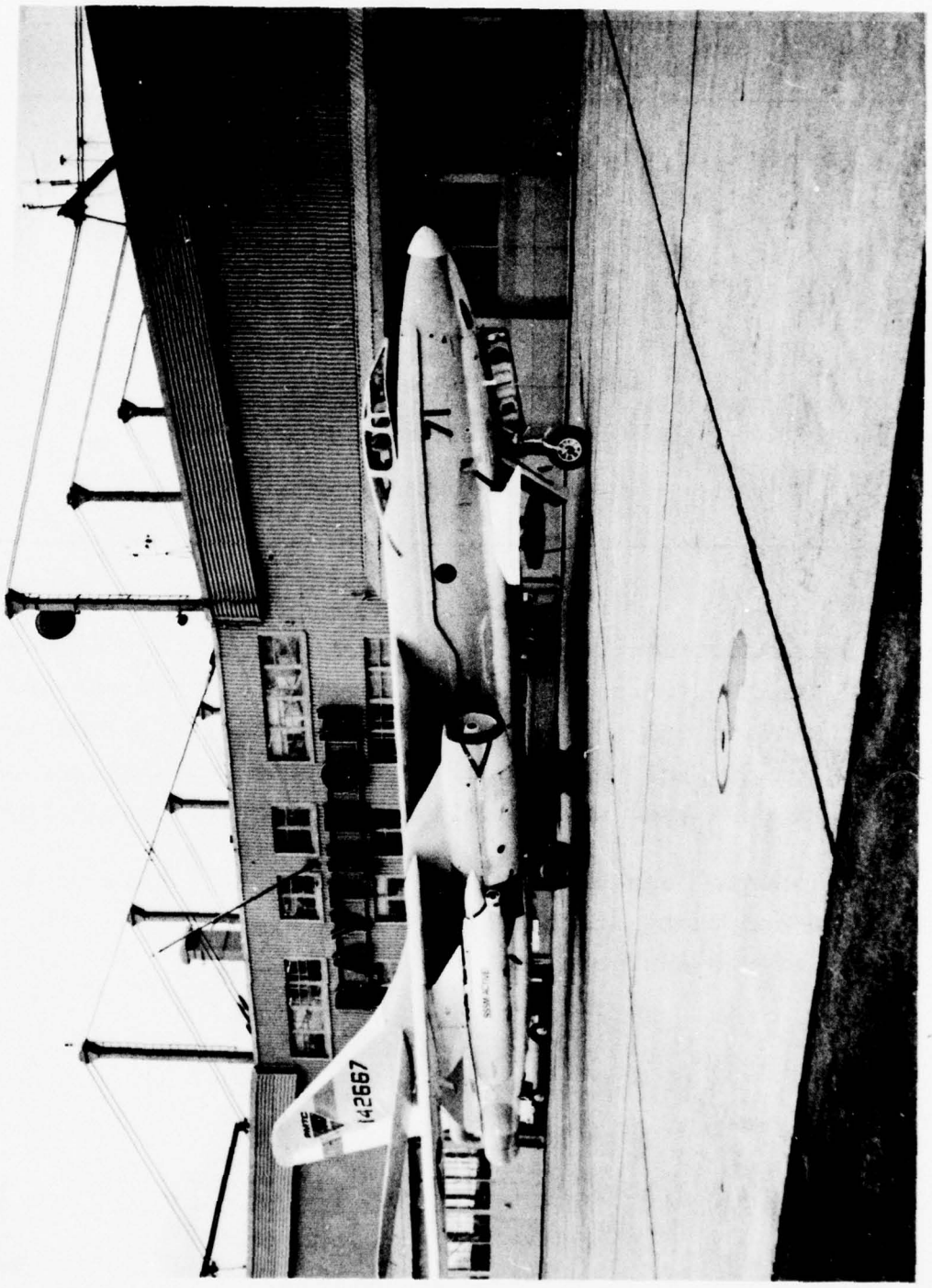

CN-6-3540

Figure 7-6 A-3 Aircraft

TABLE 7-2
CONTROL AND RECORDING EQUIPMENT

1	HP141 Spectrum Analyzer
2	HP7418A 8 Channel Recorder
1	HP181AR Oscilloscope
1	Tektronics 454R Oscilloscope
1	Seeker Patch Panel
1	Data Conditioning Unit
1	MINCOM PC500B Magnetic Recorder

Data Reduction Equipment, Figure 7-8, is part of Raytheon's standard Data Reduction Facility. All of the equipment shown was used for reading the analog tape, reducing the data, and re-recording on digital tape. The EMR1510 spectrum analyzer and the X-Y plotter were used specifically for quick-look analysis.

No special equipment was used for further data analysis. A CDC-6700 computer with associated plotters comprised the remainder of the analysis equipment.

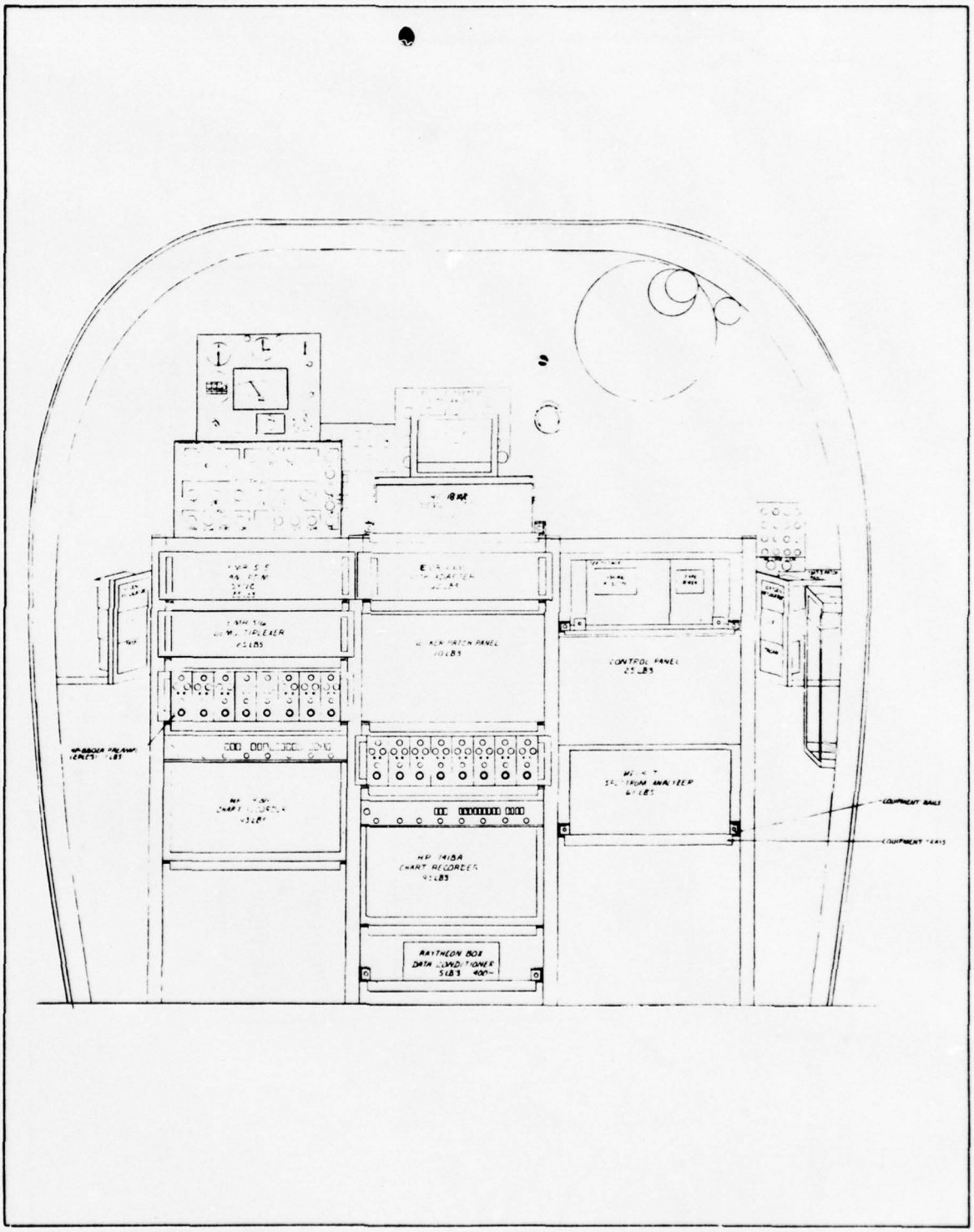

Figure 7-7 ARTS Control and Receiving Equipment

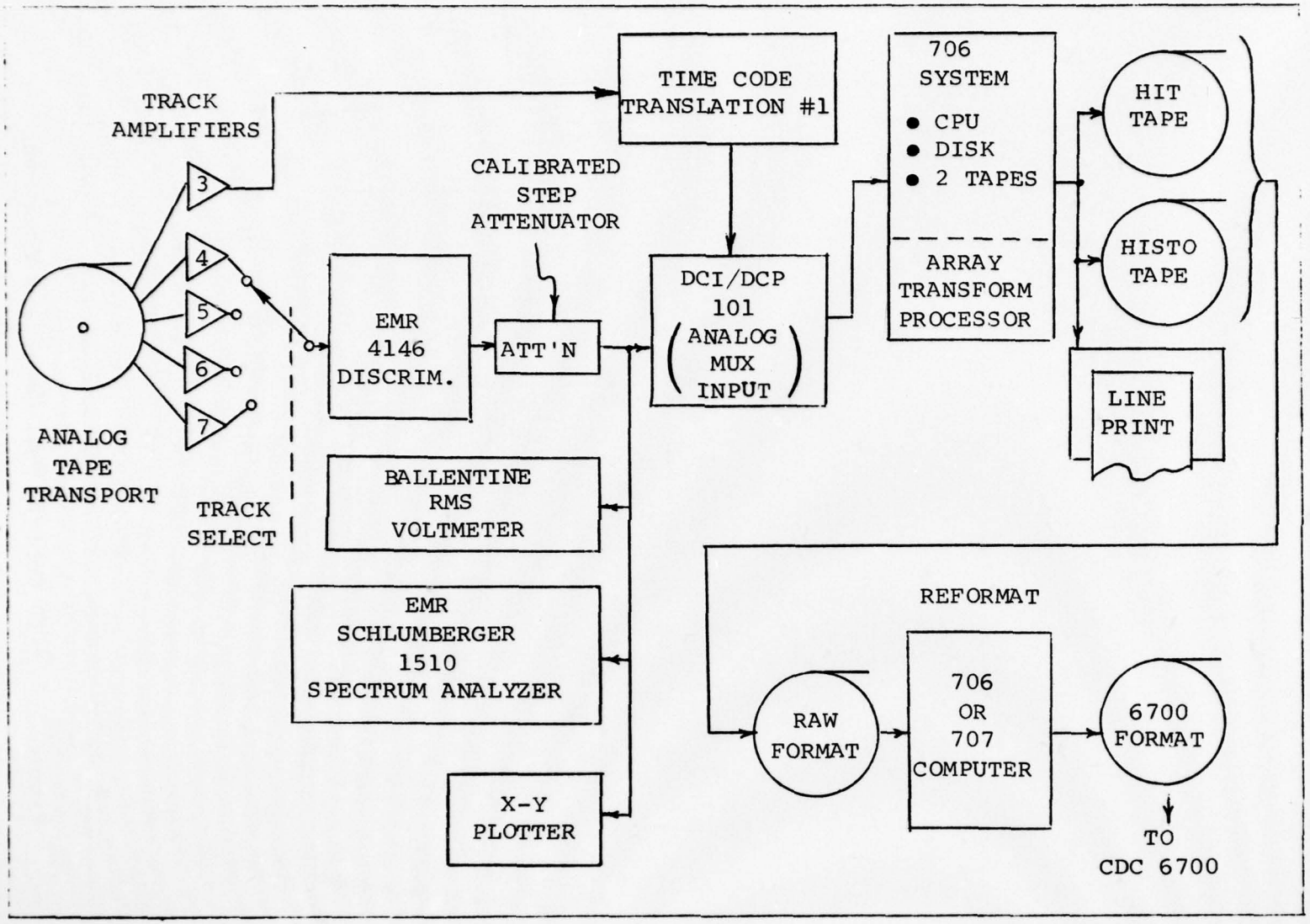

Figure 7-8 Data Reduction Equipment

8. PROCEDURES

This section describes the flight and other procedures used to process the raw system inputs so as to develop the desired outputs. These outputs were used for three basic purposes; to develop clutter models, to obtain insight into the nature of the phenomenon, and to validate measurements and procedures. Outputs of the processes fall into these basic families:

A. HISTOGRAM ANALYSIS provides description of the probability distribution of sea clutter and measures directly related to this probability distribution.

B. HIT ANALYSIS investigates subsets of returns much larger than usual. Here we are interested in describing those relatively rare large returns that most effect false alarms in a detection system. The interrelationship of hits (large returns) is also investigated as this could impact design and performance of candidate acquisition systems working in sea clutter. The roots of this analysis lies in the question "Do large returns come in clumps or herds?"

C. MEAN ANALYSIS is defined by averaging over various subsets of the data for investigation in some detail. The interest in mean analysis lies in its potential use in acquisition systems. Means were plotted and distribution and spectral content were investigated in some detail.

D. SPATIAL AND TEMPORAL ANALYSIS relates individual resolution cells to their neighbors in space and time. These relationships are expressed in terms of spatial and temporal autocorrelations functions and spectra.

The procedual descriptions to follow in-general emphasize what was done to obtain the desired outputs rather than how to process the data. However, description in terms of the mechanics involved is used when this approach provides a better understanding of the procedure involved.

Emphasis in the reduction and analysis procedures was on the relative characteristics of the data as opposed to absolute characteristics of the data. In fact, the only absolute measure is of the mean backscatter coefficient with many of the other clutter measures normalized to this mean. This emphasis was chosen as more responsive to the needs of system designers, simulators, and evaluators. Those wishing to interpret the sea characteristics in terms more suitable to their own use can find the available data on environmental characterization in the appendices.

The following description of procedures has been broken down as a tree-chart organization with each subsection describing a portion of the procedure. In many subsections an overview is first presented and then the procedures are described in detail.

8.1 Overview

8.1.1 Overview of Procedure

The basic capabilities and constraints together with program objectives were used to develop an overall program plan as illustrated in Figure 8-1.

The ARTS radar was modified as requires and integrated with the aircraft and recording equipment to form the TAGSEA clutter measurement system. This system was then tested and calibrated.

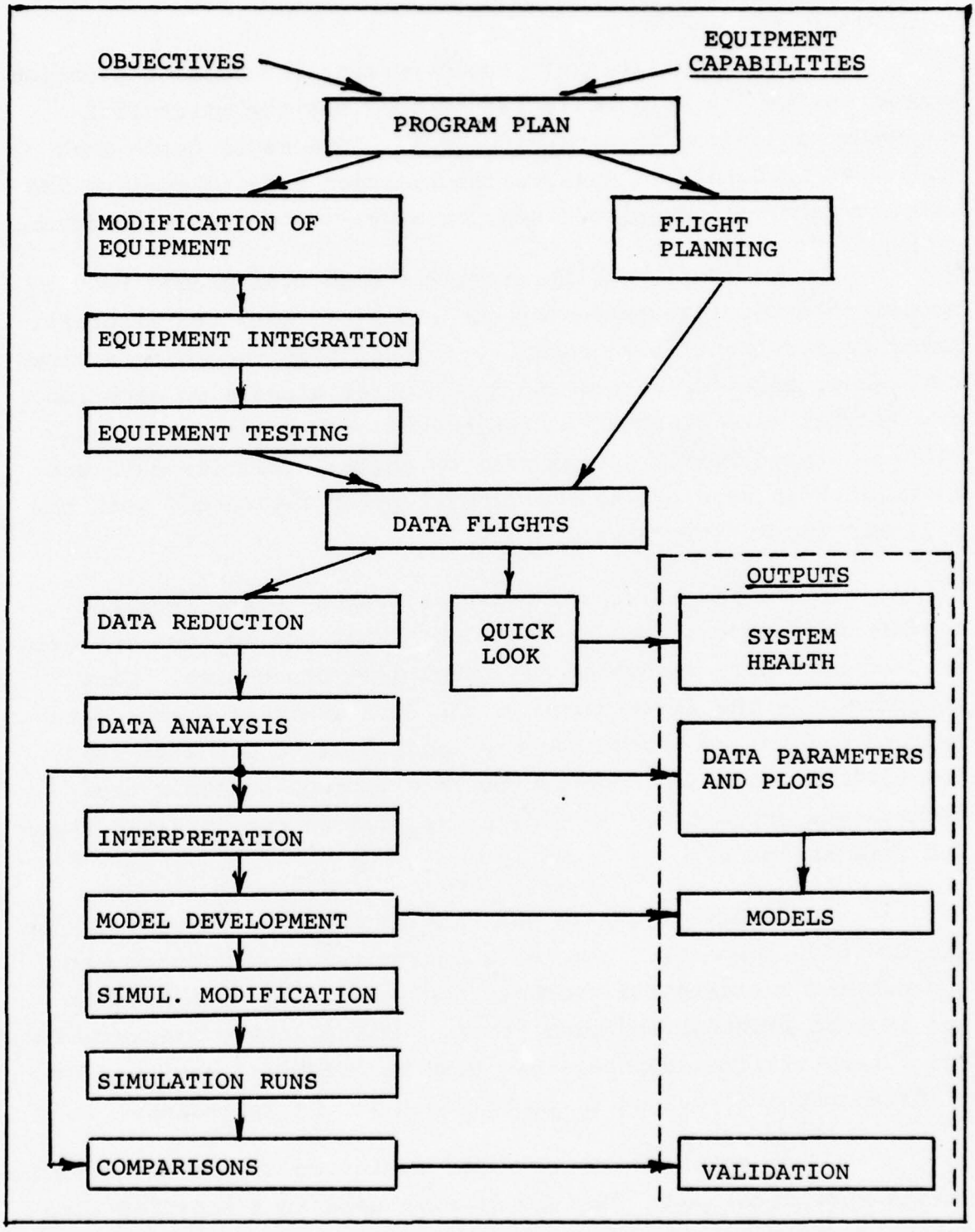

Figure 8-1 Overview of Procedures

After initial ground testing the major validation procedure for the data collection system was the quick look procedure described in Subsection 8.11. The major quick look tool was the Schlumberger spectrum analyzer used to analyze and compare receiver noise, calibration signals and clutter returns.

Initial calibration was done with ground test equipment after integration of the radar pod with the aircraft. Later calibration was achieved by sequentially recording a known CW signal, receiver noise, and the clutter signals on each run. The flights were planned to obtain data over a variety of sea states, wind directions, and grazing angles. Clutter data was taken at both vertical and horizontal polarization off both the Atlantic and Pacific coasts.

The clutter returns as well as other required signals were recorded on analog tape. This analog tape was used to feed both data reduction and quick look procedures. Data reduction was the first stage in the data analysis path. Data reduction first converted the raw radar data to map form then the basic information required for the various analysis procedures was extracted. This data was written onto digital tapes for data analysis.

Data analysis was done primarily with software in the CDC 6700 computer. Some hand analysis was used to augment, support and validate the computer analysis. Computer outputs are in both printout and plot forms. To facilitate understanding and interpretation, emphasis has been on graphical outputs. Much of this graphical output is to be found in the appendices.

After review and interpretation of the data, clutter models were developed. The models were used in a modified simulation to produce simulated sea clutter which was analyzed in the

same manner as real sea clutter. Comparisons of results were used to validate modeling and simulation.

8.1.2 Clutter Data Information Flow

The processing of clutter information was divided into several stages, each of which is defined by the facilities and equipment used. The major data processing stages are: data collection, data reduction, data analysis, interpretation, modeling, simulation, and simulation validation. A basic information flow diagram is shown in Figure 8-2. The remainder of this section described the major blocks in this order: data collection, data reduction, data analysis, and validation.

8.2 Flight Scenarios

The flight scenarios were chosen to obtain a large data base over a variety of conditions. A scenario component matrix is shown in Table 8-1.

TABLE 8-1
FLIGHT SCENARIO COMPONENTS

1.	East Coast - West Coast
2.	Depression (grazing) Angle
3.	Polarization (vertical-horizontal)
4.	Wind Direction (up-down & cross wind)
5.	State of the Sea (environmental characteristics)

Flights were flown in approximately equal numbers off both east and west coasts. Differences in clutter have been noted on other programs and a direct comparison using the same equipment was deemed to be of interest.

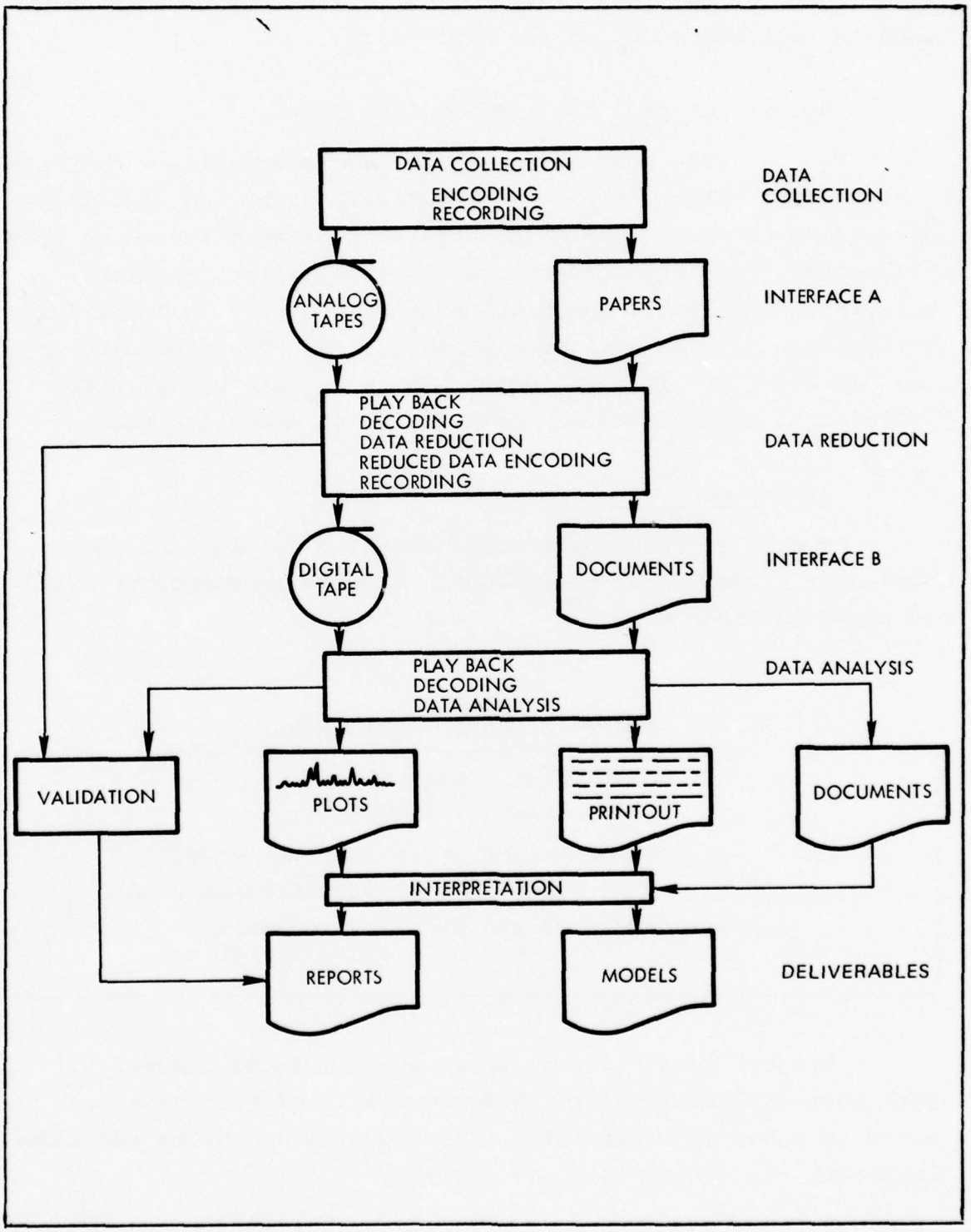

Figure 8-2 Clutter Data Information Flow

In order to obtain both a large data base and fine resolution on the sea, the data was taken in synthetic aperture (side-looking) configuration. The basic flight configuration and observation zone are shown in Figure 8-3. The aircraft flew straight and level for approximately 5 minutes at one of the three basic altitudes (1100, 2200 or 3300 feet) thereby setting the grazing angle for that run. All other parameters were then fixed by the ARTS and data reduction characteristics.

The area for east coast test flights is shown in Figure 8-4. Each flight started at the Nantucket Shoals Lightship (69° 26' W, 40° 28' N) and was contained roughly within the marked 20 mile radius circle in an L-shaped pattern. The test area on the west coast is indicated in Figure 8-5. For the west coast the primary operating areas were divided by flight with roughly half off the east coast of San Clemente Island and half off the west coast. The flight zones were chosen for open sea conditions at convenient locations. Availability of reports from the Nantucket Shoals Light Ship on sea conditions was a consideration in choosing the east coast location. Reports on the west coast were obtained from a dedicated boat in the operating area.

During these flights clutter was gathered at the three basic altitudes of 1100, 2200 and 3300 feet and at 500 feet for special low grazing angle flights. The 16 range gates gave a spread in depression angle at each altitude as shown in Table 8.2

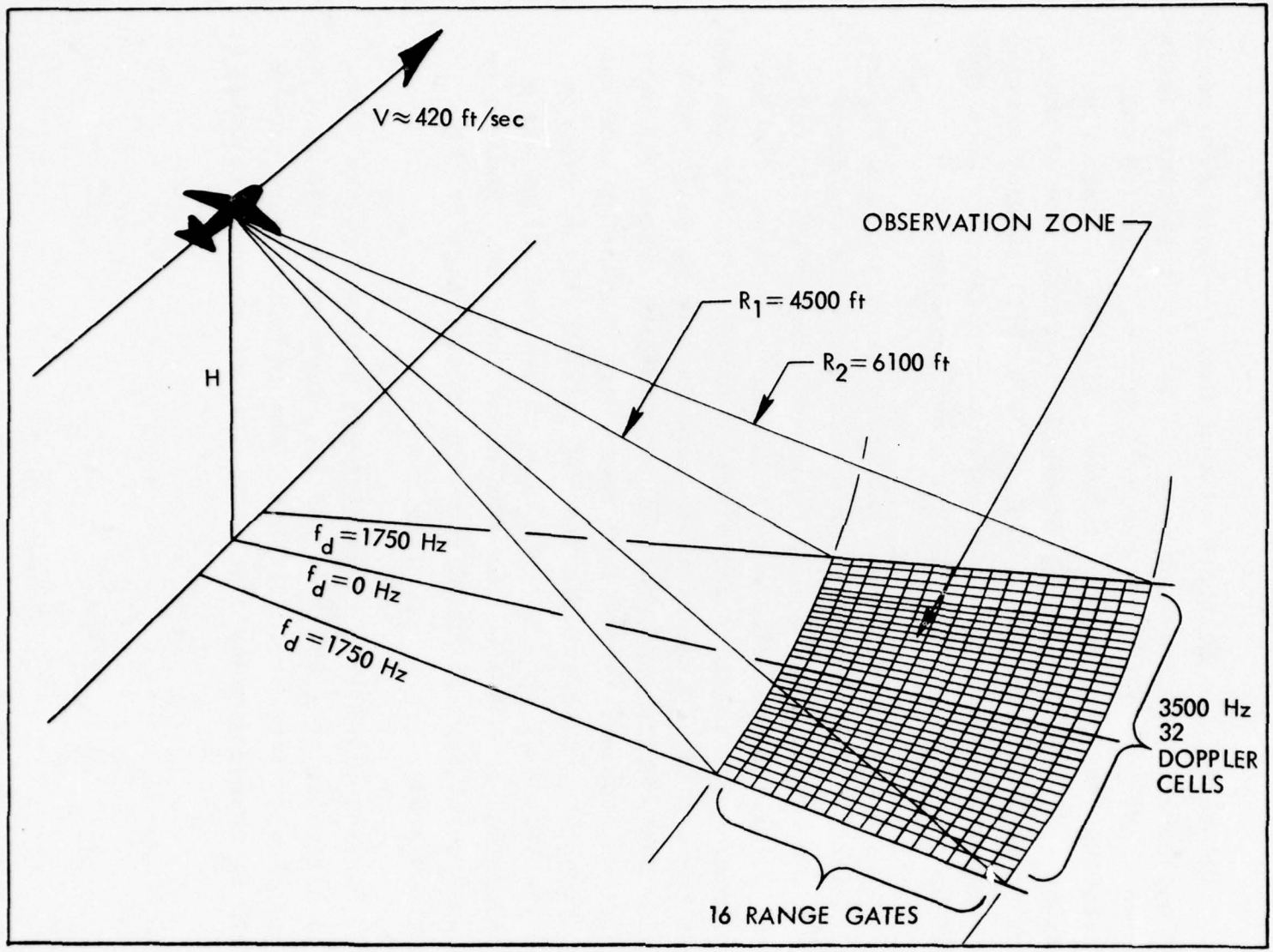

Figure 8-3 Clutter Flight: Range/Doppler Geometry and Observation Zone

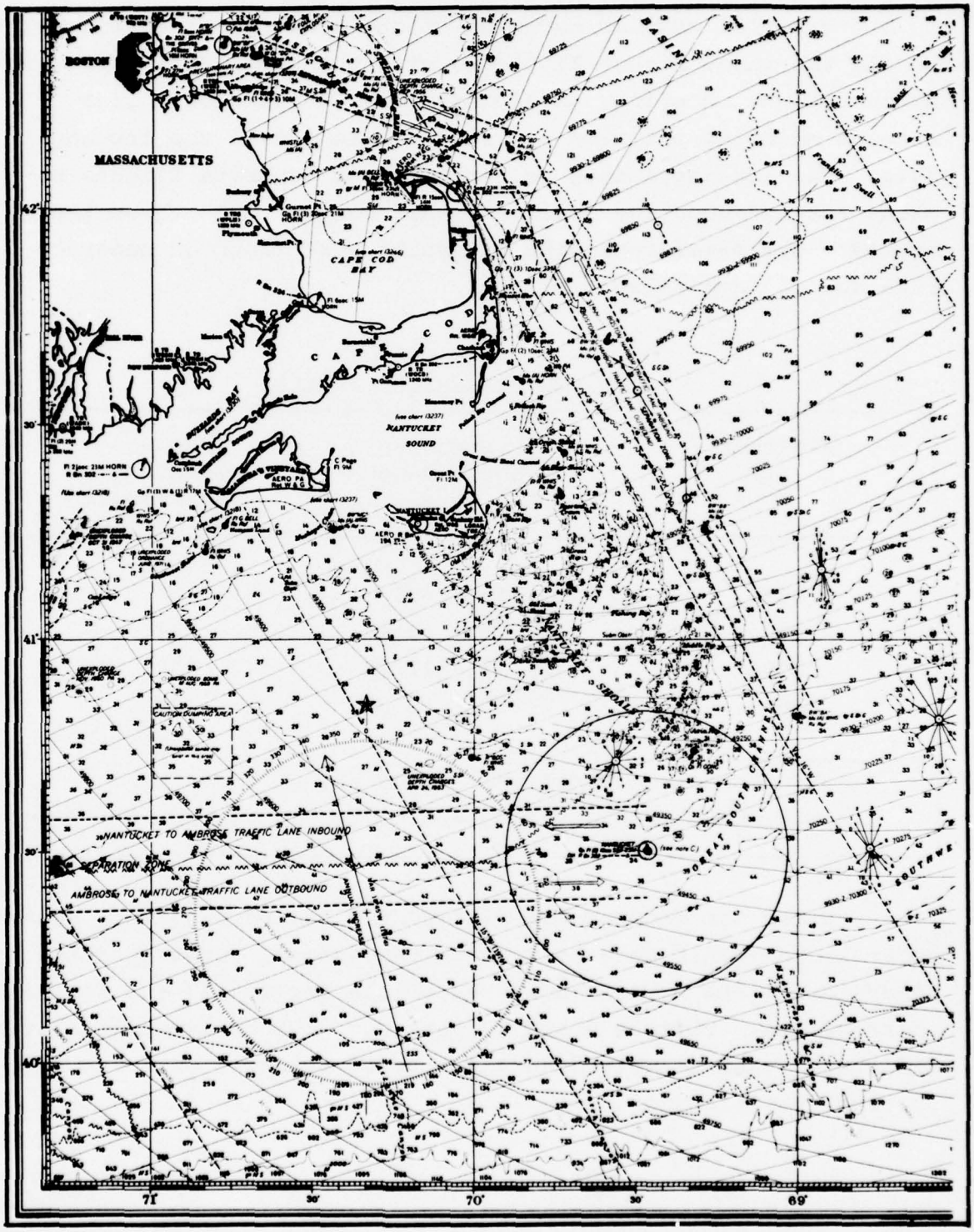

Figure 8-4 East Coast Map

Vertical angular coverage of the antenna was sufficient to fly the three higher altitudes with the same (30°) depression angle antenna mounting. A different (0° depression angle) antenna mounting position was required to obtain the low angle data. The low angle data is derived from separate flights because antenna mounting position could only by changed on the ground. The three remaining altitudes were flown on separate runs during each flight.

TABLE 8-2
SCENARIO DEPRESSION ANGLES

Altitude (ft) M	Depression Angle Range θ_1 to θ_2	Antenna Mounting Depression Angle
500	6.4° - 4.7°	0°
1100	14.3° - 10.4°	30°
2200	29.3° - 21.1°	30°
3300	47.2° - 32.8°	30°

Minimum Slant Range, R_1 = 4500 ft.
Maximum Slant Range, R_2 = 6100 ft.

Since the antenna was fix mounted for each flight, changing polarization could only be done on the ground. Consequently separate flights were required to obtain horizontal and vertical polarization. Flights 7 and 17 were run with horizontal polarization, all other flights (the majority of flights) were run with vertical polarization.

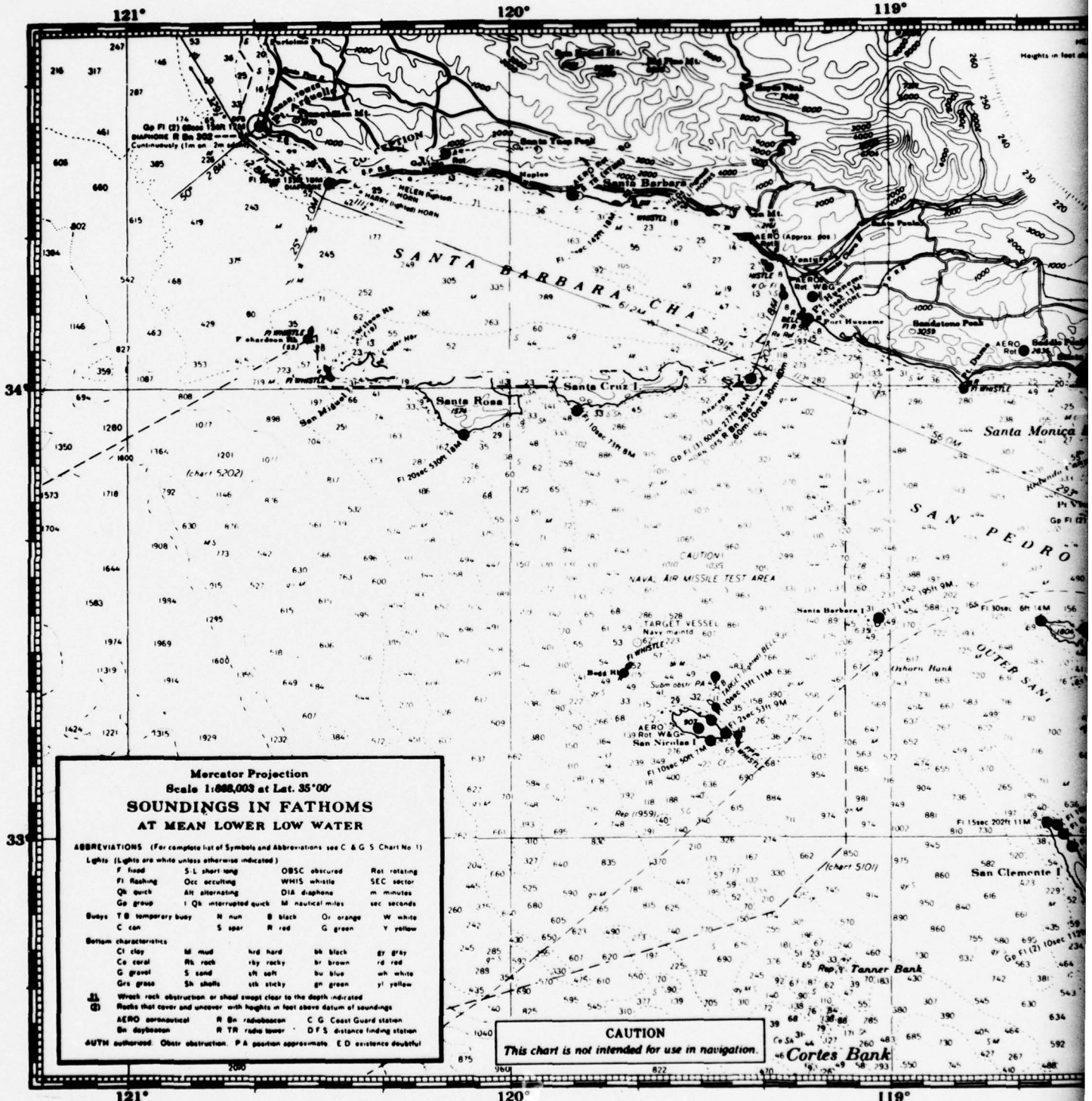
121°
120°
119°
34°
33°
SANTA BARBARA CHA
SAN PEDRO
Santa Barbara I
Santa Cruz I
Santa Rosa I
San Nicolas I
San Clemente I
Santa Monica
Cortes Bank
Tanner Bank
Osborn Bank
Santa Rosa
Santa Cruz
Santa Barbara
Ventura
Port Hueneme
Sandstone Peak
Santa Ynez Peak
Mercator Projection
Scale 1:888,003 at Lat. 35°00'
SOUNDINGS IN FATHOMS
AT MEAN LOWER LOW WATER
ABBREVIATIONS (For complete list of Symbols and Abbreviations see C & G S Chart No 1)
Lights (Lights are white unless otherwise indicated)
F fixed
Fl flashing
Qk quick
Gp group
S-L short long
Occ occulting
Alt alternating
I Qk interrupted quick
OBSC obscured
WHIS whistle
DIA diaphone
M nautical miles
Rot rotating
SEC sector
m minutes
sec seconds
Buoys T B temporary buoy
C can
N nun
S spar
B black
R red
Or orange
G green
W white
Y yellow
Bottom characteristics
Cl clay
Co coral
G gravel
Grs grass
M mud
Rk rock
S sand
Sh shells
hrd hard
rky rocky
sft soft
stk sticky
bk black
br brown
bu blue
gn green
gy gray
rd red
wh white
yl yellow
Wreck rock obstruction or shoal swept clear to the depth indicated
Rocks that cover and uncover with heights in feet above datum of soundings
AERO aeronautical
Bn daybeacon
R Bn radiobeacon
R TR radio tower
C G Coast Guard station
D F S distance finding station
AUTH authorized Obstr obstruction P A position approximate E D existence doubtful
CAUTION
This chart is not intended for use in navigation.
NAVAL AIR MISSILE TEST AREA
TARGET VESSEL
Navy maintd
(chart 5202)
(chart 5101)
Rep 1959
Rep 1959
Subm obstr PA
Heights in feet

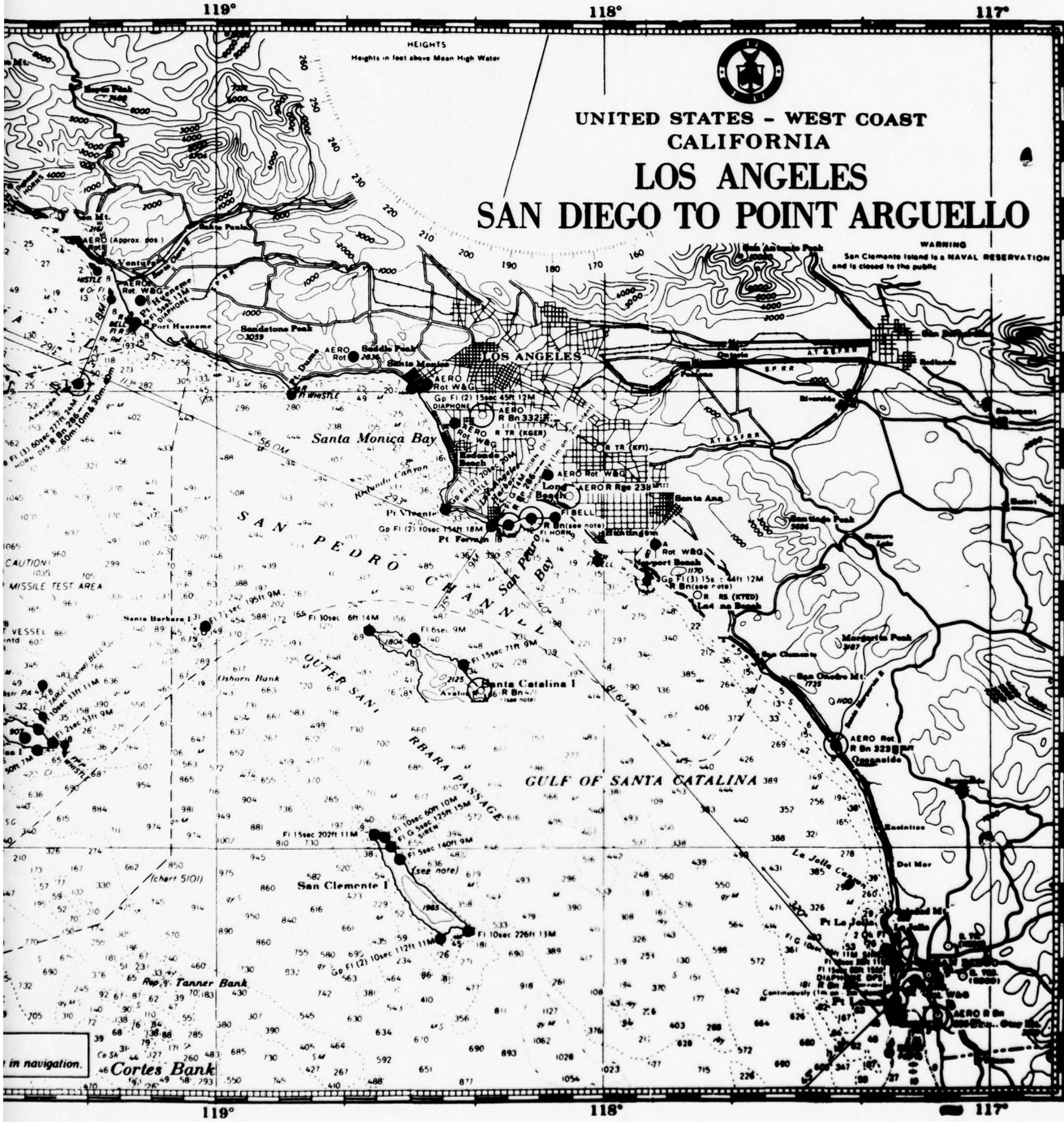

Figure 8-5 West Coast Map

2

In order to obtain data looking upwind, downwind and crosswind the trajectory shown in Figure 8-6 was flown at each altitude.

On each of the three legs at each altitude 5 minutes of clutter data was taken. Calibration data was taken as part of each run. Data flights contained up to 10 runs plus possible repeats. Run 0 was a camera run used to obtain sea pictures for analysis of sea state. There were usually 9 clutter runs as shown in Table 8-3. Low altitude flights however had only 3 clutter runs as shown in Table 8-4. Repeats of runs were sometimes done. In this case the run number was preceeded by a 1, e.e. 16. In any case the last digit of the flight number identifies run conditions.

TABLE 8-3
FLIGHT RUN MATRIX FULL FLIGHT

Run 0	Camera Run		300'	1 min.
Run 1	Radar Looking	Upwind	1.1Kft	5 min.
2	Radar Looking	Downwind	1.1Kft	5 min.
3	Radar Looking	Crosswind	1.1Kft	5 min.
4	Radar Looking	Upwind	2.2Kft	5 min.
5	Radar Looking	Downwind	2.2Kft	5 min.
6	Radar Looking	Crosswind	2.2Kft	5 min.
7	Radar Looking	Upwind	3.3Kft	5 min.
8	Radar Looking	Downwind	3.3Kft	5 min.
9	Radar Looking	Crosswind	3.3Kft	5 min.

TABLE 8-4
FLIGHT RUN MATRIX LOW ALTITUDE FLIGHT

Run 0	Camera Run		300'	1 min.
Run 1	Radar Looking	Upwind	500'	5 min.
Run 2	Radar Looking	Downwind	500'	5 min.
Run 3	Radar Looking	Crosswind	500'	5 min.

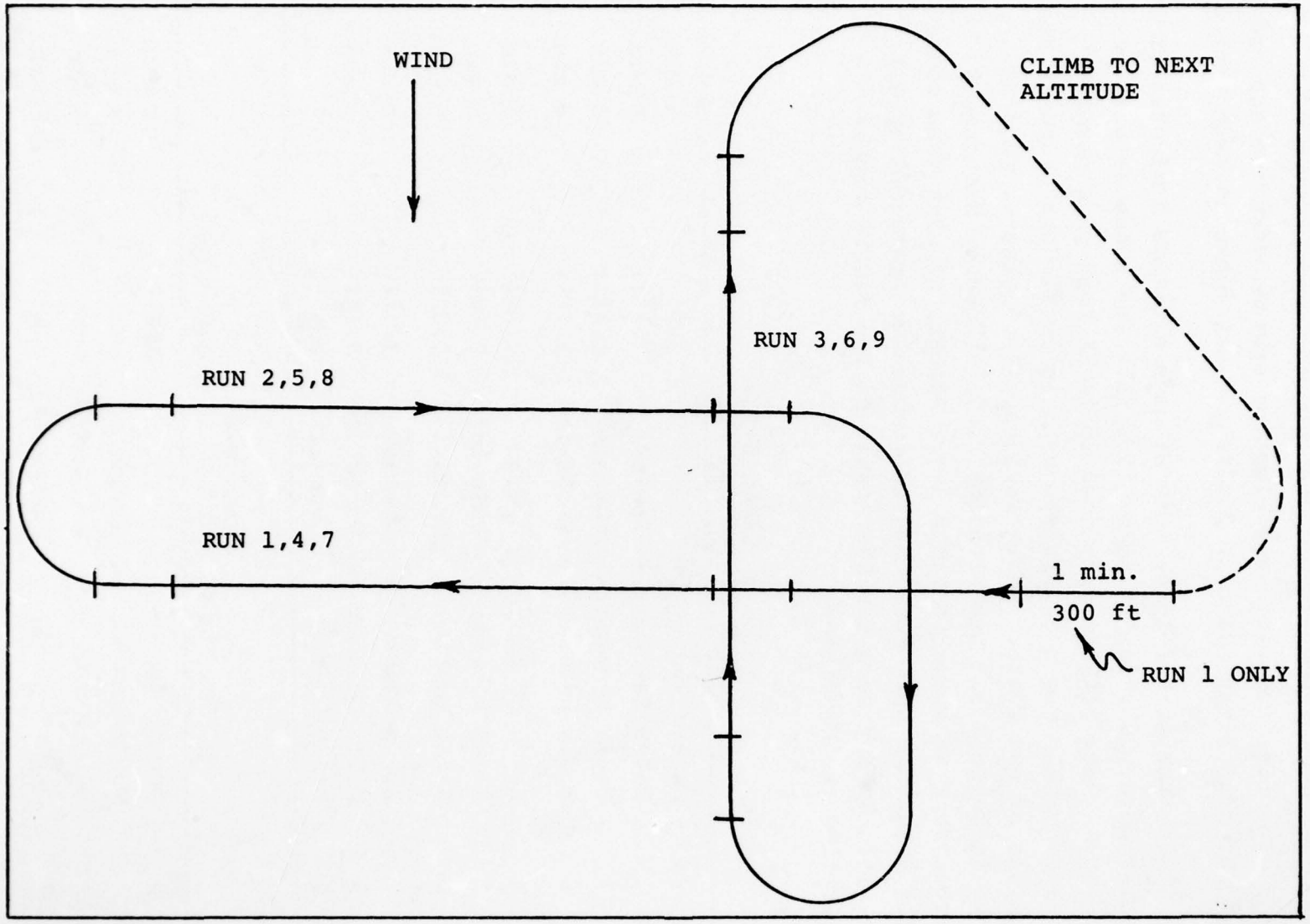

Figure 8-6 Typical Flight Pattern

UNCLASSIFIED

A sequence of events for a run is shown in Figure 8-7. The aircraft is first brought to the correct altitude and heading. ① At the start of each run the altitude is encoded on the camera data be clearing the camera the appropriate number of time. ② (1 frame for 1.1Kft, 2 frames for 2.2Kft, 3 frames for 3.3Kft). This allows better coordination of camera and radar data. The camera has two purposes; characteristic of the sea, and recording the existence of ships in the scene. The camera and tape recorder are then turned on ③ and camera frames snapped automatically every 5 to 6 seconds. The gain adjustment sequence begins ④ and ends ⑤ . This gain is set on clutter with the RMS meter and is done with the transmitter on. The calibration signal is turned on ⑥ and the VCXO adjusted to 4kHz offset ⑦ . The calibration signal is then recorded, ⑧ , for 10 seconds. The calibration signal is turned off, ⑨ , and 10 to 15 seconds of receiver noise is recorded, ⑩ , with with transmitter off. The transmitter is then turned on, ⑪ , and 5 minutes of clutter data recorded. At the end of the clutter run receiver noise, ⑬ and CW calibration signals, ⑭ , are again recorded before turning off recorders and camera ⑮ .

In a zero run, ⑯ , only low altitude pictures of the sea are recorded for sea characterization.

8.3 Environmental Characterization

8.3.1 Introduction

Environmenal characterization of the sea describes in non-radar terms the surface effects which ultimately results in signals into the ARTS system. Ideally such a description should be deterministic and be able to be correlated with the ARTS returns. Photographs, weather reports, wind and wave measurements and human observation were all used prior to, during and

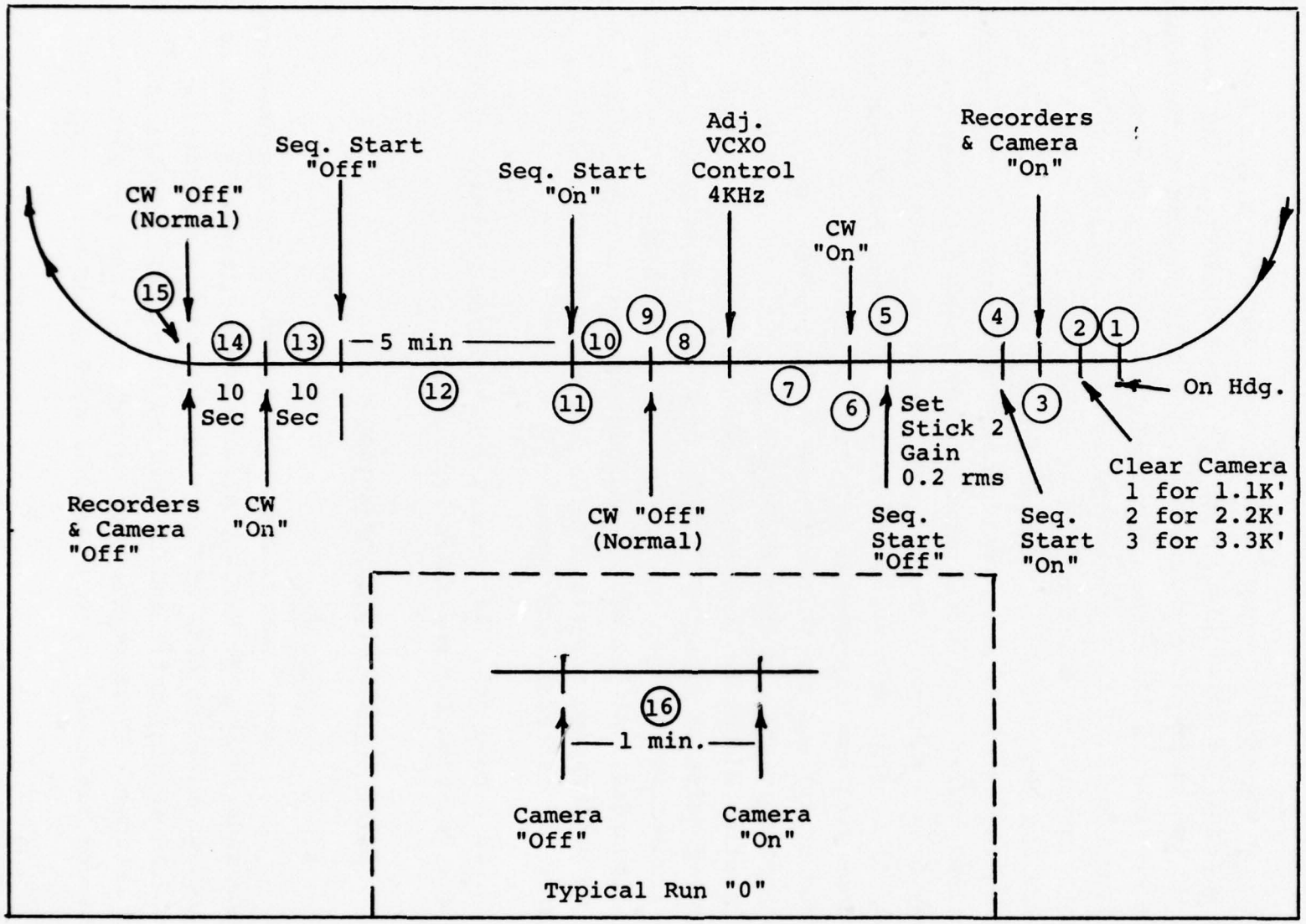

Figure 8-7 Event Sequence for Run

after flight. Objects other than the sea which would result in large returns (e.g. ships) are also of interest and were identified as part of the environment.

Except for unique events such as ships, the objective was to characterize the surface of the sea with a sea-state number. All of the work was done by General Dynamics as part of their flight test work. A preliminary copy of a description of this work is included here as Subsection 8.3.2 for the convenience of the reader.

8.3.2 Determining Sea Conditions for TAGSEA Clutter Flights

A. Method

The method used for determining sea conditions for TAGSEA clutter flights consists of the following steps:

1. General Description - Close observation of the still photos taken during flight will reveal the general condition of the sea (smooth seas through high seas). The amount of white caps present and the type of motion taking place (foam streaks, spindrift, etc.) are the main points of observation. These observations are compared to "A Guide to Sea State" (Figure 1*) as an aid in determining sea state. Once sea state is determined, values of wave height, period, wave length, wave velocity and wind velocity are approximated from the chart in Figure 8-8.

---

*"A Guide to Sea State" was developed by BUNKER RAMO, ELECTRONIC SYSTEMS DIVISION from information contained in "American Practical Navigator" by Bowditch and published by the U. S. Navy Department, Hydrographic Office. (Not reproduced here)

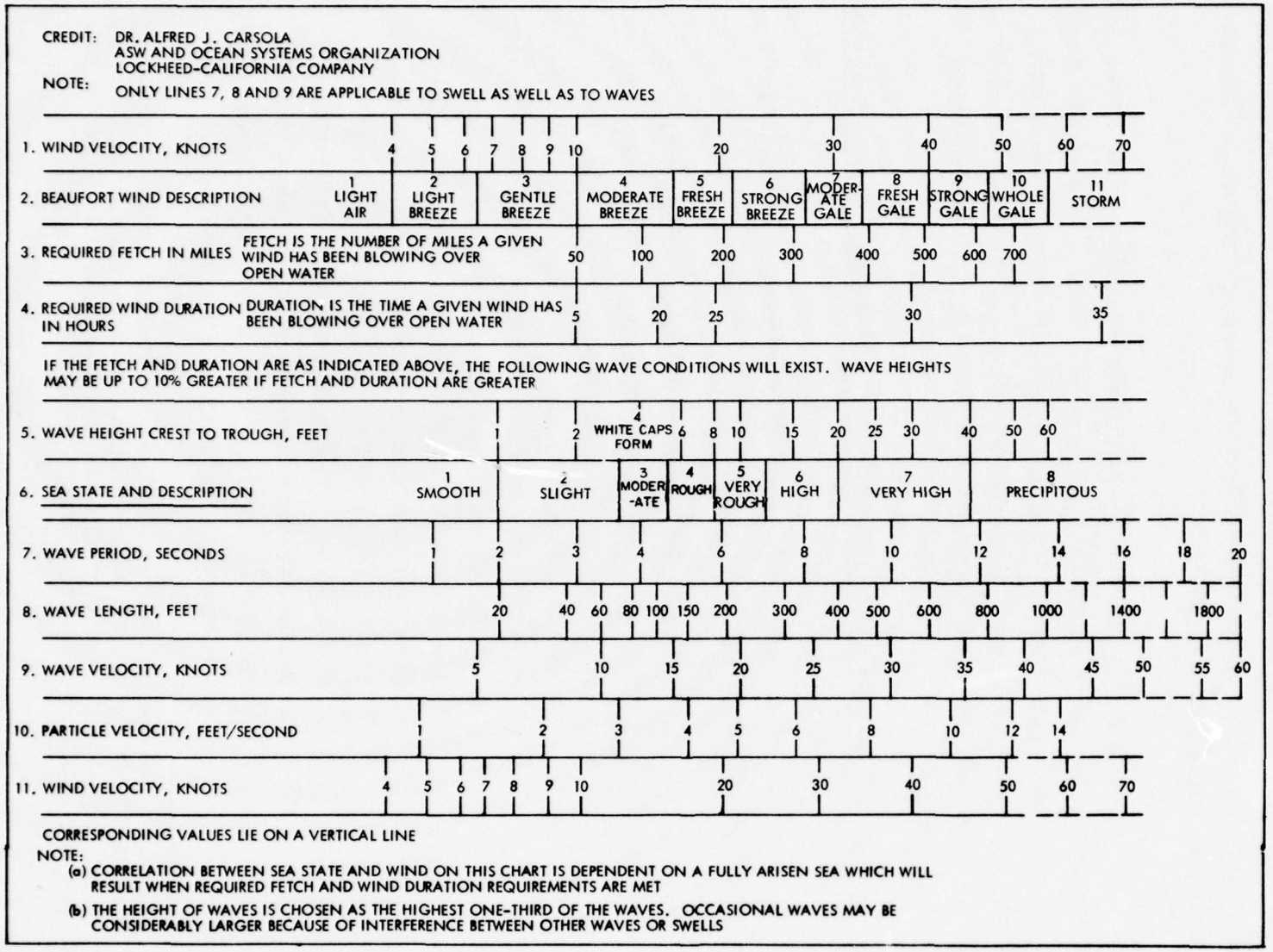

Figure 8-8 Sea State vs. Surface Environment

2. Computation of Sea State Parameters ** - Parameters relating to sea state are determined from the still photos as follows:
   a) Wave Direction - The direction of the waves is determined either by observing the trough lines in the film and then computing direction from known aircraft heading or by relating wave direction to wind direction provided wind direction is known and has been blowing for a sufficiently long time and with sufficient velocity to produce waves that are large with respect to swells.
   b) Wave Length - Wave length is determined by counting the number of waves in a given portion of the film frame and relating this to the field of view and surface area computed from test geometry.
   c) Wave Period - Once wave length has been determined, wave velocity can be approximated from the wind velocity provided that the wind velocity is known. Wave period, then, is simply the wave length divided by the wave velocity.

3. Correlation with Meteorological Data - Conditions determined in 1 and 2 above are compared with existing meteorological data to verify that the determined conditions are consistent with reported information on weather and sea conditions.

** In the case of a confused sea, these comparisons are only rough approximations.

B. Example of Sea State Determination

Sea conditions for Data Flight No. 5 (East Coast) on 12 February 1976 were determined as follows:

1. Description of Sea State - Observation of the still photographs obtained during the flight reveals that the sea was somewhat confused. However, some uniformity can be noticed in the pictures taken at the higher altitudes. A 2.2Kft upwind, for example, uniform trough lines can be seen in the upper portion of each picture.

   The pictures at 300 ft reveal the "heaping up" action of the sea. The sun glare in this case is convenient since it intensifies the contrast between the crest and trough of the large waves.

   The pictures at 1.1Kft, 2.2Kft and 3.3Kft reveal a large amount of white cap action. This action is especially noticeable at 1.1Kft upwind where foam streaking and spraying can be seen due to breaking crests and high winds.

   Based on the above observations and using Figure 1 as a guide, the sea in this case can be classified as Sea State 5 or Very Rough.

2. Computations - The following parameters were calculated for Data Flight No. 5:

a) Wave Direction - In order to compute wave direction the pictures at 3.3Kft upwind were chosen since the pattern of the trough lines are most noticeable at this altitude and windage. Since the camera line-of-sight is perpendicular to the aircraft heading, the arrow at the center of each picture indicates the direction of the aircraft heading. The trough lines are coming from a direction 73 degrees relative to this arrow. Since the aircraft heading was recorded as 220 degrees magnetic, then the wave direction is from 220 + 73 or 293 degrees magnetic.

b) Wave Length - The wave length for Data Flight No. 5 was calculated using frame No. 8 at 3.3Kft upwind as follows:

S = Distance perpendicular to the troughs in a half frame.

N = Number of troughs in a half frame=43

and L = Wave Length

Then,

$$L = \frac{S}{N} = \frac{S}{43}$$

S was calculated from the formula

$$S = \frac{F}{\sin\theta}$$

Where F = Distance perpendicular to the aircraft heading in top half of frame,

and θ = Angle between aircraft heading and trough line direction = 73°

From camera coverage geometry

$$F = H(1/\tan \psi_{min} - 1/\tan \psi_{max})$$

Where H = Altitude of aircraft = 3.3Kft

ψ_{min} = Camera field of view minimum grazing angle = 12.4°

ψ_{max} = Camera field of view grazing angle at half frame = 33°

From frame No. 8 then,

$$S = \frac{F}{\sin\theta} = \frac{(3300)(1/\tan 12.4° - 1/\tan 33°)}{\sin 73°}$$

$$= 10381 \text{ ft.}$$

and $L = \frac{S}{N} = \frac{10381 \text{ ft}}{43} = 241.4 \text{ ft.}$

From Figure 8-8 the wavelength for Sea State 5 ranges from approximately 180 ft to 265 ft.

c) Wave Period - The wave period for Data Flight No. 5 was calculated using frame No. 8 at 3.3Kft upwind as follows:

Let L = Wave Length

V = Wave Velocity

and P = Wave Period

Then,

$$P + \frac{L}{V}$$

For Frame No. 8 L = 241.4 ft and V = 34ft/sec***

*** Approximate value based on information received from Nantucket Light Ship Weather Log.

Therefore, $P = \frac{L}{V} = \frac{241.4 \text{ ft}}{34 \text{ ft/sec}} = 7.1$ seconds

From Figure 8-8 the period for Sea State 5 ranges from approximately 5.8 sec to 7 sec.

3. Conclusions - Existing meteorological data from Nantucket Light Ship was compared to the sea conditions determined for Data Flight No. 5. The following data was revealed:
   a) Wind - The wind velocity over a period of at least 25 hours was 20 knots on the average.
   b) Waves - Wave height was 10 to 12 feet from crest to trough.

   The above information was used as a final indication that a Sea State 5, as described in Figure 1 (not reproduced here) and Figure 8-8, existed during Data Flight No. 5.

8.4 Radar and Recording Operation

A three-man technical flight crew provided all the control and monitoring functions for ARTS and the recording equipment during flight. With the exception of the radar transmitter, all equipment was turned on shortly after take-off to provide maximum warm-up. The flight director in seat number one was responsible for the overall conduct of the flight and was in direct control of the on-board temeletry sub-carrier oscillators and chart recorders. He also provided the bulk of the voice annotation and written flight records. The operator in seat number two had control of the magnetic tape recorder and changed reels as required. He also provided manual control of the camera and snapped one, two, or three frames between runs as the aircraft was banked up. The resultant frame(s) of the sky served as run locators on the film strip.

The operator in seat number three controlled the radar. His duties included turn-on of the equipment, checking stability of the spectrum analyzer, setting radar gain using the RMS meter, setting the doppler offset to 4kHz, monitoring the system operation and checking the level of each range gate to be recorded. The sequence of operation during a flight and during a run is described in Subsection 8.2.

8.5 ARTS Calibration

Calibration of ARTS was accomplished in several steps and at three levels of overall assembly. The levels were: measurements made on individual units, tests and calibration of the radar, and calibration of the total ARTS systems including control and recording equipment. Basic measurements on hardware items were made only once to obtain a definitive level for such items as the antenna horn. Measurements on overall assemblies, as for example the radar, were made at least once and oftener if required. Finally, calibration and noise levels were made on each run. A block diagram of the hardware involved is shown in Figure 8-9.

A. ANTENNA MEASUREMENT

The antenna gain was measured in an anechoic chamber, using a 22dB standard horn as a reference. The measured gain was 11.2dB at the waveguide flange. A loss of 0.2dB is assumed for the waveguide to coax transition giving a gain of 11.0dB at the coaxial connector. The accuracy of measurement was $\pm$1dB.

B. TRANSMITTER POWER MEASUREMENT

The transmitter power output was measured at the antenna coaxial connector using a calibrated coupler and an average power meter. Duty cycle was measured using a detector and an oscilloscope. The peak power was found to be 29.6dBw, or 910W. At the same time, the average power at the transmitter test point was measured and found to be -8dBm. (See Figure 8-10)

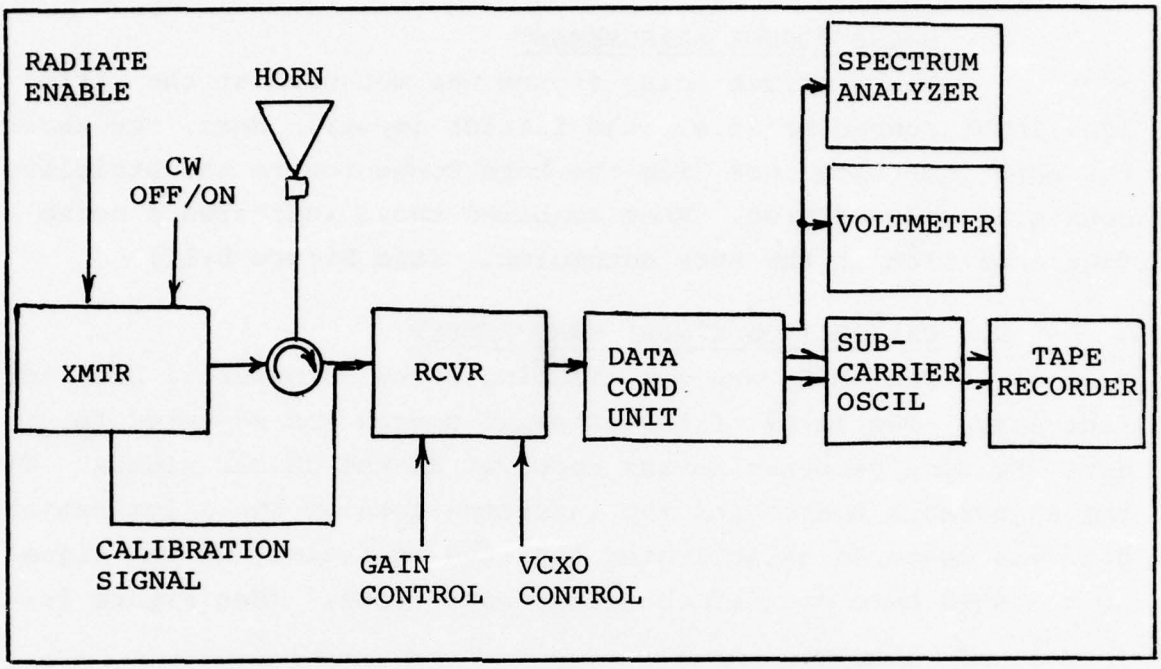

Figure 8-9 Radar and Recording Equipment

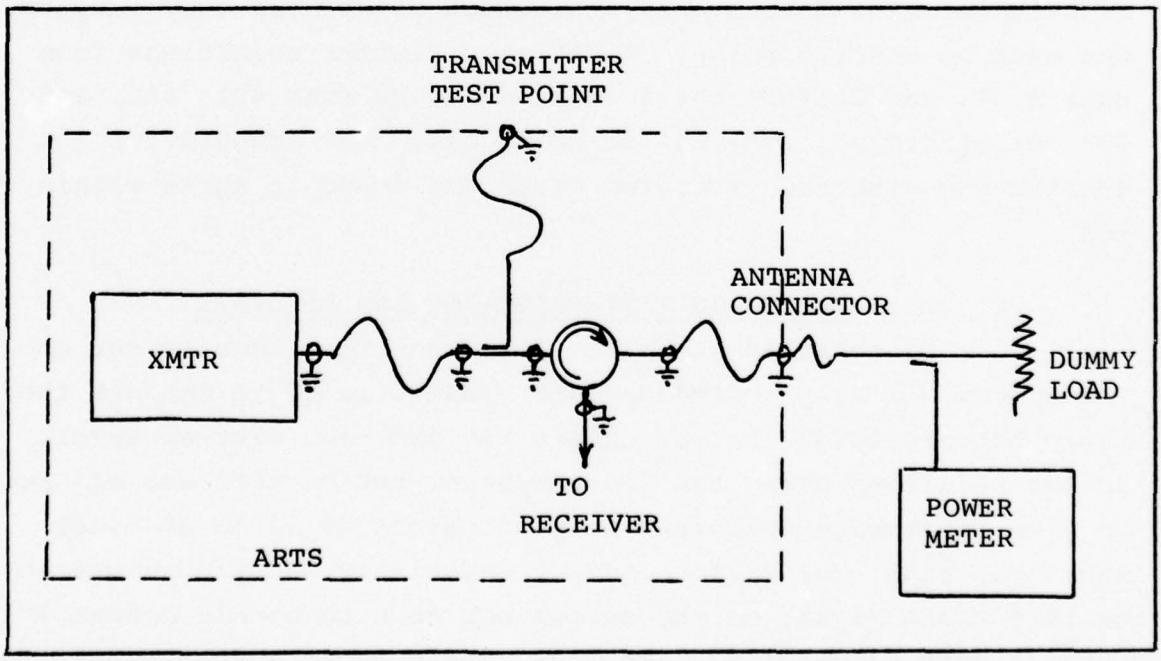

Figure 8-10 Transmitter Power Measurement

C. NOISE FIGURE MEASUREMENT

The receiver noise figure was measured at the stripline input connector (i.e., the limiter input). Next, the receiver path insertion loss from the horn connector to the stripline connector was measured. When combined these indicated a noise figure of 11dB at the horn connector. (See Figure 8-11)

D. CALIBRATION SIGNAL MEASUREMENT

The ARTS horn was illuminated by an external horn ten feet away. The level of the external source was adjusted to give the same response in the receiver as the CW CAL signal. Then the adjustable source and the insertion loss of the illumination path was measured establishing that the equivalent CW CAL signal at the ARTS horn coaxial connector was -78dBm. (See Figure 8-12)

E. PLAYBACK CHECK

After flight 4 (Data Flight 2), selected portions of data tapes were checked for consistency with expected results. A Schlumberger spectrum analyzer, which gives hard copy outputs, was used to observe noise, CW CAL, and clutter recordings from runs 1, 2, and 3 of Flight 4 (designated as runs 401, 402, and 403 respectively). The CAL to noise ratio was checked for consistency with the predicted value and found to agree within 1dB.

F. CALIBRATION IN DATA REDUCTION AND ANALYSIS

As detailed in Volume III, the prime requirement on the system was to provide adequate dynamic range to measure the ratio between large clutter echoes and the mean clutter level. In the reduction using the 706 computer, the clutter was adjusted to give an average spectrum analyzer output of 10 to 20 class marks per bin. The maximum output capability was programmed to be 1024 class marks, so the system was able to handle echoes 17dB above a mean value of 20. This was found to be adequate down to

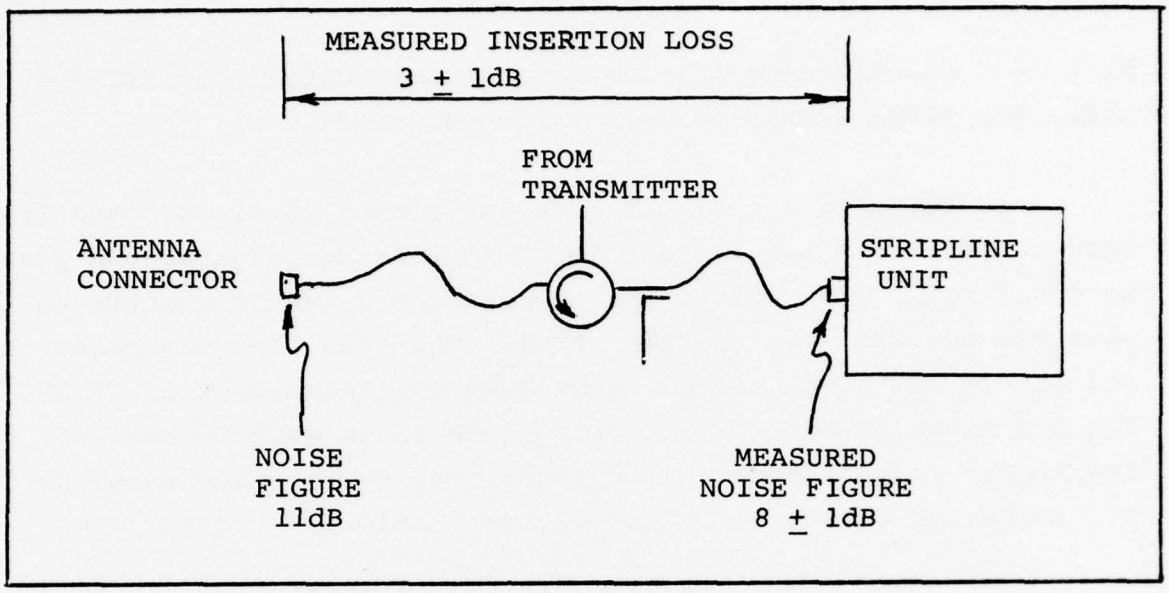

Figure 8-11 Noise Figure Measurement

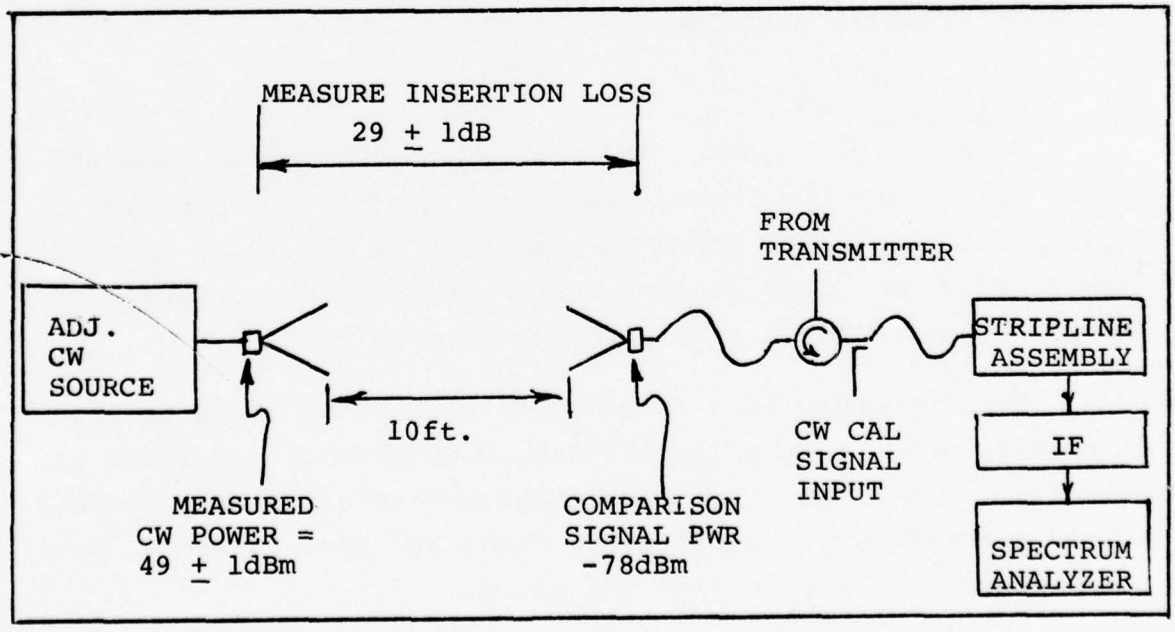

Figure 8-12 Comparison Method for Measuring CW CAL Signal Power

$P_f = 10^{-6}$ for all except a few runs in horizontal polarization where the large return-to-mean ratio exceeded 17dB.

In reducing a run, the tape was played 16 times, once for each range gate. Before reducing the first range gate, the playback voltmeter was used to set the average value of clutter to give the desired mean clutter value. Then the tape was backed up and the CW CAL level noted. Subsequently, this value of CW CAL was set manually before processing each range gate in the run, relying on computer-controlled range scaling to compensate for the variation of the CW CAL to clutter ratio with range.

The determination of σ_o, which was a secondary requirement required measurements of absolute clutter level. This was done by using receiver noise as a reference. The receiver noise level, which was a function of receiver gain setting, was estimated by combining all valid noise estimates obtained from the range gates in each run.

8.6 Data Coverage

Radar observation of the sea can be located in time and space. Since the sea is a surface, two surface coordinates suffice for positional location with time as the third observation coordinate. This section described the radar coverage in terms of these spatial and temporal coordinates.

Data coverage is a function of both radar and geometric parameters which in turn is a function of aircraft position and velocity. The single map "instantaneous" coverage with respect to the aircraft will be discussed first and then extended to the overall coverage in time and space.

A. Single Map Coverage

The basic system used is a synthetic aperture operating radar in a side-looking mode as shown in Figure 8-3 of Subsection 8.2.

The antenna had sufficient beamwidth to cover the range-doppler area and was not fundamental to coverage consideration. The coverage was restricted in cross range (perpendicular to flight path) by the 16 adjacent range gates centered 100 feet apart. The coverage along the flight path (parallel to aircraft flight path) was limited by the doppler zone process. A spread of $\pm$1750 Hz in doppler was processed in developing the data base. This doppler spread was divided into 32 doppler resolution cells for each range gate.

Control of grazing angle was achieved by selecting the altitude of the aircraft for each run. The four altitudes used were 500, 1100, 2200 and 3300 feet yielding grazing angles of 5 to 6 degrees, 10 to 14 degrees, 21 to 29 degrees and 33 to 47 degrees respectively. Each of the altitudes resulted in a different surface coverage as shown in Figure 8-13.

Computer plots of nominal surface coverage in aircraft coordinates are displayed for 500, 1100, 2200 and 3300 feet in Figures 8-14 through 8-17. Coordinates of the plots are feet from the nominal aircraft position down range and cross range with each cross representing the center of a range-doppler cell.

B. Total Coverage

During a clutter run a large number of overlapping maps were made. Since the aircraft flew approximately 20 miles during a 300 second (5 minute) run, the total sea area covered was approximately 1600 feet by 20 miles.

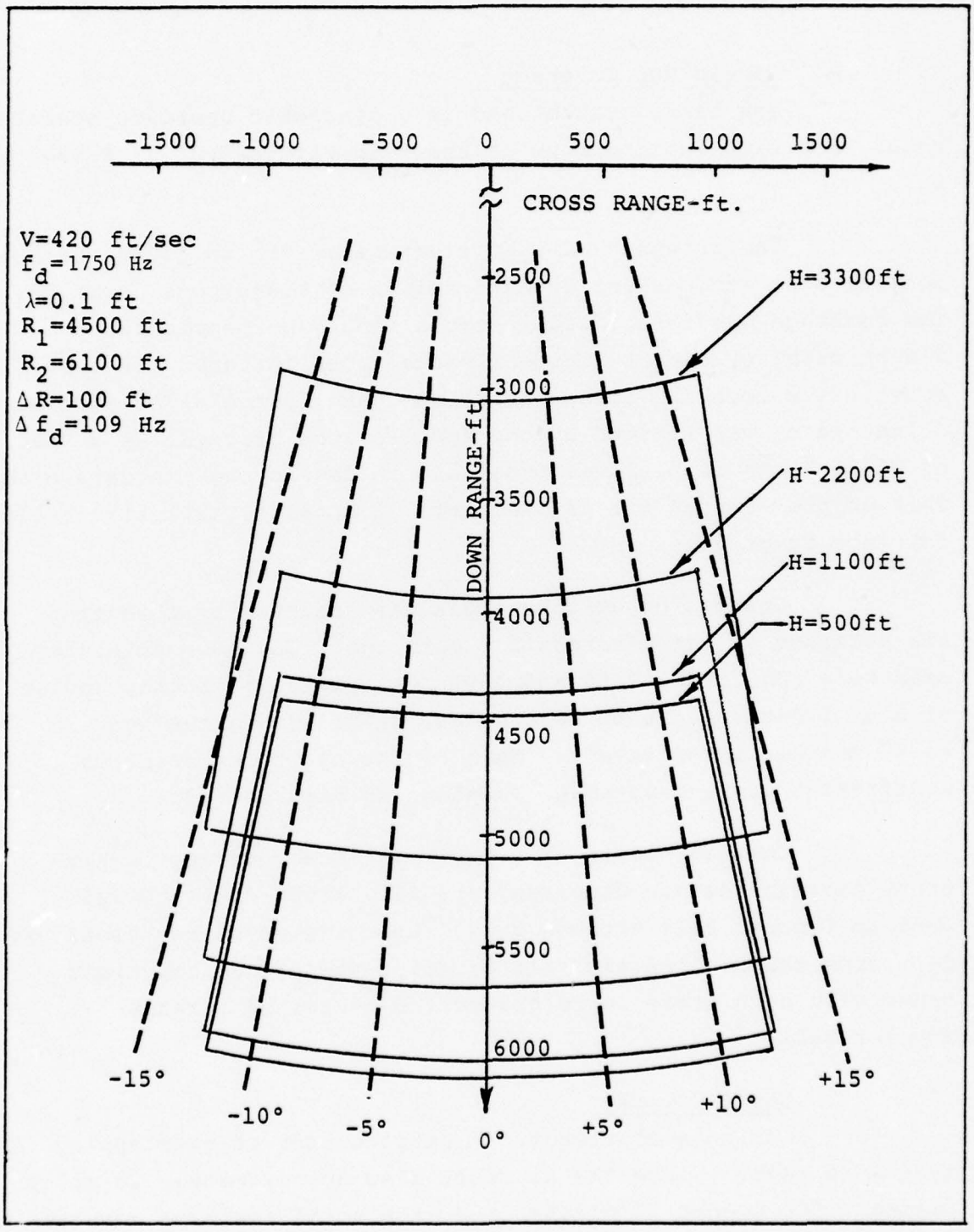

Figure 8-13 Surface Coverage

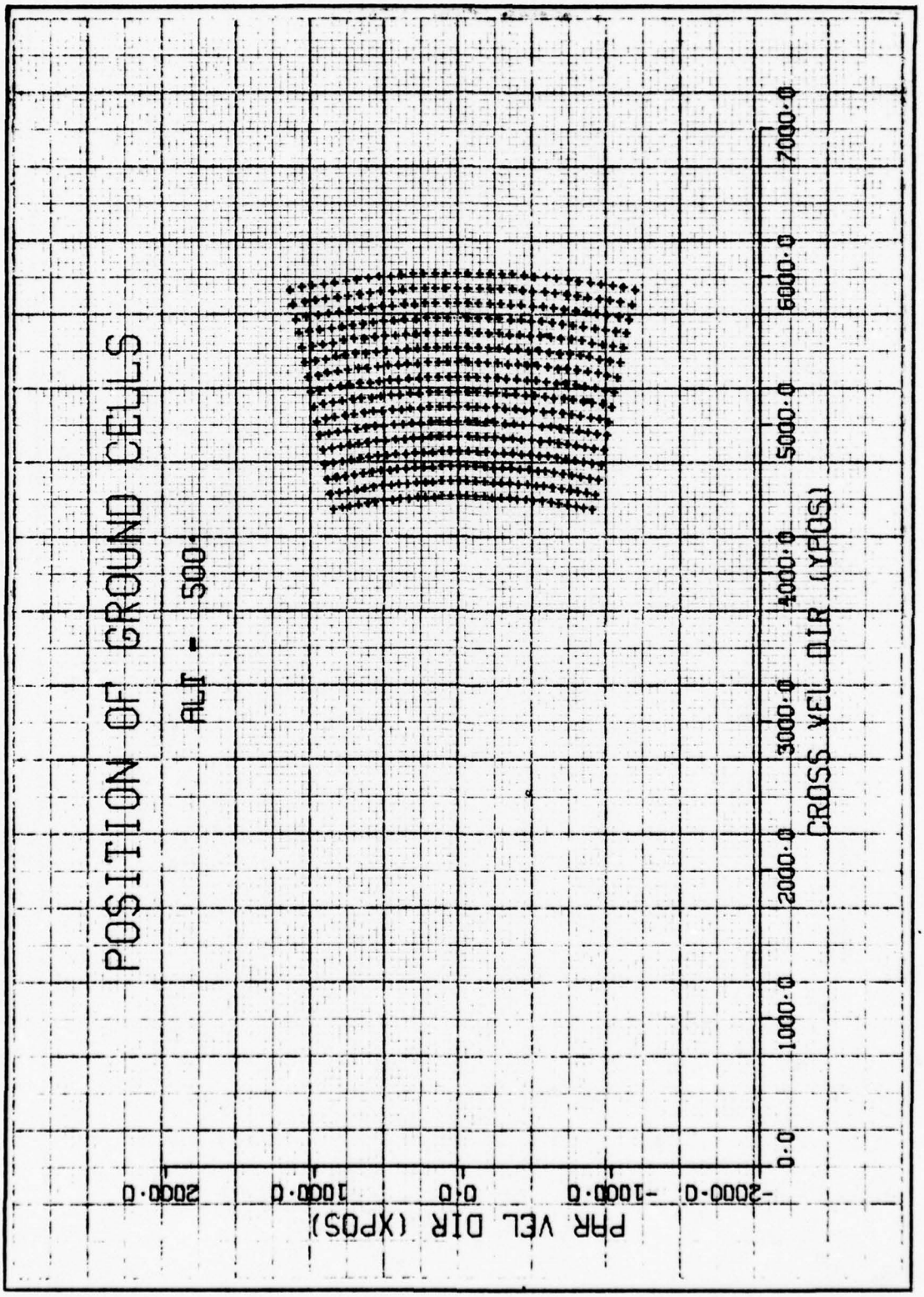

Figure 8-14 Surface Cells at 500 Foot Altitude

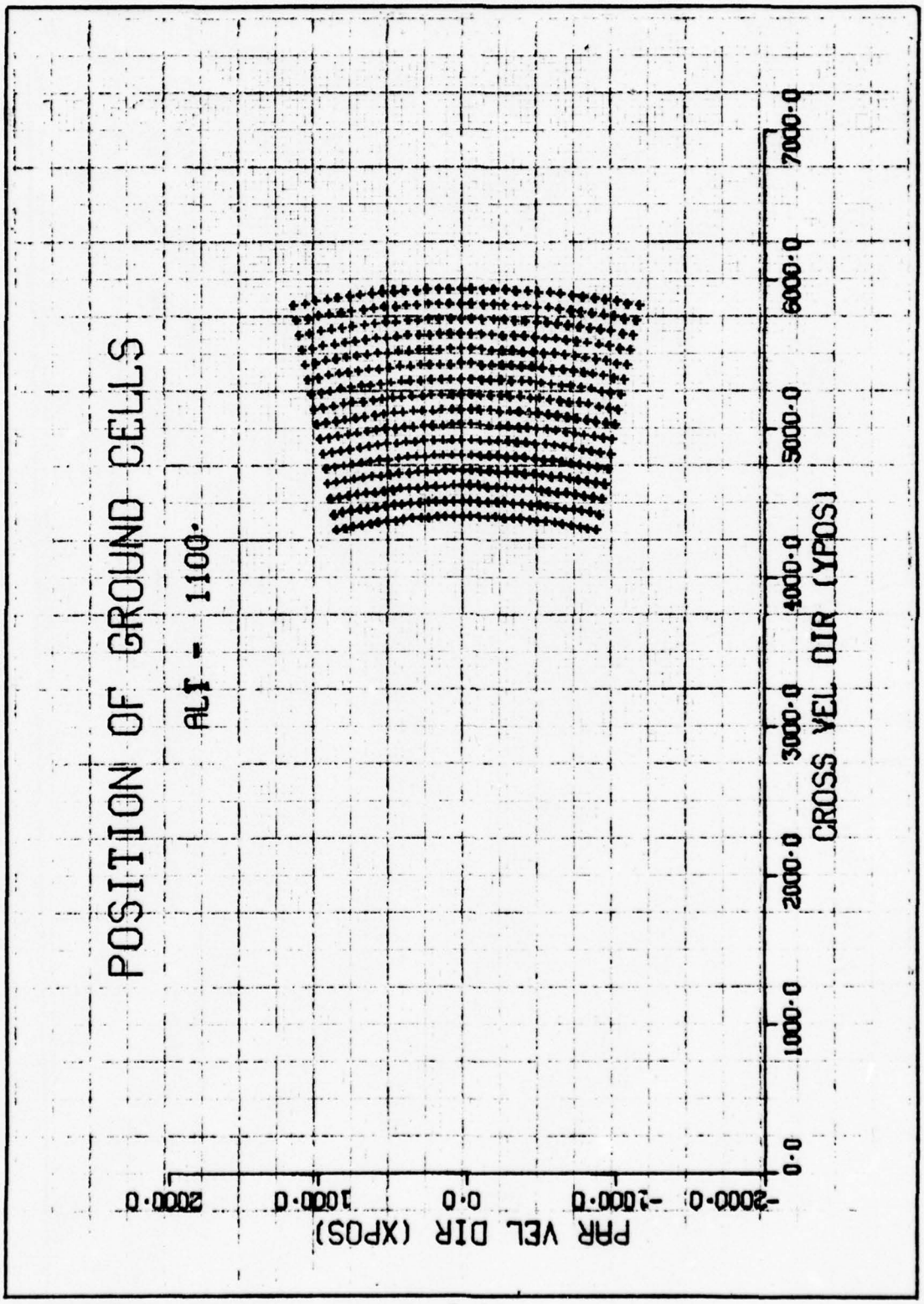

Figure 8-15 Surface Cells at 1100 Foot Altitude

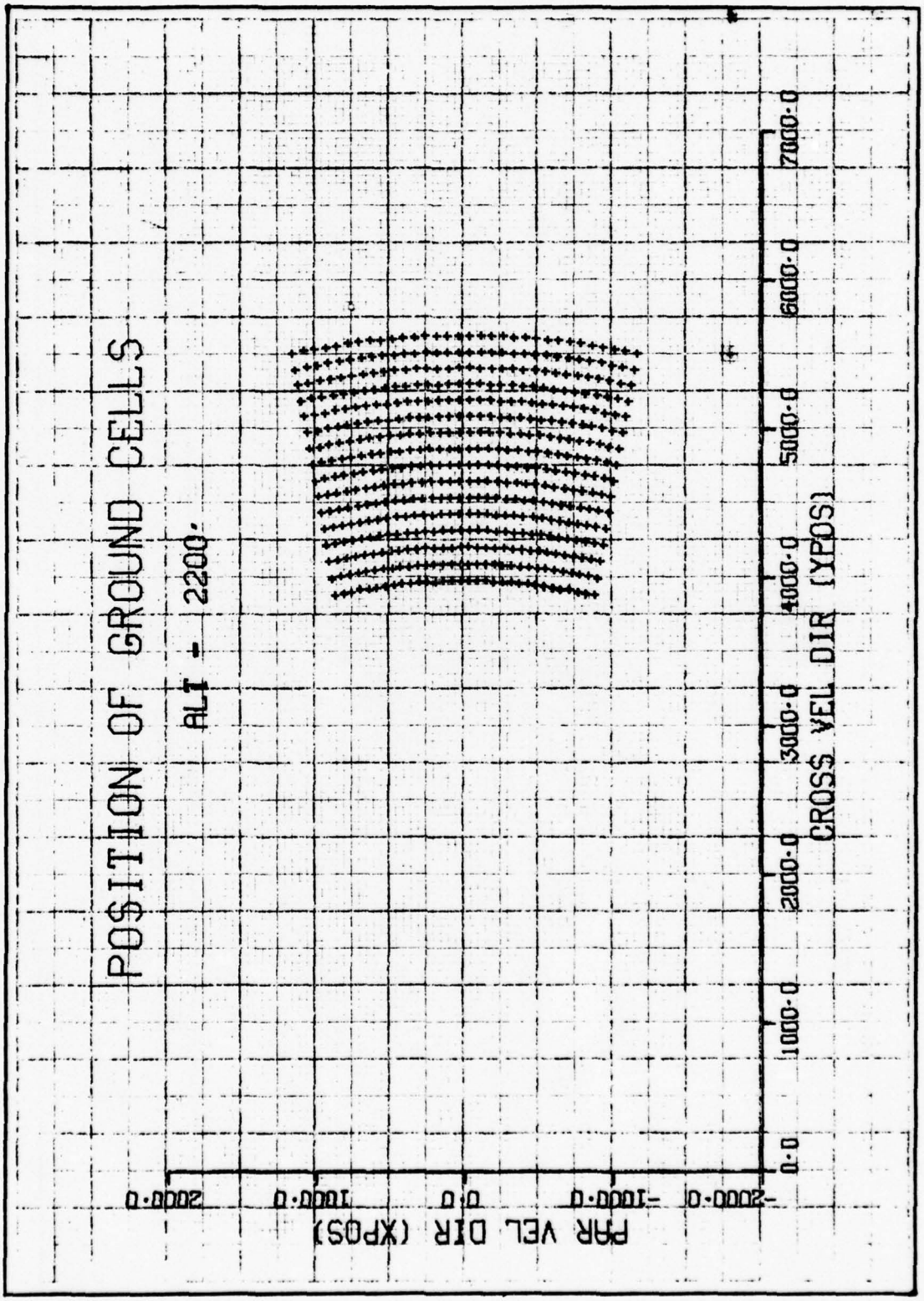

Figure 8-16 Surface Cells at 2200 Foot Altitude

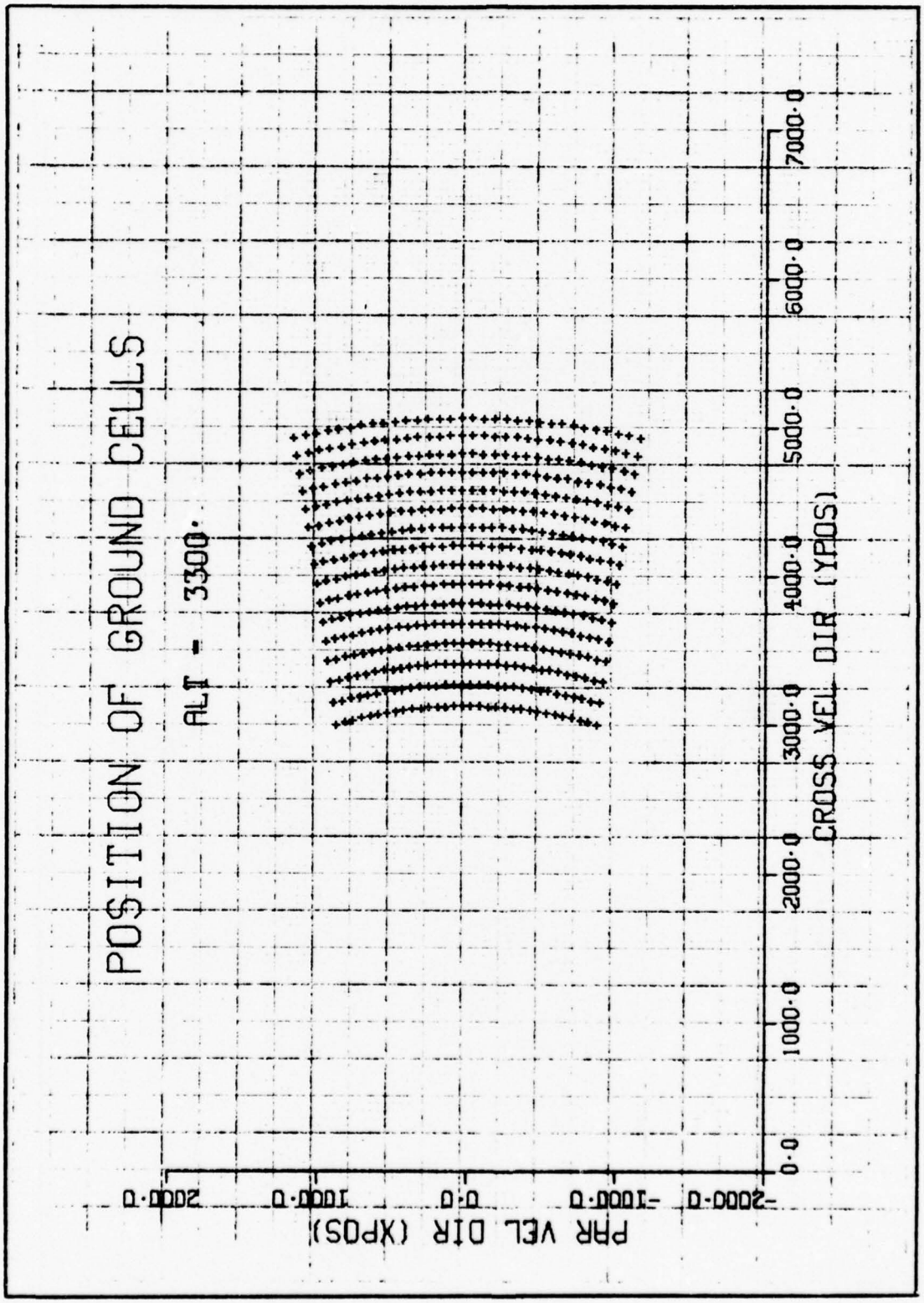

Figure 8-17 Surface Cells at 3300 Foot Altitude

The time separation of each 16 X 32 (range X doppler) map was approximately 0.009 second. At an aircraft velocity of 420ft/sec the aircraft traveled a little less than 4 feet between maps. Since the maps were about 2000 feet long in the flight direction the coverage was highly overlapped as illustrated in Figure 8-18. The data from each run can be thought of as an approximately rectangular parallelepiped with a base of 16 X 32 cells (1600 X 2000 ft), height of 300 seconds (33000 maps) and skewed approximately 20 miles (1750 cells). Size and resolution of these cells is shown in Volume III, Appendix A.

Much of the data reduction involved performing operation within this data space. Hit maps involved projections on the X, Y plane. Hits/time maps and mean maps are projections of data on the Y, t plane.

Histogram analysis slices the data into smaller parallelepipeds by slicing in time and by range gate. The initial data reduction step handled one range/time slice at a time and recorded this information for further analyses.

8.7 Recorded Data and Format

Data collected during the clutter runs was recorded in-flight by an on-board seven channel analog magnetic tape recorder. Frequency multiplexing was used on each of the seven channels or tracks. The track and subcarrier frequency allocations and the recorder data is summarized in Table 8-5.

Information in range gates 1 through 16 is the clutter data gathered during each run as well as the noise level and calibration before and after each run. The other channels and subcarriers recorded auxiliary data such as IRIG time. PAM parameters included calibrate enable, camera enable, VCXO offset, gain setting, radiate enable and radar status.

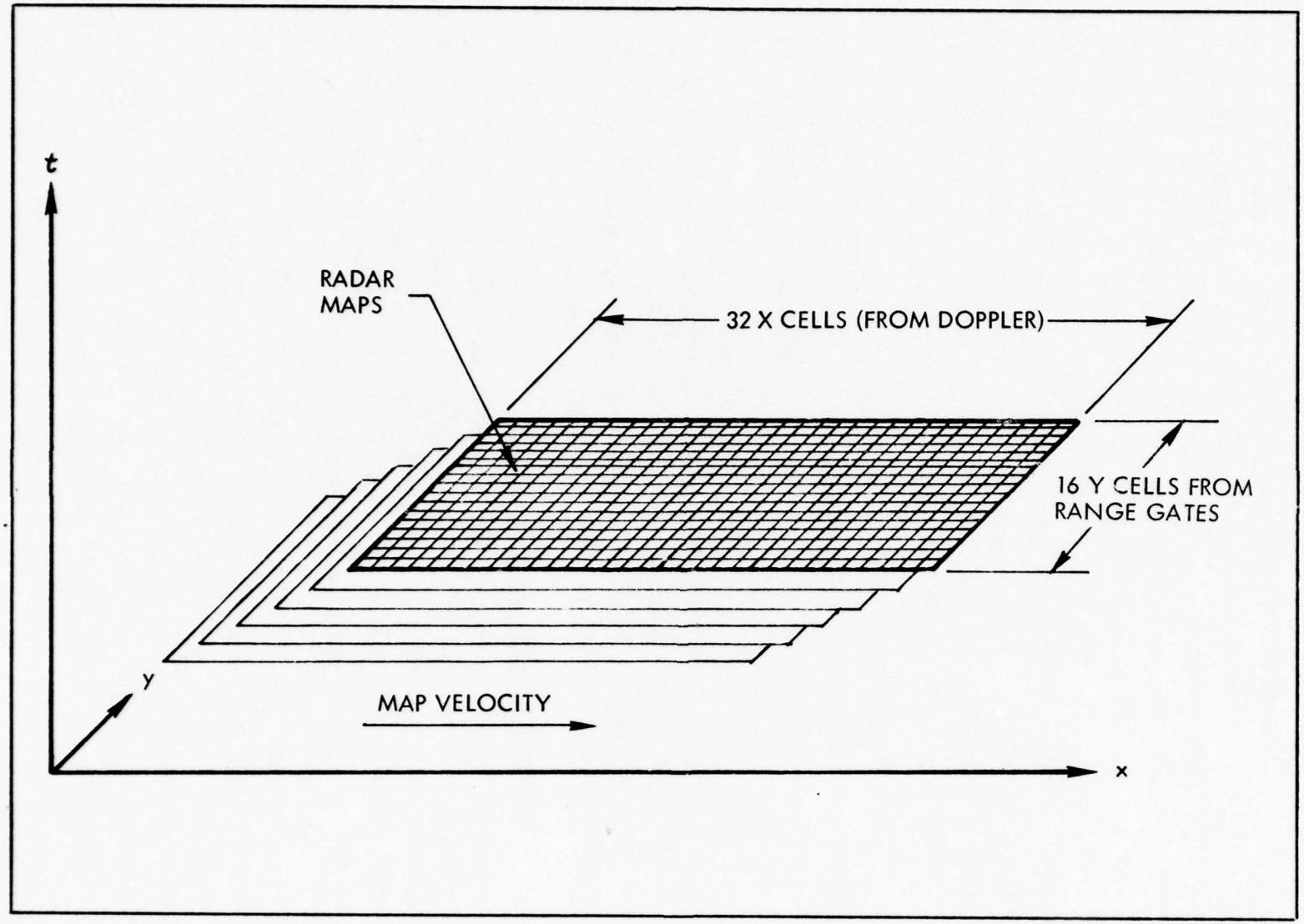

Figure 8-18 Basic Data Set

TABLE 8-5
SUBCARRIER FREQUENCY

TRACK	AUDIO/VIDEO	70KHz ±15%	124KHz ±15%	165KHz ±7.5%	240KHz ±15%	455KHz ±40%
1	None	Scan Sync	None	None	None	PAM
2	None	Doppler Error	None	None	None	None
3	None	Spare	None	None	None	None
4	IRIG Time	Range Gate #1	Range Gate #2	Range Gate #3	Range Gate #4	None
5	ICS Audio	Range Gate #5	Range Gate #6	Range Gate #7	Range Gate #8	None
6	Δ_{fi}	Range Gate #9	Range Gate #10	Range Gate #11	Range Gate #12	None
7	Δ_{fq}	Range Gate #13	Range Gate #14	Range Gate #15	Range Gate #16	None

8.8 Data Reduction

Data reduction was a stage in the processing of data from the raw radar returns into final analysis outputs. It is distinguished by the facility and equipment utilized more than by strong conceptual differences.

The data for all range gates was collected simultaneously. The data reduction function, however, required processing the clutter data one range at a time. The sequential processing of the recorded radar signals (one range gate at a time) must be kept in mind to understand some of the material that follows.

Data reduction was accomplished in the Raytheon Telemetry facility. Those data manipulation tasks best able to be accomplished within the telemetry facility were done under the data reduction task. Those tasks better done with the CDC-6700 were done under the heading of data analysis.

8.8.1 Equipment Set-Up for Data Reduction

Data reduction in terms of equipment is diagrammed in Figure 8-19. Analog tapes recorded in flight were played back and decoded. The clutter data was played back one range gate at a time at half the recorded speed. Each range gate was picked sequentially by selection of tape track and central frequency of the tunable discriminator. The output of the discriminator corresponded to the raw radar data for the selected range gate. The gain was set on this signal to best use the dynamic range of the equipment. Finally, the signal from the attenuator was sampled at 7kHz (corresponding to a real time sampling of 14kHz) and converted to a digital word.

The digital words were then processed by the Raytheon 706 computer with an Array Transform Processor (ATP) to create digital data tapes. Line printer outputs were also

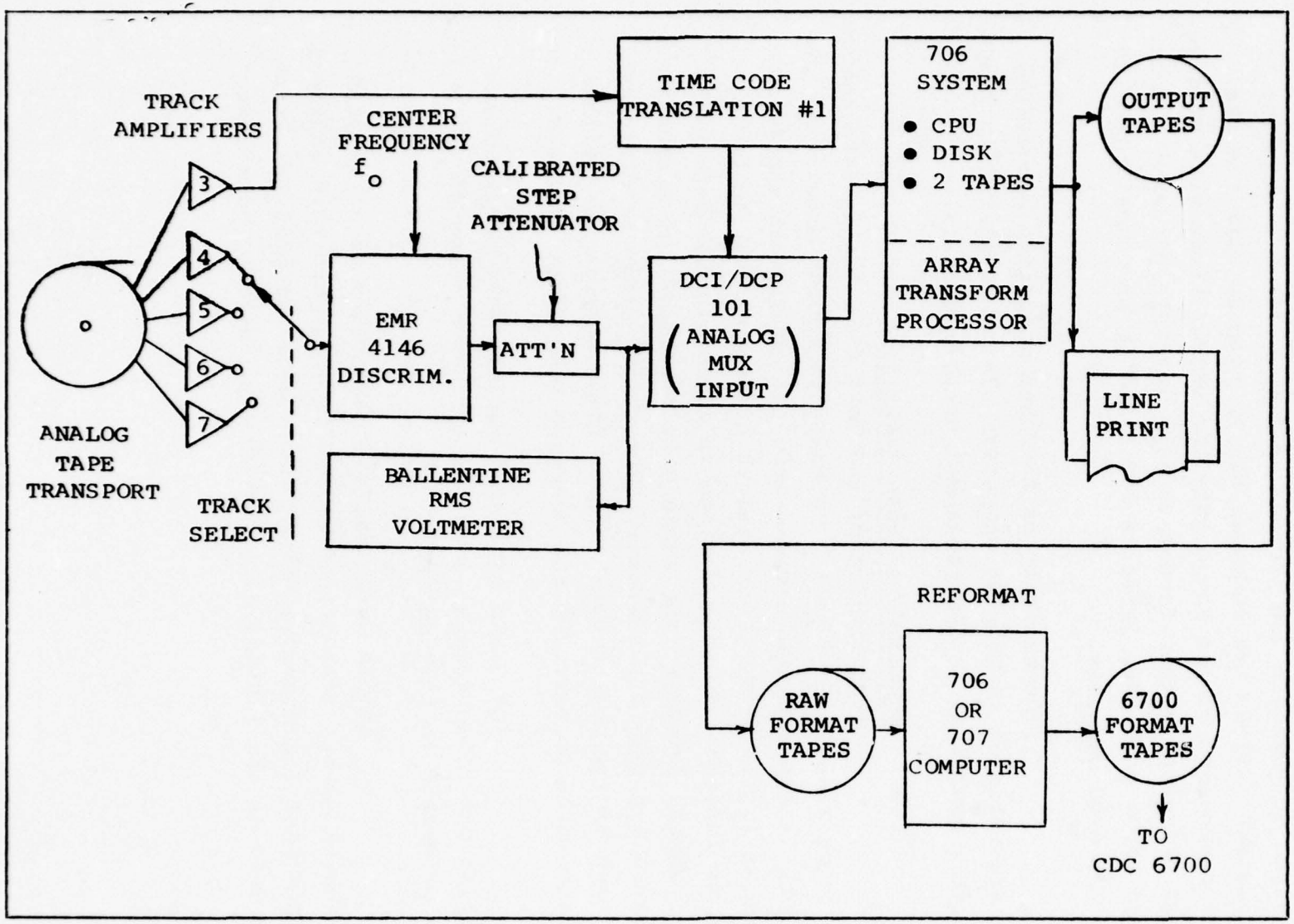

Figure 8-19 Data Reduction Equipment Set Up

obtained to validate the processing and obtain reformatting parameters. Since the computer had to keep up with the real time processing of the range gate, the output tapes were written in an efficient output format to save valuable processing time. These tapes were then later re-formatted to be compatible with the CDC 6700 computer.

The majority of the data reduction processing was accomplished in the 706 computer. This processing is functionally described in the remainder of this section.

8.8.2 Breakdown of Data Reduction

Manipulation of the data done during data reduction is rather complex in detail. In order to better understand the process it has been sub-divided into two conceptual stages as shown in Figure 8-20. These stages are sequential in terms of data processing. The first stage is common to all data paths. This process developed the range gate stripe of the synthetic aperture map from the raw data. The second stage is different for each of the output data tapes. These outputs were either selected data or selected raw measures taken from the data.

The "full data set" outputs were obtained in parallel one range gate at a time. All range gates of valid data were processed in this manner.

Sample data analysis required a separate pass through the data. All of the sample data outputs were obtained in this pass since only a single range gate was used to obtain this data as the limited data provides an adequate data base.

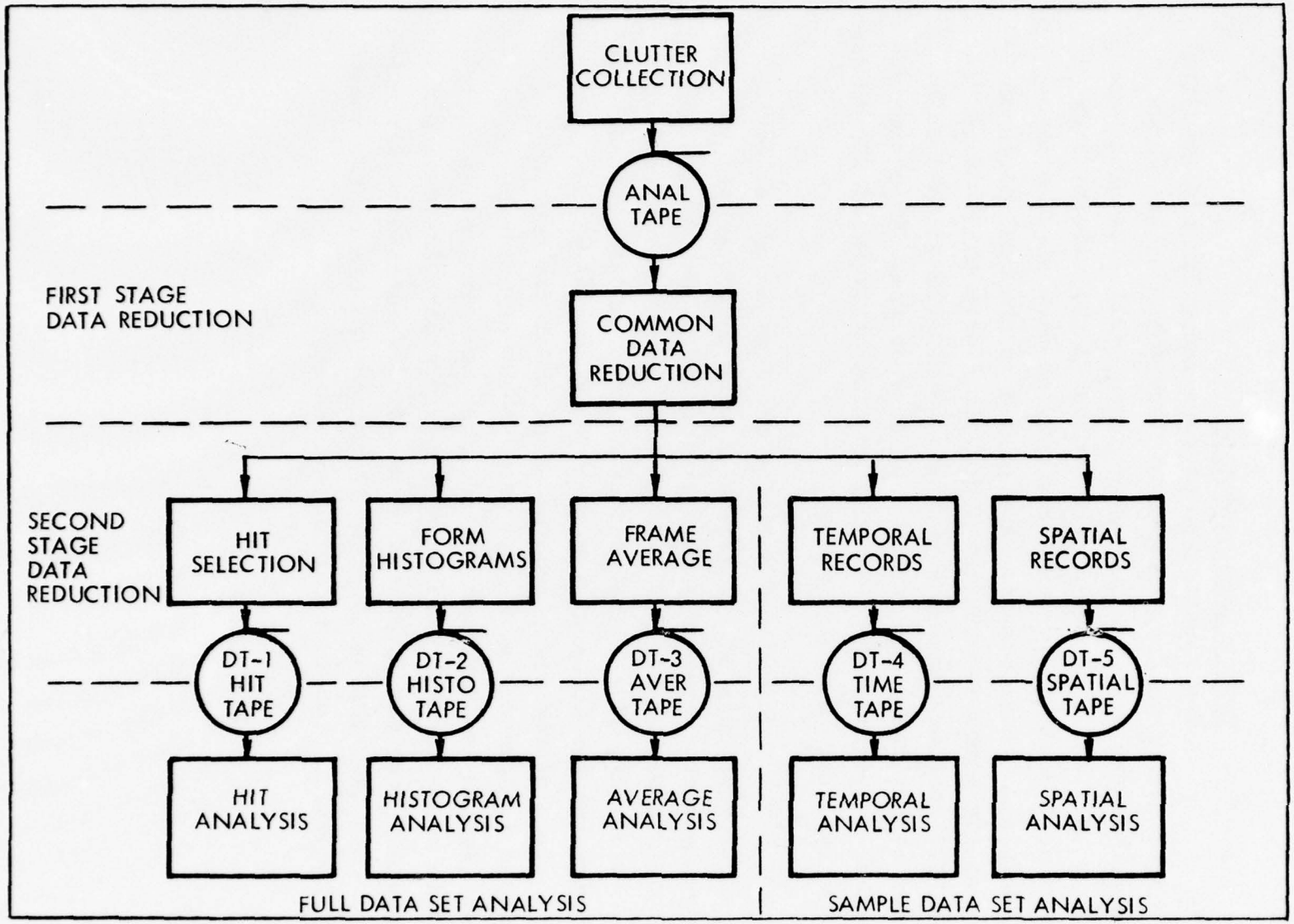

Figure 8-20 Analysis Path Breakdown

UNCLASSIFIED

8.8.3 Common Data Reduction

The first stage of data reduction resolved the raw radar data into doppler dwells. Estimates of the known bias terms were also removed (see Figure 8-21). Samples were first converted to 10 bit digital words at the rate of 7kHz (14kHz real data time). Next the samples were blocked into 128 samples. These samples were placed in the real parts of 128 complex words and the imaginary parts were set to zero. These 128 complex numbers were than fourier transformed using an FFT technique to obtain the complex spectrum. This spectrum was then converted into the power spectrum by summing the squares of the real and imaginary parts.

Thirty-two cells of the output were selected for further processing. These cells were then weighted to remove best estimates of known gain biases. Each of the thirty-two outputs was multiplied by a number obtained from estimates of doppler bias of the antenna, range gate, radar altitude, geometry and the spectral effects of the data samples. A complete description of the weighting functions and their development is found in Appendix A, Volume III. Data weighting based on known factors was used for two reasons; to maximize the use of dynamic range for the clutter,and to compensate the data before histograms were developed to avoid adding returns with different gains into the same histograms. A terse synopsis of the common data reduction process is given in Table 8-6.

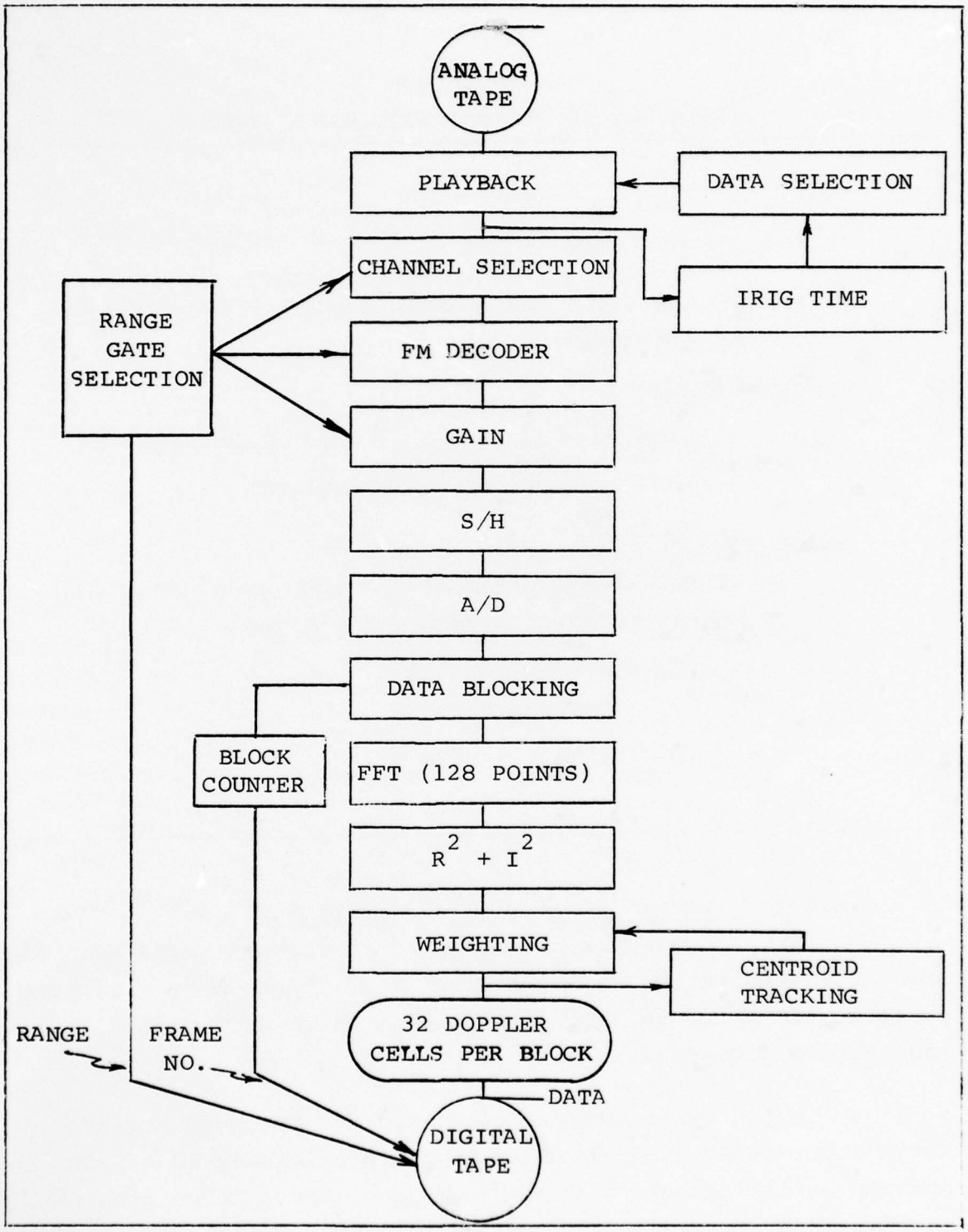

Figure 8-21 Data Reduction Common Processing

TABLE 8-6

TAGSEA PRE-PROCESSING ROUTINES - SUMMARY

FFT

- INPUT - TIME POINTS
  - 128 I @ 7 KHZ SAMPLE, 10 BIT (RECT. WINDOW)
  - 128 Q SET TO "0"
- OUTPUT
  - 128 SQUARE MAGNITUDE $I^2 + Q^2$ (AMBIGUOUS)
  - SELECT 32 OUT OF 64 UNAMBIGUOUS

NORMALIZED-WEIGHT

- 32 POINTS/FFT CENTERED @ 2 KHZ (4KHZ REAL TIME)
- COMPOSITE ARRAY MULTIPLY TABLE FOR:
  - NORMALIZE, $1/R^4$
  - ANTENNA PATTERN
  - OTHERS AS REQ'D

8.8.4 Second Stage Hit Data Reduction

The objective of hit data reduction and analysis was the investigation of large hits (i.e., those most likely to cause system problems, and false alarms in radar detection and acquisition processes.)

Second stage data reduction recorded all hits above a pre-chosen threshold (set at approximately 10^{-3} probability on the detection curve). Each of these large hits was registered by recording the power level of the return, range gate of the return, doppler cell of the return, and time of the

return (frame number). (See Figure 8-22). In order to better pack the data on the digital tape the time was recorded as the change in FFT frame number since the last hit. These changes in frame number were accumulated in data analysis to obtain the absolute frame number (time from the beginning of the run).

The result of this segment of the total data reduction process was a digital tape (DT-1, Hit Tape) on which was recorded each return within one resolution cell which had an amplitude greater than the threshold together with its (relative) location in space and time.

8.8.5 Second Stage Histogram Data Reduction

Second stage histogram processing created histograms of blocks of data. A block consists of 600 FFTs each contributing 32 data points for a total of 19200 data points. Each of these points was sorted into a 1024 size array by using the amplitude as the address to be stored in the array. A flow diagram of this process is found as Figure 8-23.

This process produced a large data base since the sample rate was 14kHz and 128 samples were used for each FFT. Thus an FFT frame represented 128 samples divided by 14,000 samples/sec or 0.009 second. Six hundred of these frames represents a time sample of 600 times 0.009 second or approximately 5.4 seconds. Since a run collected about 5 minutes or 300 seconds of data, approximately 50 histograms were created for each range gate on each run. With 16 range gates this yeilded approximately 800 histogram per run.

The source data for each histogram is portrayed in Figure 8-24 for a typical run. Note that histograms were also collected for noise and CW calibration periods of the run. Each square in this histogram matrix is an array of 1024 numbers based on 19,200 data samples. This information was recorded in digital form on DT-2, Histogram Tape.

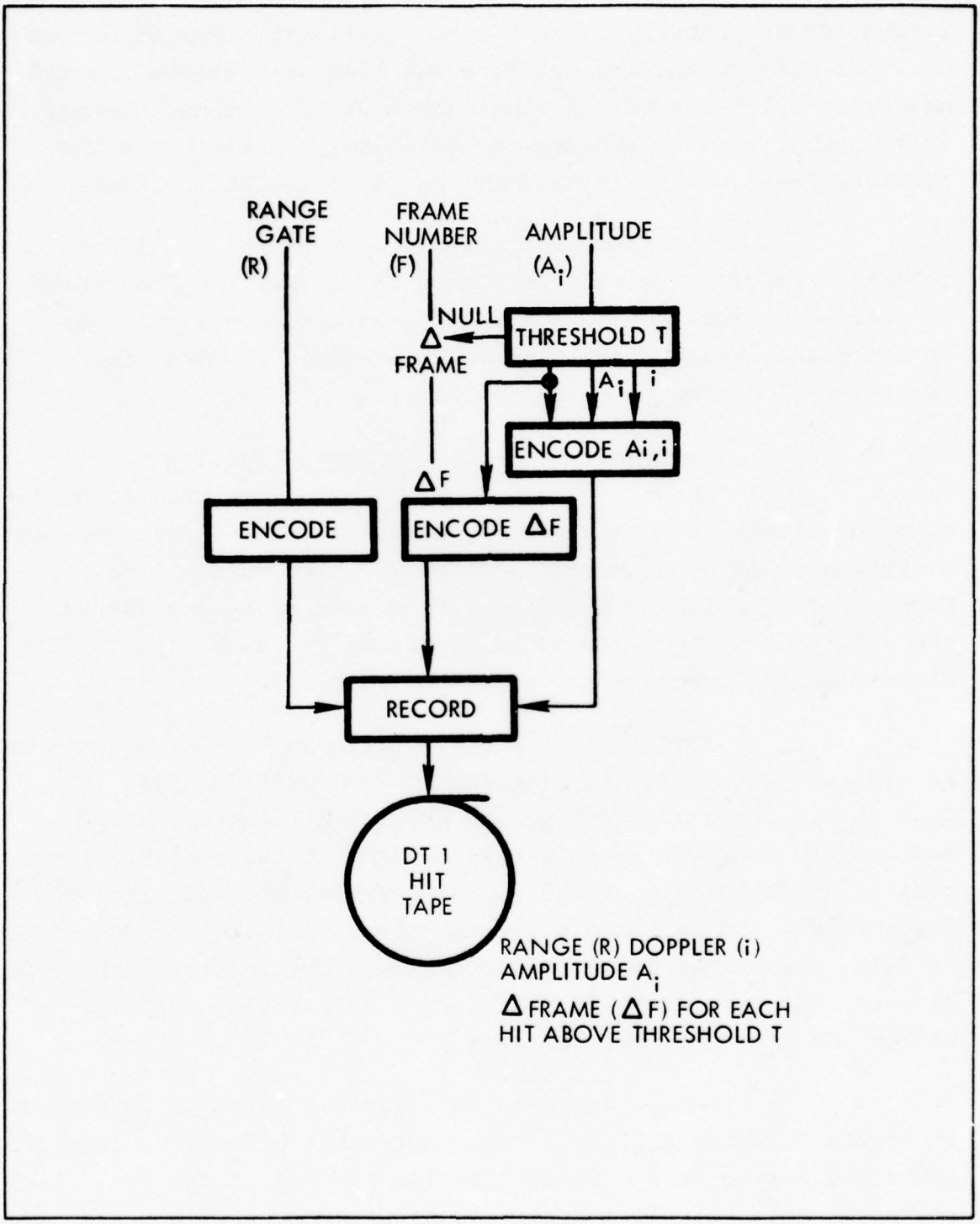

Figure 8-22 Second Stage Hit Data Reduction

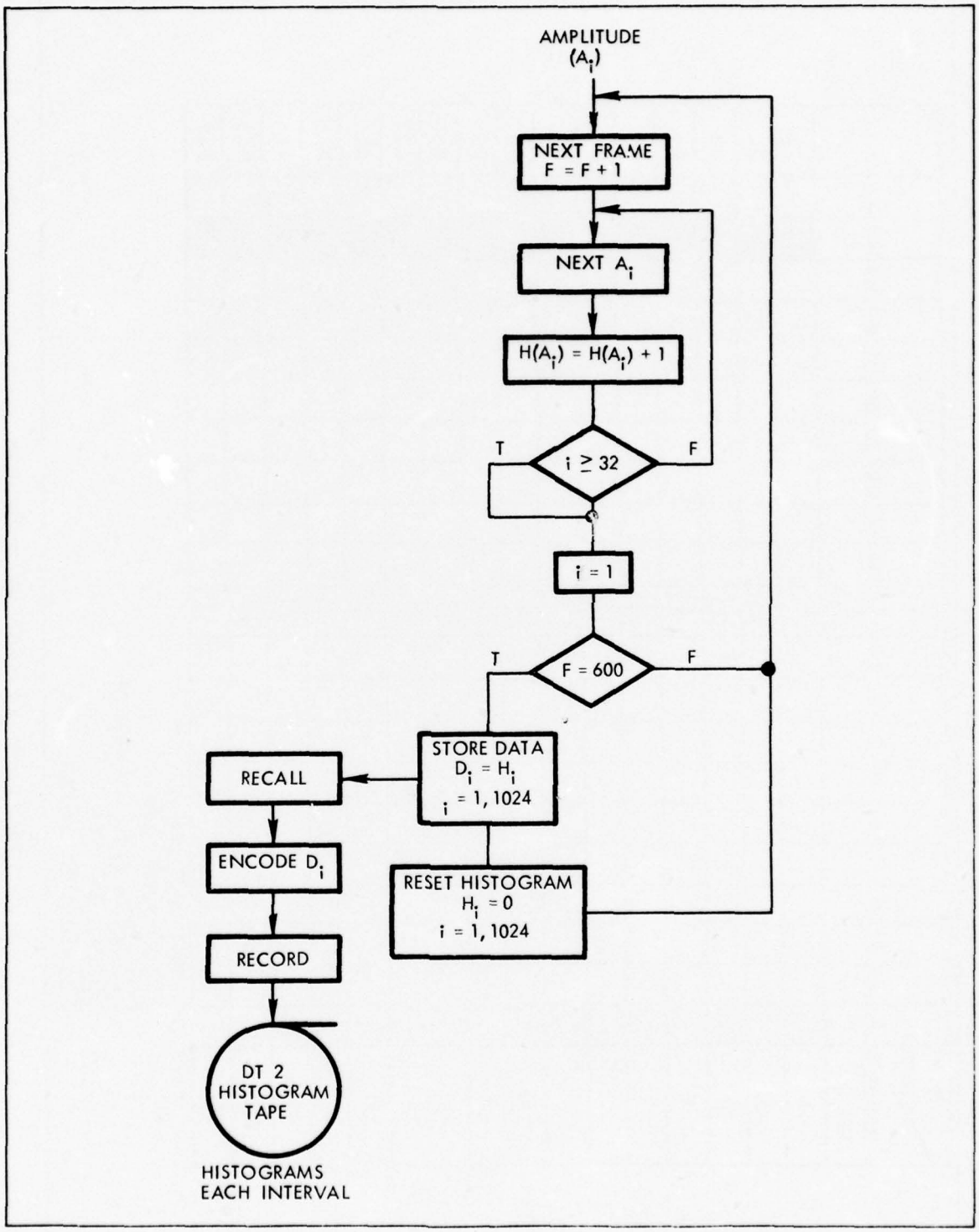

Figure 8-23 Second Stage Histogram Data Reduction

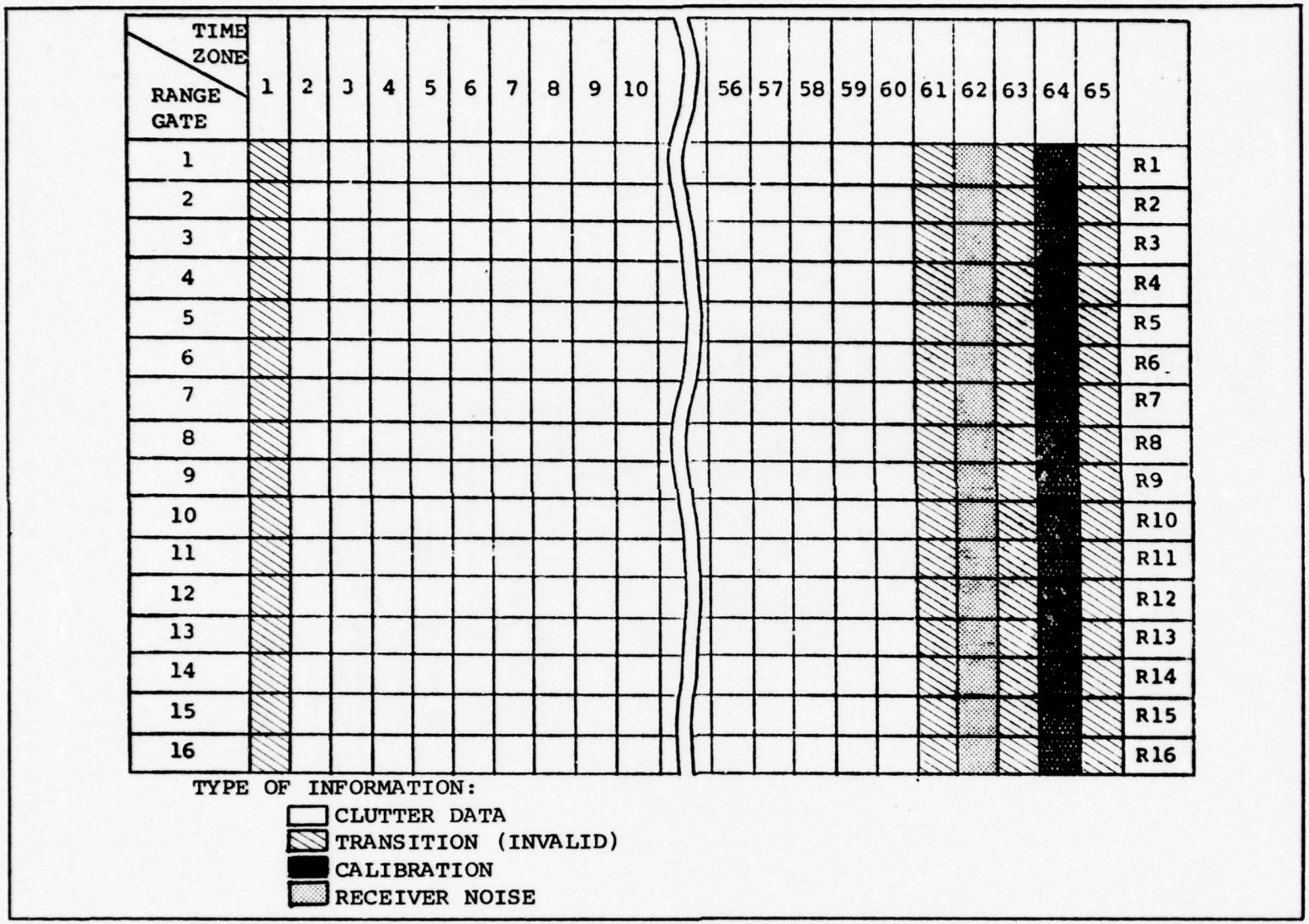

Figure 8-24 Histogram Matrix

8.8.6 Second Stage Mean Data Reduction

Second stage data reduction of the mean data is quite simple. The 32 weighted returns from each FFT were summed to obtain a single number (see Figure 8-25) and these numbers were recorded as the mean data.

Each range gate yielded approximately 30,000 mean numbers for a total of approximately 500,000 frame means per run. In practice the mean and histogram data were combined on a single tape for transfer to data analysis.

8.8.7 Second Stage Data Reduction-Spatial/Temporal Analysis

For spatial and temporal analysis the second stage of data reduction was simply a process of selecting appropriate data from a single range gate. The data available from a range gate is portrayed in Figure 8-26. This data set is a constant range slice of the data base. Three types of data were selected for spatial/temporal analysis; Spatial Data, Radar Temporal Data, and Surface Temporal Data.

For spatial analysis entire frames of 32 FFT cells were written onto tape. The frames were time separated to avoid correlation between the frames. The 32 doppler cells were the largest spatial extent of data at any one time. In terms of the diagram of Figure 8-26 regularly spaced horizontal rows of data were extracted for spatial analysis.

For Radar Temporal Analysis the data in a prechosen doppler cell was selected from each frame. In terms of the diagram of Figure 8-26 radar temporal data is a vertical column of data.

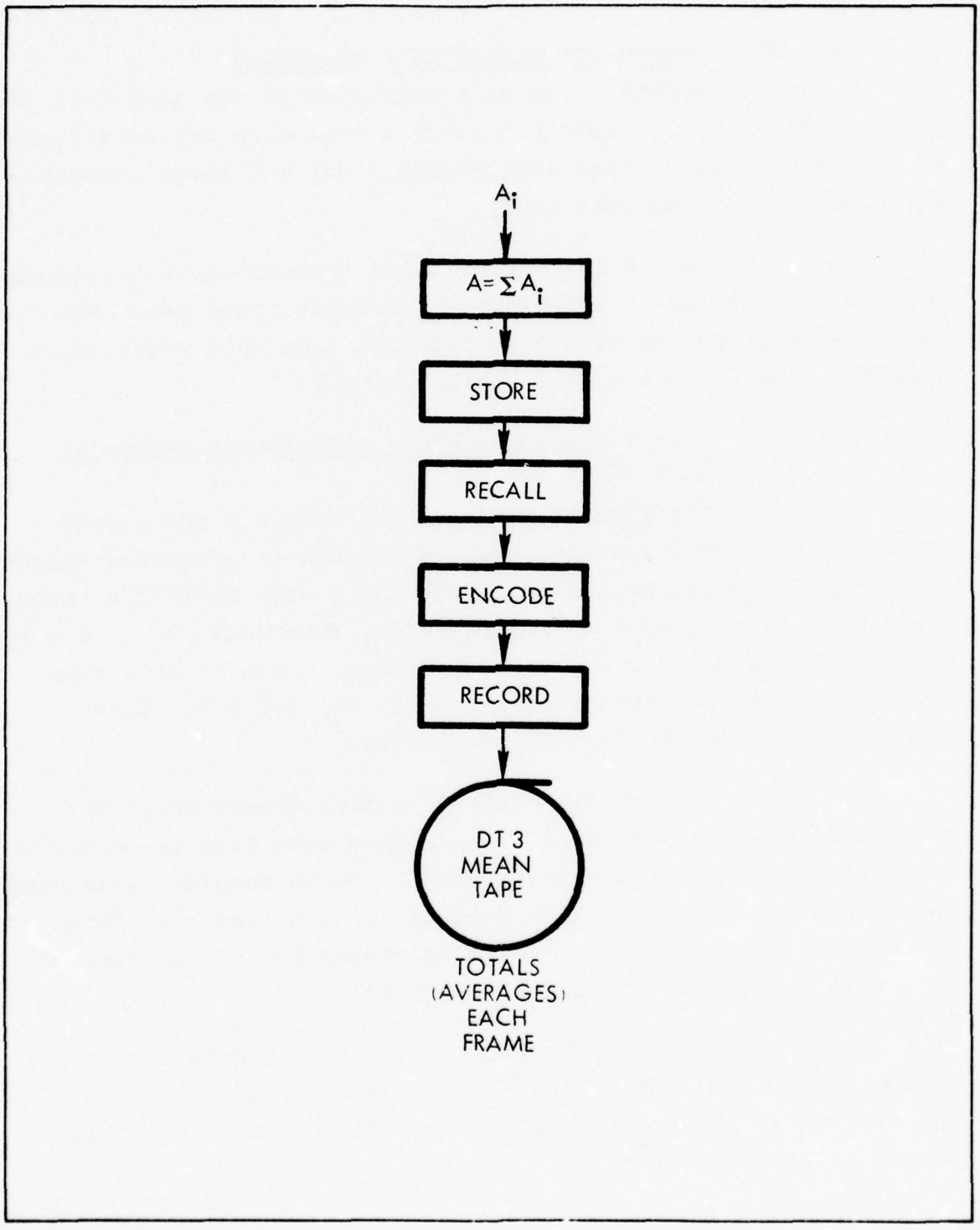

Figure 8-25 Second Stage Mean Data Reduction

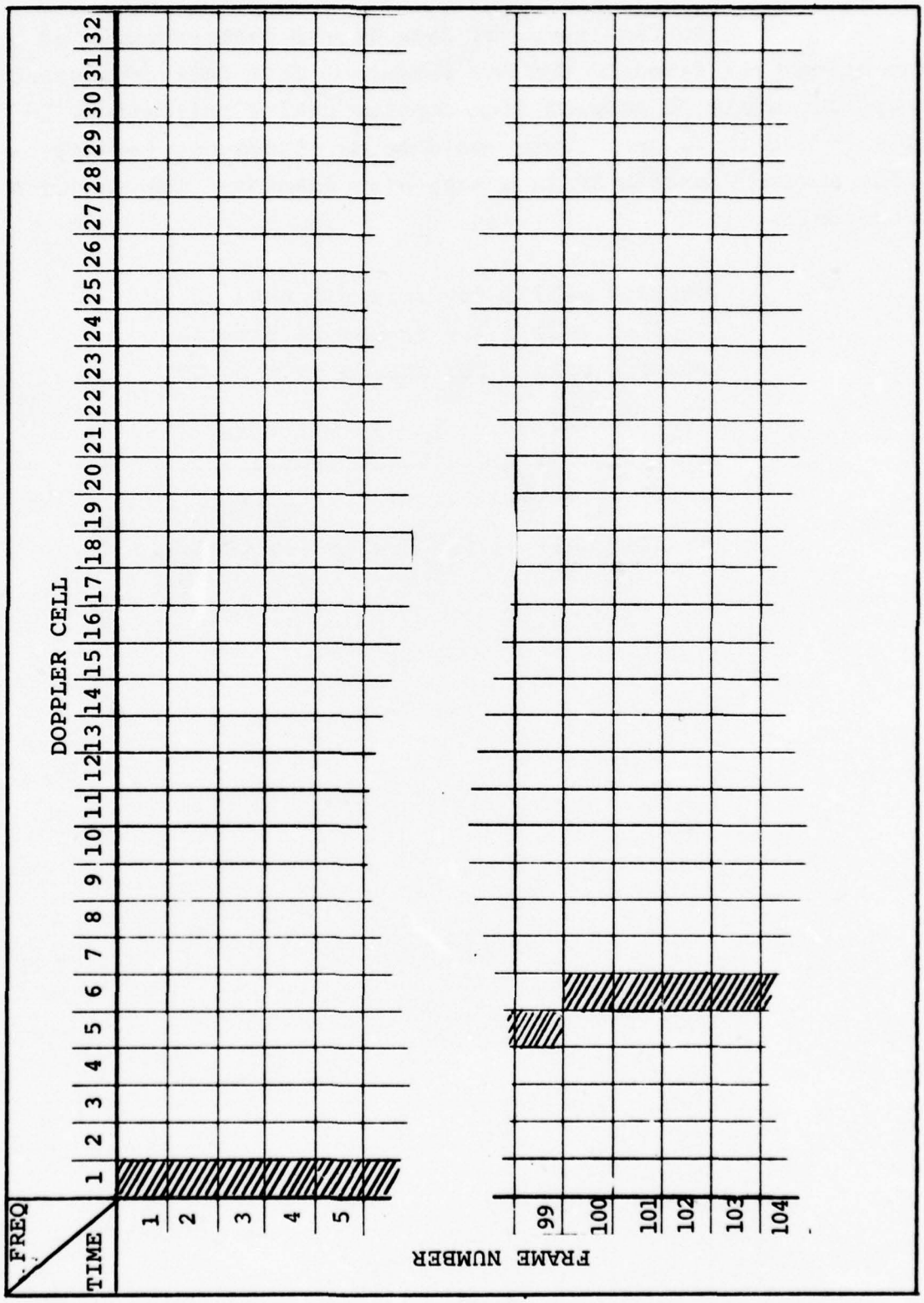

Figure 8-26 Data Base for a Range Gate

Surface temporal data is the best estimate of a resolution cell fixed on the sea surface. This data consisted of approximately 20 samples from doppler cell 1 bollowed by 20 cells from cell 2, etc. This would be an elongated diagonal stripe across Figure 8-26 in a step-wise fashion. The sequence is nominally:

Doppler cell 1 for frames 1 thru 20,
Doppler cell 2 for frames 21 thru 40,
Doppler cell 3 for frames 41 thru 60,

.....
.....
.....

Doppler cell 32 for frames 620 thru 640

8.9 Reduced Data Transfer and Formats

Reduced data was prepared for further analysis by formating for CDC 6700 processing on seven track digital tape in one of two formats; Histogram tape, or Hit tape. Each tape had the same header information format before the data for each run. This header in ASCI-II form contained information on flight number and date, run number, start IRIG time and end IRIG time, tape ID (Histogram/Hit-Temporal/Spatial), range gate number used for gain setting, altitude code, and weighting matrix offset.

The Histogram magnetic tapes for use on the CDC 6700 had the following formats:

(1) The first record on each Histogram data tape contained Header Information in ASCI-II format packed into 12 CDC words (60 Bits per word).

(2) Each following HISTOGRAM RECORD consisted of 1630, 16 bit Ray 706 words which were mapped into 489 60-bit CDC 6700 words. Each 16 bit Ray 706 word was packed onto 7-track magnetic tape in an 18 bit format as illustrated in Figure 8-27.

The information format contained on the HISTOGRAM tape is defined in Figure 8-28. A string of "ones" after (A) and (C) and a string of "zeros" after (B) in Figure 8-28 were used as flags.

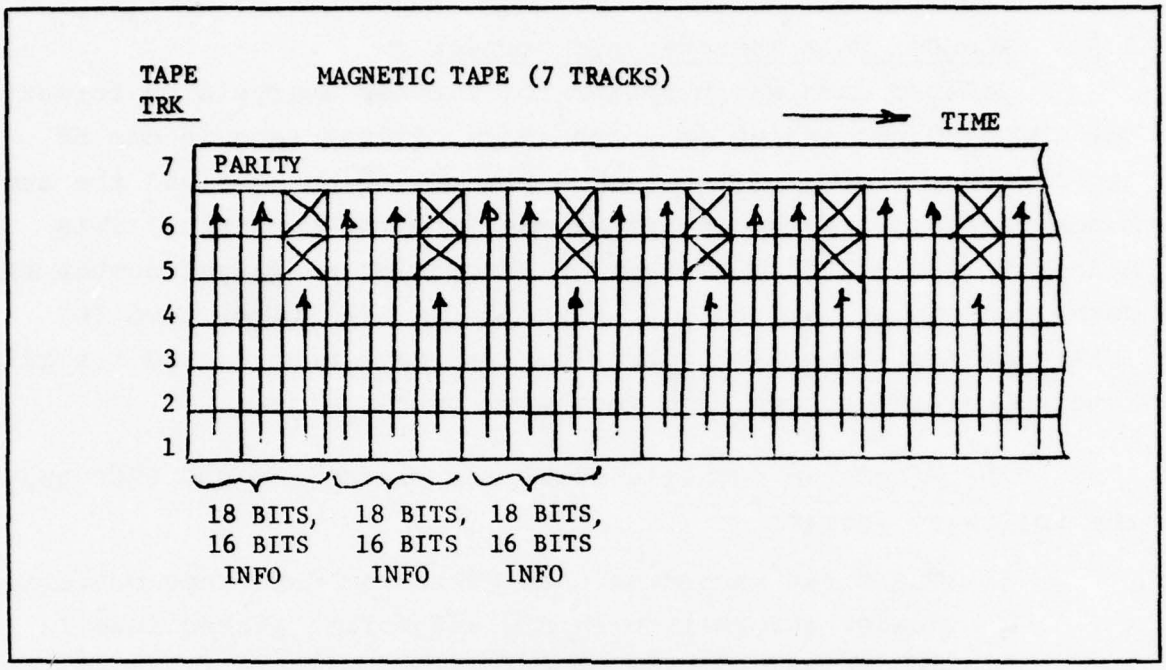

Figure 8-27 Histogram Format

The Hit tapes had the following format:

(a) ASCI-II Header same as HISTOGRAM tape except tape label to read "HIT DATA"

(b) Data = 2560, 12-bit words 120 bits reserved for header on each 2560 bit record. (2560/5 = 512, 60 bit words).

(c) Each data word contained three items per bit.

1. Error Flag(1 bit). If "Zero" format as follows:
2. Δ FRAME NO. = frame number since last hit was recorded 8 bits (0-255)
3. doppler cell no. 6 bits (0-63)
4. power amplitude (30dB range) 10 bits(0-1023)

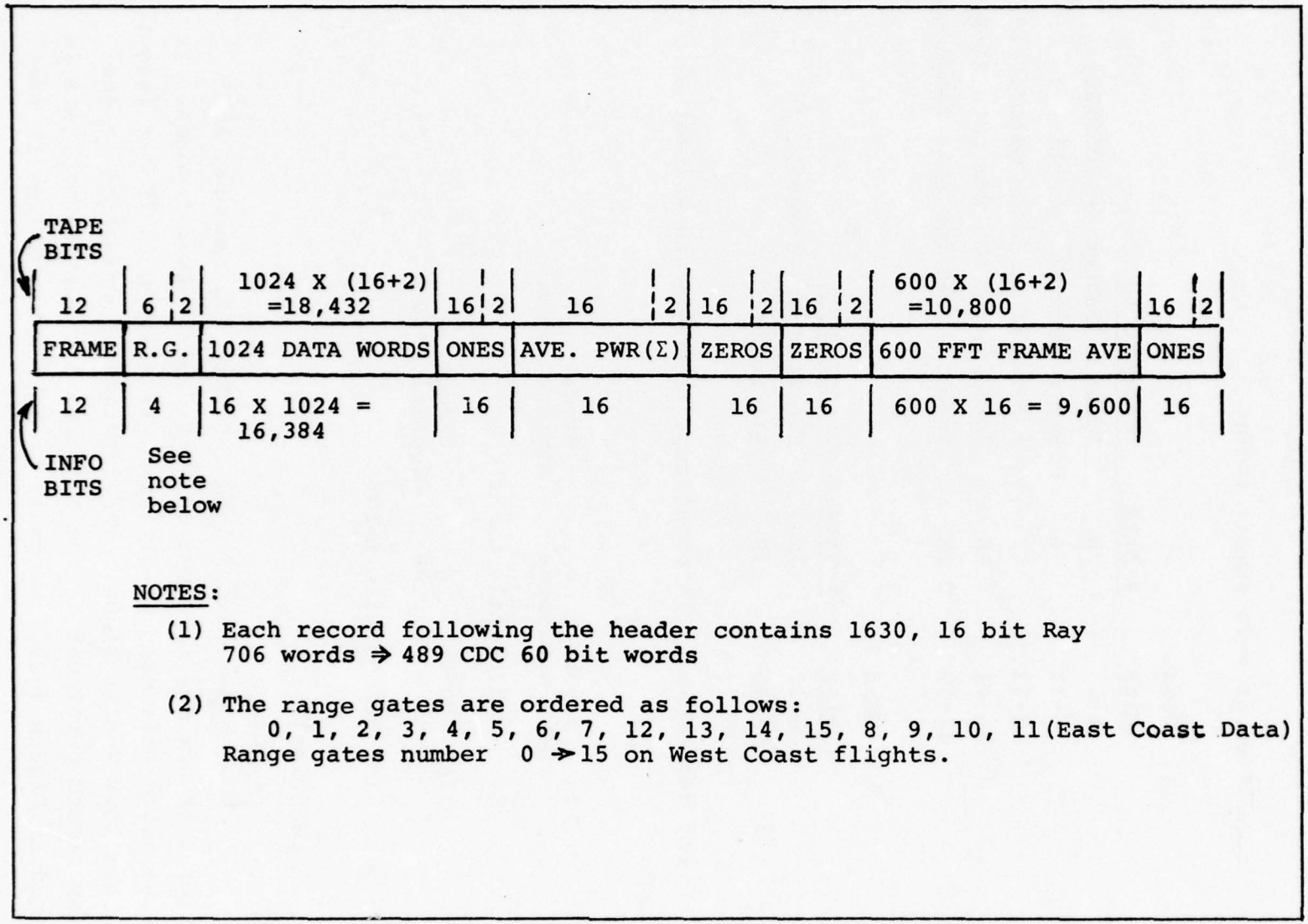

NOTES:

(1) Each record following the header contains 1630, 16 bit Ray 706 words ⇒ 489 CDC 60 bit words

(2) The range gates are ordered as follows:
0, 1, 2, 3, 4, 5, 6, 7, 12, 13, 14, 15, 8, 9, 10, 11(East Coast Data)
Range gates number 0 →15 on West Coast flights.

Figure 8-28 Data Format for Histogram Tape Information

UNCLASSIFIED

HEADER words = 2, 60-bit words

(a) Word 1

Bits	# Bits	Description
0-5	6	Record counter (MODULO128)
6-11	6	Range Gate No. (0-31)
12-23	12	# Records in Range Gate (1-4096)
24-41	18	Total frame no. for gate (1-N)
42-59	18	Last Δ frame for this range gate

(b) Word 2

Bits	# Bits	Description
0-11	12	Hit counter (1-4096)
12-59	48	All zeros

For each Spatial/Temporal run, the data was written as follows:

1. Record Header
   Next N-Records Temporal Data
2. End-of-file marks
   (a) Record Header
   Next M-Records Spatial Data
   (b) End-of-file marks

Specifically:

Header

The header record used for both the temporal and spatial data was the same and consisted of 54 16-bit words. It must be noted that each 16-bit word was written in 18-bit format with the last 2-bits blank. The information contained in the header record pertinent to the temporal and spatial analysis is defined in Figure 8-29. Words 15 to 54 contain Hollerith text.

WORD	BITS 0 1 2 3	4 5 6 7	8 9 10 11	12 13 14 15	COMMENTS
1	1 1 0 0	1 0 0 0	1 0 1 0	0 0 0 0	144240_8 = Hollerith "H"
2	← — DELTA FRAME FOR SPATIAL DATA — — — — →				
3	← — — RANGE GATE USED — — — — — — — — — — →				Range gate from which data is gleaned
4	← — — ALTITUDE CODE — — — — — — — — — — — →				
5	← — — FIXED CELL NUMBER FOR TEMPORAL DATA — — →				
6	NOT USED	FLIGHT (BCD)	FLIGHT (BCD)	RUN(BCD)	
7	RUN(BCD)	RUN(BCD)	IRIG START 10'S HRS (BCD)	IRIG START HRS (BCD)	
8	IRIG START 10'S MIN'S (BCD)	IRIG START MIN'S (BCD)	IRIG START 10'S SECS (BCD)	IRIG START SECS (BCD)	

Figure 8-29 Temporal and Spatial Data Header Record

Temporal Data

The temporal data was written in logical records of 1440 16-bit words which correspond to 432 60-bit CDC words $\left[\frac{(1440)(16+2)}{60} = 432\right]$. Each logical record contained 360 4-word blocks where each block contained the following data:

(1) Snap back factor
(2) Variable cell number
(3) Variable cell power
(4) Fixed cell power

The snap back factor indicated how many sweeps were made through the 32 doppler cells for the variable cell. The variable cell number was the particular doppler cell being recorded at the time.

The variable cell power was the power in the ground fixed doppler cell and the fixed cell power was the power in the radar fixed doppler cell as indicated in the 5th word of the header.

The end of data was indicated by two consecutive words of all "ones".

Spatial Data

The spatial data was also written in logical records of 1440 16-bit words which corresponds to 432 60-bit CDC words. Each logical record contained 45 32-word blocks where each block contained the power in the 32 doppler cells.

The power in the 32 cells was recorded every "Delta frame" where delta frame is indicated by the second word of the header.

Again, the end of the data was indicated by two consecutive words of all "ones".

8.10 Data Analysis

Data analysis descriptions will be subdivided corresponding to the natural data flow. This follows directly from the data reduction description of histograms, hit, mean, spatial and temporal analyses. Histogram analysis deals with the statistical distribution of the data. Hit analysis is concerned with the relatively rare large clutter returns. Mean analysis is a detailed investigation of the average backscatter cross section. Spatial and temporal analyses simply extract the respective spectra and autocorrelation functions over space and time.

8.10.1 Histogram Analysis

First it is appropriate to introduce some notation simplifying the discussion of histogram processing. Then there will be a discussion of the data analysis procedures. Let the histograms (1024 arrays) be denoted by capital letter H and the element of the histogram by the corresponding lower case.

$$H = (h_K) \qquad K = 1, 2, 3, \ldots\ldots\ldots 1024$$

Let us denote the histogram for range gate i and time zone j by H_{ij}. Let the elements of this histogram be h_{ijK} $K = 1, \ldots. 1024$.

The sum of Histograms is defined by:

$S = P + H_{ij}$ as the histogram where P is any other histogram.

$$s_K = p_K + h_{ijK} \text{ for each } K \qquad K = 1, \ldots. 1024$$

i.e., we will sum histogram by summation of their letter elements.

Let us further denote the mean of a histogram B by $\bar{b}$ where:

$$\bar{b} = \sum_{K=1}^{1024} K_{bK}$$

and the normalized histogram by

$$\hat{B} = \frac{10}{\bar{b}} \cdot B = \left\{ \frac{10.b_K}{\bar{b}} \right\}$$

a normalized histogram is one scaled to have its mean at 10.

A. Analysis of Histograms

In the data reduction stage each range gate was broken up into blocks of 600 FFT's i.e., 19,200 points. Clutter data trailing noise records and calibration were also blocked in this way. Each of these blocks of data was then sorted into 1024 bins by amplitude. Each histogram transferred was an array of 1024 numbers listing the number of occurances of that class interval in the original 19,200 data samples and the total corresponded to a probability density function. A large number of histograms were transfered from data reduction for each run. The sequence of these on the tape is shown in Figure 8-30. Not all of the histograms contained useful clutter data as indicated by the shaded portions. Also start-up problems sometimes caused erroneous results in the first histogram in each range gate and such data was discarded. At the end of each range gate receiver noise and calibration were also recorded. When analyzing clutter these were also ignored along with transition histograms built by combining two types of data. An example of this is zone 61 of Figure 8-30.

The paperwork accompanying histogram tapes from data reduction indicated the location in time zones of various kinds of data. This facilitated the data analysis by processing the different types of histograms in different manners.

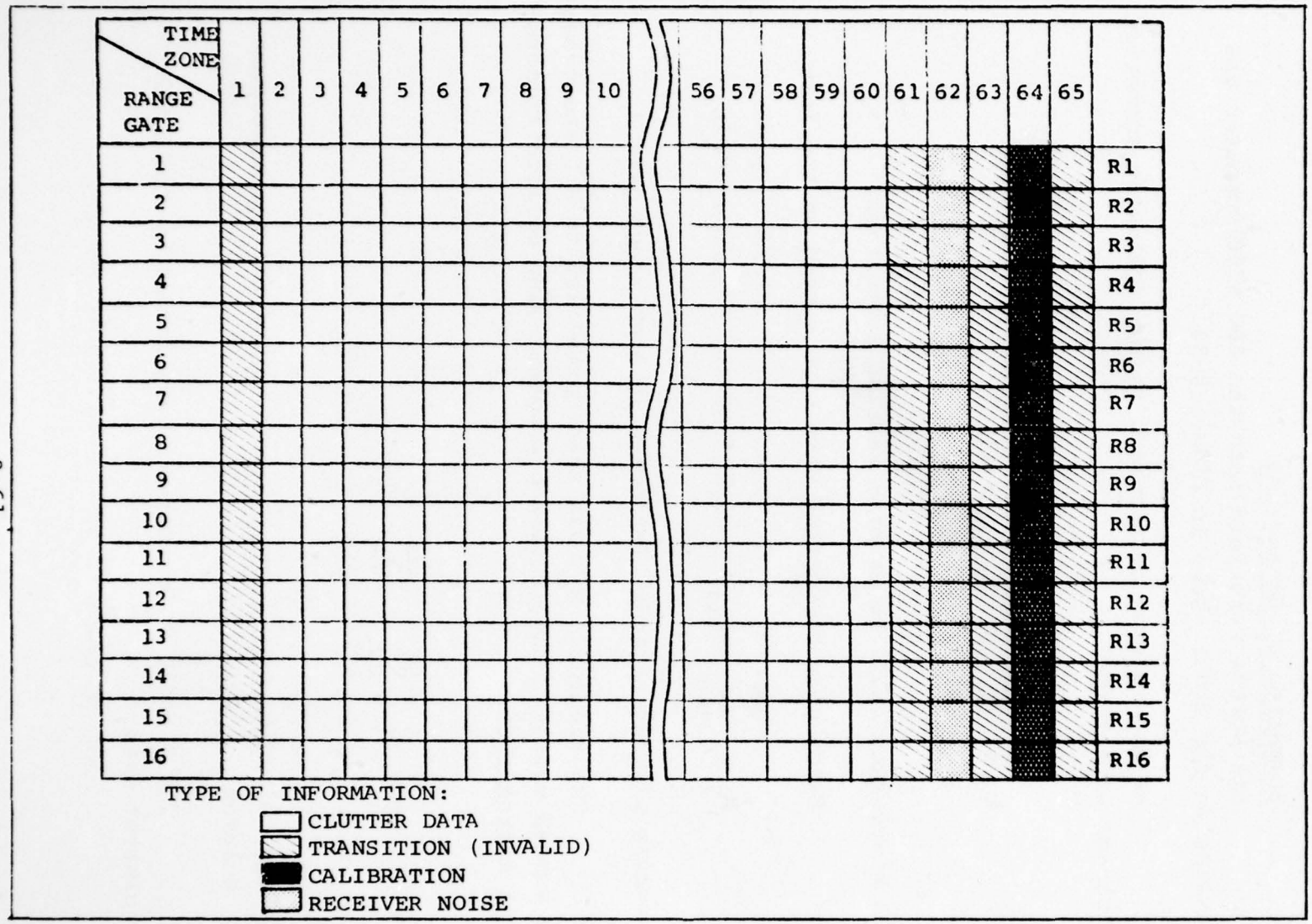

Figure 8-30 Contents of Histograms from Data Reduction for Typical Run

B. Summation of Histograms

Histograms were read into the CDC 6700 computer one at a time in the order shown in Figure 8-30.

As each histogram was read in the following summation histograms were formed.

$$T_j = \sum_{i-1}^{16} H_{ij} \qquad \text{for all } j$$

These histograms shall be denoted as time histograms.

Range gate histograms were also summed in the form

$$R_j = \sum_{j \epsilon c} H_{ij}$$

by summing all the clutter histograms in each range gate.

The histogram H_{ij} was then normalized to $\hat{H}_{ij}$ and these were summed over all the clutter histograms (sum of locally normalized histograms).

$$TOT_N = \sum_{i=1}^{16} \sum_{j \epsilon c} H_{ij}$$

NOTE: The column or time histogram was formed for all histogram columns.

The R and TOT_N hisotgrams were formed by including only clutter data.

Two other types of total histograms were formed these are:

$$TOT_A = \sum_{j=1}^{16} \hat{R}_j \quad \text{and} \quad TOT = \sum_{j=1}^{16} \sum_{jec} H_{ij}$$

These are the summation of the range gate normalized histograms and a total histogram without normalization.

C. Statistical Parameters of Histogram Data

Standard statistical measures of the histograms are listed in Table 8-8. These parameters were computed for each histogram, each range sum histogram, R_i, and each time sum histogram, T_i. These parameters were also computed for each of the total histogram listed above, i.e., TOT_N, TOT_A, TOT. These were stored on tape for post processing.

TABLE 8-8
STATISTICAL PARAMETERS OF HISTOGRAM $H=(h_i)$

- Absolute moments a_1 (=mean), a_2, a_3, a_4

$$a_K = \sum_{i=1}^{1024} i^K h_i \Big/ \sum_{i=1}^{1024} h_i$$

- Central Moments $C_2 (=\sigma^2)$, C_3, C_4,

$$C_K = \sum_{i=1}^{1024} (i-a_1)^K h_i \Big/ \Sigma h_i$$

- Distribution Cuts Q = .5(median), 10^{-1}, 10^{-2}, 10^{-3}, 10^{-4}, 10^{-5}, 10^{-6} where a cut is for K defined as

$$\sum_{i=1}^{K} h_i = (1-Q) \sum_{i=1}^{1024} h_i$$

The absolute moments, a_i, were computed directly by summation and a_1 is the mean. The central moments c_i were computed from the absolute moments by the following formulas (obtainable by binominal expansion):

$$c_2 = a_2 - a_1^2$$

$$c_3 = a_3 = 3a_2a_1 + 2a_1^2$$

$$c_4 = a_4 = 4a_3a_1 + 6a_2a_1^2 - 3a_1^4$$

It should be noted that c_2 is the variance.

The distribution cuts are simply points on the Q curve where Q = 1-P and P is the cumulative probability. These were computed by summing until the threshold was exceeded and the index was then noted.

D. Computer Procedures

The computer procedures for histogram processing are outlined in Figure 8-31.

The basic histogram analysis program computed and recorded on an output magnetic tape as shown in Table 8-9.

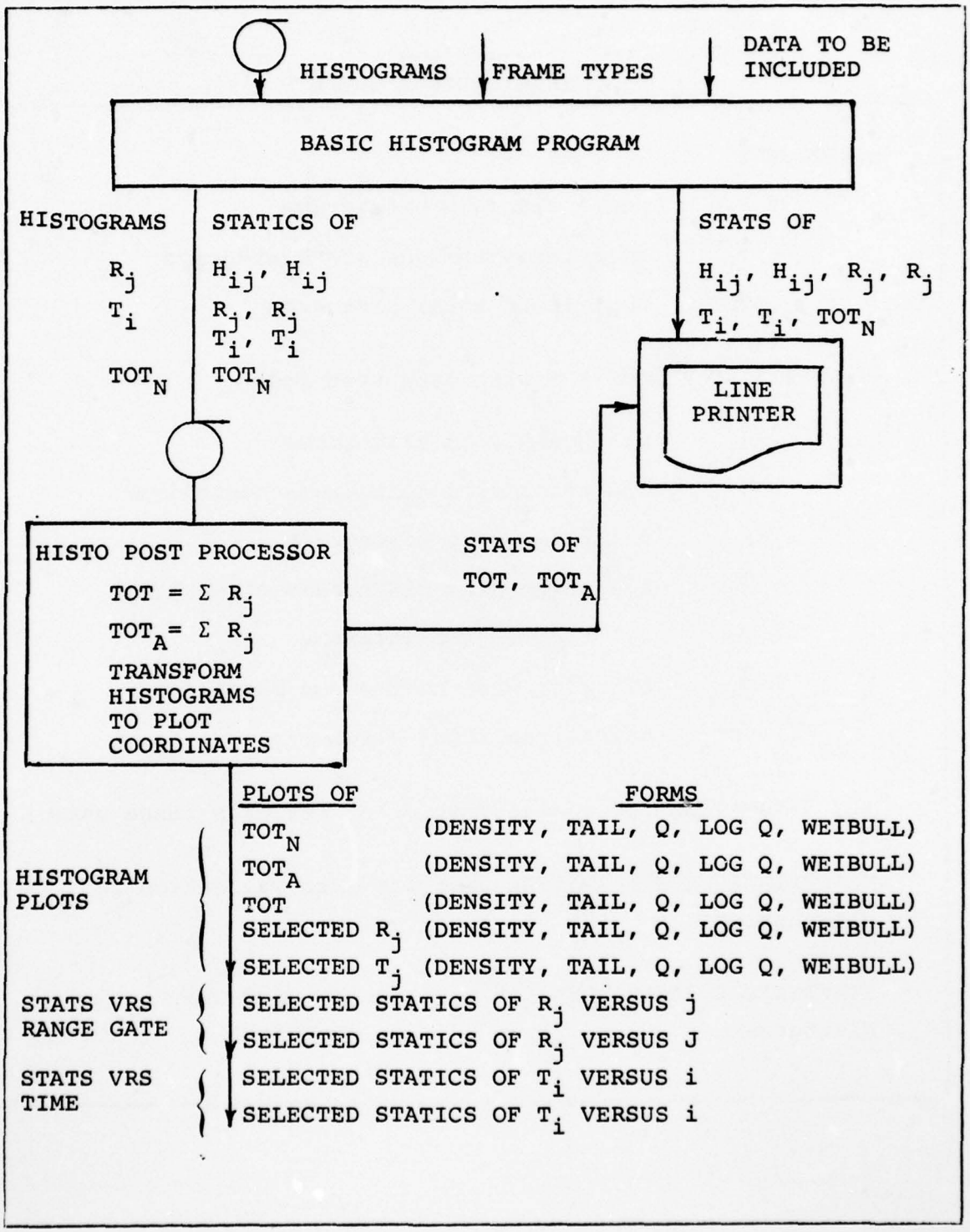

Figure 8-31 Computer Histogram Processing

TABLE 8-9
HISTOGRAM PROGRAM OUTPUTS

-HISTOGRAM

- R_j range gate sum histograms
- T_i selected time zone sum histograms
- TOT_N normalized total histogram

-STATISTICAL PARAMETERS with data type code

- H_{ij} all transfered histograms
- $\hat{H}_{ij}$ all transfered histograms normalized
- R_j all range gate histograms
- $\hat{R}_j$ all range gate histograms normalized
- T_i all time zone histograms
- $\hat{T}_i$ all time zone histograms normalized
- TOT_N normalized total histogram

-KEY PARAMETERS for computation of σ_o for each range gate.

-MISCELLANEOUS INFORMATION used for data validation and diagnostics

-STATISTICAL PARAMETERS for range gate, time and total histograms.

8.10.2 Hit Analysis

Hit analysis data processing is used for characterization of sea clutter radar echoes exceeding an amplitude threshold. A "hit" is defined as an echo large enough to have a probability of occurance of about 10^{-3} or less. Hit analysis outputs plots show behavior of sea clutter out in the tails of probability density functions.

Outputs from hit analysis were used for validation of the TAGSEA data base. In a few cases system anomalies were clearly identified from hit analysis plots and/or printouts. Targets present in the sea, such as ships or buoys, may also be identified from hit data.

Statistical behavior of hits are of interest to designers in terms of evaluation of constant false alarm rate (CFAR) and Sequential Detection (verification) schemes.

Hit analysis outputs for the TAGSEA program are as follows:

- Hit Counts vs. Time (temporal data)
- Hit Maps (spatial data)
- Conditional Probability Maps (temporal and spatial plots of hits in the immediate vicinity of very large hits)

These outputs show the behavior of sea clutter as a function of the following parameters:

- Altitude or grazing angle
- Sea State (1 - 5)
- Wind Direction (up, down and cross)
- Polarization (vertical and horizontal)
- East Coast vs. West Coast (continental USA)

Hit counts vs. time plots provide sums of hits within each range gate and total hits over a block of time equal to either 20 (fine gain) or 100 (coarse) FFT frames. Hit maps and hit counts vs. time plots indicate behavior within each range gate.

Hit map plots show position of sea clutter scatters in a Cross-Range vs. Down-Range coordinate system. Range-doppler information gathered by the radar was processed using synthetic aperture techniques to generate a hit map.

Targets present in flight test data can be detected from hit map and fine gain hit counts vs. time plots. A target with dimensions less than the nominal 100 ft X 100 ft resolution cell will appear as a sharp spike in one or two range gates of the hit map. The same target will appear in the hit counts vs. time plot for a time period of a few seconds at a level of one or two hits. Nominal clutter appears as a few tenths of a hit.

Conditional probability maps provide means for characterizing clutter properties in the vicinity (i.e., time, range, doppler) of large hits exceeding a threshold corresponding to 10^{-5} hit probability. The problem posed by conditional probability maps processing may be stated as follows:

> Given a hit exceeds the 10^{-5} threshold, what is the probability that hits in the immediate space-time vicinity of the referenced hit will exceed a 10^{-3} threshold? The processing algorithm considers an ensemble of such events from which an ensemble average of hits in each surrounding range-doppler-time resolution cell is computed. The term "vicinity of the referenced hit" refers to spatial and temporal

dimensions of ±7 range gates (cross range), ±7 doppler filters (down range), and ±7 FFT time frames (±128/14kHz=±0.064 seconds) with respect to position of the referenced hit.

A. DT-1 Hit Tape Data

Hit data for each run of each flight was stored on a DT-1 reformatted digital hit tape generated by the data reduction process. The DT-1 hit tape is compatible with the CDC-6700 digital computer. Each hit was identified by its power, range gate numbers, doppler filter number and delta FFT frame number (i.e., delta time). Delta FFT frame number was accumulated after reading each hit such that total FFT frame count and therefore time could be computed for each hit. An FFT frame was based on a sample rate of 14kHz and 128 points in the FFT. Time for processing one FFT frame was therefore 128/14kHz = 0.0091428571 second.

B. The SORT Process

The DT-1 hit tape was re-alphabetized using a sorting process programmed on the CDC-6700 computer. During data reduction, hits on the DT-1 tape were packed sequentially in time from minimum to maximum FFT frame number within each range gate processed. Data reduction processed each range gate sequentially from minimum range to maximum range as is indicated in Figure 8-32.

Hit data analysis required that hits be available sequentially in time irrespective of range gate or doppler filter number. This requirement came about from a desire to present data as originally observed by the radar; i.e., in time sequence.

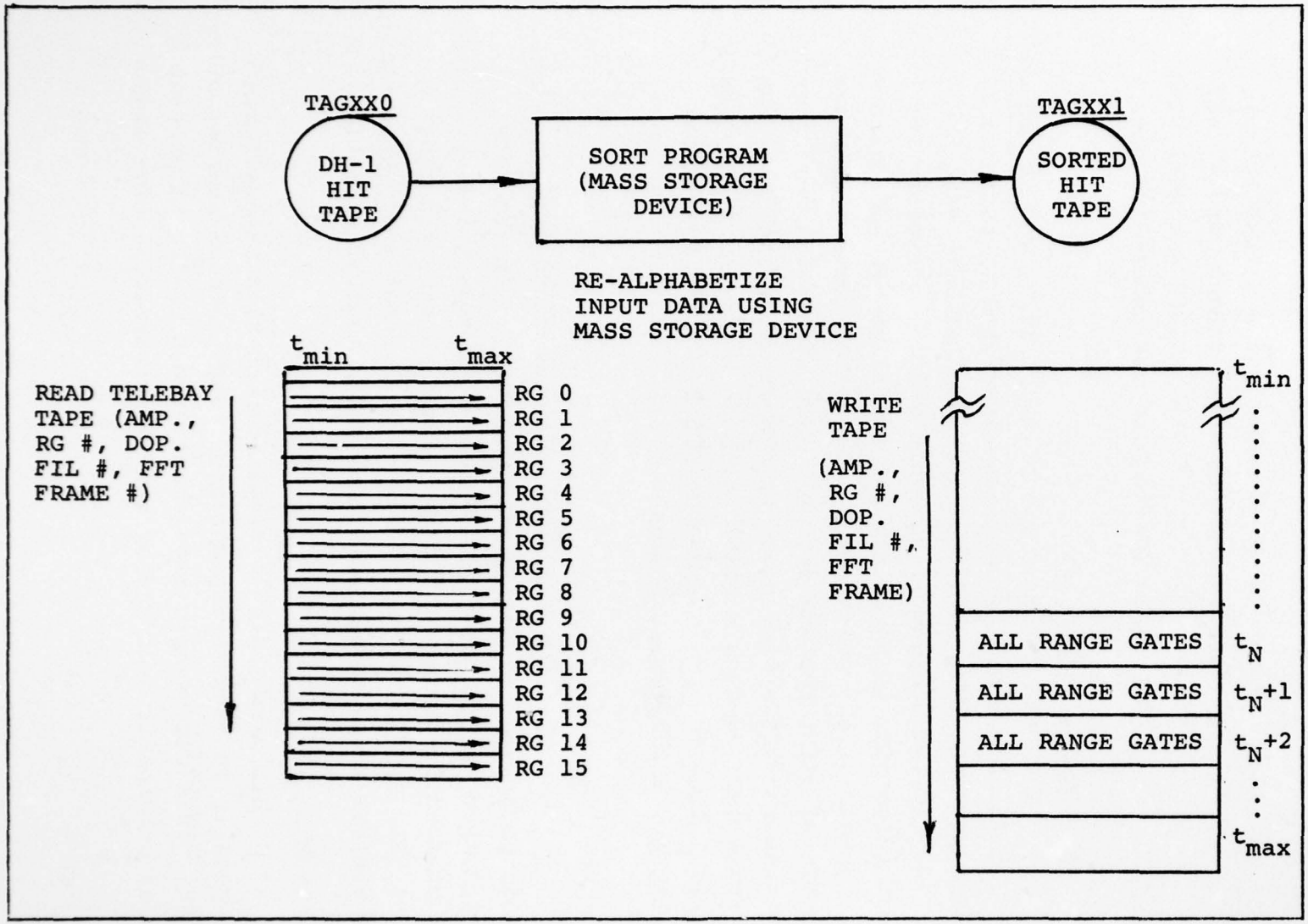

Figure 8-32 The SORT Process

AD-A036 972 GENERAL DYNAMICS/POMONA CALIF POMONA DIV F/G 17/9
TAGSEA PROGRAM. VOLUME II. PROCEDURES AND OUTPUT FORMS.(U)
AUG 76 N00017-73-C-2244
UNCLASSIFIED NL

2 OF 2
AD A036972

END
DATE FILMED
4-77

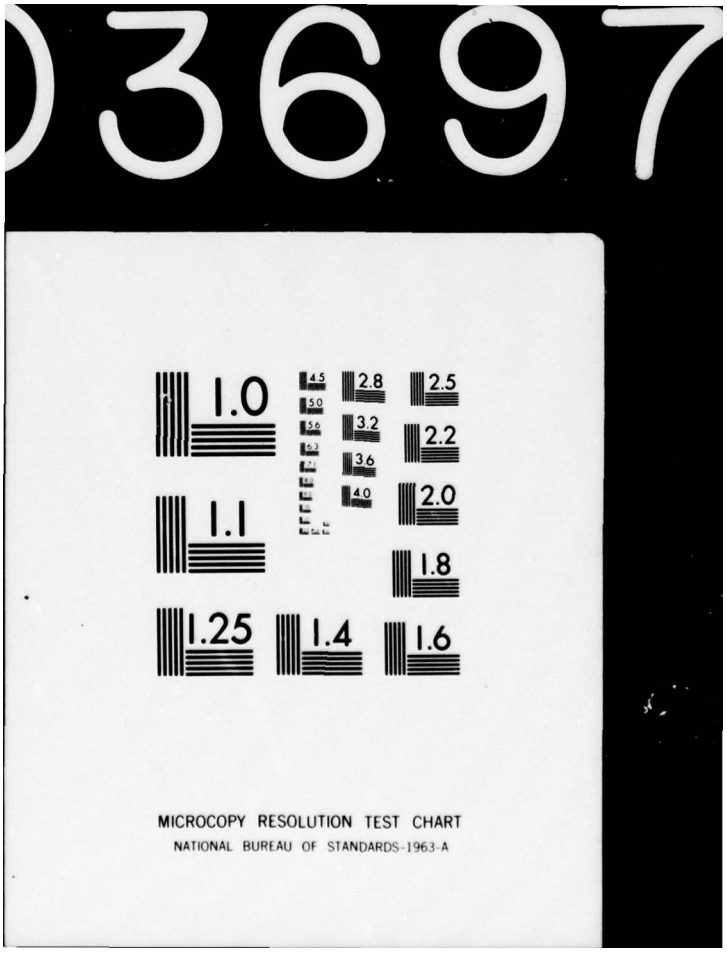
03697
1.0
1.1
1.25
1.4
1.6
1.8
2.0
2.2
2.5
2.8
3.2
3.6
4.0
4.5
5.0
5.6
MICROCOPY RESOLUTION TEST CHART
NATIONAL BUREAU OF STANDARDS-1963-A

The SORT process in Figure 8-32 was used to read the DT-1 hit tape onto a mass storage device present within the CDC-6700 computer. The data was re-alphabetized such that all hits were sequential in time and an output tape was written. The "sorted" hit tape was used as input for all subsequent hit data analysis.

C. Hit Data Analysis - Flow Chart

Hit data analysis flow chart in Figure 8-33 indicates the sorted hit tape drives three data processing programs:

- Hit Counts vs. Time
- Hit Maps
- Conditional Probability Maps

Each program generated an output data tape that was used to drive each of three plot programs. The plot programs read the data tape, performed a minimum amount of processing, and wrote plot tapes from which Cal. Comp. plots were produced. Each program had control card data inputs and a label card input for plot identification by run type, flight/run code, sea state, altitude and wind direction.

Hit counts vs. time and hit map plots are multi-trace amplitude vs. time or down-range presentations in which each of 16 range gates and the range gate sum were plotted on separate traces.

Conditional probability maps are contour plots of selected slices through the conditional probability code.

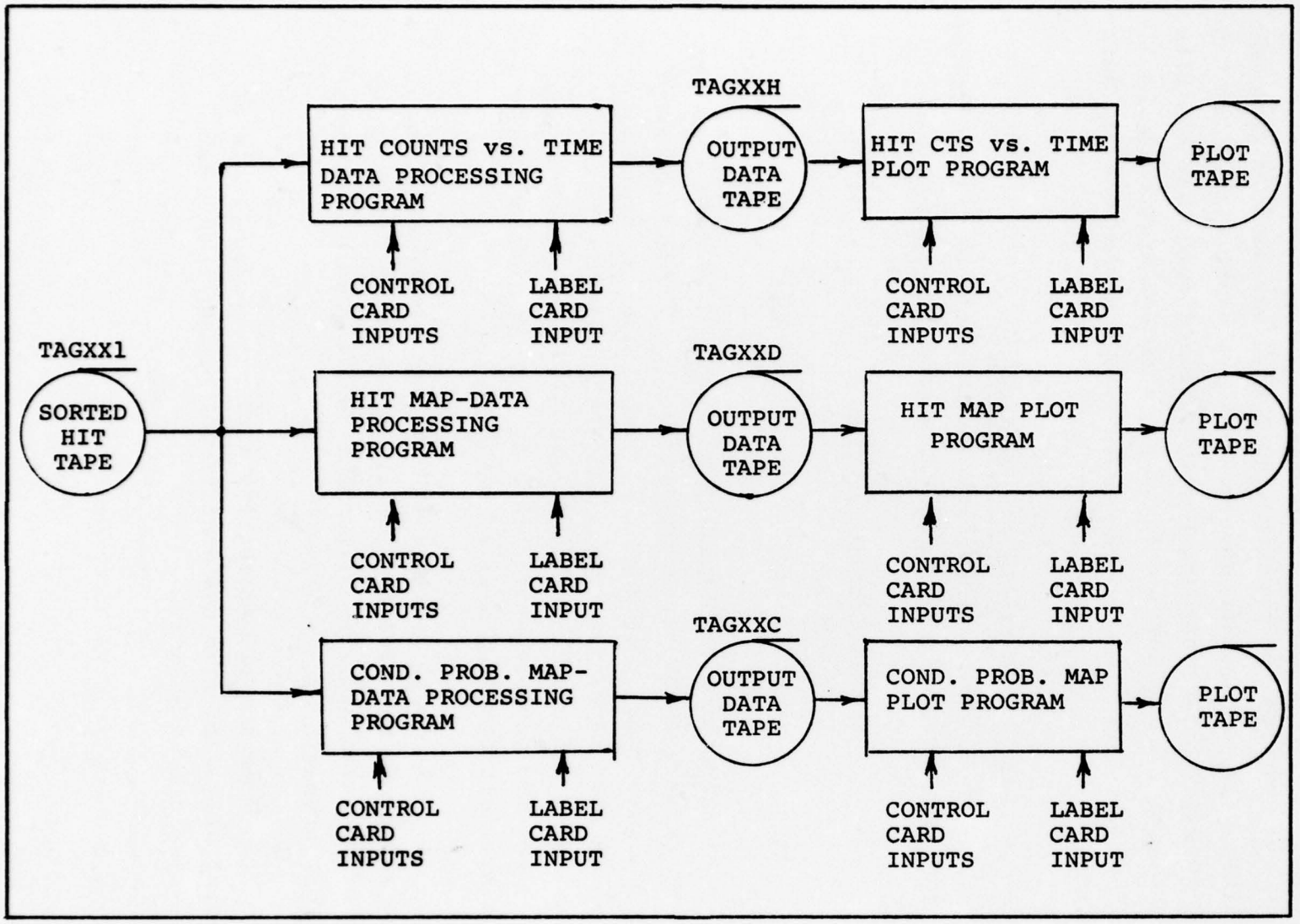

Figure 8-33 Hit Data Analysis Flow Chart

UNCLASSIFIED

D. Hit Counts vs. Time Analysis

Hit counts vs. time analysis provides a time history of hits exceeding a set threshold. Details regarding data processing are flow charted in Figure 8-34.

Hits from the sorted hit tape were read, thresholded and mean normalized. Hits within each range gate and hit totals were accumulated within each FFT frame. The range gate sums and total hits per FFT frame were written onto the output data tape. An option exists for line pronter output.

A second accumulation was used to sum hits within a block of FFT frames (nominally 20 or 100). A "quick-look" line printer output summary listed total hits/block and the last FFT frame number at which a hit occured within each block.

The plot program read hits/range gate/FFT frame from the data tape. Hits were accumulated into blocks and written into the plot arrays. After normaliztion by the block size, the plot tape was generated. The plot program provided a quick look output summary and an option for printout of hits/range gate/FFT frame.

E. Hit Map Analysis

Hit data was processed using synthetic aperture techniques to produce hit maps.

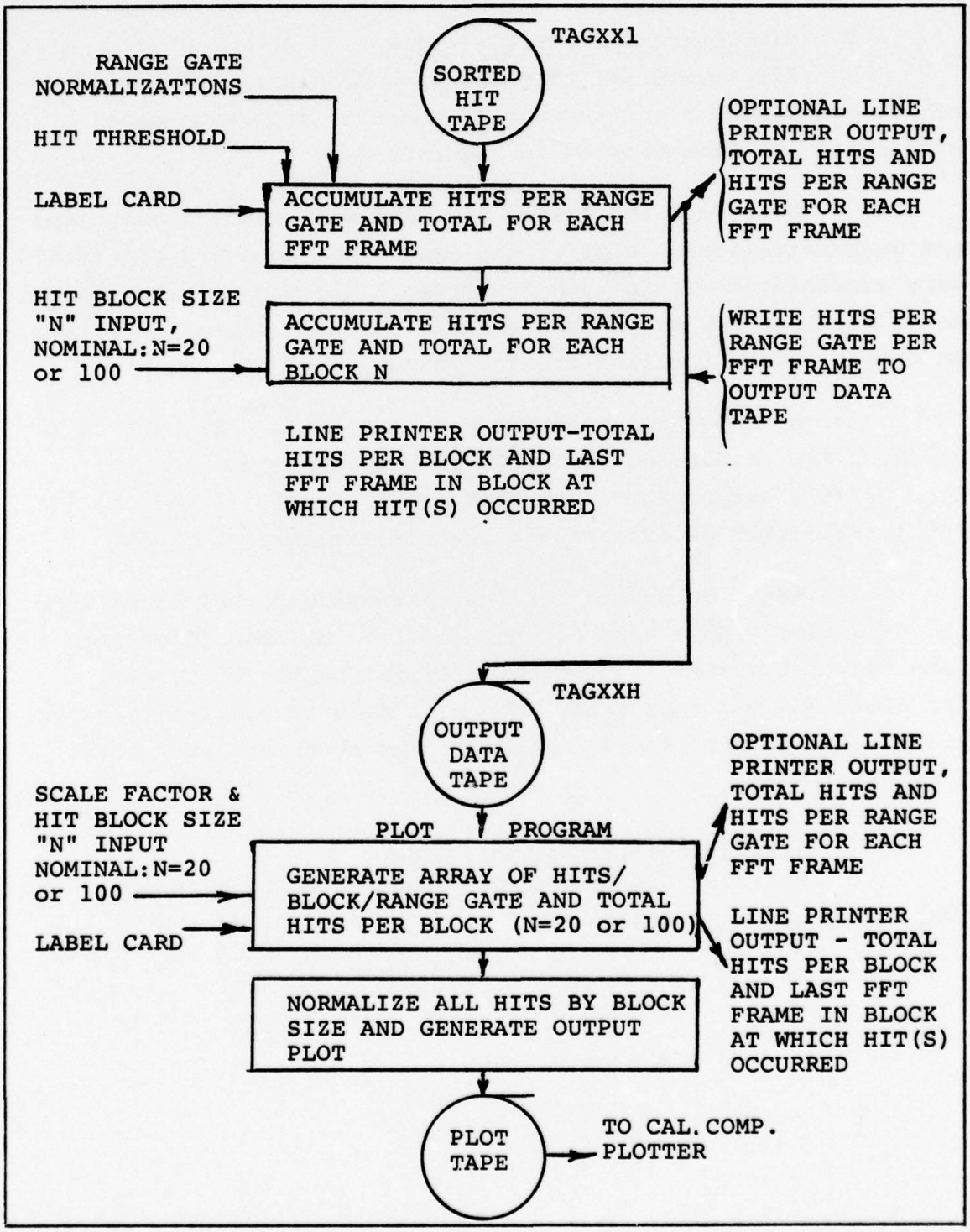

Figure 8-34 Hit Counts vs. Time Detailed Data Processing Flow Chart

Each hit read from the sorted hit tape was mean normalized provided that its amplitude (A) exceeded the threshold. Range gate number (R), doppler filter number (D), and FFT frame time (T) from hit data were used along with radar wavelength, doppler resolution, aircraft velocity and altitude to compute the true spatial portion of each hit in sea space. Four sea space overlays in Figure 8-35 illustrate the hit map boundraries for altitude of 500 ft, 1100 ft, 2200 ft, and 3300 ft. Each are mapped by the TAGSEA system was subdivided into 16 down range cells by 32 cross range cells. Key system parameters are listed in the Figure. These are aircraft velocity, V, maximum doppler frequency, f_d, wavelength, λ, minimum range, R_1, maximum range, R_2, range resolution, ΔR, and doppler resolution, Δf_d.

As the aircraft flew in the cross-range direction, hit map "snapshots" were taken every FFT frame ($\simeq$ 9.14ms). The amount by which the hit map contours moved in the cross-range direction in one FFT frame, or "range slip", was simply aircraft velocity multipled by FFT frame time; 420 ft/sec X 0.00914 sec = 3.84 feet.

A second mapping was used for display of hits using computer processing. The sea was conceptually divided into nominal 100 ft X 100 ft cells. The true spatial portion of each hit as computed from range-doppler information was quantized into a particular cell in the rectangular grid. The number of hits in each cell of the grid was accumulated as the aircraft flew by. Figure 8-36 shows the conceptual form of hit map output. Hit map contours in Figure 8-36 have a mean cross-range extent of about $\pm$1200 ft or a total span of about 2400 ft. The total number of hits possible per resolution cell was roughly estimated from total cross-range extent and range slip:

$$\text{Max. No. Hits} = \frac{\text{Cross Range Extent}}{\text{Range Slip}} = \frac{2400}{3.84} = 625$$

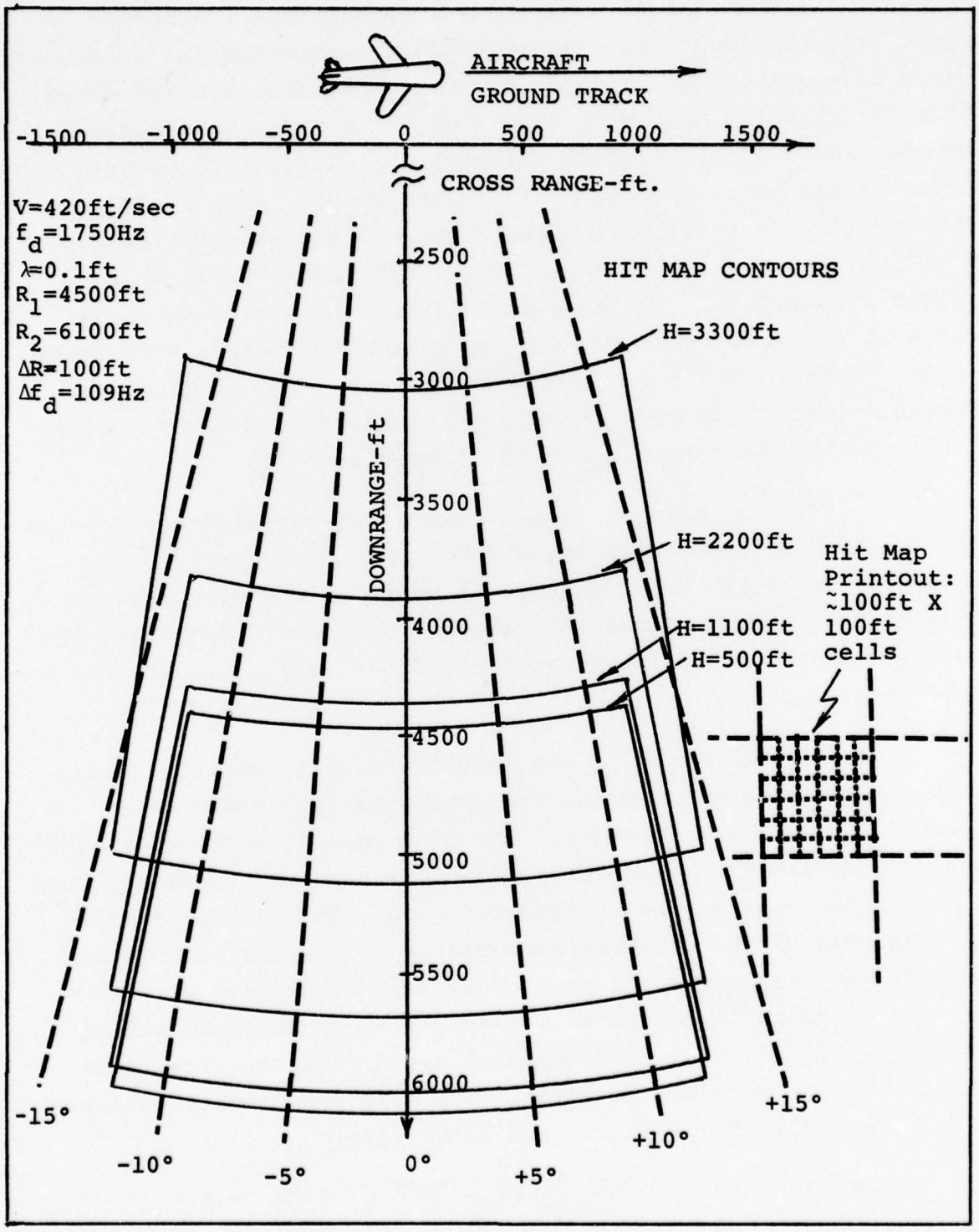

Figure 8-35 Sea Space Overlays

CROSS RANGE, FEET	DOWNRANGE					SUM
	1	2	3	. . . . .	16	
100	1	3	2	. . . . .	5	10
200	2	1	3	. . . . .	4	21
300	6	3	2	. . . . .	3	36
400	4	1	3	. . . . .	2	32
.	.	.	.	. . .	.	.
.	.	.	.	. . .	.	.
.	.	.	.	. . .	.	.
.	.	.	.	. . .	.	.
.	.	.	.	. . .	.	.
125800	3	1	2	. . . . .	4	30
125900	2	5	6	. . . . .	1	28
126000	1	3	5	. . . . .	2	38
	3780	3690	3801	. . . .	3695	60480

Figure 8-36 Hit Map Output Concept

For hit probability of 10^{-3} a hit is expected about every other FFT frame (2 frames X 16 range gates X 32 doppler cells = 1024 trials). There are roughly 400 cells in a hit map and about 300 hits; therefore, the expected number of hits per cell is about 0.75.

Hit analysis flow is indicated in Figure 8-37. Fixed system parameters in Figure 8-35 were used to compute scale factors for the hit map. Scale factor equations are listed in Table 8-10. Hit map scale factors are: minimum down range position (Y_{min}), maximum down range position (Y_{max}), and minimum cross range. These factors vary with velocity and altitude of the run. Maximum doppler frequency, $f_d(max)$, is the number of filters in the FFT filter bank (16) multiplied by doppler resolution Δf_d ($\simeq$109 Hz).

The scale factors are required as input to Transformation Equations in Table 8-11. Hit map processing in Figure 8-37 indicates an R-X presentation (range gate number vs. cross range) was available as an option. If the option were selected the J index of the hit map was referenced directly to range gate number. The option was used to maintain the integrity of data within each range gate. The hit map was distorted slightly when the R-X option was selected due to small curvature in ground range contours. On the other hand, the true X-Y mapping sufferes from "fringing" minimum and maximum down range due to curvature of the range gates. The R-X option was chosen for all hit map processing to avoid mixing data from adjacent range gates and to facilitate data validation.

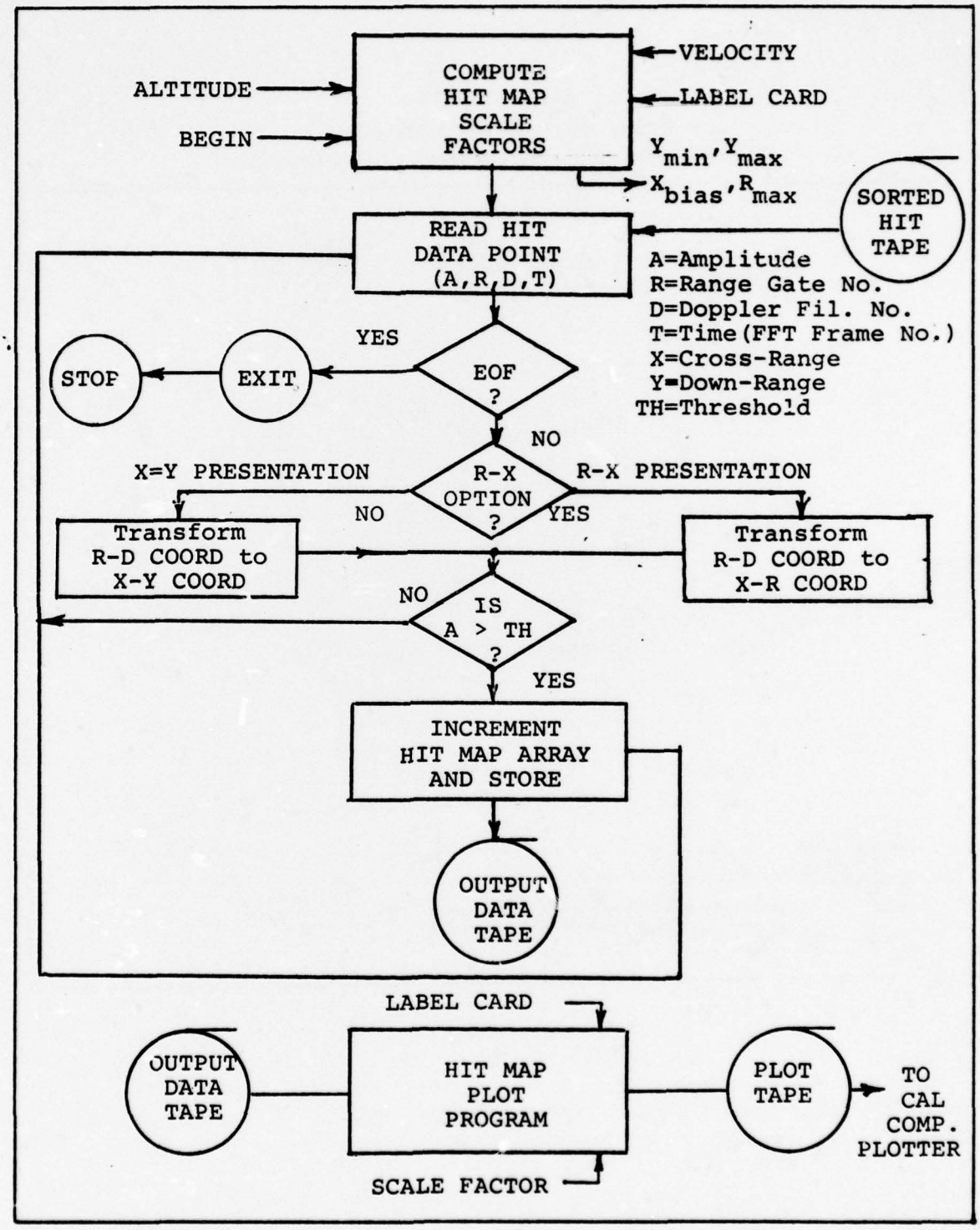

Figure 8-37 Hit Data Processing for Hit Map and Large Hit Detection

TABLE 8-10

SCALE FACTOR EQUATIONS -
TRANSFORMATION TO GROUND COORDINATES

$$R_{max} = \left(\frac{\lambda}{2}\right)\left(\frac{14000}{128}\right)\left(\frac{f_{d(max)}}{\Delta f_d}\right)$$

$$X = (R_{min})\ (\dot{R}_{max}/V)$$

$$Y_{min} = \sqrt{R_{min}^2 - X^2 - H^2}$$

$$Y_{max} = \sqrt{R_{max}^2 - H^2}$$

$$X_{bias} = -(R_{max})\ (\dot{R}_{max}/V)$$

NOTE:

$$\Delta f_d = \frac{\text{sample rate}}{\text{no. points in FFT}} = \frac{14000\ \text{Hz}}{128}$$

TABLE 8-11
TRANSFORMATION EQUATIONS—R-D TO X-Y COORDINATES

RANGE $R = R_{min} + (R.G.\ \#)\ \Delta R + \Delta R/2$, $(R.G.\ \# = 0, 1, \ldots, 15)$

RANGE RATE $\dot{R} = \left(\frac{\lambda}{2}\right)\left(\frac{14000}{128}\right)\left((DOP.\ FIL.\ \#) - 35.5\right)$, $(DOP.\ FIL.\ \# = 20, 21, \ldots, 51)$

TIME $T = (FFT\ Frame\ \#)\ (128/14000)$

CROSS RANGE $X = R\ (\dot{R}/V) + (V)\ (T)$

DOWN RANGE $Y = \sqrt{R^2 - X^2 - H^2}$

True spatial coordinates in sea space

HIT MAP GRID INDICES (INTEGERS)

$I = (X - X_{bias})/\Delta R$ $(\Delta R = 100\ ft.)$

$J = (16)\ (Y - Y_{min})/(Y_{max} - Y_{min}) + 1$ (X - Y option)

$J = R.\ G.\ \# + 1$, If R-X option selected

If A(X,Y) > threshold, then increment hit map (I,J) by 1.

F. Conditional Probability Analysis

Software procedure for conditional probability map processing is described by the flow chart in Figure 8-38. Hits read from the sorted hit tape were searched until one exceeds threshold TH1 (10^{-5} hit probability). After such a hit was found a three dimensional range doppler and time "grided" cube was formed with dimensions $\pm$7 cells surrounding the vicinity of the hit. The total number of cells in the volume is 15 X 15 X 15 =3375. Time (FFT frame) is regarded as always extended by $\pm$7 cells except in the vicinity of the beginning and end of the run. However, range and doppler were restricted to 16 range gates and 32 doppler cells. A normalization array was constructed to take into account the finite extent of range-doppler information. Each time a hit exceeds TH1 the normalization array was incremented by one in those relative range-doppler cells where it is possible for a hit to take place. For example, if a hit exceeds TH1 in the smallest range gate and doppler filter, only positive values of relative range-doppler exist. Therefore, the normalization array was incremented by one only in the positive relative range-doppler positions. Hits exceeding the TH2 (10^{-3}) threshold were used to increment the 3375 cell range-doppler-time cube at positions to the location of the hit > TH1.

The process was repeated for all hits > TH1 on the sorted hit tape. For each hit > TH1 the normalization array was incremented only in range-doppler cell for which it was possible for hits to occur. Hits > TH2 were used to increment the 3375 cell range-doppler-time cube at $\pm$7 cells relative to the co-ordinates of a large hit.

When end of file was reached the grided cube was nromalized by the normalization array on a cell-by-cell basis in the range-doppler dimension. The normalized cube is the condition-al probability map. Clearly, all hits that exceed the 10^{-5}

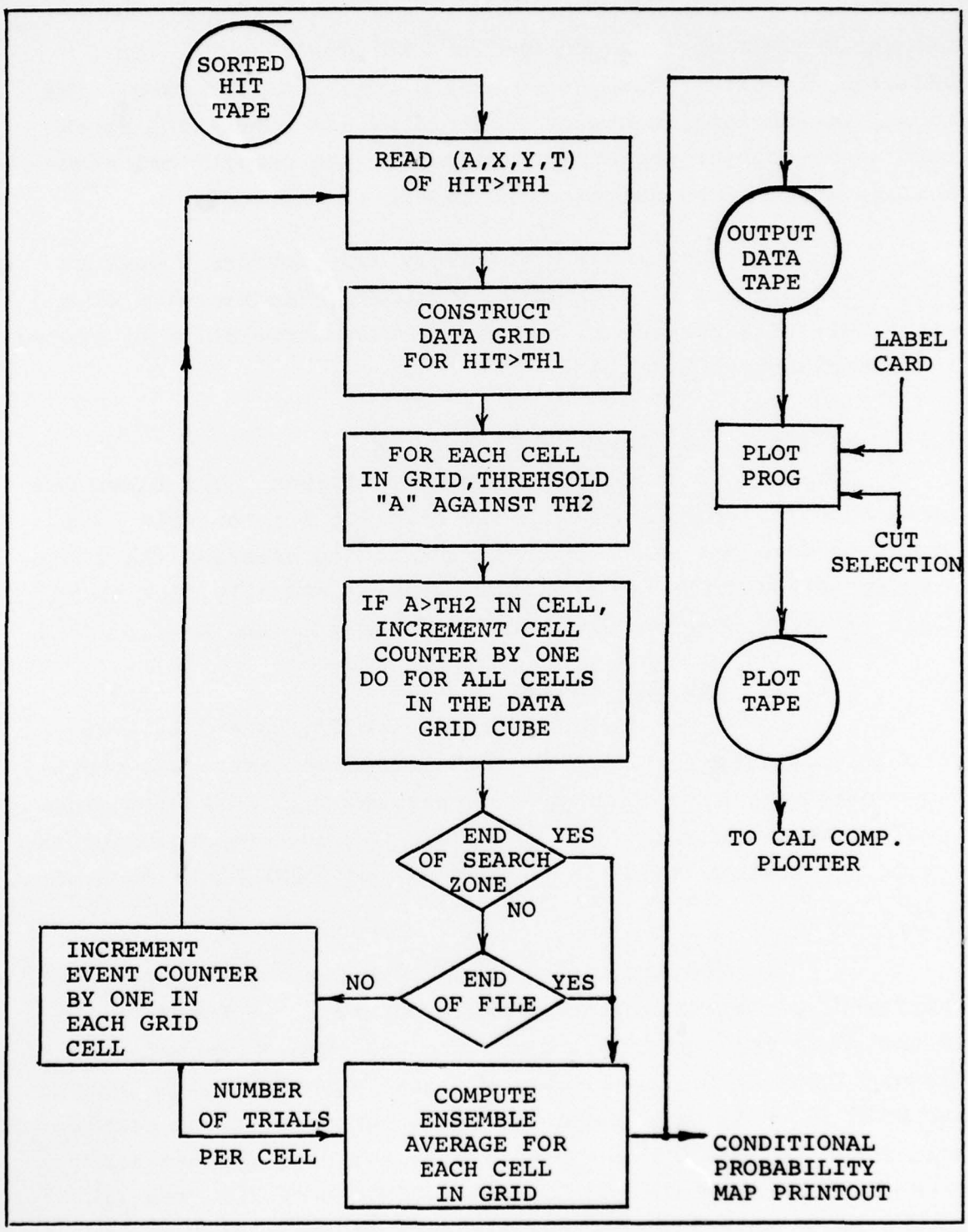

Figure 8-38 Software Procedure for Conditional Probability Maps

threshold (TH1) must exceed the 10^{-3} threshold (TH2). In addition all hits > TH1 reside at the center of the cube. The normalization array contains a record of all hits > TH1 at the zero range-doppler position. Therefore, the conditional probability map must be unity at the center of the cube.

The conditional probability map provides a measure of the correlation between hits surrounding the vicinity of a hit > TH1. Its purpose is to measure such correlation by processing sea clutter hit data.

8.11 Validation of Data and Procedures

Three types of validation were performed. The first ensured that the process used in the aircraft for gathering and recording data was satisfactory. The second assessed the credibility of reduction and analysis outputs. Finally, the third class of procedures checked the credibility of the data.

8.11.1 Data Gathering

After flights 4 and 6 (on 2/9/76 and 2/12/76 respectively), the ratio of CW CAL to receiver noise was checked for consistency with other system measurements. A Schlumberger spectrum analyzer with 40 Hz bandwidth was used to determine the ratios. These are shown in Table 8-12, together with the predicted value.

The prediction was obtained by calculation from radar and spectrum analyzer parameters. Refer to Figure 8-39. If the power gain between the antenna and the sample and hold circuit input is G, the calibrate signal variance at the sample and hold input is GP_{CAL}, and the noise variance at the sample and hold input is $2G\ KTB_nF = P_nG$. (The factor of 2 appears since frequencies both above and below the VCXO contribute the the second mixer output.) Now the variance at the output of the sample and hold equals the variance at the input of the sample and hold.

TABLE 8-12
CAL TO NORM RATIOS

Flight	Run	Gate	CAL/Noise (dB)	Mean (dB)	Std. Dev. (dB)
4	1	5	40.0		
	2	5	39.5		
	3	5	39.8	39.8	0.3
6	2	0	41		
		1	40.5		
		2	39.5		
		3	40		
		4	41		
		5	40.5		
		6	40.5		
		7	39		
		8	41		
		9	41		
		10	40		
		11	40		
		12	40		
		13	40.5		
		14	38.5		
		15	39.5	40.2	0.8
Calculated Value				40.1	1.2

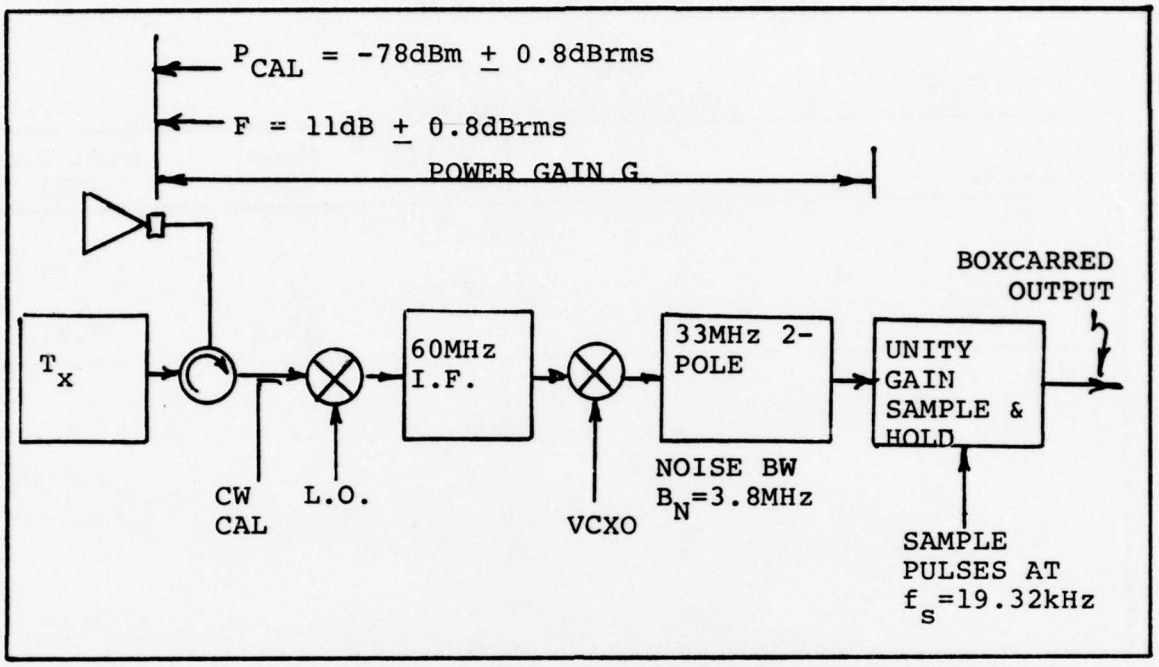

Figure 8-39 Block Diagram for CAL/Noise Calculation

Then the noise power spectral density is given by:

$$S_{N\ out} = P_n G \frac{2}{f_s} \left(\frac{\sin \pi \frac{f}{f_s}}{\pi \frac{f}{f_s}} \right)^2$$

We are also interested in the level of the first line of the calibrate signal, which is given by:

$$P_{CAL\ OUT} = P_{CAL}\ G \left(\frac{\sin \pi \frac{f}{f_s}}{\pi \frac{f}{f_s}} \right)^2$$

Then the output CAL to noise ratio is:

$$\frac{P_{CAL\ OUT}}{S_{N\ OUT}} = \frac{P_{CAL}}{P_N} \times \frac{f_s}{2}$$

If a spectram analyzer with noise bandwidth B_{SA} is used to measure the CAL to noise ratio,

$$P_{N\ OUT} = S_{N\ OUT}\ B_{SA}$$

Then,

$$\frac{P_{CAL\ OUT}}{P_{N\ OUT}} = \frac{P_{CAL}}{P_N} \times \frac{f_s}{2B_{SA}} = \frac{P_{CAL}}{4KTB_nF} \times \frac{f_s}{B_{SA}}$$

	+	-
P_{CAL}	-78.0dBm$\pm$0.8dbrms	
f_s = 1932 Hz	42.9dB	
4		6.0dB
KT		-174.0dBm/Hz
B_n = 3.8 MHz		65.8dB
F		11.0dB $\pm$ 0.8dbrms
B_{SA} = 40 Hz		16.0dB
	-35.1dB	-75.2dB
	75.2	
	40.1dB $\pm$1.2dbrms	

The measured values shown in Table 8-12 were well within the range of this predicted value.

8.11.2 Output Procedures Validation

1. Histograms and Distribution Functions
   Noise and CAL signals were processed and found to exhibit the required dynamic range.

2. Temporal & Spatial Autocorrelation Functions
   Test signals were processed and found to behave as predicted.

3. Hit Maps
   The Nantucket Lightship was mapped and found to have the expected extent.

4. Conditional Probability Maps
   The Nantucket Lightship, again, was mapped and indicated the expected extent.

5. Statistics of the Mean
   FFT sums were used for this purpose. These were compared with the histogram means and found to agree.

6. Sea Reflectivity (σ_o)
   No absolute reference such as a standard target was used here since the prime purpose of the program was to gather relative data. However, values for reflectivity are available at reduced accuracy. Receiver noise was used as the reference for the received signal. The contributors to error are listed below, together with the size of errors. (All uniform distributions were assumed to have a value of $E_{MAX} / \sqrt{3}$ rms.)

Transmitter Power	0.6dB rms
Antenna Gain (2 way)	1.2dB rms
Noise Figure	0.8dB rms
Aircraft Velocity	0.4dB rms
Combined error	1.5dB rms

Thus the 2σ error is ± 3.0 dB due to hardware and calibration errors. In addition, errors in estimating sea state could introduce approximately 4dB per sea state error.

Since the values obtained for σ_o were several decibels higher than values obtained by previous observers, the lightship cross-section was estimated from data as an additional check. Schlumberger spectra of the lightship were obtained at intervals of one second while the lightship was in the radar's field of view. These returns were compared with receiver noise and indicated an average cross-section of 160 square meters for the lightship which is credible.

8.11.3 Data Validation

The data was screened at three levels. First, data tapes were reduced only if the equipment showed evidence of operating correctly during the flight. This was determined by noting whether monitoring instruments behaved normally. Second, during initial reduction, the clutter-to-noise ratio at the A/D converter input was observed. Range gate recordings with less than a 4dB clutter plus noise-to-noise ratio were not reduced. Finally, the histograms and hit data were examined for dropouts or spurious signals which were not typical of target responses. Range gates with data containing such responses were removed from the data base. The criteria for rejecting such data were:

1) Excessively long time responses at high level (more than 15 seconds) in one range gate.

2) Very short time responses (one or two FFT intervals) in which most filters in one range gate responded at high level simultaneously.

These criteria would not exclude surface targets, which typically responded over a few adjacent doppler cells, for seven seconds or less.

8.11.4 Quick-Look Verification

Verification of the data gathering and recording process was obtained after flights using the set-up of Figure 8-40. The elements unique to the quick look process are the Schlumberger Spectram Analyzer and the X-Y plotter. Other elements are part of the normal data reduction path.

Data from each range gate is available by selecting a track amplifier and tuning the EMR 4146 Discriminator to the appropriate subcarrier frequency. The spectrum analyzer then processes the incoming data by doing a 512 point FFT with a resolution of 40Hz, applying weighting and averaging the outputs for approximately 25 seconds. This is done three times for each range gate; with noise only, with noise plus calibration, and with noise plus clutter.

The results are plotted using the X-Y plotter as shown in Figure 8-41. The x-axis covers approximately 10KHz and the y-axis has a 60dB range. Several points are of interest on the resultant plot. Noise is noted as being recorded at

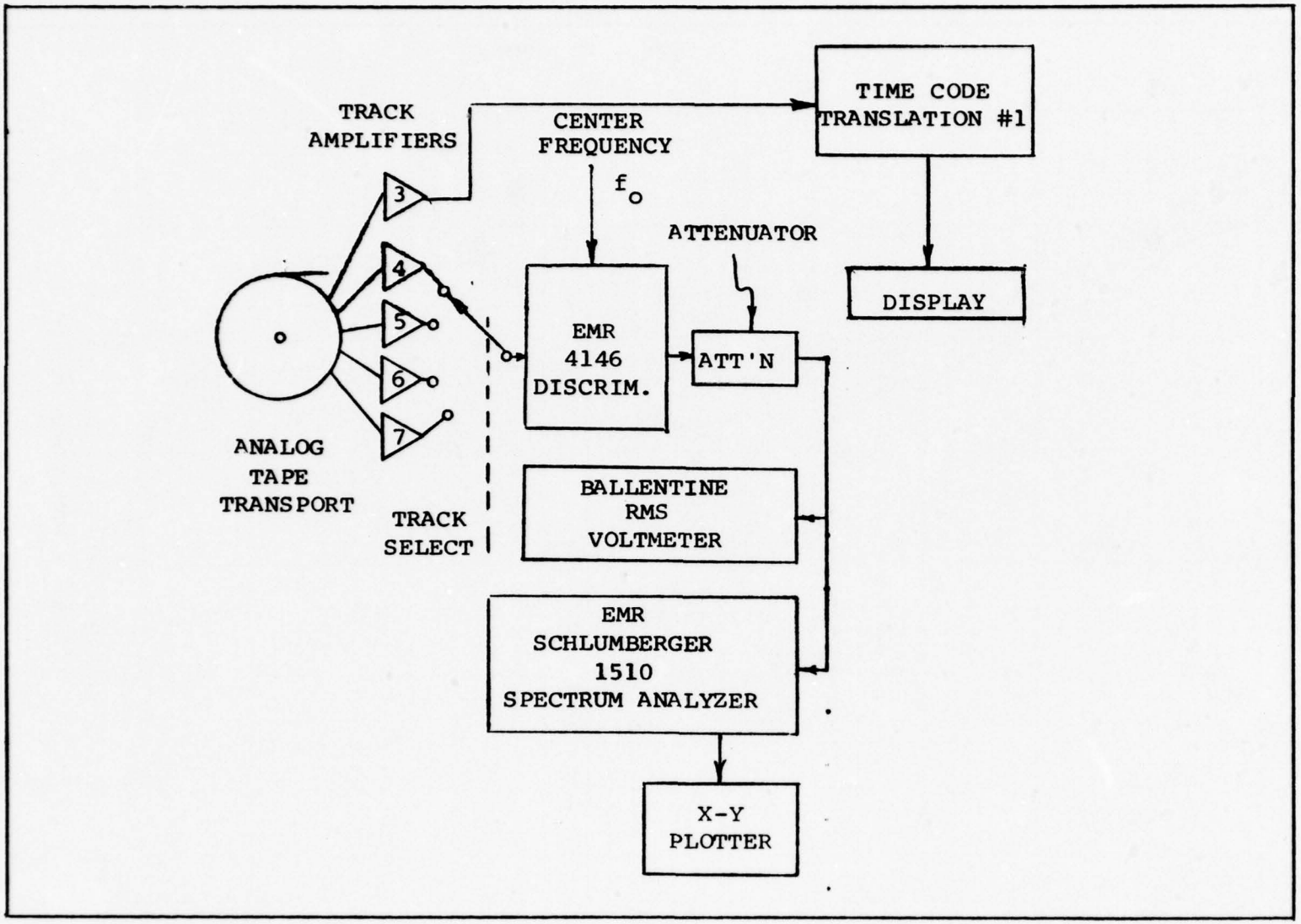

Figure 8-40 Quick Look Equipment Set Up

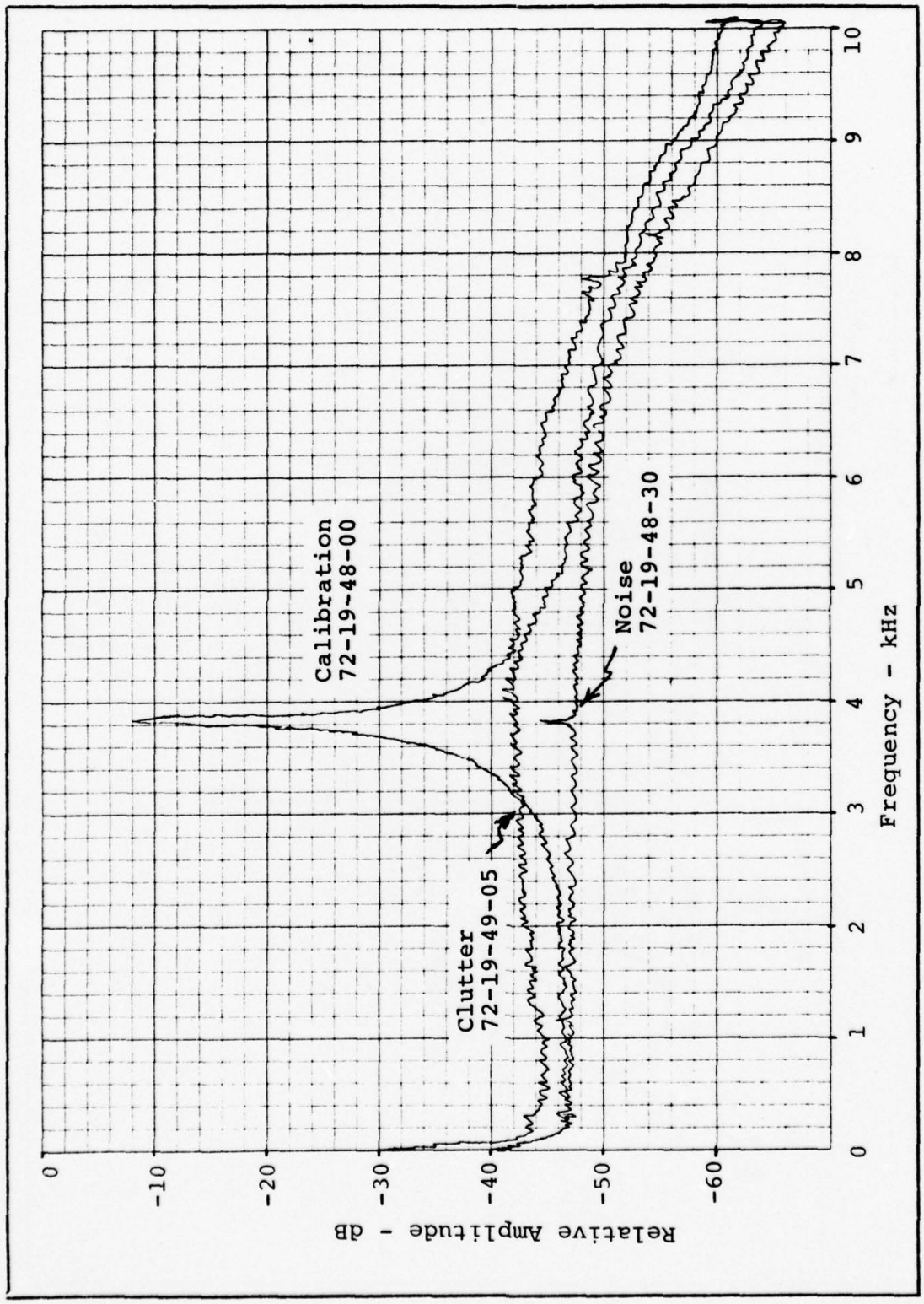

Figure 8-41 Quick Look Analysis

IRIG time 72-19-48-30, is flat over the spectrum of interest, and rolls off above 6.3KHz as determined by the anti-alising filter in the discriminator. Also note that a slight amount of CW leakage appears on the noise plot at 4KHz which serves as a convenient zero-doppler marker. Calibration plus noise follows noise closely except in the CW calibration area around 4KHz where the calibration is placed to provide an absolute measure of the system level. Clutter plus noise is above noise (about 5dB in this example) and has a slight shape due to the antenna beam shape.

From this composite plot the health of the system can be determined and the quality of the data judged for use in further analysis. This quick-look capability also proved to be of great use and flexibility as a diagnostic tool during the flight test program.

The above description covers the quick-look processing for the East Coast flights. On the West Coast General Dynamics used a similar setup with an Ubiquitous spectrum analyzer, A/D converter, digital tapes, a programmed 516 computer and plotter in place of the Schlumberger and X-Y plotter. The functions performed were the same.

9. OUTPUTS (FORM AND MEANING)

This section will describe the output figures and tables. Most of the data presented elsewhere in this report is of such a speciallized nature that it is necessary to define in some detail the form and meaning of the computer generated curves, the summary tables, and the outputs which resulted from special analyses. Subsections covering Histograms, Hit Ananlysis, Average Analysis, Spatial Analysis, Temporal Analysis, Special Data Analysis and Mean Backscatter Coefficient follow.

9.1 Histogram Analysis Outputs

Data distributions were obtained from all the valid data in each run. The resulting data was displayed in a number of forms. Each of these are analytical derivable from one another. The display forms are:

1. P.D.F. = Probability density function	Plot
2. P.D.F. tail = high return tail of above	Plot
3. $Q(x) = 1-P_{cum}$ = 1 - cumulative probability	Plot
4. Log(Q) = Log of above	Plot
5. WEIBULL	Plot
6. Statistical Parameters	Numbers

Data distributions were obtained from the full run data sets with various normalization and for selected subsets of the data. A matrix of data type and presentation form is shown as Figure 9-1.

DATA TYPE	PDF (histogram)	PDF TAIL	Q	LOG Q	WEIBULL	STATISTICAL PARAMETERS
Single Histogram H_{ij}	I	I	I	I	I	I
Range Gate Histogram	I	I	I	I	I	I
Time Zone Histogram	I	I	I	I	I	I
Total Histogram (RAW)	S,R	S,R	S,R	S,F	S,R	S,F
Total Histogram (A) (range gate normalized)	S,R	S,R	S,R	S,F	S,F	S,F
Total Histogram (N) (locally normalized)	I,R	I,R	I,R	I,F	I,R	I

S = Standard Output

F = Full Outputs in Appendices

R = Representative Outputs in Appendices

I = Intermediate or Check of Data Analyses

Figure 9-1 Distribution Outputs - Type & Form Matrix

Selected statistical parameters were plotted versus time and range gate. These are also included in the report. Figure 9-2 shows a matrix of these outputs.

9.1.1 Total Histogram (RAW)

For each run all the valid clutter histograms were added to form a total histogram for the run. This is the total histogram. Due to uncompensated differences in σ_o and data processing the range gates had somewhat different mean clutter levels.

	RAW	Normalized by Mean
Statistics versus Range Gate	S,F	S,P
Statistics versus Time Zone	S,F	S,F

S = Standard Output Plot
P = Partial Output in Appendices
F = Full Output in Appendices

Figure 9-2 Statistical Plots Matrix

These differences were not removed in the total histograms. Figure 9-3 shows a raw histogram as collected. This is the probability density function estimate extracted from the data. It is normalized ($p(k) = h_k / \sum_{i=1}^{1024} h_i$) to probability density form. Figure 9-4 expands the high amplitude/low probability tail of this function.

To form Figure 9-5, Q(x), the cumulative probability function (P) was formed by integrating (summing) the probability density function. Then the cumulativity probability function was subtracted from one to obtain Q (i.e., Q = 1-P).

$$Q_I = 1 - \sum_{k=1}^{I} p(k)$$

We next developed the Log Q representation of the data Figure 9-6. To obtain this plot the logrithm of Q is taken to obtain the abscissa.

$$A_I = \text{Log}_{10}\, Q_I$$

This curve is the most useful in picking the levels of the various tails, e.g., the 10^{-5} and 10^{-6} points are readily found and read. This form of the curve is the form most familiar to radar designers when computing false alarm probability for detection systems.

The final type of representation found is the Weibull plots (Figure 9-7). Here the double natural logarithm of Q is taken and plotted against the class interval in dB. The change in sign is necessary to preclude taking the logarithm of a negative number.

$$W_i = \ln(-\ln Q_i) = \ln\left[\ln\left(\frac{1}{(1-P_i)}\right)\right]$$

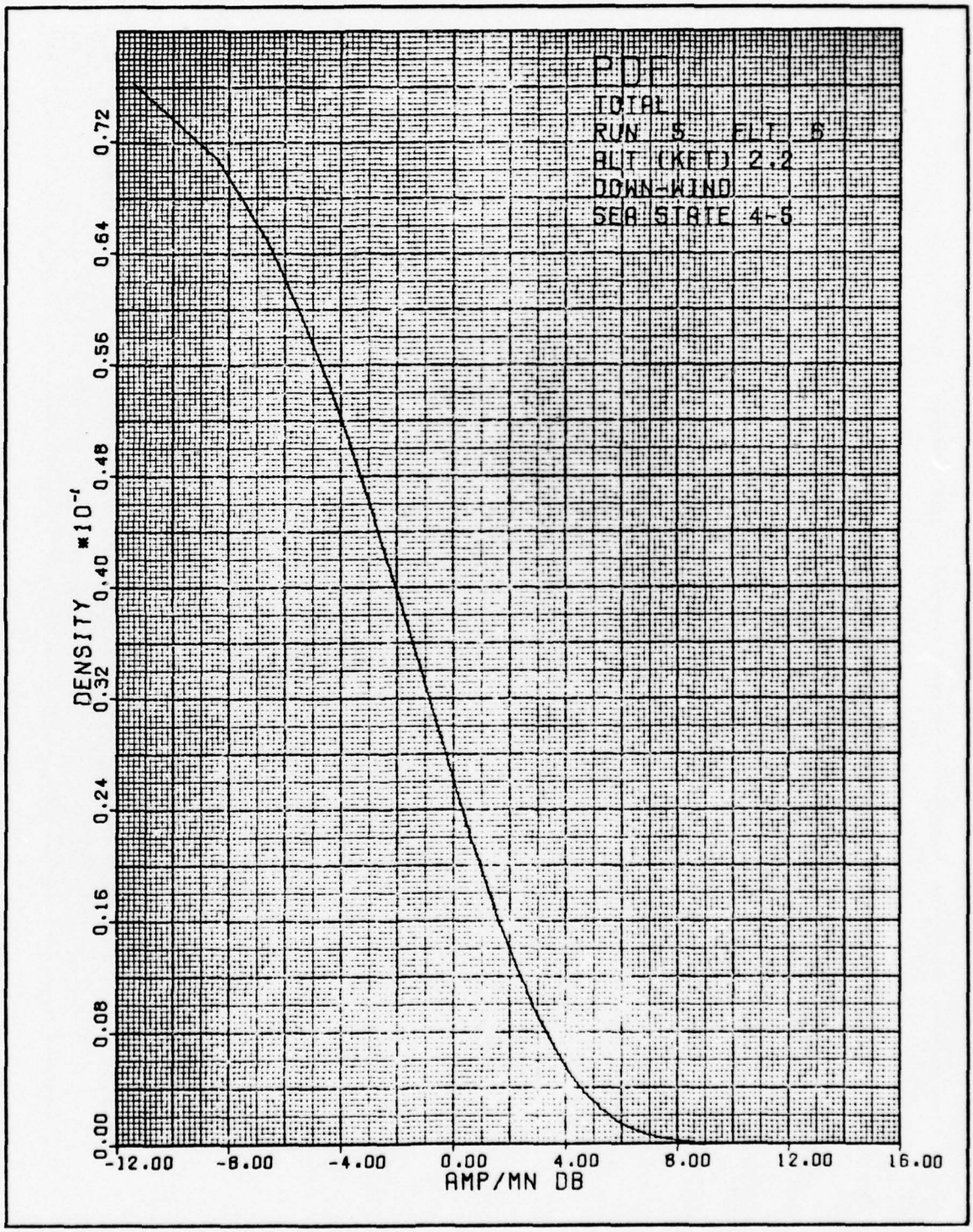

Figure 9-3 Total PDF

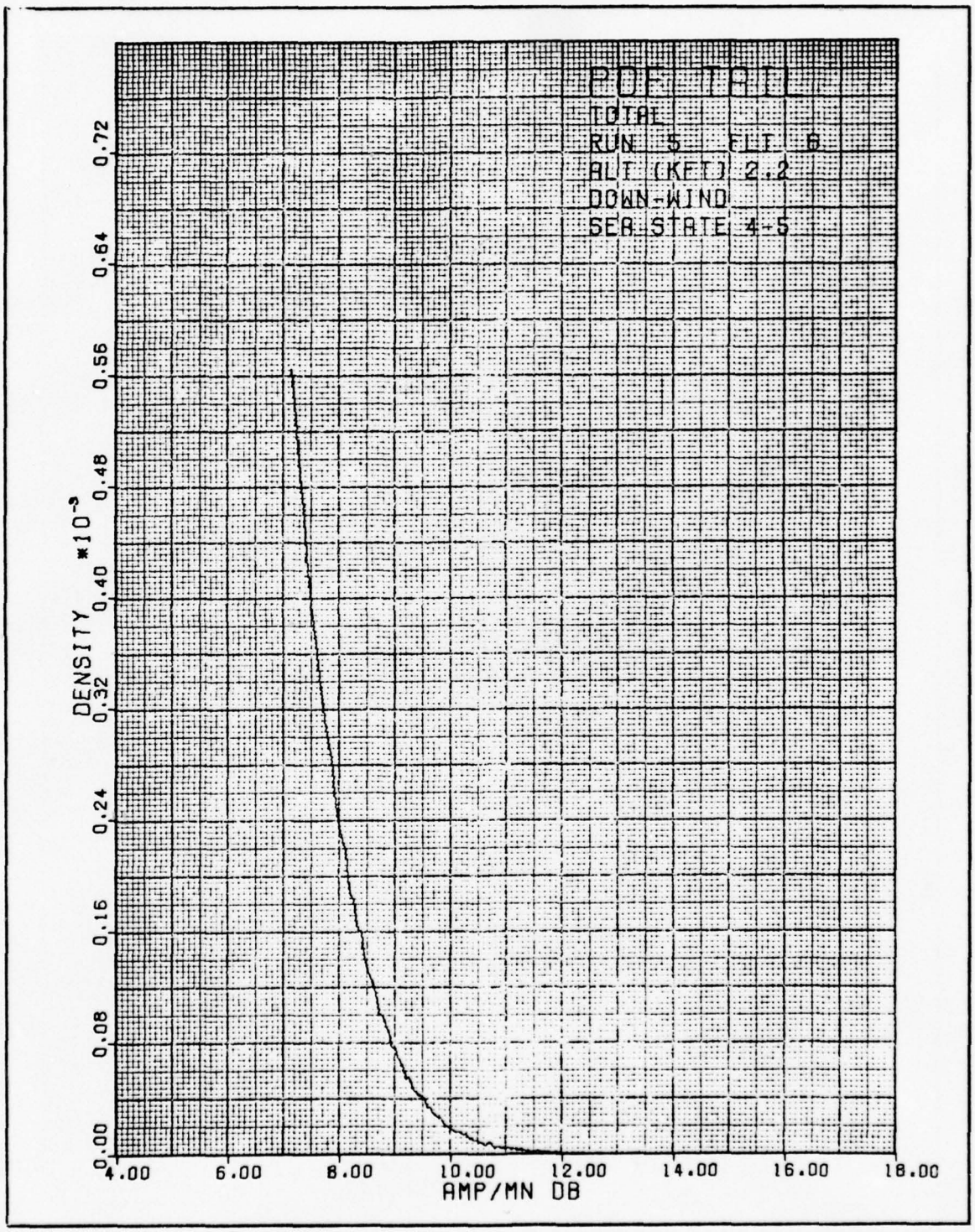

Figure 9-4 PDF Tail

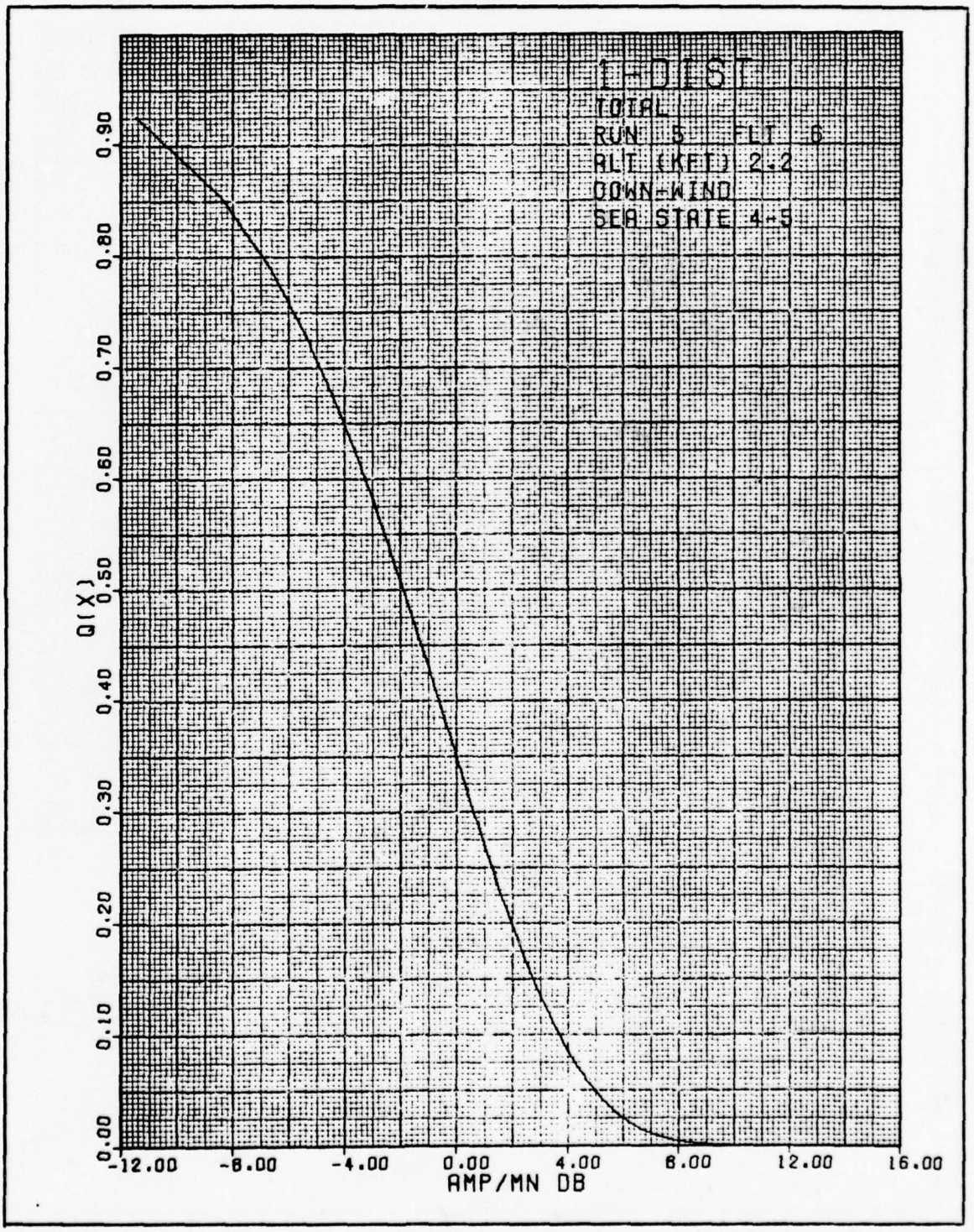

Figure 9-5 Q Plot (1-Dist)

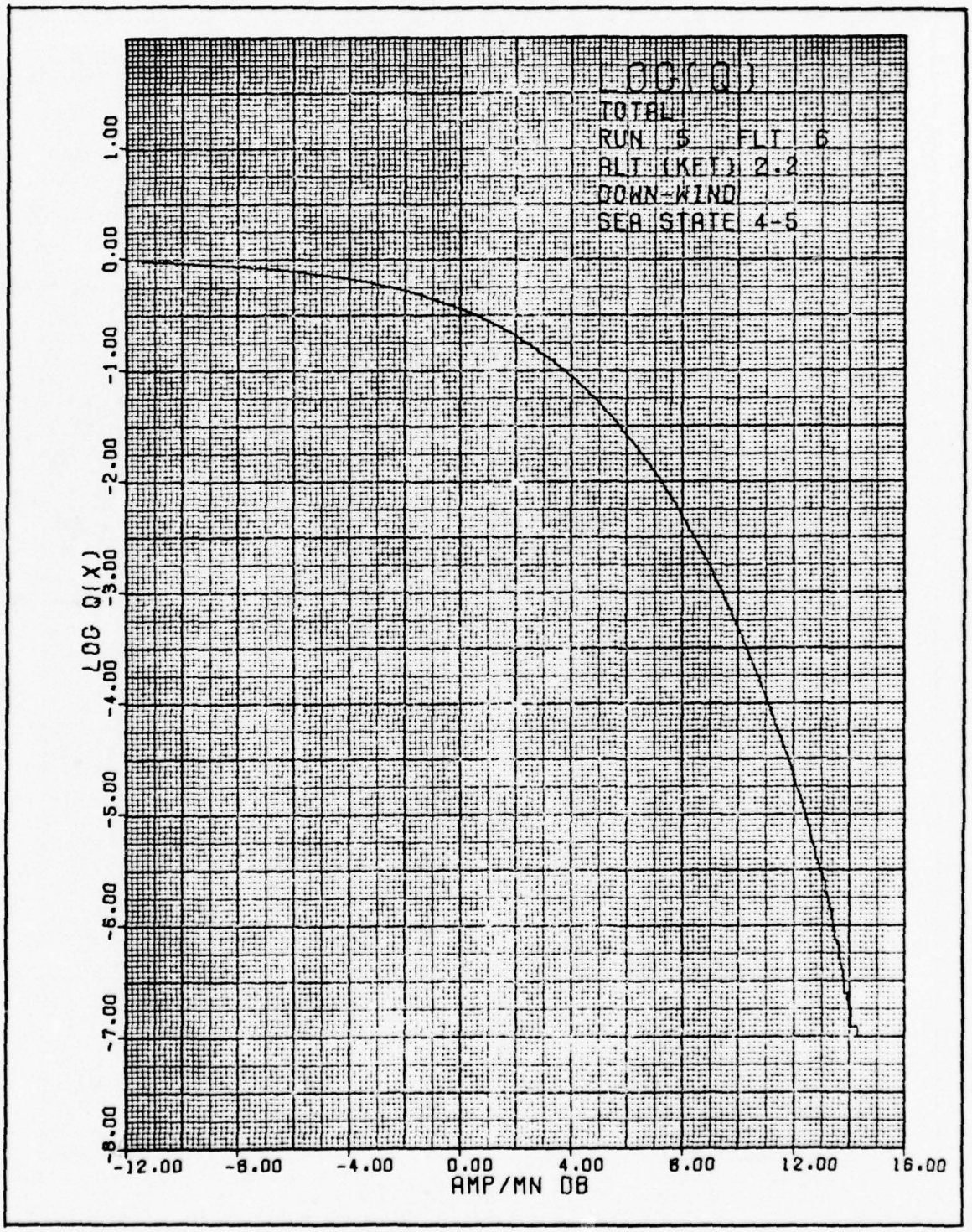

Figure 9-6 Log (Q)

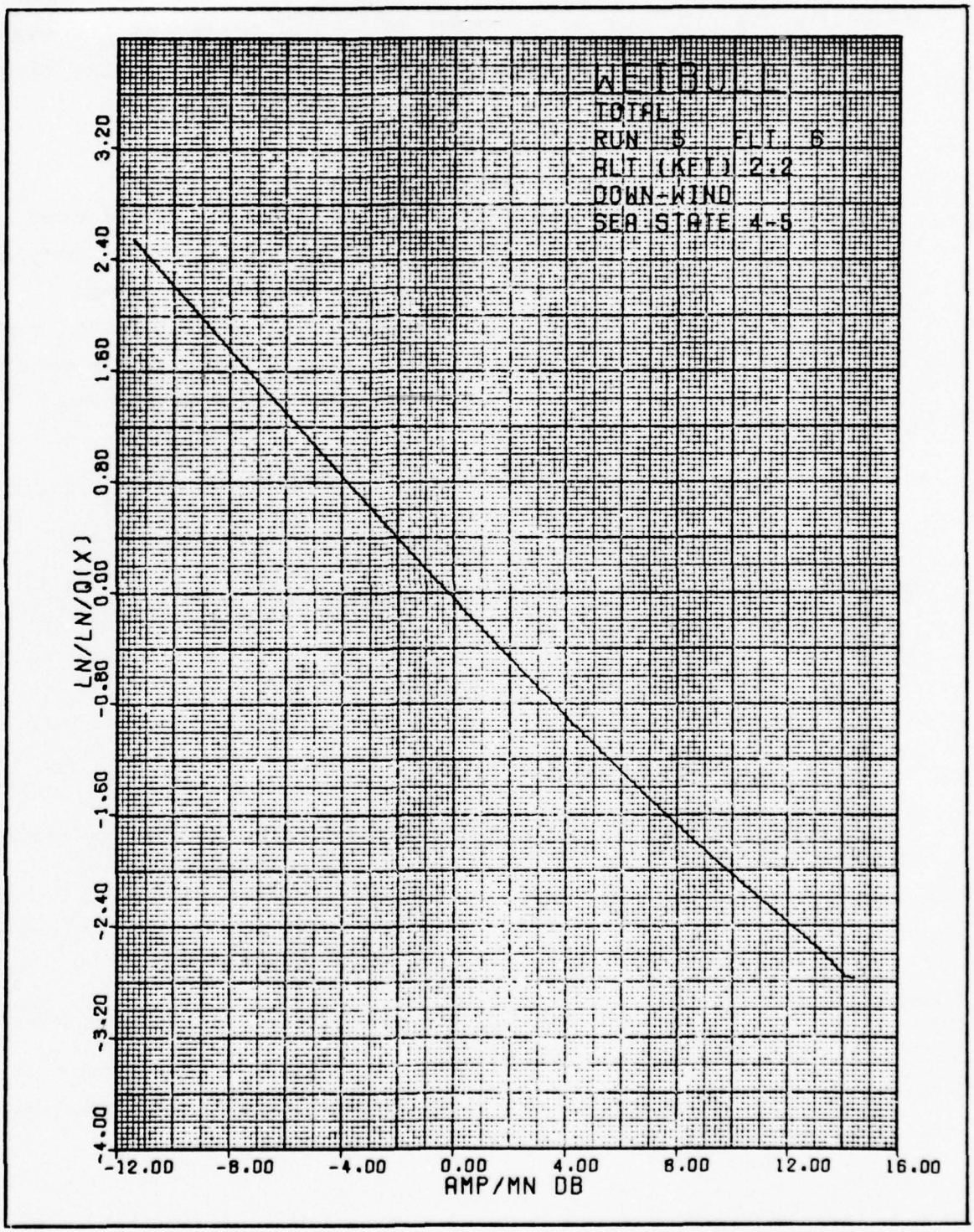

Figure 9-7 Weibull Plot

Weibull plots are used in a number of specialty fields for statistical analysis. This representation is presented to give those familiar with it a better insight into the data.

9.1.2 Total Histograms (A)

Total-A Histograms are again constructed from all the valid data in a run. Type-A histograms however remove the gain variation from range gate to range gate. (These variations are more due to to collection system variations than in the data.) To form these Type-A histograms the range gate histogram R_j is created for each range gate by summing the clutter histogram in that range gate.

$$R_j = \sum_{i=1}^{N\tilde{}50} H_{ij}$$

Each of these is then normalized to place the mean at 10.

$$R_j = r_{jk}$$

$$r_{jk} = r_{jk} \cdot 10 \Big/ \sum_{L=1}^{1024} L \cdot r_{jL}$$

These normalized range gate histograms are then summed to obtain the TOTAL-A histogram.

$$A = \sum_{j=10}^{15} \widehat{\sum_{i=1}^{\tilde{}50} H_{ij}} = \sum_{j=0}^{15} \widehat{R_j}$$

TOTAL-A PDF is shown in Figure 9-8 and its tail as Figure 9-9.

Transformations of the data corresponding to those described in Subsection 9.1.1 were used to obtain the remaining representations:

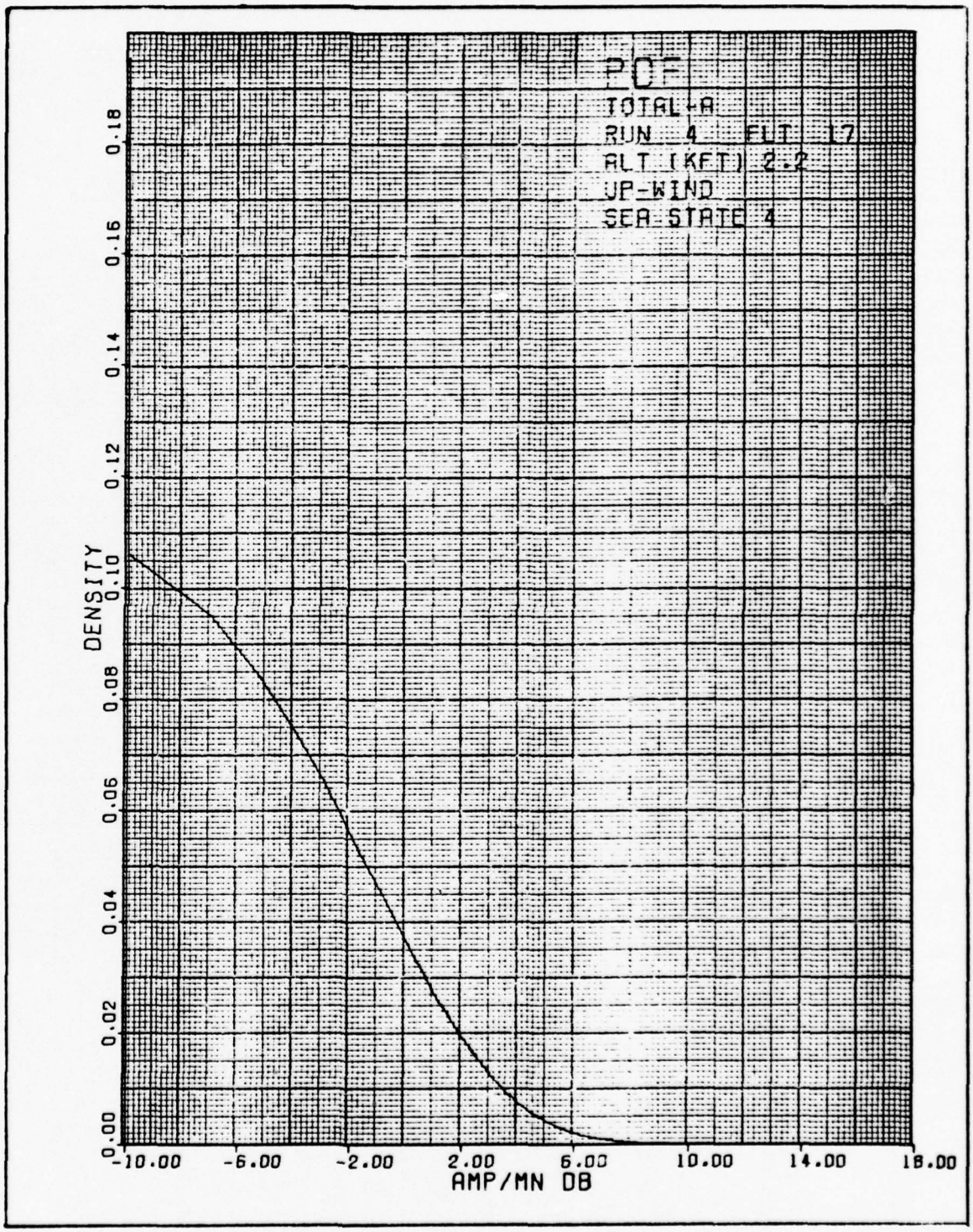

Figure 9-8 PDF Total-A

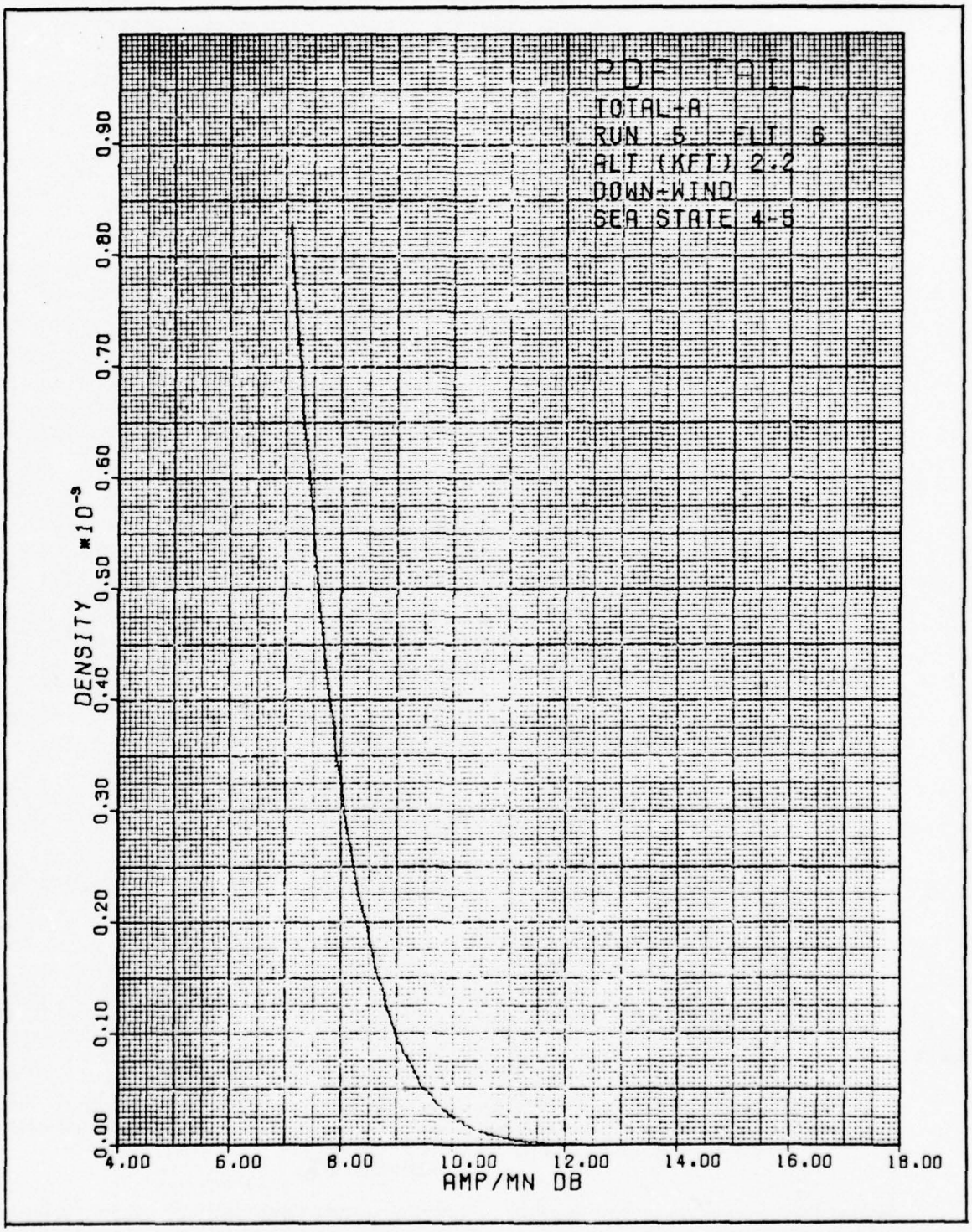

Figure 9-9 PDF Tail

TOTAL-A Q plot - Figure 9-10;
TOTAL-A Log Q plot - Figure 9-11;
TOTAL-A Weibull plot-Figure 9-12.

9.1.3 Total Histogram (N)

Type-N histograms were normalized by the local mean instead of the long term or range gate mean, i.e., each clutter histogram H_{ij} was normalized before summation.

$$N = \sum_{j=0}^{15} \sum_{i=1}^{\sim 50} H_{ij}$$

These TOTAL-N histograms are again found in each display representation with examples as follows:

TOTAL-N - PDF - Figure 9-13;
TOTAL-N - PDF tail - Figure 9-14;
TOTAL-N - Q plot - Figure 9-15;
TOTAL-N - Log Q - Figure 9-16;
TOTAL-N - Weibull plot - Figure 9-17.

9.1.4 Statistical Parameters

A number of statistical parameters are computed from each histogram. These are listed in Table 9-1. These statistical parameters are listed by the computer for each H_{ij}, R_j, T_i histogram as well as various types of Total histograms computed. The statistics of the sub sets were used to identify data problems. Since there are 500-1000 sets of parameters for each run only the parameters for the Total-A are included in the report. A typical print out of the Total-A statistical parameters is shown in Table 9-2.

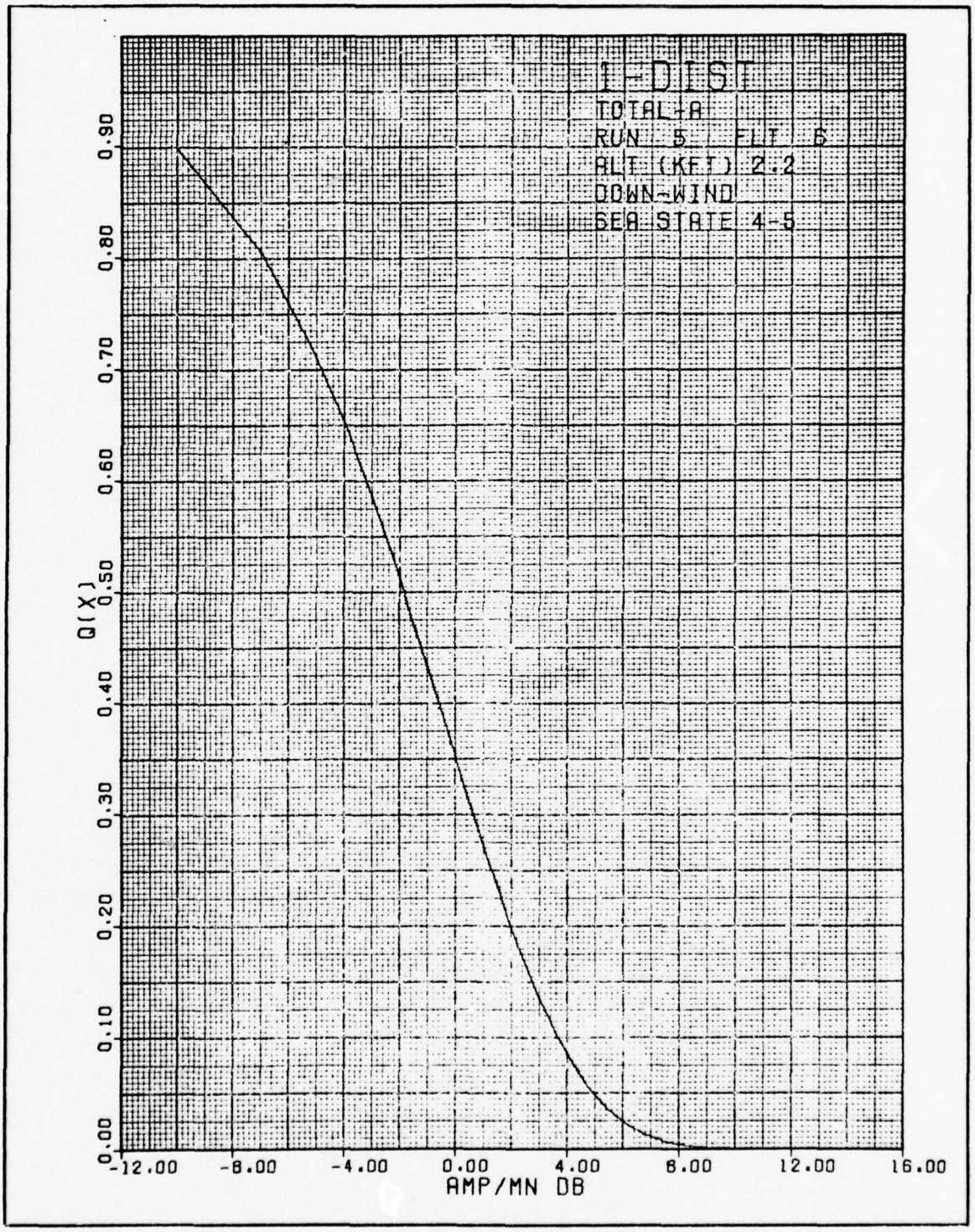

Figure 9-10 Q Total-A

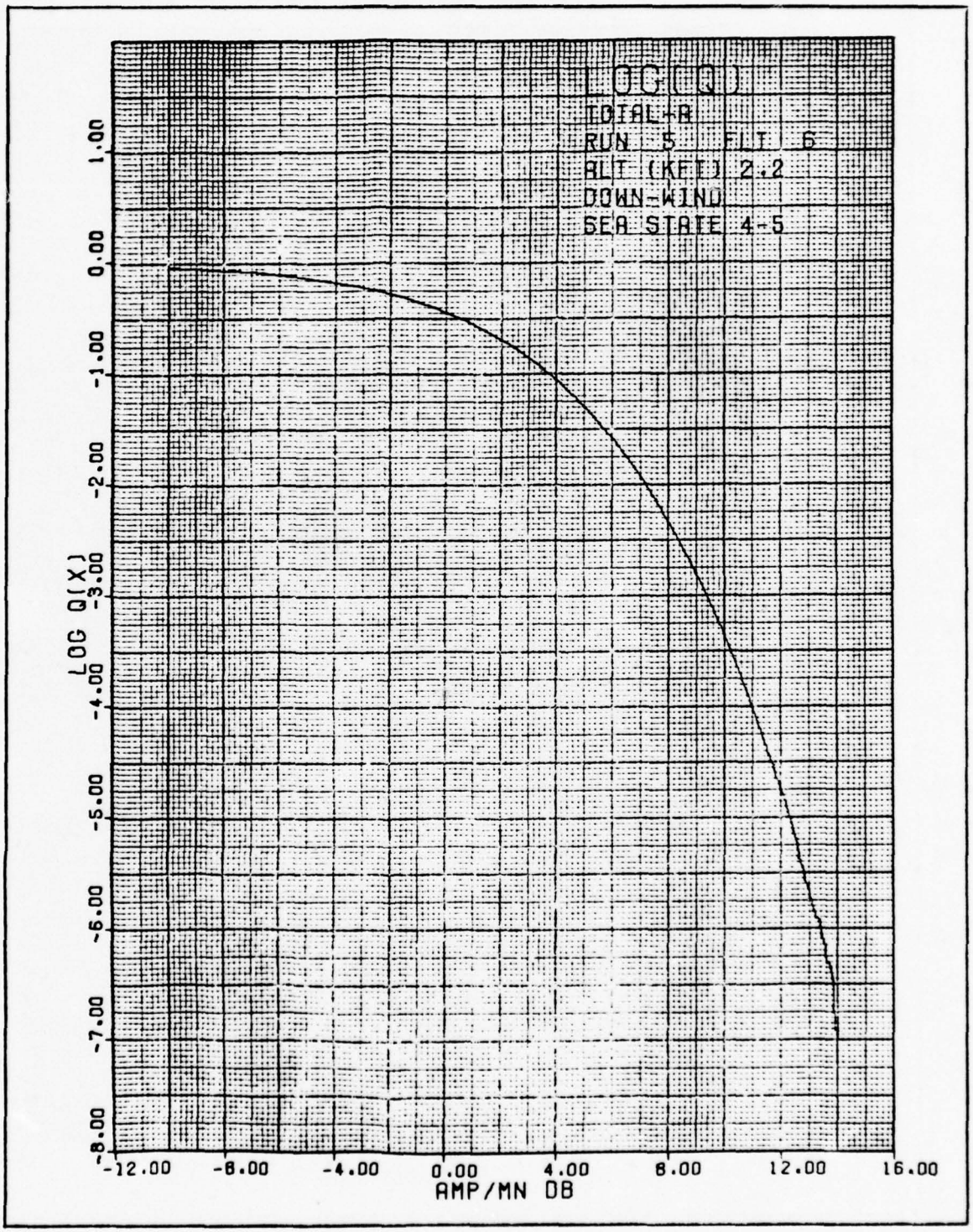

Figure 9-11 Log (Q) Total-A

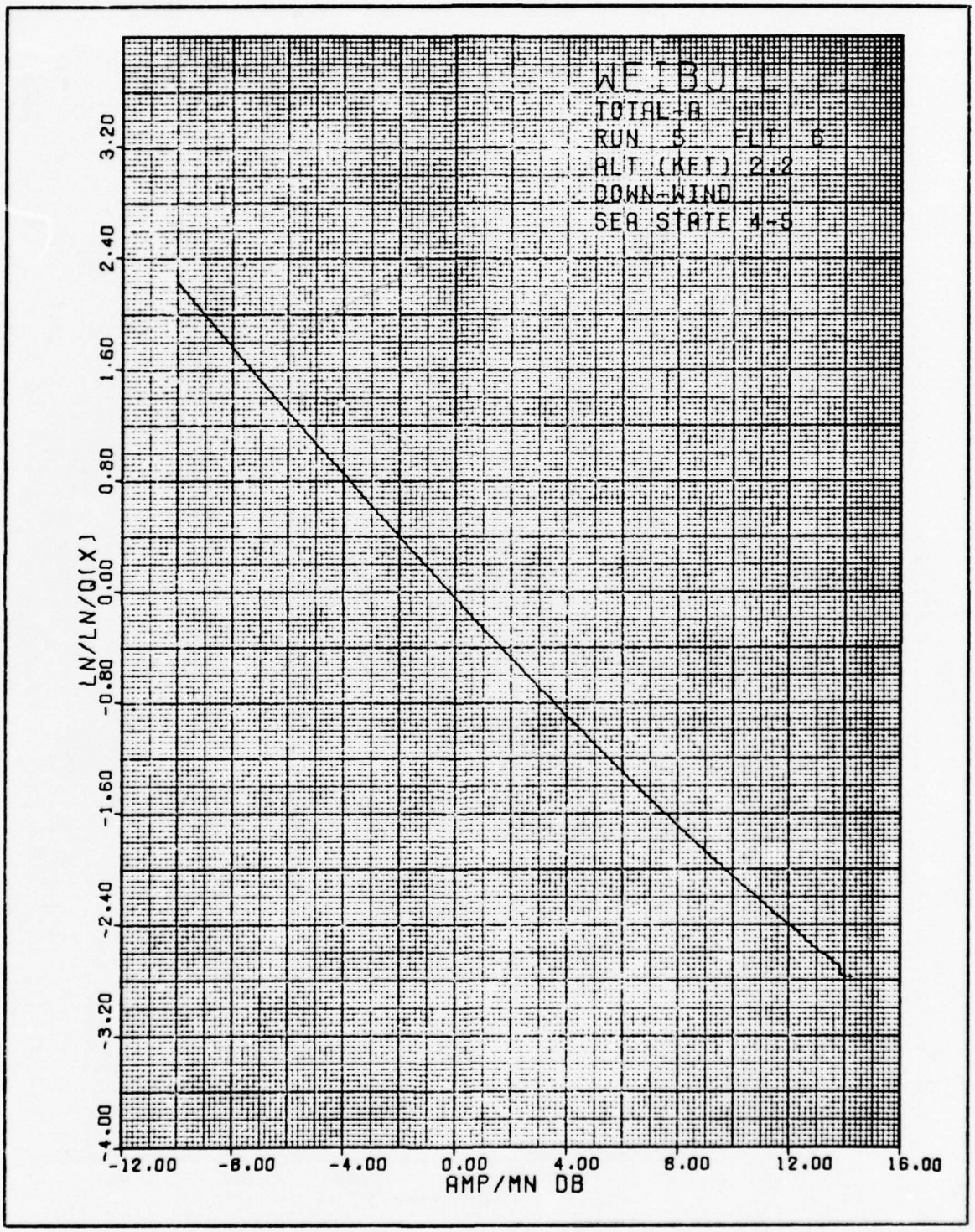

Figure 9-12 Weibull Total-A

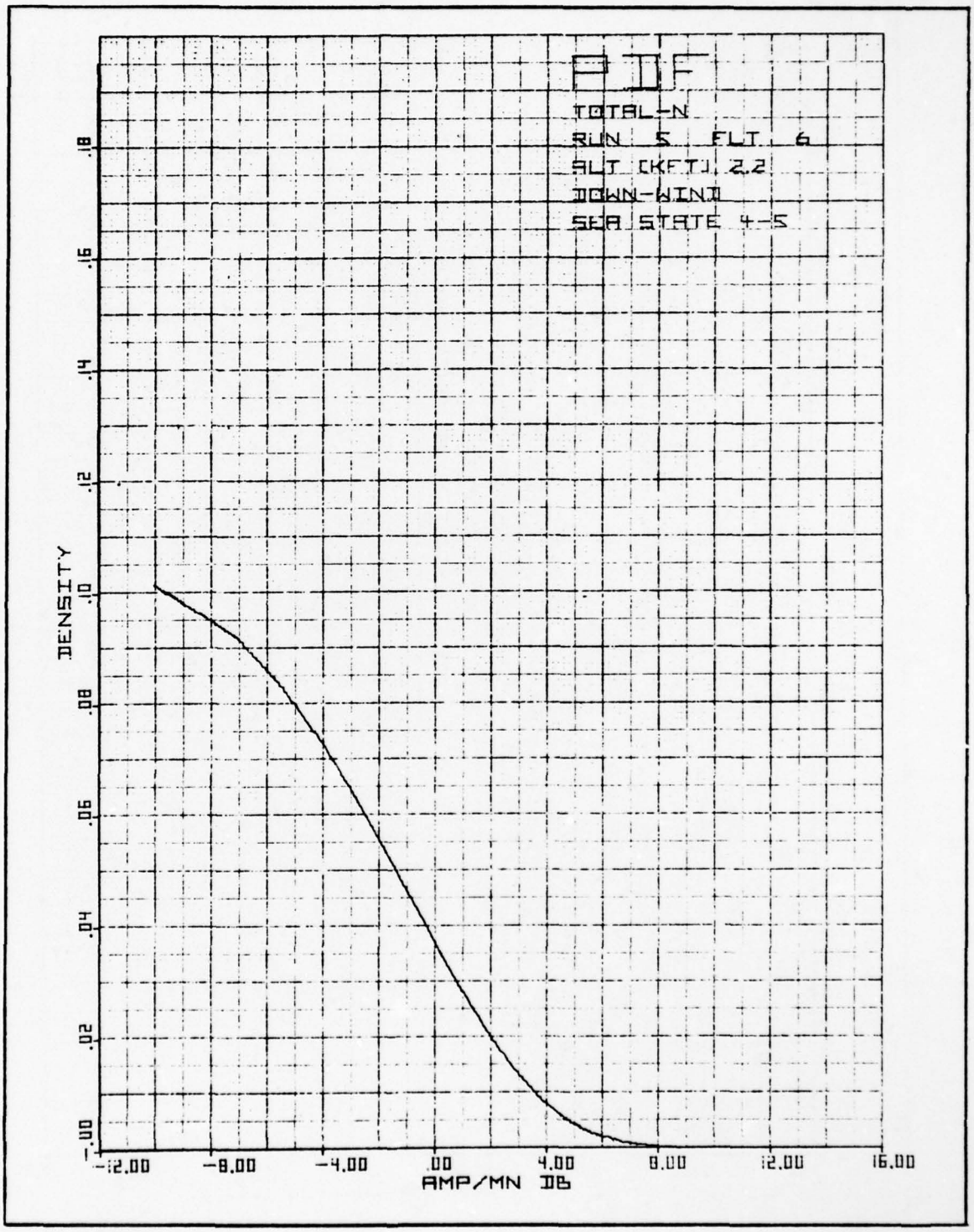

Figure 9-13 PDF Total-N

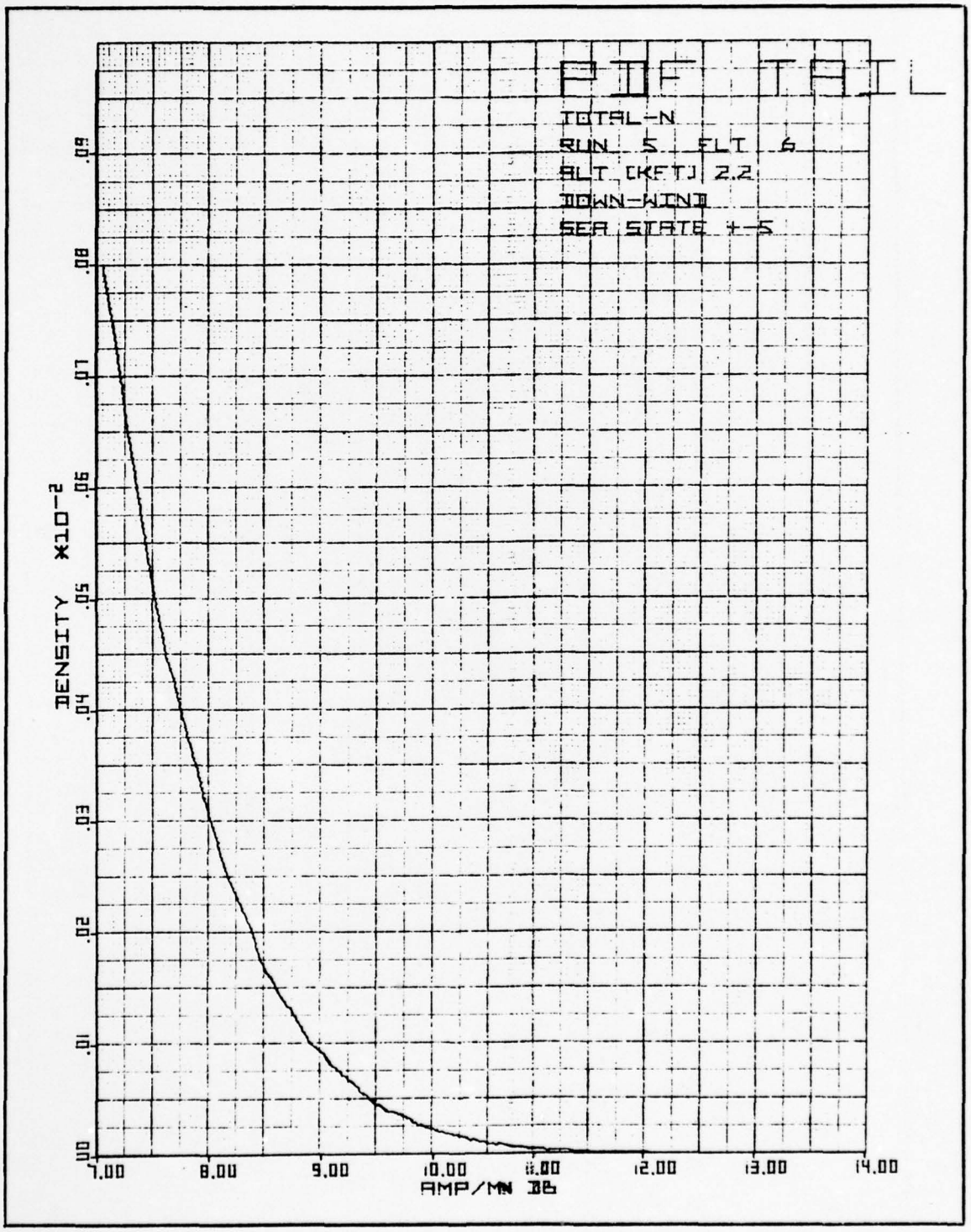

Figure 9-14 PDF Tail Total-N

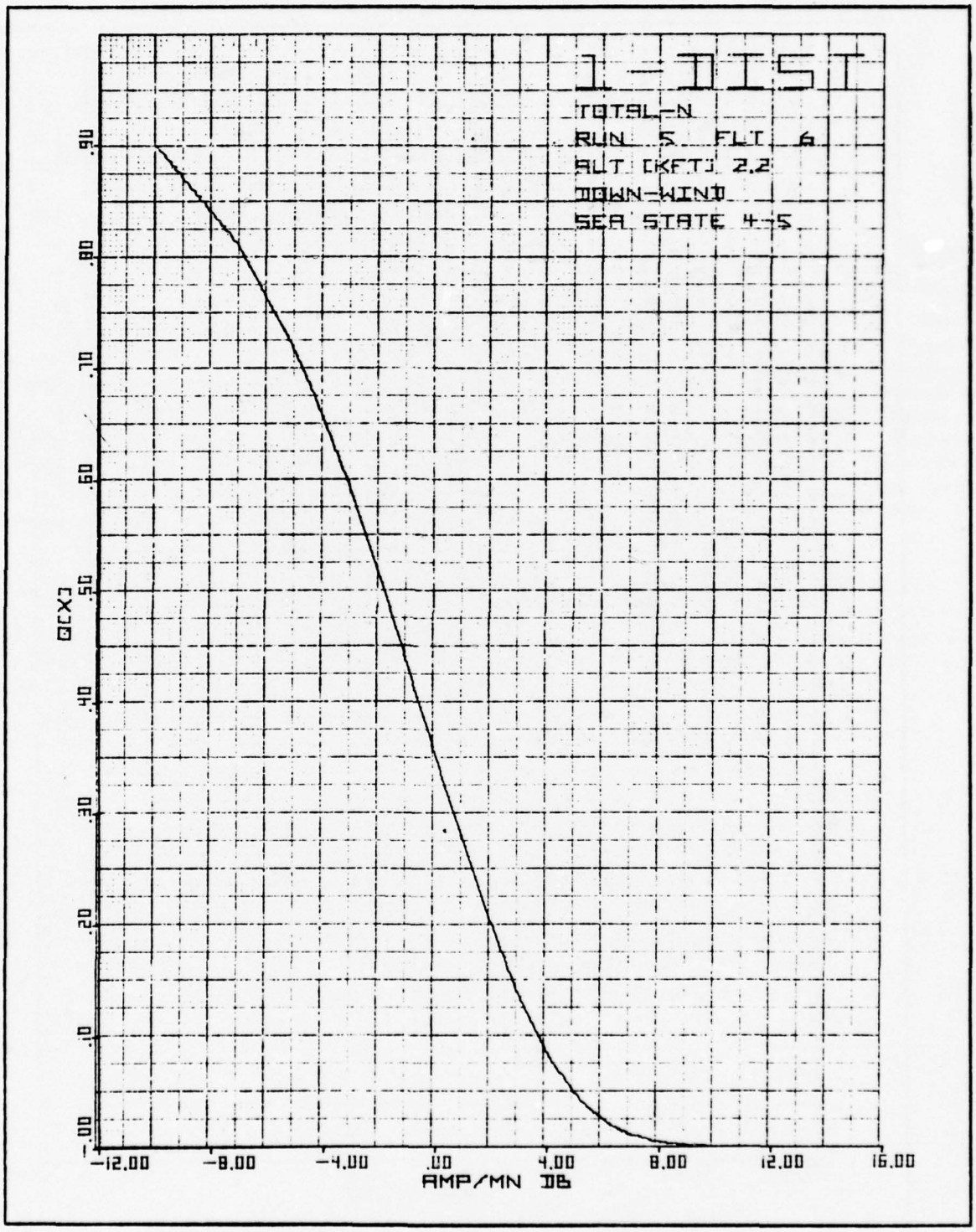

Figure 9-15 Q Plot Total-N

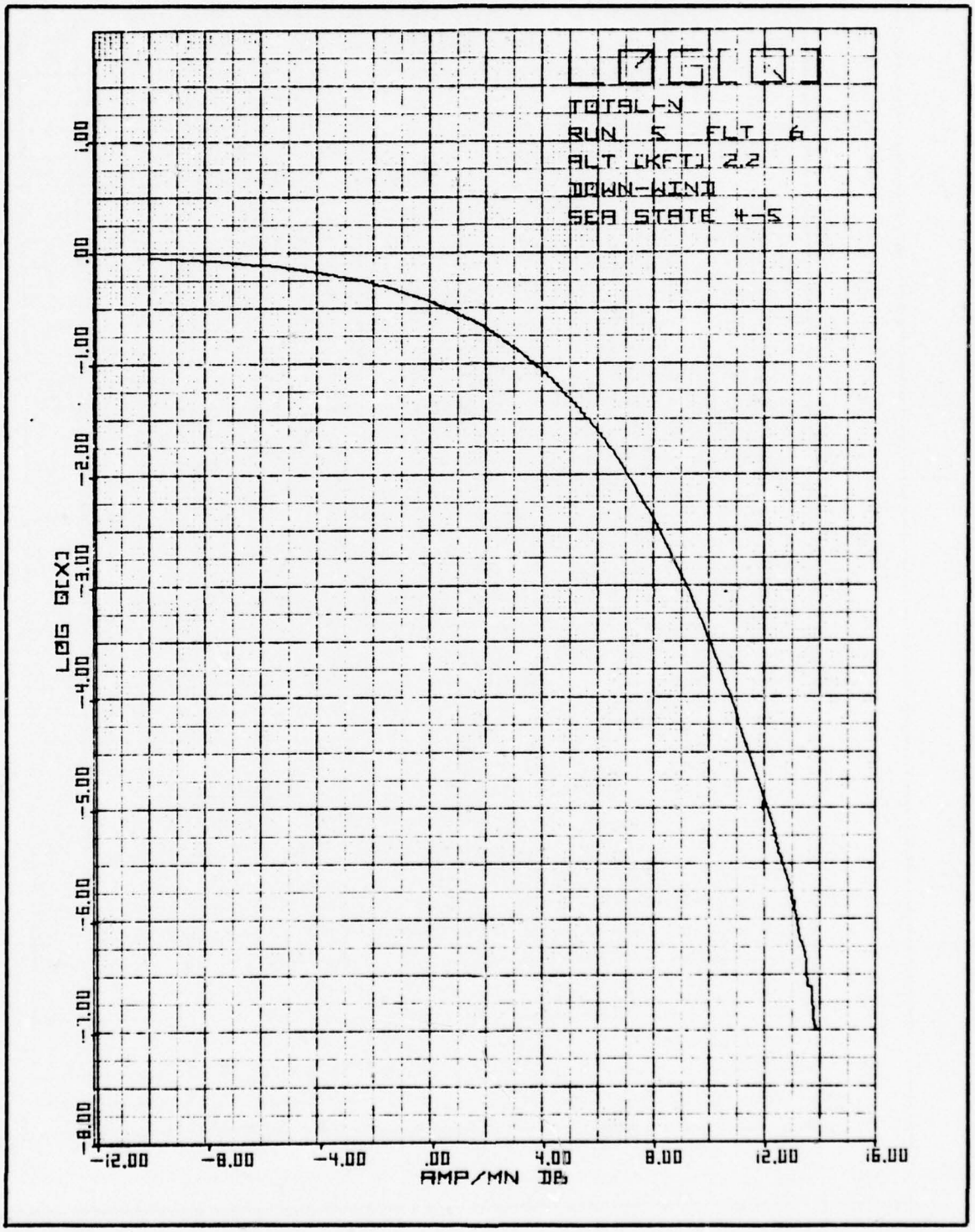

Figure 9-16 Log Q Total-N

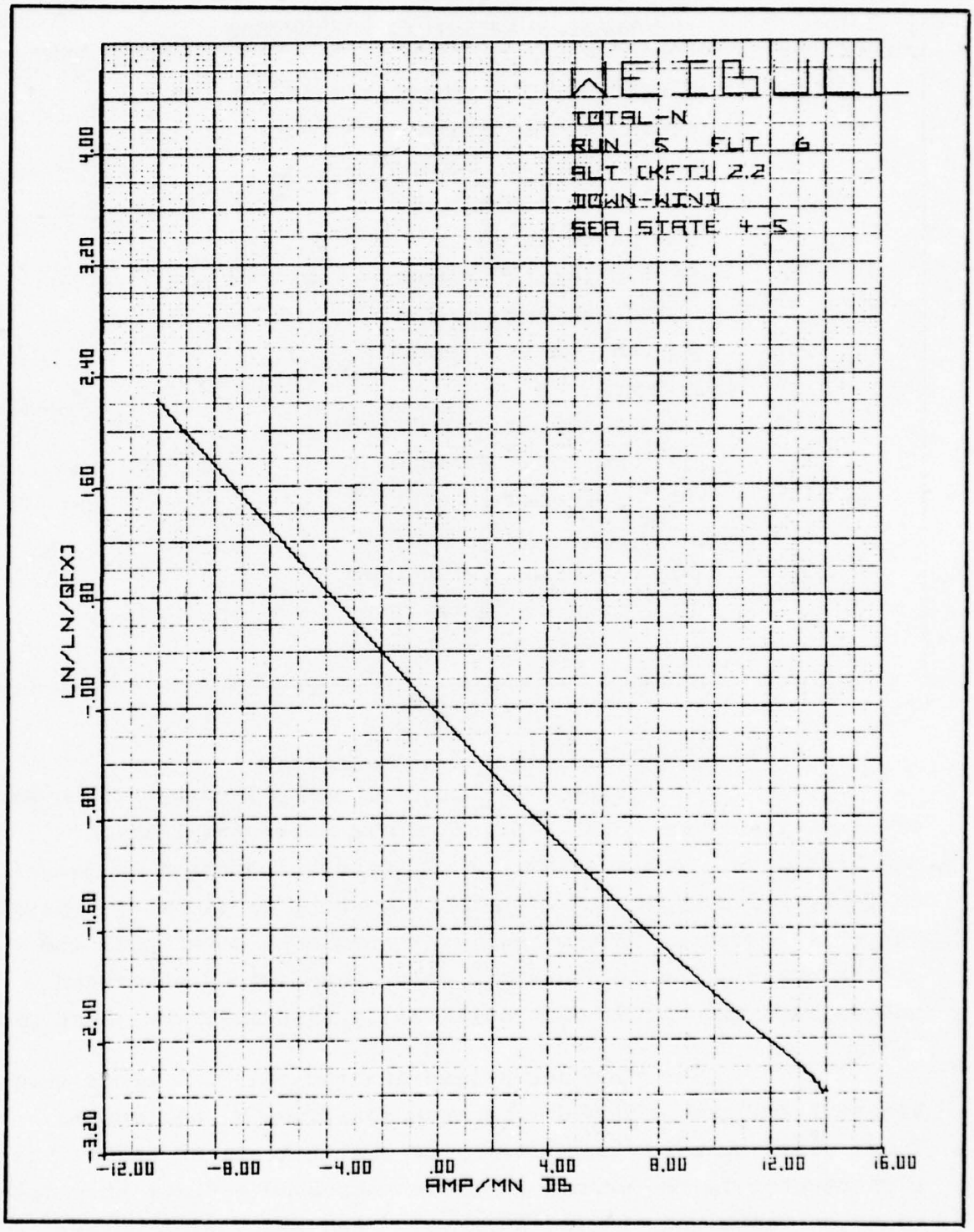

Figure 9-17 Weibull Total-N

TABLE 9-1
STANDARD STATISTICAL PARAMETERS

1*	First absolute moment = mean
2	Second absolute moment
3	Third absolute moment
4	Fourth absolute moment
5*	Max value in dB
6	Second central moment = variance
7	Third central moment
8	Fourth central moment
9*	Median
10*	10^{-1} point on Q function
11*	10^{-2} point on Q function
12*	10^{-3} point on Q function
13*	10^{-4} point on Q function
14	10^{-5} point on Q function
15	10^{-6} point on Q function

9.1.5 Statistics versus Time Plots

Histograms, T_i, are formed by summing histograms within a time zone. The statistics are extracted from this sum histogram. The statistical parameters indicated by asterisks on Table 9-1 are plotted as a function of i or time. A typical output is shown as Figure 9-18. It should be noted that the differential gains in the range gates have not been removed before summation producing artificially high tails on these plots.

The mean normalized statistical line plots (e.g., Figure 9-19) are produced from mean moralized T_i histograms. These plots show the consistency of the statistical parameters with respect to the mean. Note the increased effects of sample noise on the higher tails, i.e., 10^{-5} and max. value points.

TABLE 9-2
TYPICAL PRINTOUT OF THE TOTAL-A STATISTICAL PARAMETERS

J	AA(J)	Description
1	10.00390908	Absolute moment 1 (mean)
2	221.39338474	Absolute moment 2
3	8122.29036380	Absolute moment 3
4	437393.91676312	Absolute moment 4
5	24.26511261	Maximum value (dB)
6	121.21320290	Central moment 2 (σ^2)
7	3479.91574387	Central moment 3
8	215277.90684270	Central moment 4
9	7.78151250	Median
10	13.61727836	10^{-1} on Q (dB)
11	17.07570176	10^{-2} on Q (dB)
12	19.29418926	10^{-3} on Q (dB)
13	20.93421685	10^{-4} on Q (dB)
14	22.27886705	10^{-5} on Q (dB)
15	23.36459734	10^{-6} on Q (dB)

UNCLASSIFIED

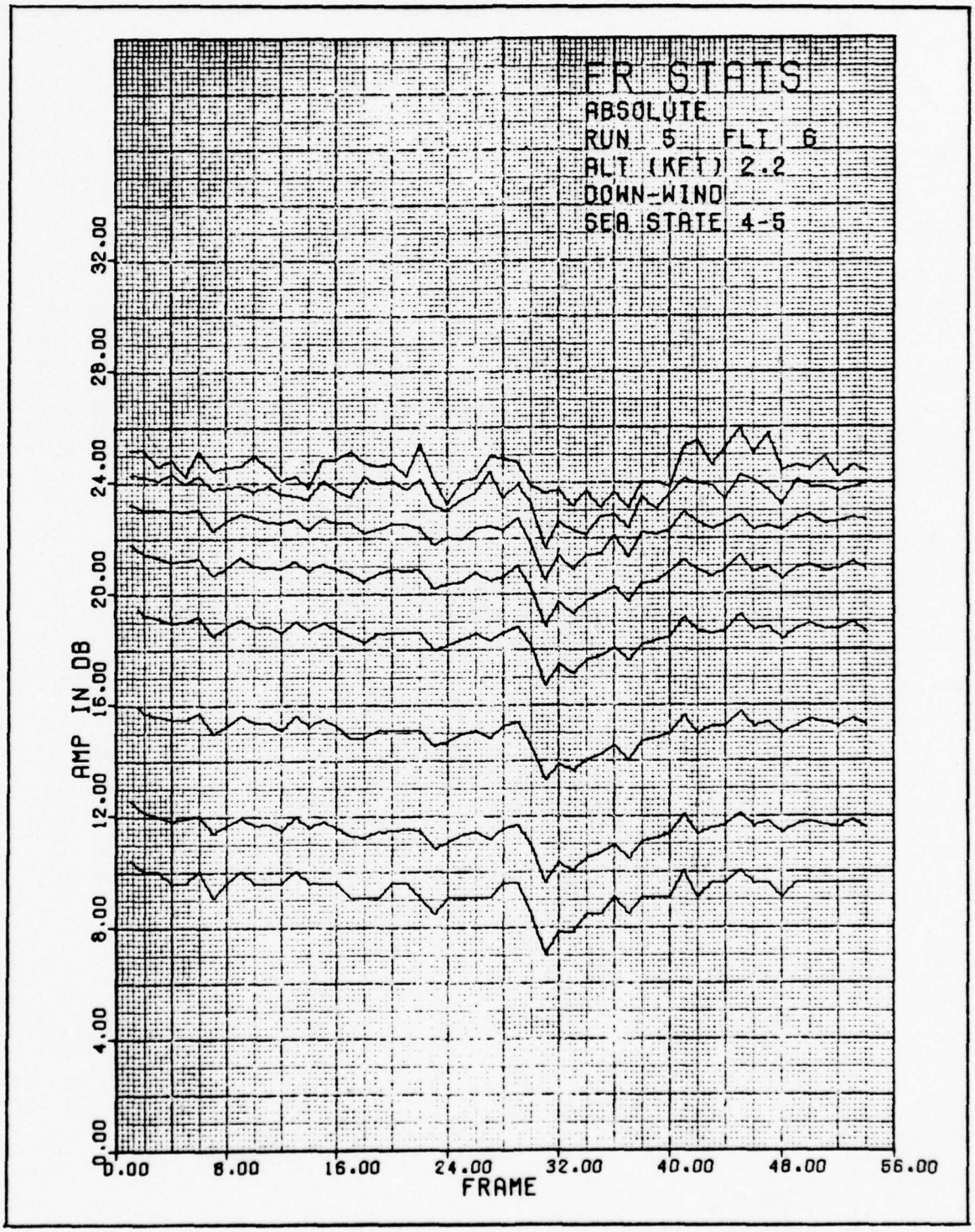

Figure 9-18 Frame Statistics-Absolute

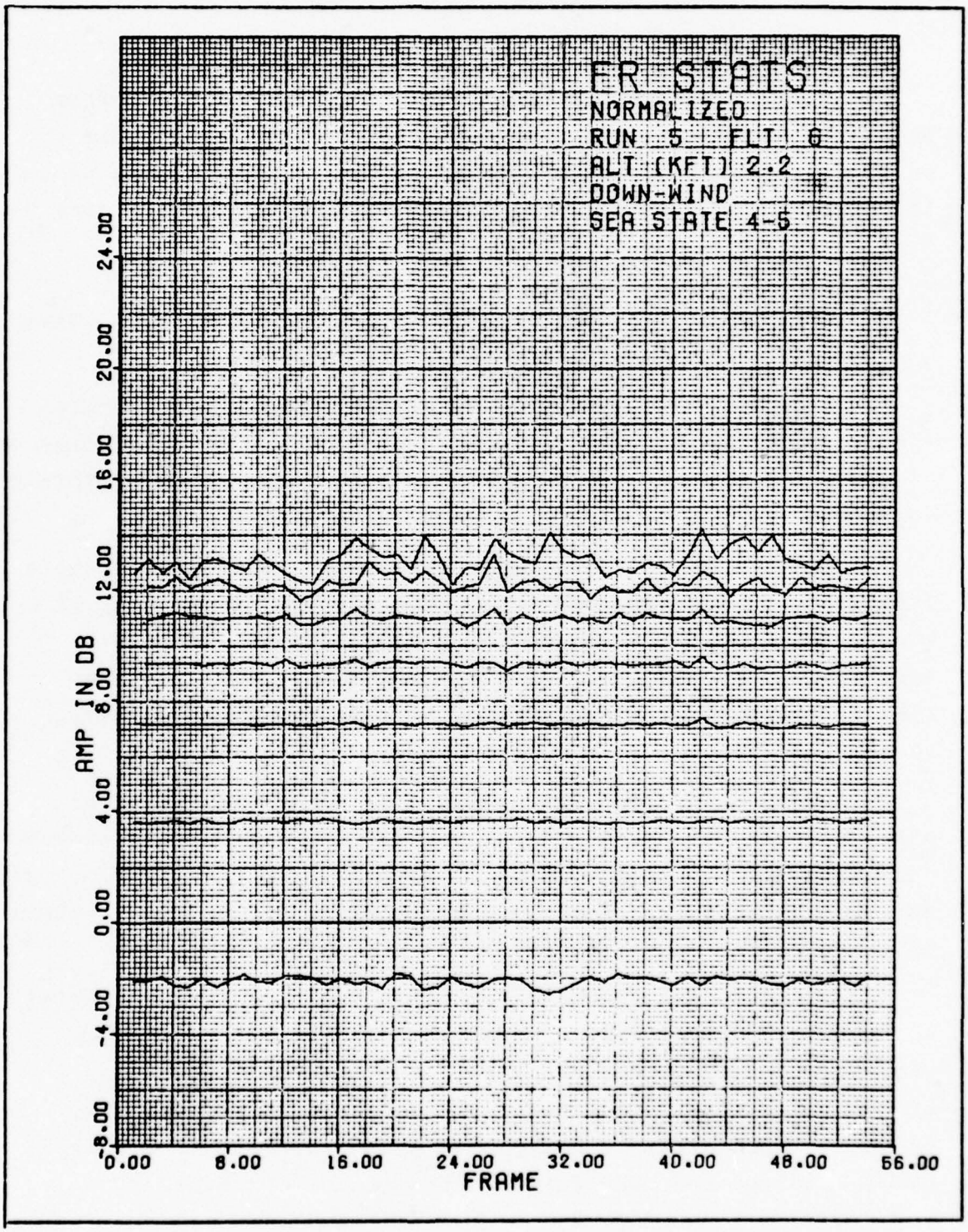

Figure 9-19 Frame Statistics-Normalized

9.1.6 Statistics versus Range Gate Plots

The same starred statistics in Table 9-1 from the range gate histogram R_j are plotted against range gate (j) in Figure 9-20. In the normalized range gate statistics plots these parameters from $\hat{R}_j$ are plotted against j. (See Figure 9-21)

9.2 Hit Analysis Outputs

Hit Analysis outputs are Hit Maps, Hit Counts vs. Time and Conditional Probability Maps.

Hit Maps are generated by synthetic aperture mapping techniques. The hit map is used to provide a graphic display of sea clutter echoes in a cross-range vs. down-range coordinate system.

Hit Count vs. Time plots are generated by summing hits within each range gate and total hits for all range gates in blocks of either 20 (fine grain) or 100 (coarse grain) FFT time frames (one FFT = 0.009142857 second). Hit Counts vs. Time plots provide temporal information regarding the nature of sea clutter.

When used together Hit Maps and Hit Counts vs. Time plots provide data validation information and generally expose any anomalies out in the tails of distribution functions. Real targets, such as ships or buoys, may be identified from spatial and temporal information contained in these outputs.

Conditional Probability Maps provide means for spatial and temporal characterization of sea clutter echoes in the vicinity of rare events. A rare event has been defined as a hit exceeding the 10^{-5} probability threshold. The vicinity of such a rare event is defined by a 15 X 15 X 15 = 3375 cell range-doppler-time cube centered on the 10^{-5} probability hit.

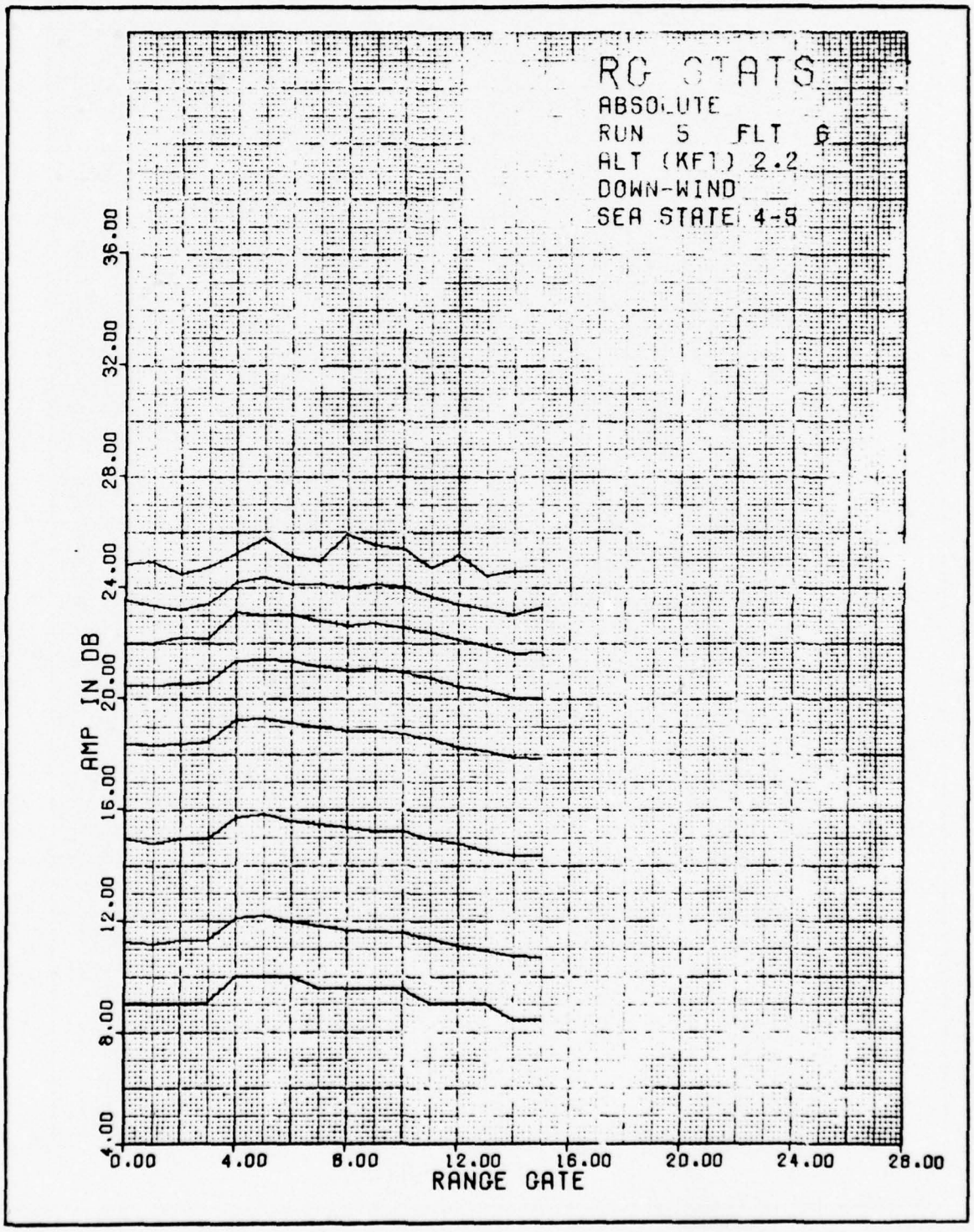

Figure 9-20 Range Gate Statistics-Absolute

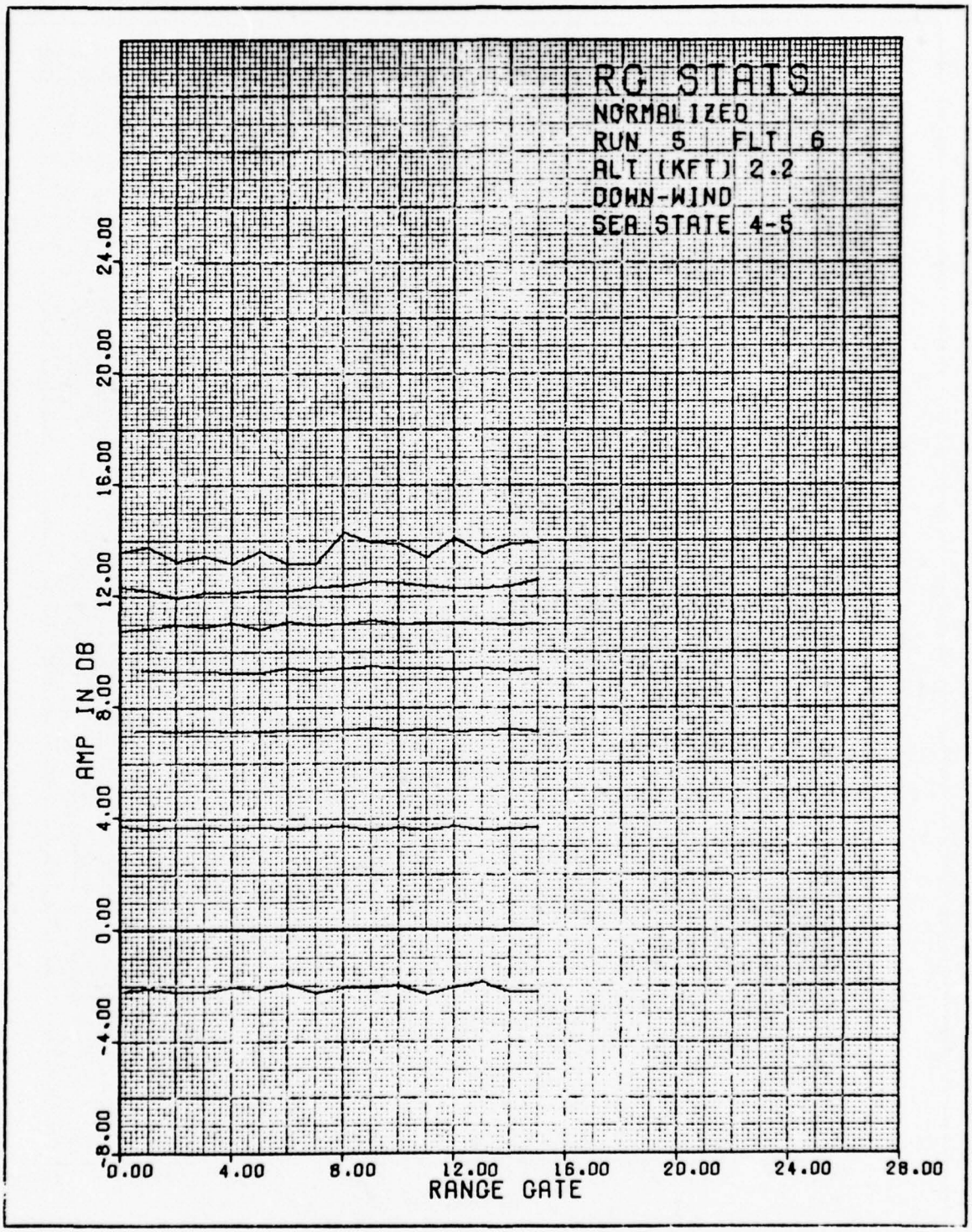

Figure 9-21 Range Gate Statistics-Normalized

These maps provide probabilistic information regarding how long events exceeding a 10^{-3} threshold persist and indicate the region of space over which such events are extended.

9.2.1 Hit Maps

A typical Hit Map plot for Flight 6, run 5 (0605) is presented in Figure 9-22. Number of hits exceeding a nominal 10^{-3} (A-type) threshold in each range gate are plotted as a function of down-range distance in 100's of feet. The range gate sum (bottom plot) is computed by summing hits in all range gates and multiplying the result by 0.2 at each down-range position.

The ordinate scale factor was set at ten hits per major division for all plots. The smallest division is one hit, the quantum level of hit data. The range gate sum scale factor is 50 hits per major division (5 hits for the smallest division).

Down-range distance for a typical hit map is determined by aircraft velocity and run time duration (set during the aircraft flight test). Nominal values are 420 ft/sec and 300 seconds. Therefore, most runs are in the neighborhood of 126,000 ft. Variations in both aircraft velocity and run time during the flight test resulted in different map lengths for each run.

Total cross-range extent varies with altitude from 1738 feet at 1100 ft altitude to 2218 feet at 3300 ft altitude. For Flight 8 run at 500 ft altitude, cross-range extent is 1706 ft. Radar slant range resolution was approximately 110 feet.

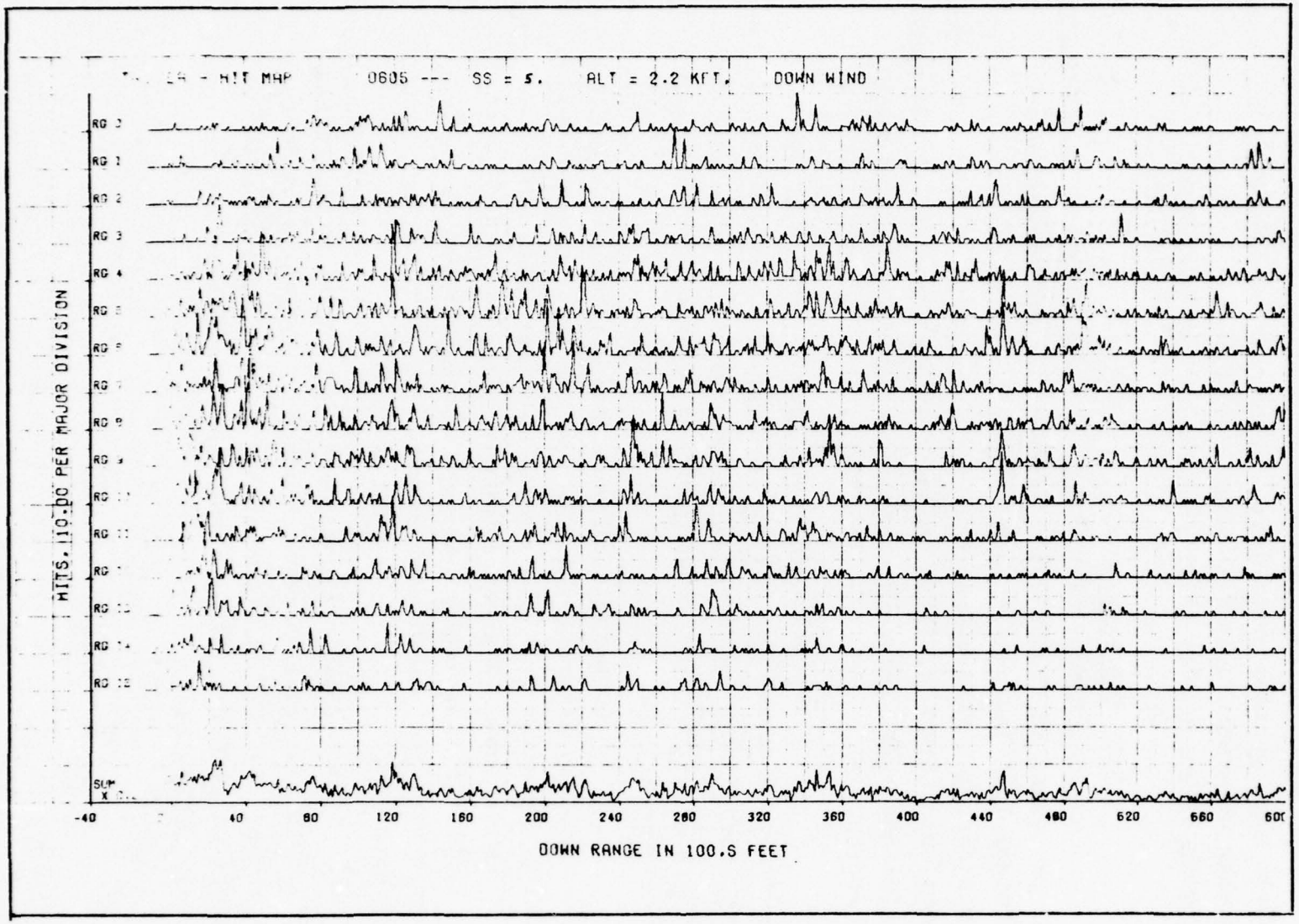

Figure 9-22 Hit Maps

The following scale factors are useful for relating hit map data to time and hit counts vs. time data:

Cross-range distance = velocity X time
One FFT frame = 0.0091428571 second
20 FFT frame = 0.18285714 second
100 FFT frames = 0.91428571 second
V = 420 ft/sec in all hit maps except Flight 6 and 8, Run 12. Velocities used for the latter flights are tabulated below:

Flt/Run	Velocity (ft/sec)
0601	470
0602	430
0603	439
0604	459
0605	430
0606	430
0607	474
0608	486
0609	436
0812	350

Each hit map plot is labeled by Flight/Run Key, sea state (1 to 5), altitude, and wind direction (up, down or cross). The flight/run key is decoded as follows:

Flight Run Key = ABCD
A = 0 for East Coast, 1for West Coast
B = Flight Number on either coast
CD = Run number (nominal 0 to 9)

In a few cases flight test runs were repeated. The "CD" number for these runs were 101, 102, ...,. For example, runs 1601 and 1602 were labeled 16101 and 16102 on the rerun.

9.2.2 Hit Counts vs. Time

Hit Counts vs. Time plots indicate mean numbers of hits exceeding a nominal 10^{-3} (A-type) threshold in each range gate. A range gate sum is computed as well. There are two sets of plots, fine and coarse, in the data base. Hit counts are averaged over 20 FFT time frames, or about 0.183 second, in the fine grain plots and over 100 FFT frames, or 0.914 second, in the coarse plots. In each presentation mean hit counts are computed by normalizing the sum by block size (i.e., 20 or 100 FFT frames). Examples of typical hit counts vs. time data are given in Figures 9-23 (Fine) and 9-24 (Coarse).

Because hit count range gate sums are normalized by block size, the scale factors were set equal to 0.2 hits per major division for both fine and coarse plots. The scale factor for the range gate sum of the bottom plot (obtained by summing over all range gates and multiplying the result by 0.2) is one hit per major division or 0.1 hit for the smallest division. Time duration for hit counts vs. time is nominally 300 seconds (32812.5 FFT frames). Receiver noise and calibration signals follow clutter data in each plot.

Each plot title lists flight/run key, sea state, altitude and wind direction.

9.2.3 Conditional Probability Maps

Examples of typical conditional probability maps are given in Figures 9-25 through 9-29. The first three plots are time, range, and doppler principal plane cuts through the

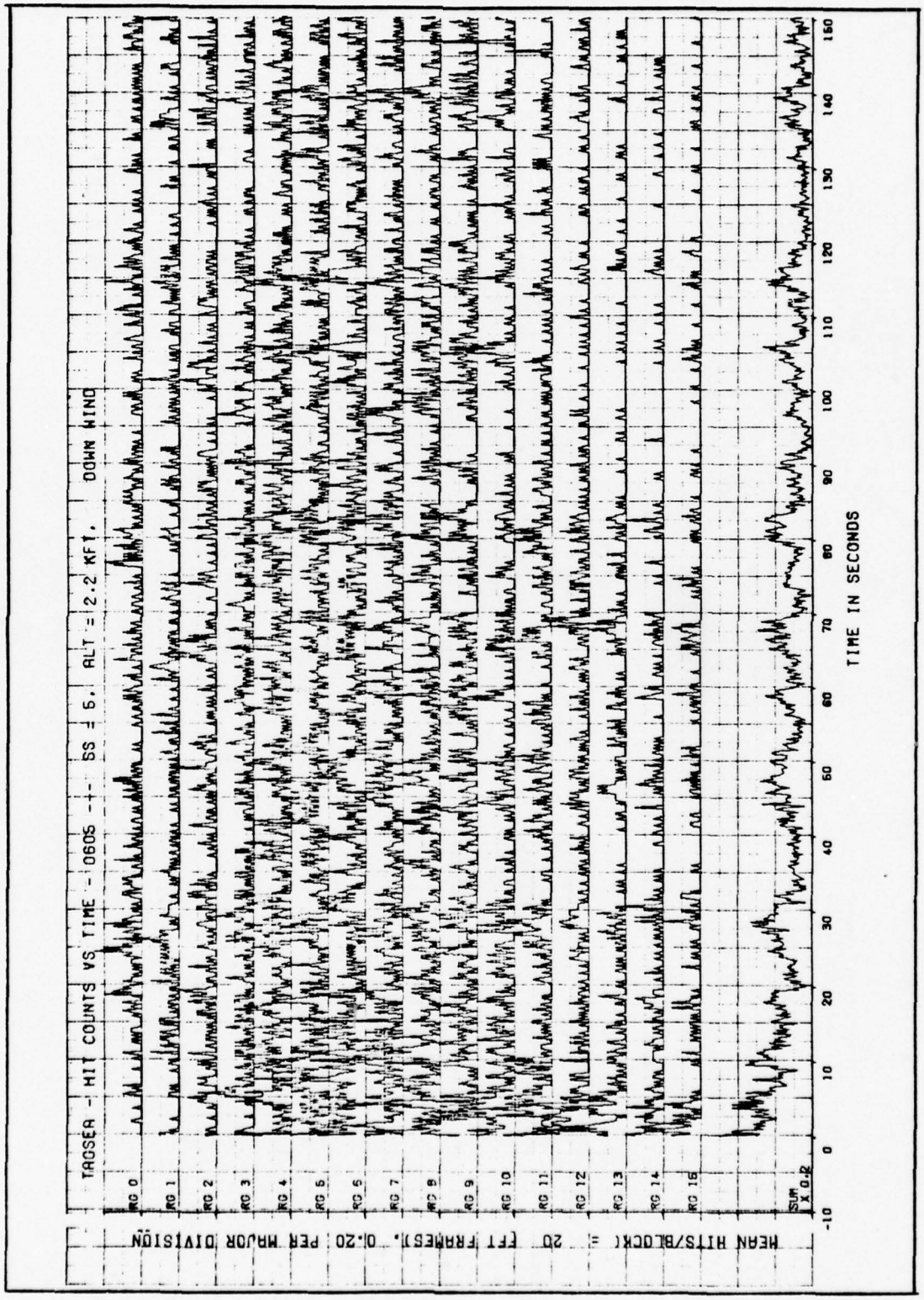

Figure 9-23 Hit Counts vs. Time (Fine Grain)

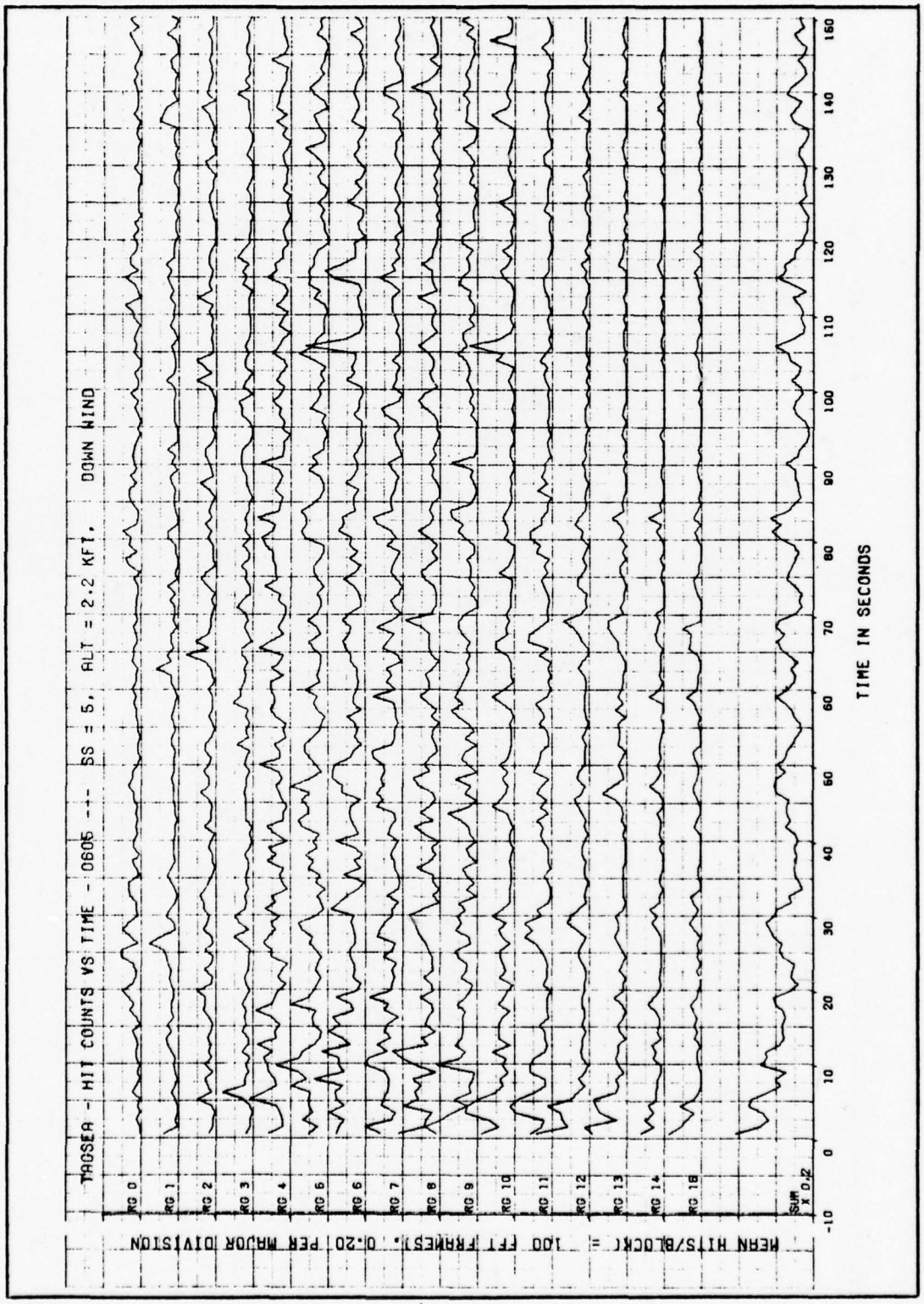

Figure 9-24 Hit Counts vs. Time (Coarse)

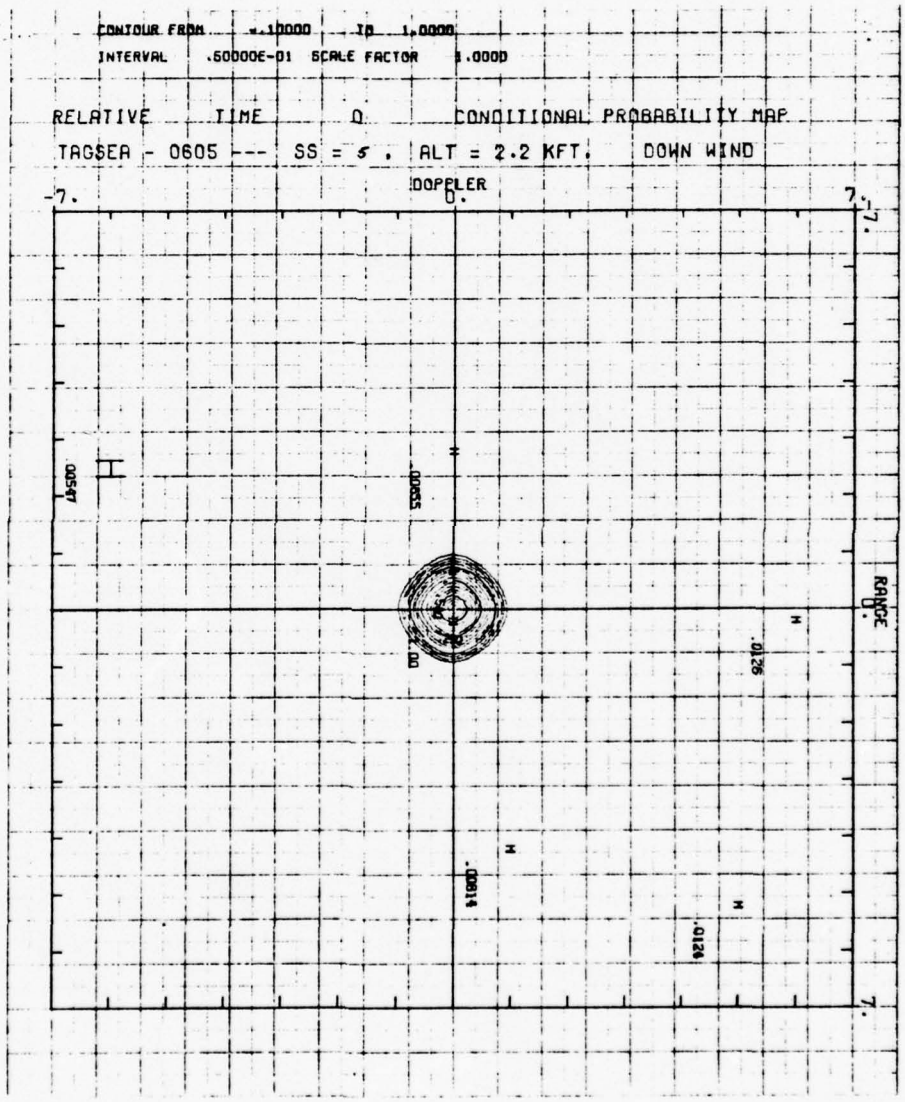

Figure 9-25 Conditional Probability Map (Time=0)

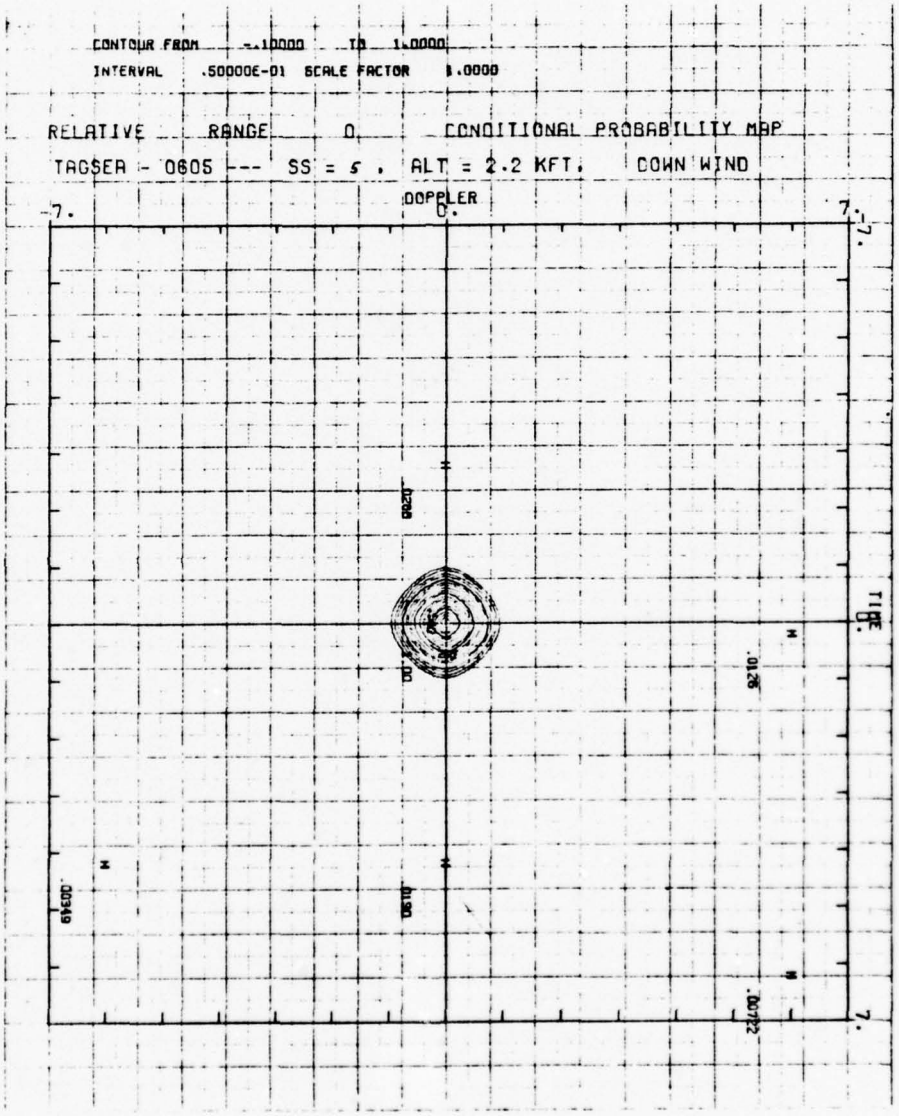

Figure 9-26 Conditional Probability Map (Range=0)

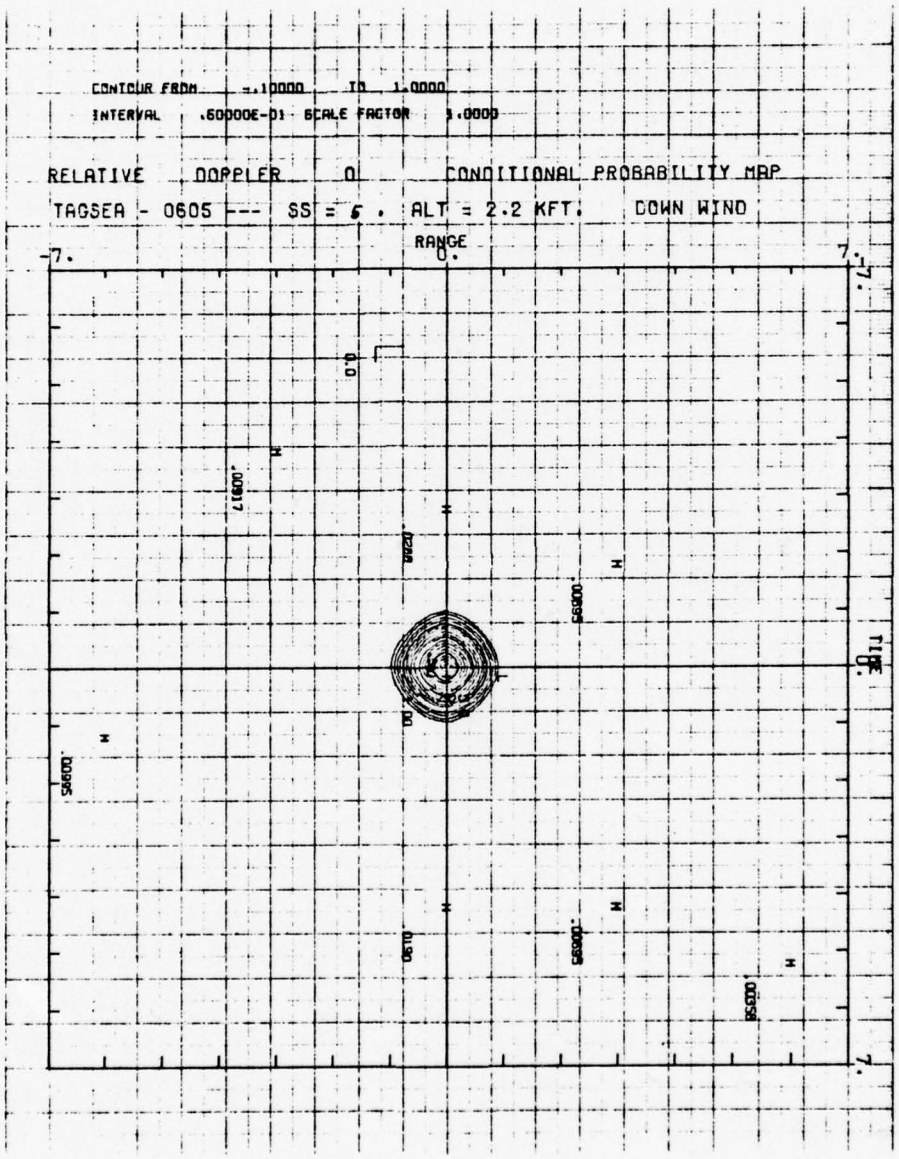

Figure 9-27 Conditional Probability Map (Doppler=0)

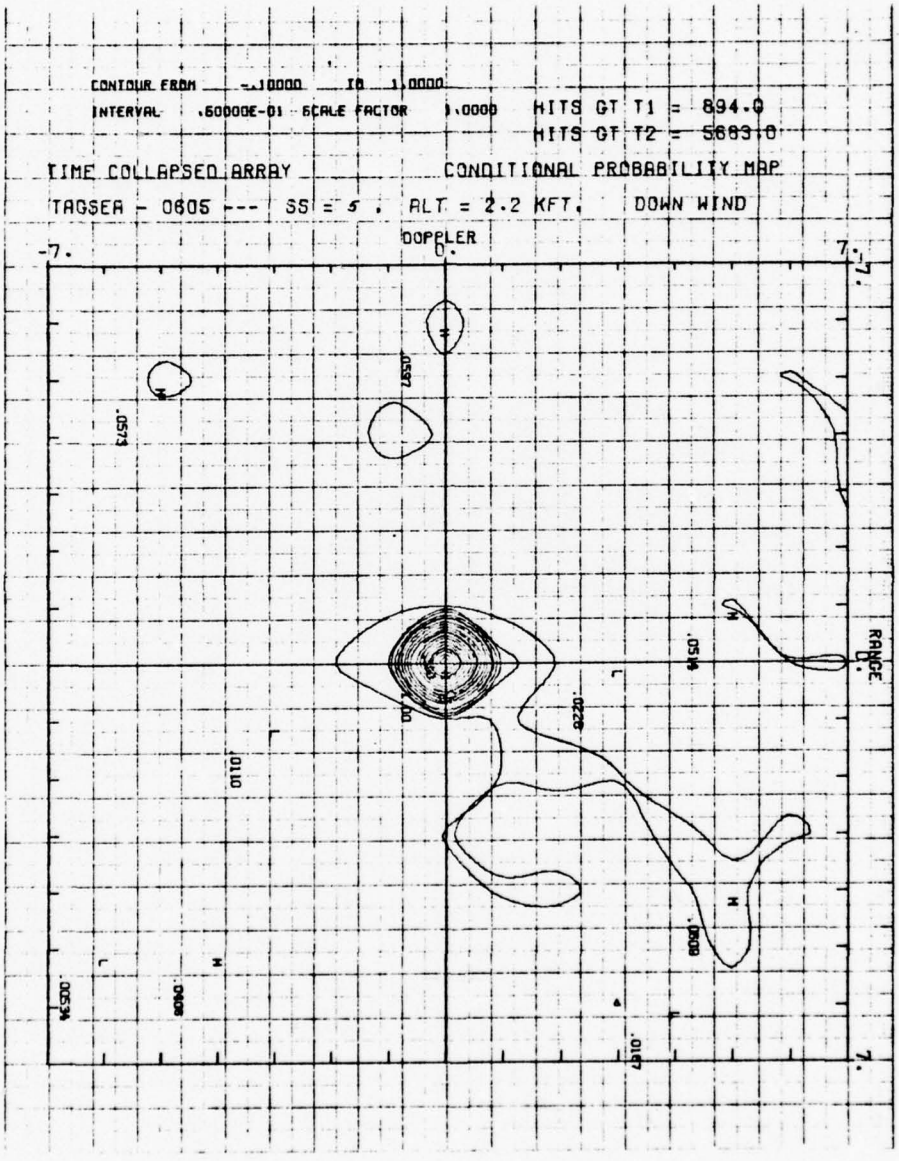

Figure 9-28 Conditional Probability Map
(Time Collapsed Array)

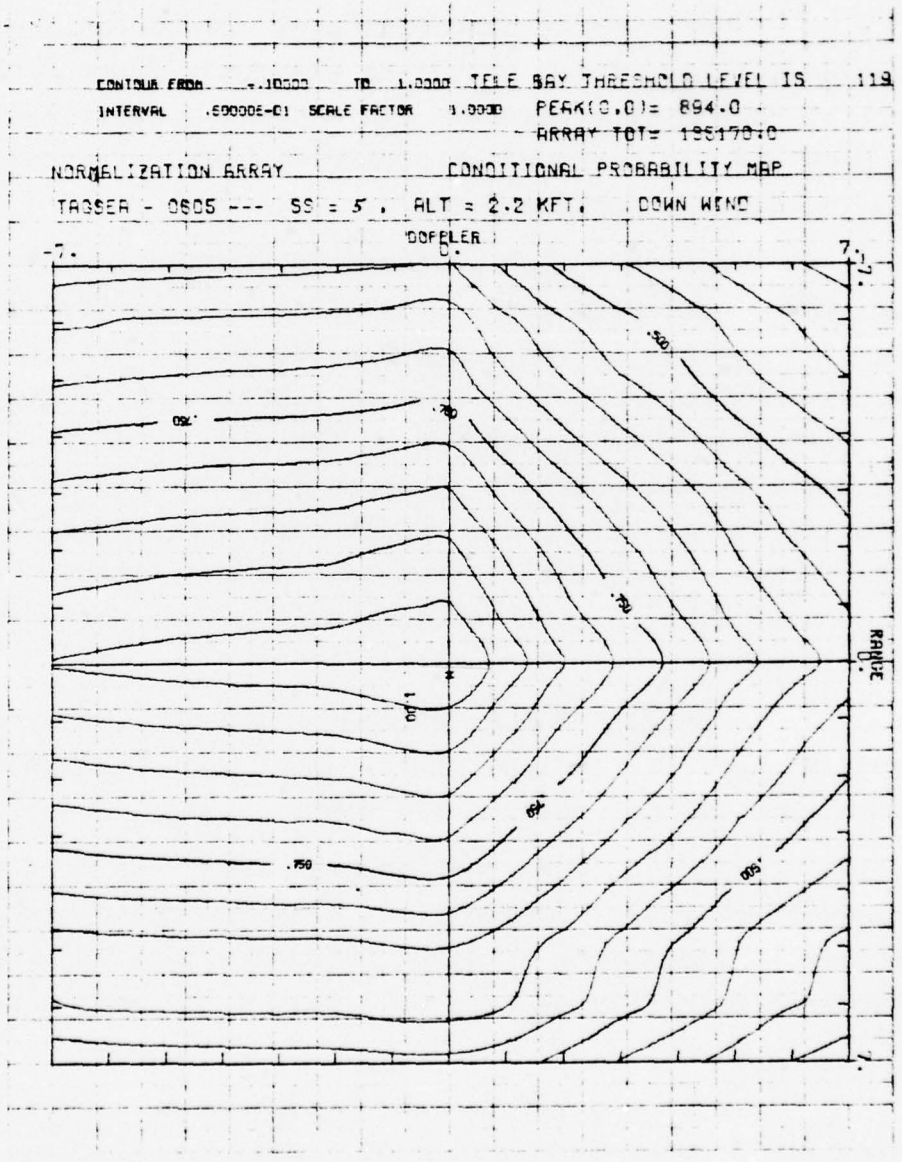

Figure 9-29 Conditional Probability Map
(Normalization Array)

15 X 15 X 15 conditional probability cube with the referenced hits (those exceeding 10^{-5} threshold) residing at the center of the cube.

Contours of probability vs. range and doppler are plotted for the Time=0 principal plane cut. Similarly, contours of probability vs. time and doppler are plotted for the Range=0 cut and contours of probability vs. time and range are plotted for the Doppler=0 cut.

A fourth plot illustrated in Figure 9-28 shows contours for a collapsed array. All 15 time cuts were summed with respect to time in the Range-Doppler plane. The resultant sum was limited to one before contour plotting the collapsed array. Probability is obtained from the plot by dividing each contour level by 15. Because large numbers for probability are hard limited to unity, the result serves primarily as a qualitative measure of the distribution of conditional hits as observed by looking down the time axis of the conditional probability cube.

Numbers of hits exceeding the 10^{-5} (A-type) threshold T_1 and 10^{-3} (A-type) threshold T_2 for the run are listed on the Time Collapsed Array plot.

In all cases the contour maps range from 0 to 1 in increments of 0.05. Dashed lines indicate regions where probability is indeterminant since no events were possible. This occurred primarily in runs with only a few usable range gates.

Contours for the normalization array are plotted vs. range and doppler in Figure 9-29. The normalization plot peaks at one in the center of the array. Number of hits exceeding the T_1 thresholds and the T_2 threshold are listed on the plot. The number of trials against the T_2 threshold

at a particular range-doppler coordinate may be computed from the product of contour level and number of trials at the center or peak of the normalization array.

The variance in estimation of conditional probability is smallest near the center of the cube. As the number of trials fall off at the edges of the cube the variance in estimation of probability increases.

For most of the runs processed the conditional probability maps have spikes at the origin with a few scattered low level probability hits elsewhere. Run 0605 illustrates this property.

9.3 Average Analysis

A characterization of the mean value of the returned clutter signal is important to completely specify its nature. Average analysis is an attempt to gather information as to the statistics and non-stationary (time variability) of the mean.

9.3.1 Average Plots

Average plots are generated as a function of time in each range gate where data is available, see Figure 9-30. The power in 100 consecutive FFT frames is averaged to produce each plotted point. This represents a time aperture of approximately 0.9 second. The amplitude scale on the plots is 2dB per major division. The scale indicated which runs a full $\pm$30dB is used only for indexing the range gates in approximately 2dB stops for clarity is not an absolute scale. Range gate "0" appears near the 20dB mark and range gate "15" appears near the -10dB mark.

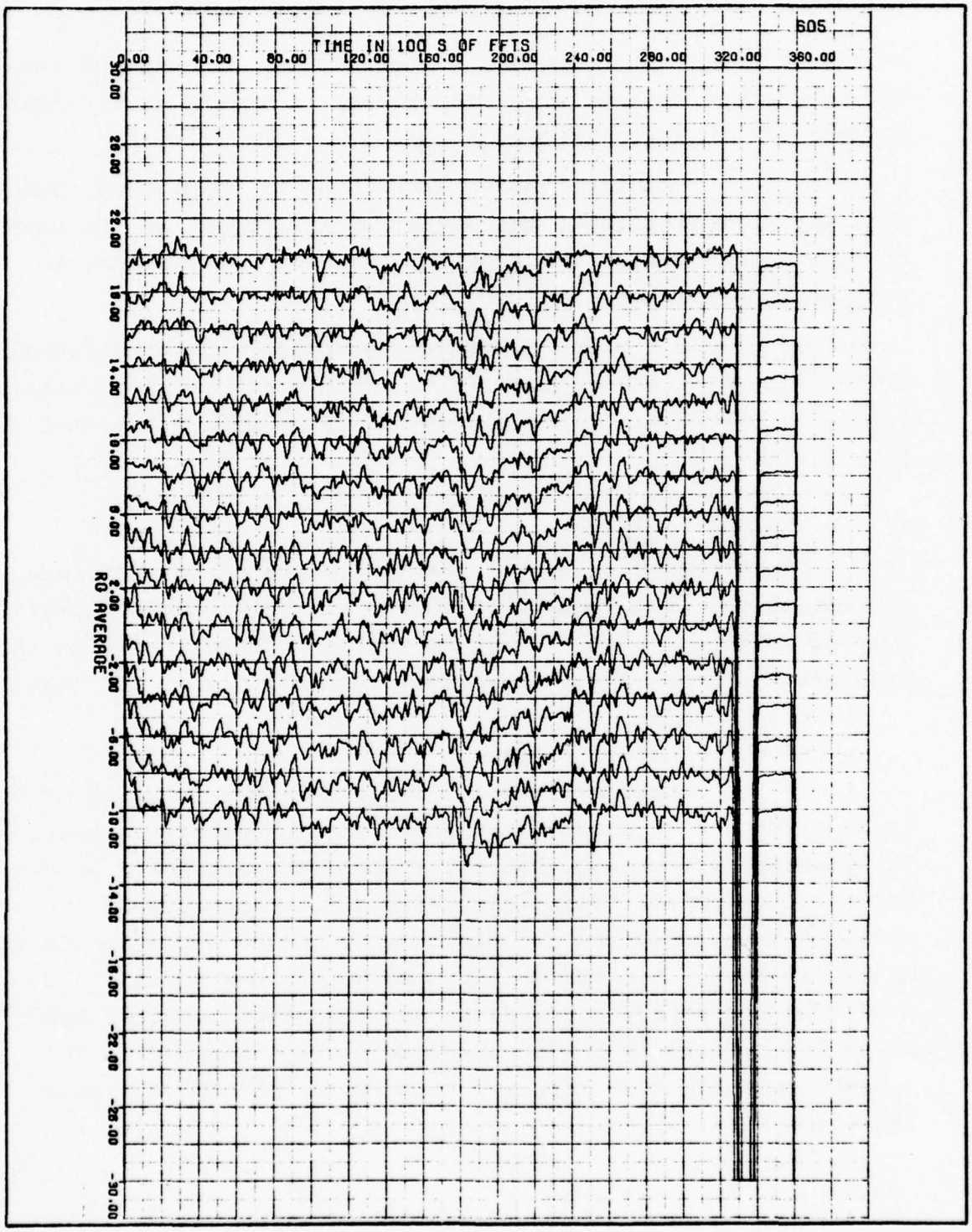

Figure 9-30 Average Plots

The sharp drop in amplitude in all of the range gates is the sample of receiver noise and the increase in amplitude after the dropoff is the calibrate signal.

Average plots serve two purposes. The first is to give an overview of the data on a quick-look basis to visually discern any anomalies in the data set, such as unexpected gain changes. The second is to observe the texural structure of the mean which relates to its stationarity. Is the mean changing rapidly or slowly, is it spikey or smooth, and does it contain decernible trends?

9.3.2 Statistics of the Mean

A sample mean is generated every 600 FFT frames (1 histogram frame) in each range gate which yields an effective time aperture of approximately 5.4 seconds. The mean and variance of the set of sample means which consists of approximately 800 points (16 range gates by 50 histogram frames)are determined and tabulated. This information yields insight into the non-stationarity of the mean.

The variance of the sample mean will be higher than the actual variance of the true mean due to variations from range gate to range gate which could not be normalized out.

9.4 Spatial Analysis

Spatial analysis characterizes the variations in clutter from one location on the sea to another. That is, as a function of "space" from doppler cell to doppler cell. This analysis is done in only one range gate.

9.4.1 Spatial Spectra

Spatial spectra are calculated from the 32 doppler cells. A spatial spectrum is the magnitude of the fourier transform squared of the power in the 32 doppler cells. Forty such spectra are averaged to remove sampling effects to produce the final spectrum, an example of which appears in Figure 9-31.

It should be noted that the "dc" component has been removed. In Figure 9-31 the abscissa is scaled in cells where each cell is approximately 2.6×10^{-4} cycles/foot wide and the ordinate has units of watts^2/cycle/foot. From Figure 9-31 it is evident that the spatial spectrum for this case is fairly flat.

9.4.2 Spatial Autocorrelation Function

The spatial autocorrelation function (ACF) is calculated directly from the spatial spectrum, that is, the ACF is the inverse fourier transform of the spatial spectrum. The ACF that is derived from the spectrum in Figure 9-31 appears in Figure 9-32.

In Figure 9-32 each cell is approximately 60.0 ft wide. It can be seen that for this example, each doppler cell is independent of all the other doppler cells since the ACF falls off sharply from 1.0 in just one cell of distance.

9.5 Temporal Analysis

Temporal analysis characterizes the variations in clutter from one instant of time to the next. This analysis is done in only one range gate since this is sufficient for the temporal characterization.

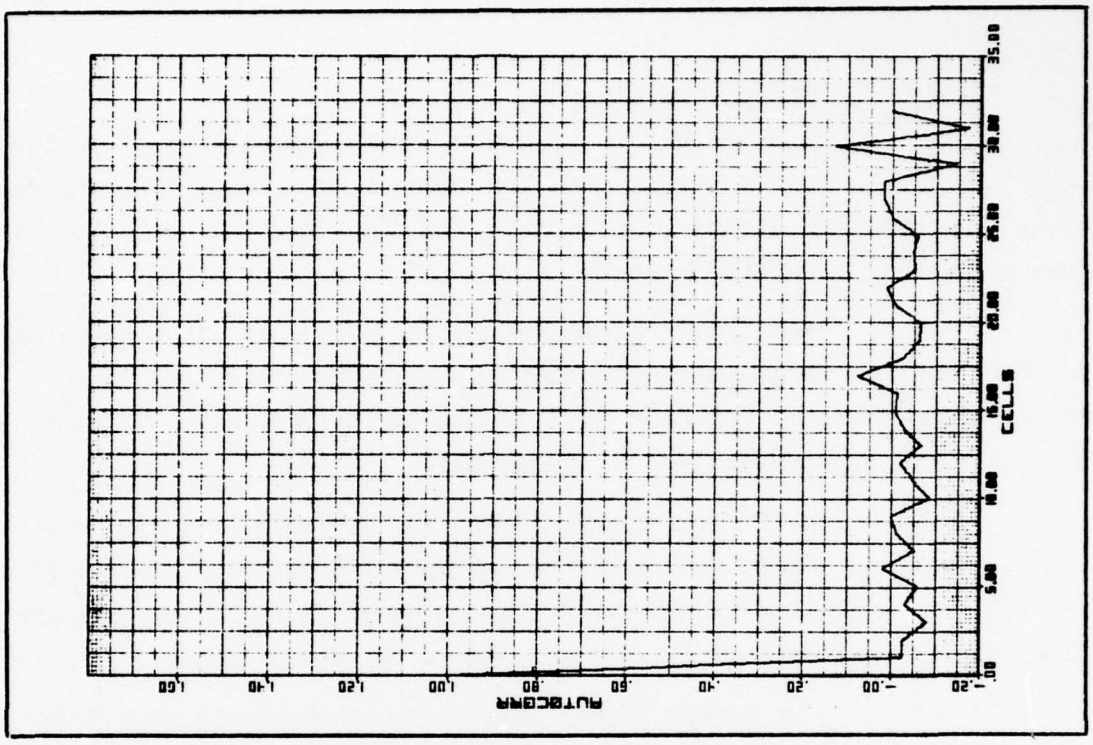

Figure 9-32 Spatial Autocorrelation

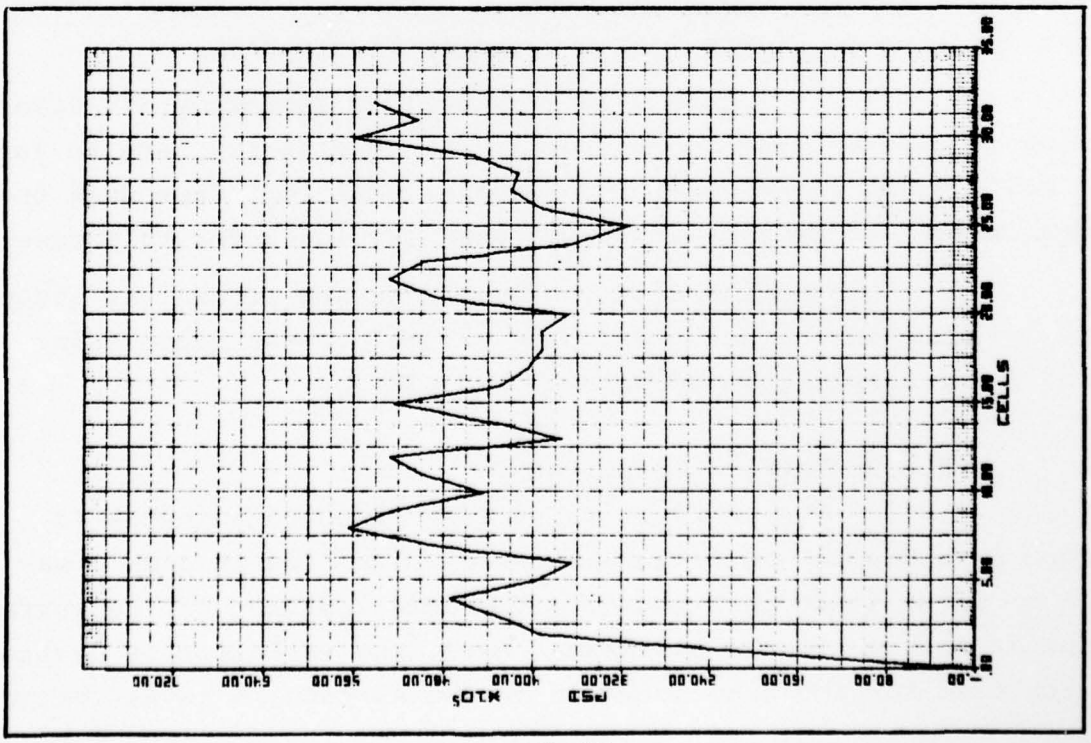

Figure 9-31 Spatial Spectrum

9.5.1 Radar Coordinates

The analysis in radar fixed coordinates is done in a single, fixed doppler cell as viewed as a function of time. The variation of clutter with time for one doppler cell within the receiver is investigated.

The radar fixed temporal spectrum is the magnitude of the fourier transform squared of the power history in a particular (fixed) doppler cell which is viewed over a time aperture of approximately 9.1 seconds.

In Figure 9-33, which is an example of a radar fixed temporal spectrum, the "dc" component has been removed. The abscissa is scaled in cells where each cell is approximately .055Hz wide and the ordinate has units of watts^2/Hz.

The radar fixed temporal autocorrelation function (ACF) is calculated directly as the inverse fourier transform of the radar fixed temporal spectrum. The ACF that is derived from the spectrum in Figure 9-33 appears in Figure 9-34.

In Figure 9-34 each cell is approximately 8.9ms wide. Since the ACF drops from 1.0 to practically zero in just 1 cell (8.9ms), the power in a doppler cell is independent from one instant to an instant 8.9ms later (at least for this case).

The increase in the ACF in and around the 1000th cell is due to the noise variance on the process since fewer and fewer samples are added into the ACF.

9.5.2 Surface Coordinates

The analysis in surface fixed coordinates is done in a doppler cell that is varied with time in such a way as to force it to correspond to the same location on the surface for as long a time as possible. Here, the variation in clutter with time for the same location on the surface is investigated.

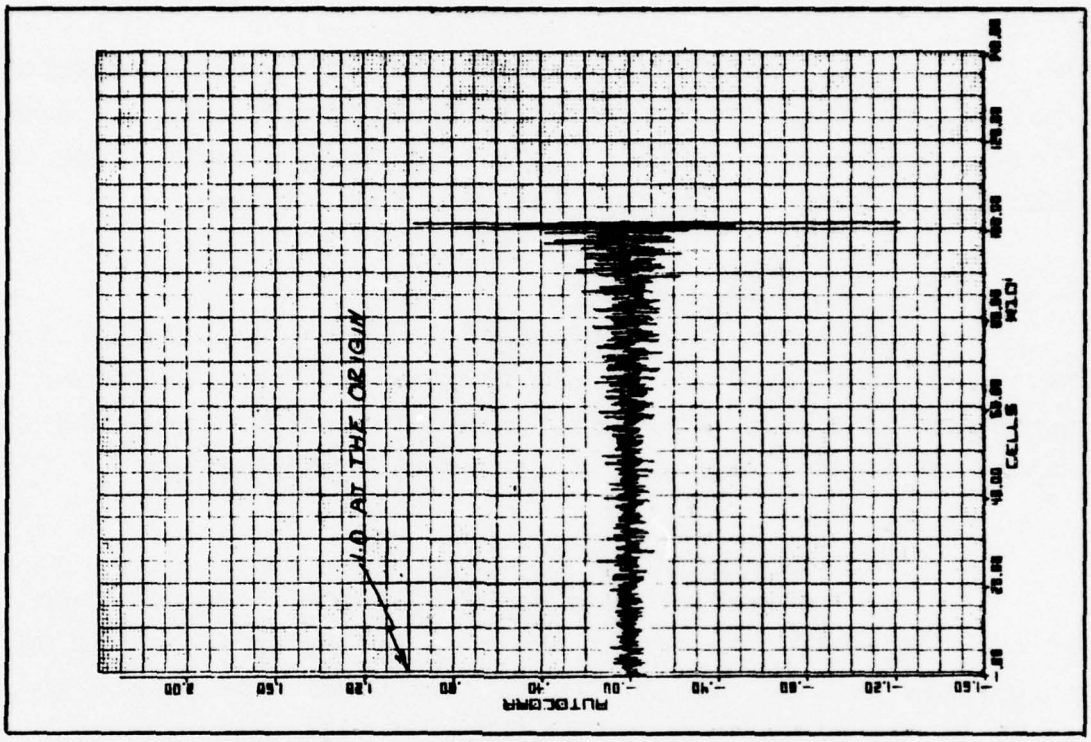

Figure 9-34 Radar Fixed Temporal Autocorrelation

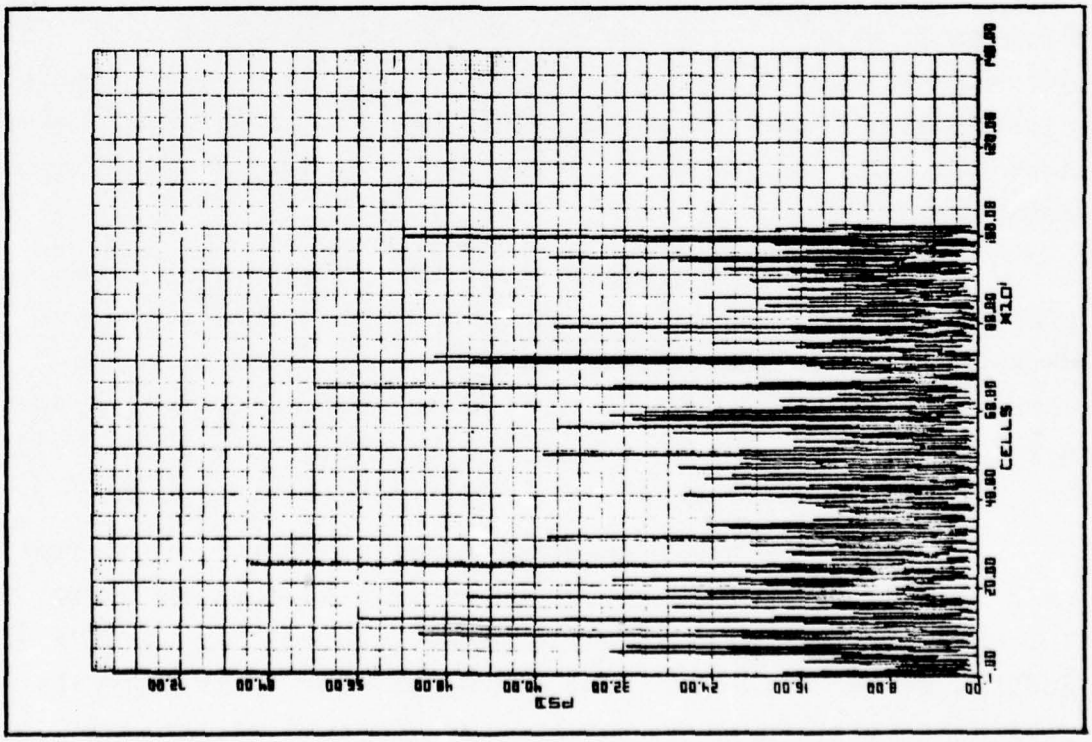

Figure 9-33 Radar Fixed Temporal Spectrum

The temporal spectra and autocorrelation functions that are generated for the surface fixed coordinates are similar in form and meaning to those generated for the radar fixed coordinates. Hence, they will not be discussed here.

9.6 Special Data Analysis

In addition to the standard (nominal) data analysis and reduction that was done for all flights and runs, it became necessary from time to time to gain more insight into some aspect of a particular set of flight/run combinations.

9.6.1 Mean Analysis

Since the mean value of the clutter was found to be non-stationary, an effort was made to characterize the mean in greater detail. In the following analysis, means are computed every 90msec and a total time window of 9.1 seconds is used.

Each mean value is normalized to eliminate variations from range gate to range gate. The entire data set in all range gates is accounted for by averaging in the range gate domain for a particular 90msec interval. This results in a "sample mean" data set. The following analysis is done using the sample mean data set.

A histogram of the sample mean data set was computed to find out its spread as well as to see if it was skewed. A typical histogram appears in Figure 9-35. The "amp" scale is the value of the sample mean as generated over a 90msec window. The data that follows in Figure 9-36, 9-37 and 9-38 is for the same sample mean data set as for Figure 9-35.

The power spectral density (PSD) of the sample mean data set was computed and an example appears in Figure 9-36. The abscissa is scaled in cells where each cell is .0055Hz wide and the units of the ordinate are watts^2/Hz. This analysis yields information as to the spectral content of the mean.

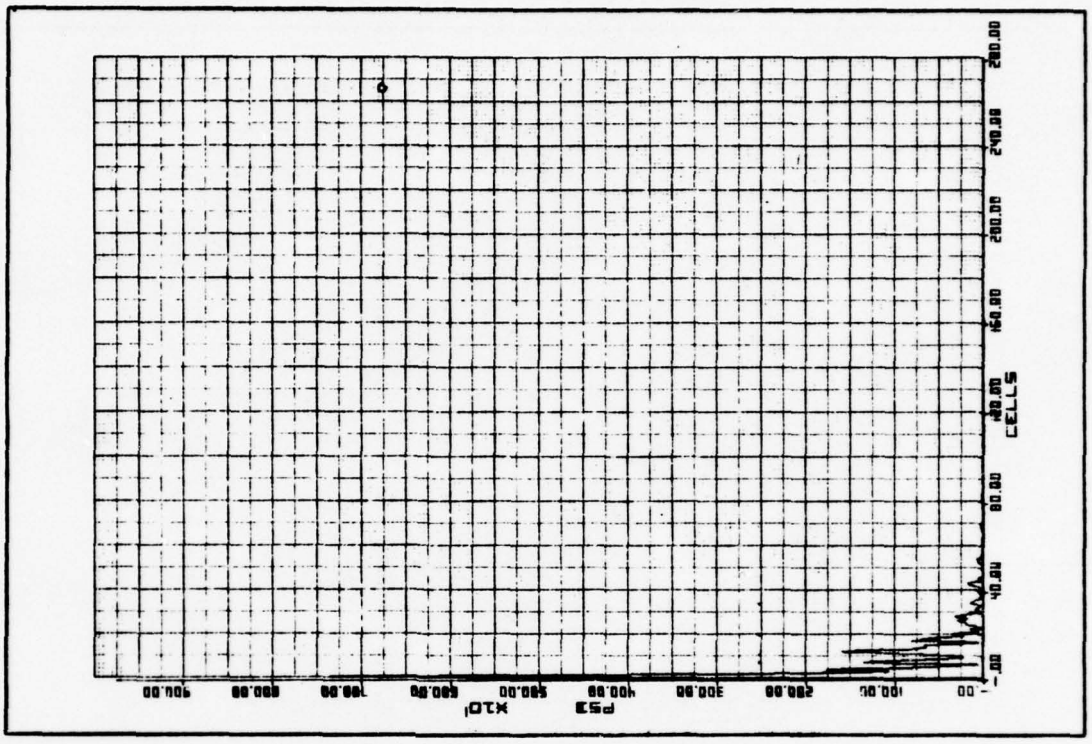

Figure 9-36 Sample Mean PSD

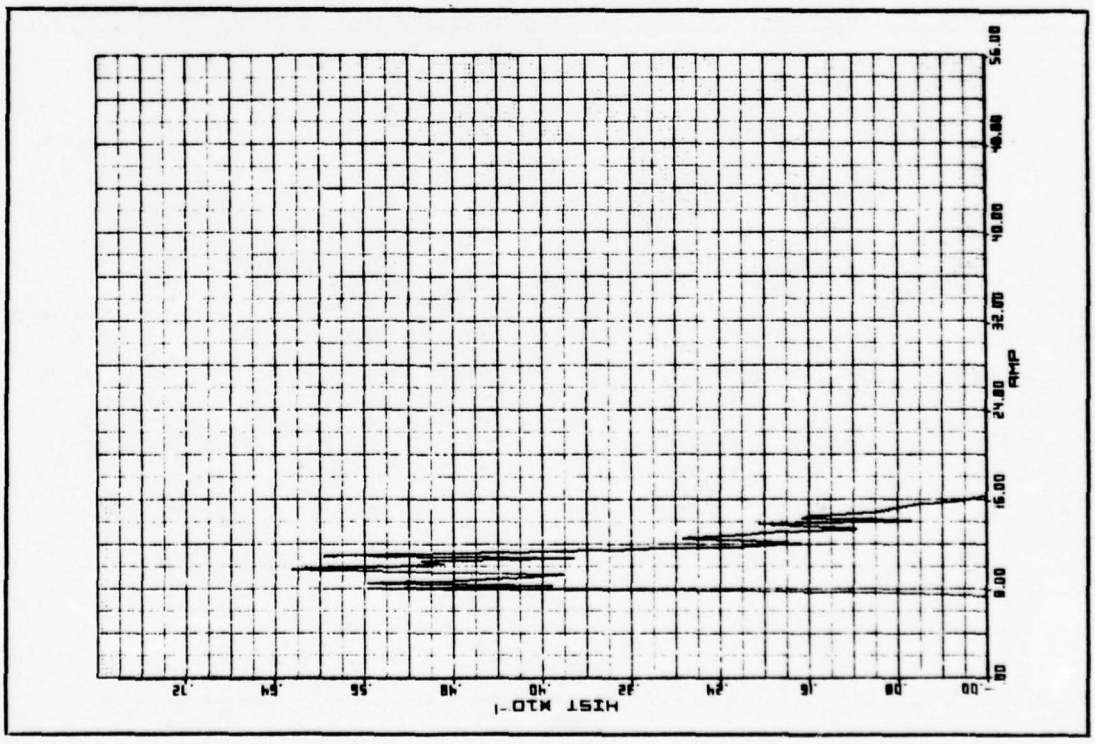

Figure 9-35 Sample Mean Histogram

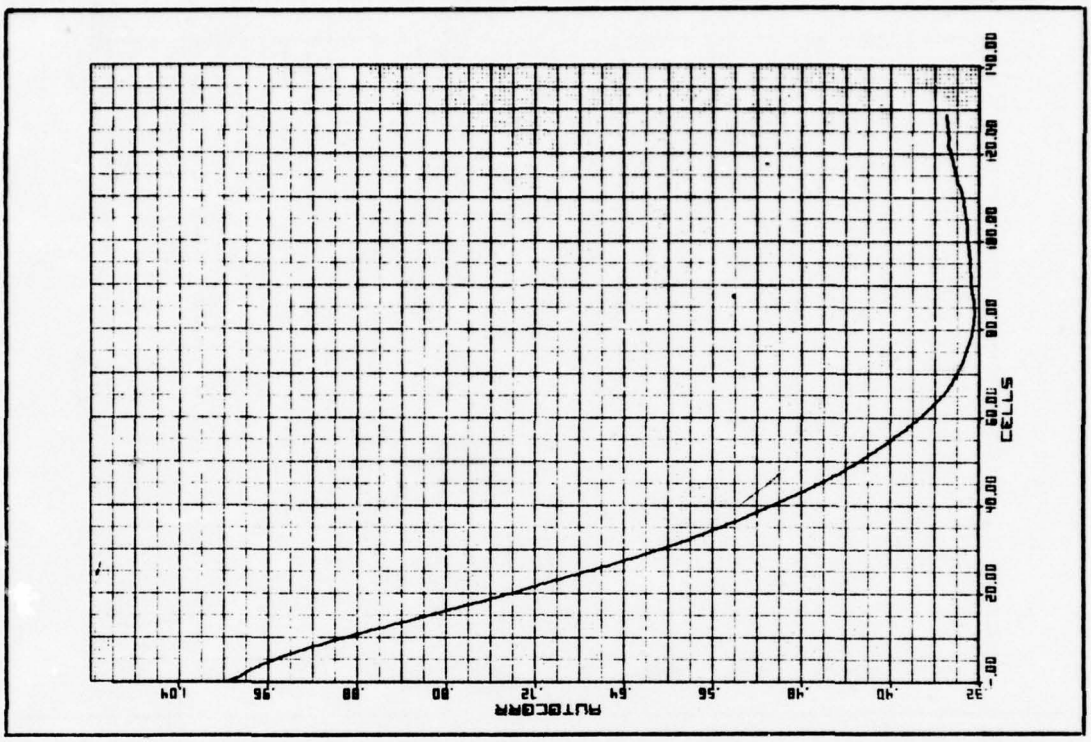

Figure 9-38 Expanded Sample Mean ACF

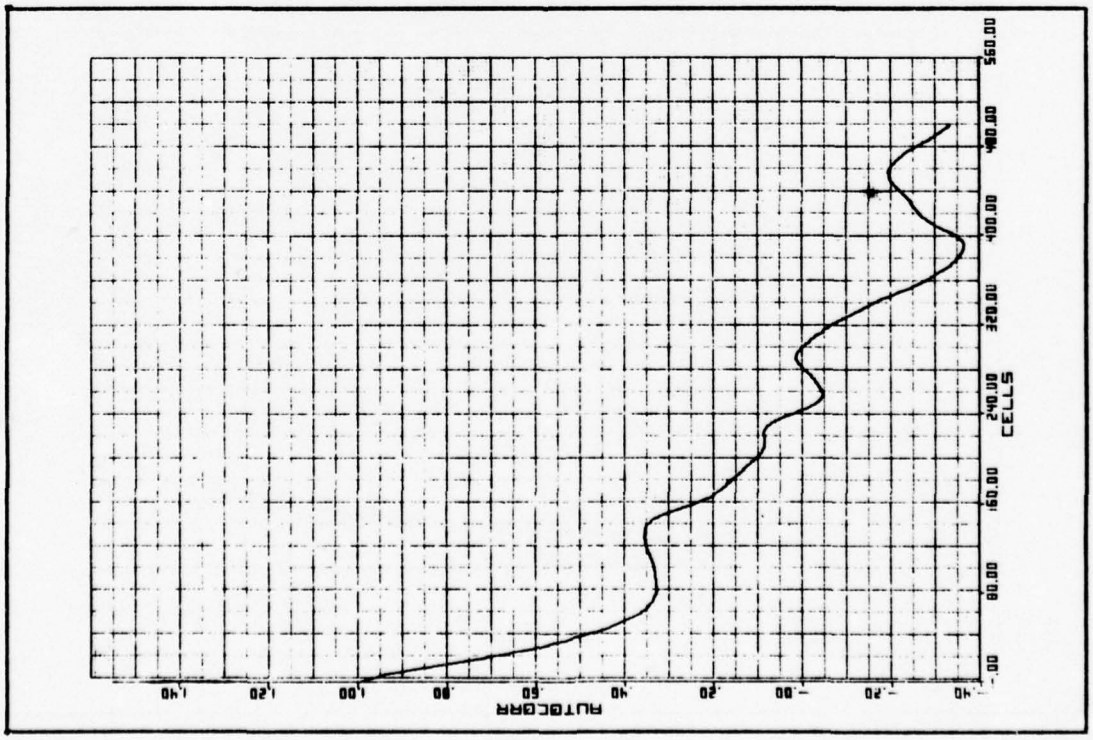

Figure 9- 37 Sample Mean ACF

The autocorrelation function (ACF) of the sample mean data set was computed as the inverse fourier transform of the PSD. The ACF is in Figure 9-37 with the abscissa scaled in cells where each cell is 90msec wide. In some cases, the first few seconds of the ACF were blown up to fill a plot page. However, the scale remains at 90msec per cell. An example of this appears in Figure 9-38.

9.6.2 Range Gate-to-Range Gate Correlation Coefficient

The correlation coefficients of the power history of the first available range gate with the power histories of the remaining range gates were computed. These coefficients give insight into the dependence or independence of the clutter signals from range gate to range gate.

The correlation coefficient was computed over approximately a 3.5 minute time window when the data was available. For runs with short power histories, the time window was shortened appropriately. This data appears in tabular form as shown in Figure 9-39 with some of it being presented graphically as well.

9.7 Mean Backscatter Coefficient

Measurements were made of the mean backscatter coefficients, σ_o, and the data is presented in two forms, plots of σ_o versus depression angle and tabulations of range gate number (grazing angle), mean and other parameters.

A typical plot, Figure 9-40, shows σ_o in dB versus depression angle in degrees for each of the nine runs during a single flight. The run numbers, 601, 602, etc., correspond to the wind direction where 0601, 0604, and 0607 are upwind looks for flight 6 with the last digit being the run number. Run numbers -2, -5 and -8 are downwind looks while -3, -6 and -9 are crosswind looks.

RANGE GATE	CORR COEF
0	1.000000
1	.567194
2	.641696
3	.562991
4	.569481
5	.537075
6	.519616
7	.524761
8	.484168
9	.470918
10	.417443
11	.437481
12	.437265
13	.41[illegible]1
14	.405542
15	.381349

Figure 9-39 Tabulated Correlation Coefficient for Flight/Run 605

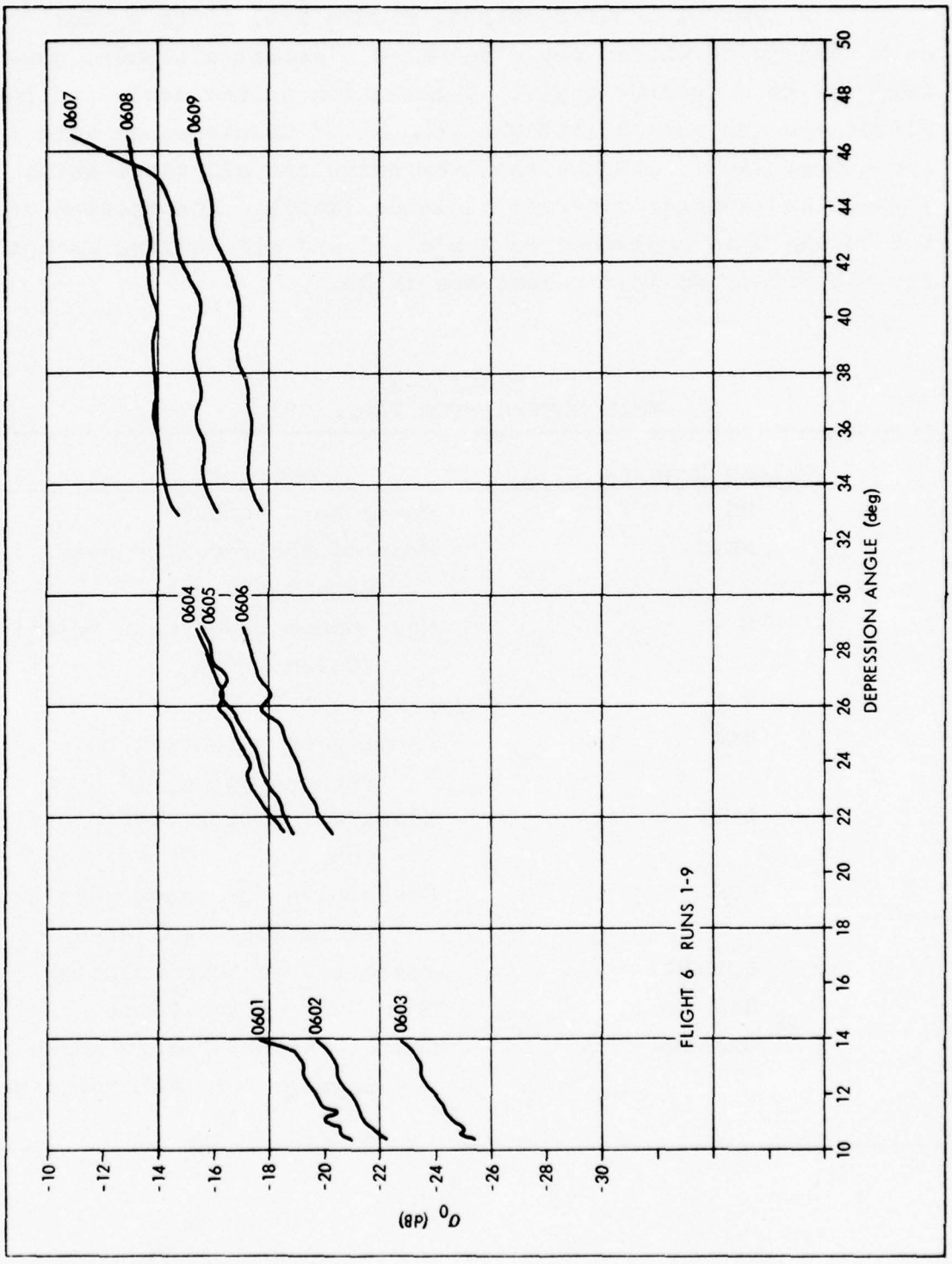

Figure 9-40 Flight 6 Mean Backscatter Coefficient Plots

A typical tabular output, Figure 9-41 lists σ_o for each range gate which, for a selected aircraft altitude, corresponds to a grazing angle. Information on the table indicates flight and run number (FLTRUN), number of usable range gate (D), run number (RUN), average receiver noise for all range gates (AVG), and nominal aircraft altitude (NALT). The meaning of the column 3 is explained in Table 9-3 and all entries except for the first and last column are in dB.

TABLE 9-3
MEAN BACKSCATTER TABLE KEY

Column Heading	Meaning
RG	Range gate number
MEAN	Mean of the receiver noise in each range gate
W	Mean minus range gate weighting (Column WTG)
X	W minus AVG
WTG	Range gate weighting corresponding to R^{-4}
SIGT	Measured clutter return during run
COR	Correction for range gate gain variations (measured)
CORSIG	Corrected measured clutter
SIG	Mean backscatter ratio
GRAZING	Corresponding grazing angle in degrees for that range gate

FLTRUN= 601
D= 16.0 AVG=-1.29 RUN= 1 NALT= 2

RG	MEAN	W	X	WTG	SIGT	COR	CORSIG	SIG	GRAZANG
0	-1.00	-1.00	.29	0.	-17.71	0.	-17.71	-18.00	13.99
1	-1.00	-1.51	-.22	.51	-18.82	0.	-18.82	-18.60	13.68
2	-.50	-1.50	-.21	1.00	-19.01	0.	-19.01	-18.80	13.39
3	-4.80	-6.28	-4.99	1.48	-19.39	0.	-19.39	-14.40	13.11
4	1.50	-.45	.84	1.95	-18.36	1.00	-19.36	-19.20	12.84
5	3.10	.70	1.98	2.40	-18.32	.91	-19.22	-20.30	12.58
6	2.60	-.25	1.04	2.85	-18.66	.82	-19.48	-19.70	12.33
7	2.60	-.68	.61	3.28	-18.89	.73	-19.62	-19.50	12.09
8	2.70	-1.01	.28	3.71	-19.12	.64	-19.75	-19.40	11.87
9	3.00	-1.12	.17	4.12	-19.33	.55	-19.88	-19.50	11.64
10	3.10	-1.43	-.14	4.53	-20.04	.45	-20.49	-19.90	11.43
11	4.00	-.99	.30	4.99	-19.70	.36	-20.07	-20.00	11.23
12	4.10	-1.21	.09	5.31	-19.82	.27	-20.10	-19.90	11.03
13	4.30	-1.39	-.10	5.69	-20.30	.18	-20.48	-20.20	10.84
14	4.80	-1.26	.03	6.06	-20.47	.09	-20.57	-20.50	10.65
15	5.20	-1.23	.06	6.43	-20.94	0.	-20.94	-21.00	10.48

FLTRUN= 602
D= 16.0 AVG= -.09 RUN= 2 NALT= 2

RG	MEAN	W	X	WTG	SIGT	COR	CORSIG	SIG	GRAZANG
0	-.50	-.50	-.41	0.	-19.71	0.	-19.71	-19.30	13.99
1	-.10	-.61	-.51	.51	-20.01	0.	-20.01	-19.50	13.68
2	.50	-.50	-.41	1.00	-20.21	0.	-20.21	-19.80	13.39
3	.90	-.58	-.49	1.48	-20.39	0.	-20.39	-19.90	13.11
4	2.30	.35	.45	1.95	-19.55	1.00	-20.55	-20.00	12.84
5	3.70	1.30	1.39	2.40	-19.51	.91	-20.42	-20.90	12.58
6	3.40	.55	.65	2.85	-19.95	.82	-20.77	-20.60	12.33
7	3.50	.22	.31	3.28	-20.19	.73	-20.92	-20.50	12.09
8	3.60	-.11	-.01	3.71	-20.51	.64	-21.15	-20.50	11.87
9	4.00	-.12	-.03	4.12	-20.63	.55	-21.17	-20.60	11.64
10	4.50	-.03	.07	4.53	-20.83	.45	-21.29	-20.90	11.43
11	5.00	.01	.10	4.99	-21.00	.36	-21.36	-21.10	11.23
12	5.10	-.21	-.12	5.31	-21.42	.27	-21.69	-21.30	11.03
13	5.20	-.49	-.40	5.69	-21.60	.18	-21.78	-21.20	10.84
14	5.60	-.46	-.37	6.06	-21.77	.09	-21.86	-21.40	10.65
15	6.10	-.33	-.23	6.43	-22.23	0.	-22.23	-22.00	10.48

Figure 9-41 Tabulation of σ_o by Range Gate

UNCLASSIFIED

10. CLUTTER SIMULATION/VALIDATION

10.1 Objectives

One of the major outputs of the TAGSEA sytudy is a detailed model of the expected clutter return of the ocean under various conditions. This model is intended for use not only for this system but also for other system design evaluations.

A simulation of the TAGSEA system has been constructed to validate the clutter model. The simulation consists of a model of the actual hardware, the proposed clutter model and a model of the first stage of analog data reduction.

Figure 10-1 shows the flowchart for the generations and validation of the model.

The major objective of this portion of the study is to validate a clutter model for use in this and other studies. The model has been verified using the simulations of the hardware and initial analog data reduction. Outputs of the simulation were designed to be compatable with existing data reduction software so that results could be compared with the actual data on a one-to-one basis.

10.2 Simulation Structure

The simulation of the ARTS system, clutter model, and analog data reduction was designed to provide accurate results while minimizing the amount of complex calculations required. Since literally millions of numbers need to be generated to simulate a run, considerable effort was devoted to improving efficiency. The simulation then is specifically designed to

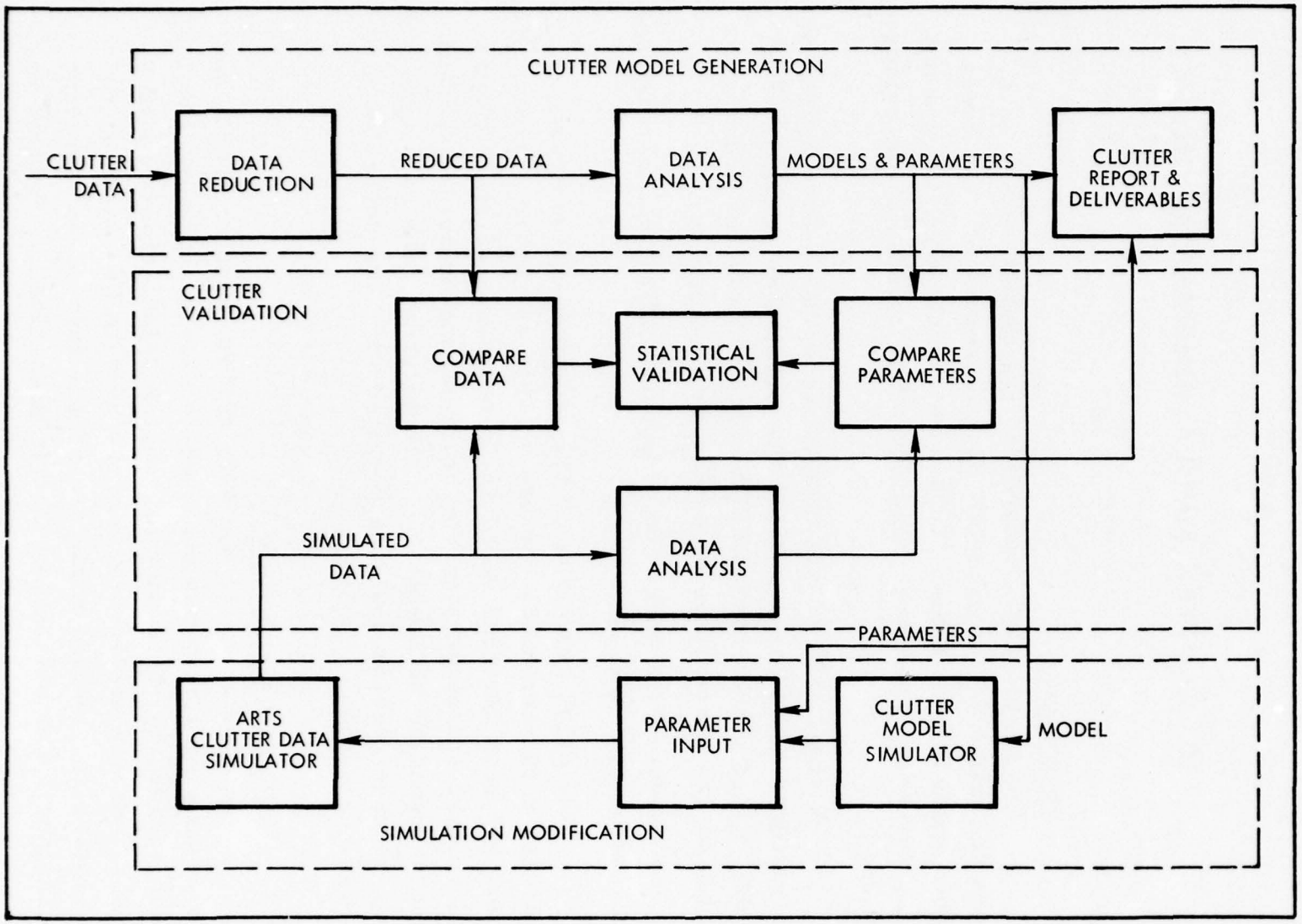

Figure 10-1 Clutter Model Generation, Simulation & Validation

model the TAGSEA system only. Ideas and sections of previously existing clutter simulations were utilized however, and the simulation is configured in such a manner that generalization and/or modification to another system could be accomplished quite easily.

A flow chart of the simulation is shown in Figure 10-2. Since a detailed description of the actual software is contained in Appendix E only the overall structure of the simulation will be discussed here.

The program starts by reading a set of inputs which define the geometry and various system parameters. Then various system parameters which can be considered "stationary" over a short period of time are generated and placed in arrays. The clutter model is then used to provide values with the correct amplitude and distribution. These values are then passed through a model of the analog data reduction processing which removes a best estimate of the clutter independent parameters. These clutter values are then written on two tapes which are equivalent to the digital tapes normally provided by data reduction. After the values have been written on tape a decision is made whether to stop or not. If the run continues a futher decision is made as to whether to update the "stationary" parameters or not. At the end of the run the tapes are sorted to the correct order and passed on for processing by the standard TAGSEA software.

10.3 Radar Model

In the clutter data gathering operation, a 200 nsec pulse was transmitted at a 19.3kHz rate. The received RF energy would be mixed down to 4kHz (I only) for a zero doppler signal and the signal passed through a series of 16 sample and holds (S/H) (See Figure 10-3).

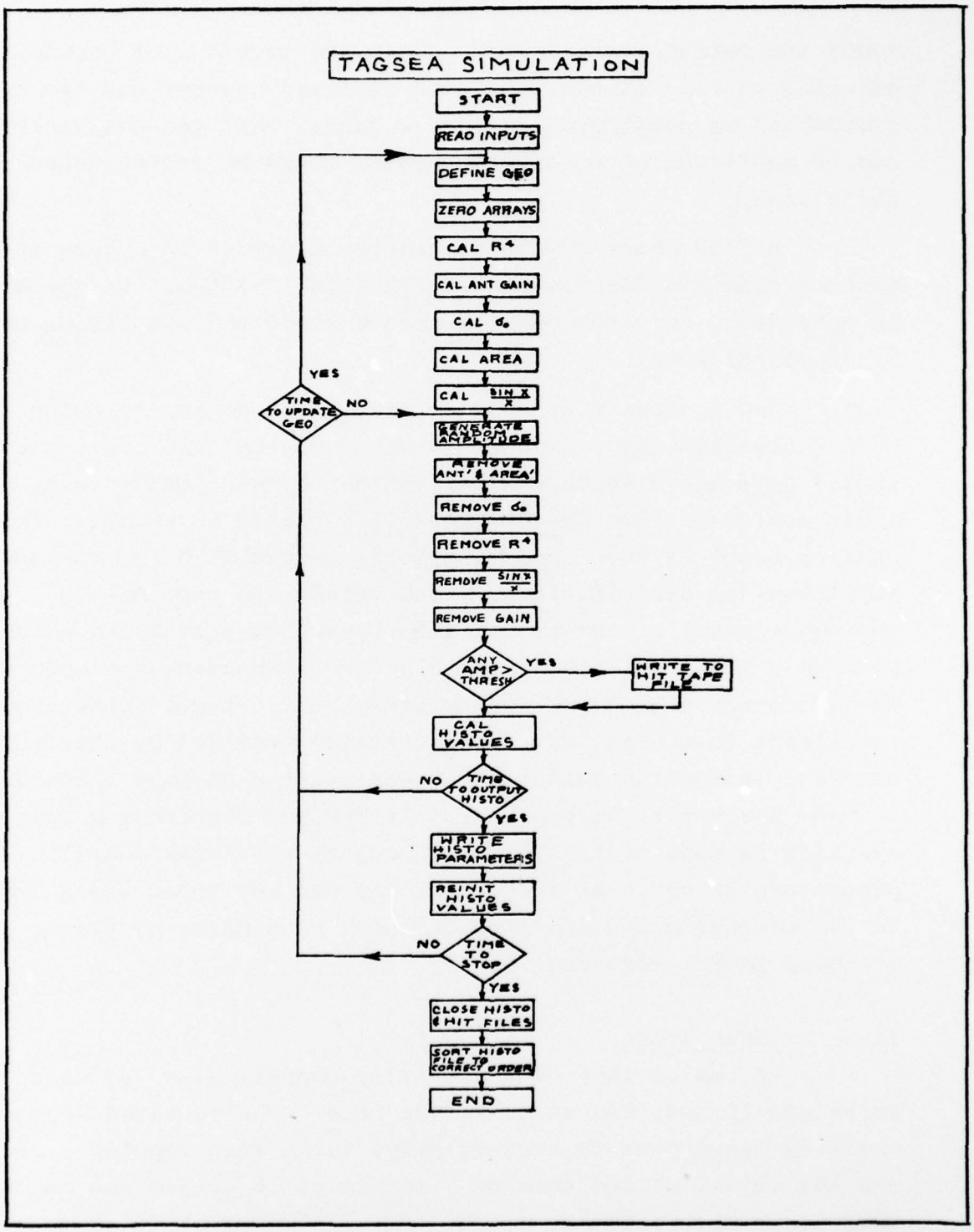

Figure 10-2 TAGSEA Simulation Flow Chart

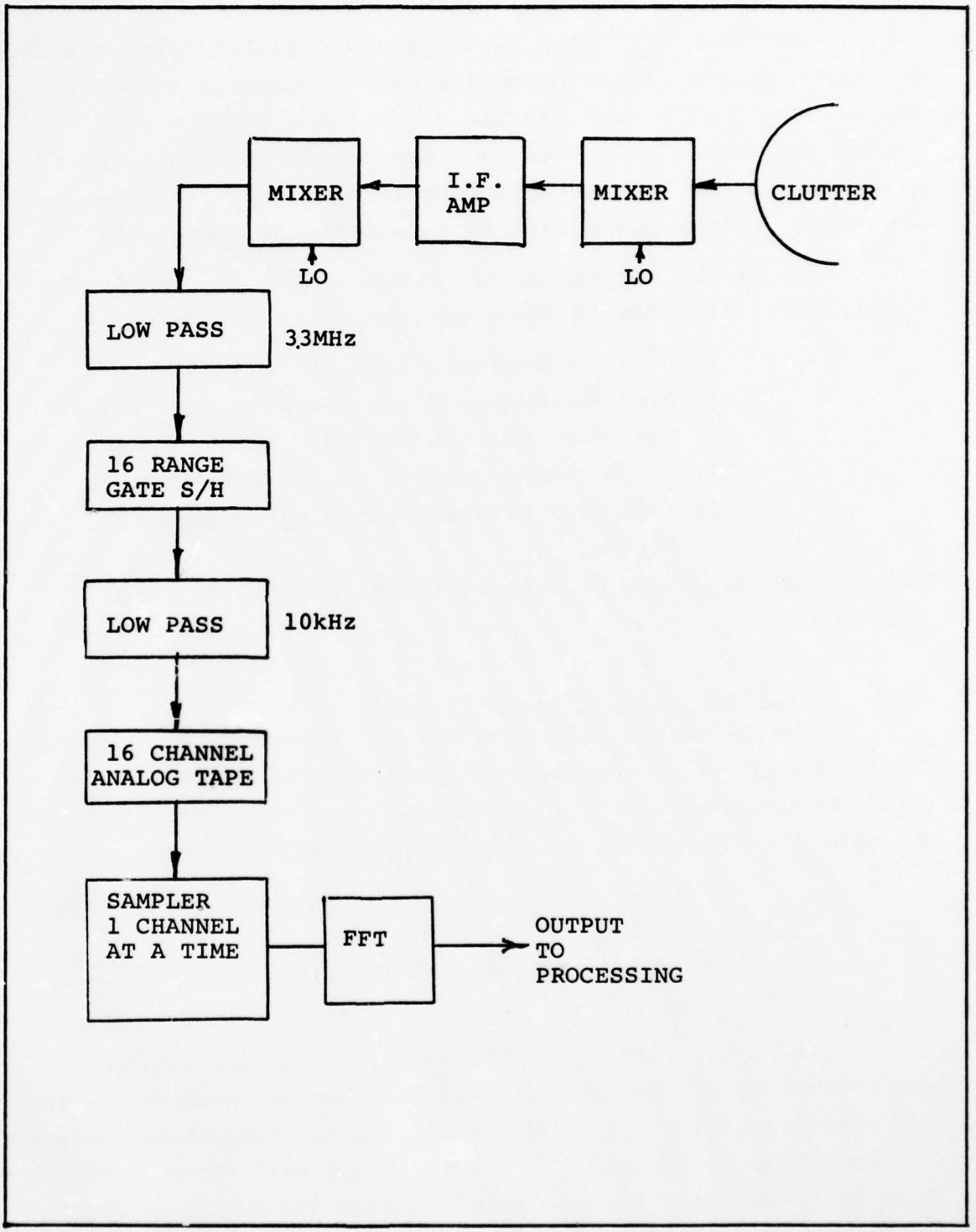

Figure 10-3 Simplified TAGSEA Data Gathering/Processing Block Diagram

The output of each range gate was passed through a 10kHz filter to remove higher harmonics and the signals stored on analog tape. This tape was digitized (at a 14.0kHz rate) and passed through an FFT. The real and imaginary components of each term in the Fourier Transform were squared and added to produce an output power term as a function of frequency.

It is the outputs of the FFT that are modeled in the simulation. Included in these outputs are:

1) R^4 for each range gate
2) Area for each clutter patch in the synthetic map
3) Gain for each clutter path in the synthetic map
4) σ_o vs. grazing angle for each range gate
5) (Sin x)/x effects from S/H for each doppler filter

The detailed modeling of each of the effects is discussed in Appendix E.

10.4 Implementation of Clutter Model

The "GENERATE RANDOM AMPLITUDE" block of Figure 10-2 is designed to produce a clutter process that is equivalent to particular measures of the data being observed. The statistical measures that have been matched include the following:

1) The overall probability density function (P_{df})
2) The P_{df} of the mean
3) The autocorrelation of the mean of the radar maps

It is worthwhile explaining certain aspects of the software reduction process which could have an influence on these observed quantities. The overall P_{df} being matched was developed by first finding the mean of 60 FFTs (each with 32 doppler cells). Once done, the data was re-scaled so that the new mean would histogram into amplitude 10. Roughly 50 such sets of 600 FFTs

were processed in this way from each of 16 range gates and the histograms were then added to form the overall P_{df}. To obtain the P_{df} of the mean, the average amplitude of each range gate (roughly 32 dopplers X 30,000 FFTs) was separately recorded. The overall average was then obtained and each data point was re-scaled by dividing by the mean for its range gate and multiplying by the overall mean. In this way, undesirable unbalances between range gates would be countered. To produce a sample of the mean of the radar map 10 adjacent FFTs (for each range) were averaged (16 range gates X 32 dopplers X 10 = 5120 points). This process was continued until 1024 such means were obtained. The P_{df} of the mean was found by placing these means into a histogram. The time autocorrelation of the mean was then established by taking the FFT of these points, finding the power spectrum, and performing an inverse transform.

The random process modelled assumes independence between the doppler cells and between the range gates. With the exception of the mean variation of the process with time, it is also assumed that there is no time correlation. The radar data was observed every 9 milliseconds with 100 feet between range gates and between doppler cells and it too shows little correlation over this time and over a distance of 100 feet. The clutter model which yields an adequate match to the data is of the form:

$$\chi = \chi_m \chi_Q$$

where χ_m provides the mean variation with time, and χ_Q is a random variable drawn from a process with a P_{df} which is identical to the observed overall pdf. The χ_Q's are independent from doppler cell to doppler cell (and in range gates and time) for all elements in the synthetic aperture map.

To develop χ_Q for each cell, the overall cumulative distribution function (cdf) of the actual data was used to develop a distribution table for the simulation. A uniform random number was generated in the computer to produce a number between 0.0 and 1.00. An actual amplitude for use in the simulation was then selected so as to yield a value on the cdf equal to that from the random number generator. Since the mapping is one-to-one, the amplitude so generated has a cdf equal to the parent cdf.

In the construction of χ_m, it became apparent that over the course of the flight there are only a few independent samples of the map mean. From the radar data, a Gaussian fit to the mean was made and an exponential fit to the time autocorrelation of the mean was found to be satisfactory. One can generate the process with these two constraints by passing "white" Gaussian noise through a low pass filter. A discussion of how to generate such a process with the desired correlation time and output variance is given in Volume III.

10.5 Data Reduction/Analysis (Simulation Data)

The output data from the simulation was constructed so as to conform to the existing software standards and hence could be processed just as the radar tapes were. The tapes produced by the simulation have been analyzed by taking the histogram, power spectral density, and autocorrelation of the map mean, by developing the cumulative distribution function of the overall process and plotting several of its characteristics, and by developing all of the standard moments. In addition, the hit counts versus time and the conditional probability maps were obtained. Figures 10-4 to 10-6 represent the simulation outputs of the autocorrelation of the mean, the P_{df} of the mean, and $Q(\chi)$ (which equals 1.00-cdf(χ)) normalized to the mean. Additional data can be found in Appendix F of Volume III.

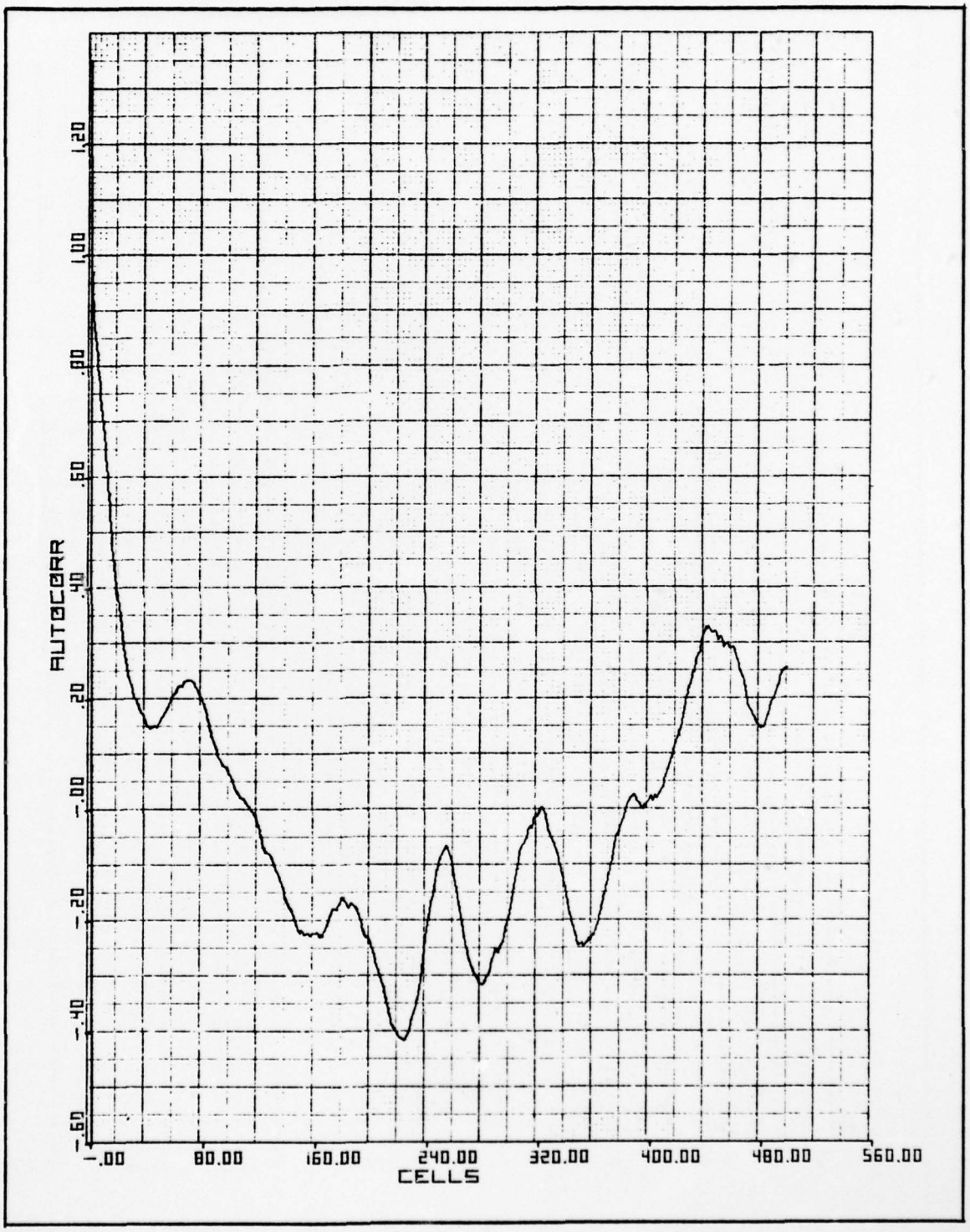

Figure 10-4 Simulation Autocorrelation Function of the Map Mean

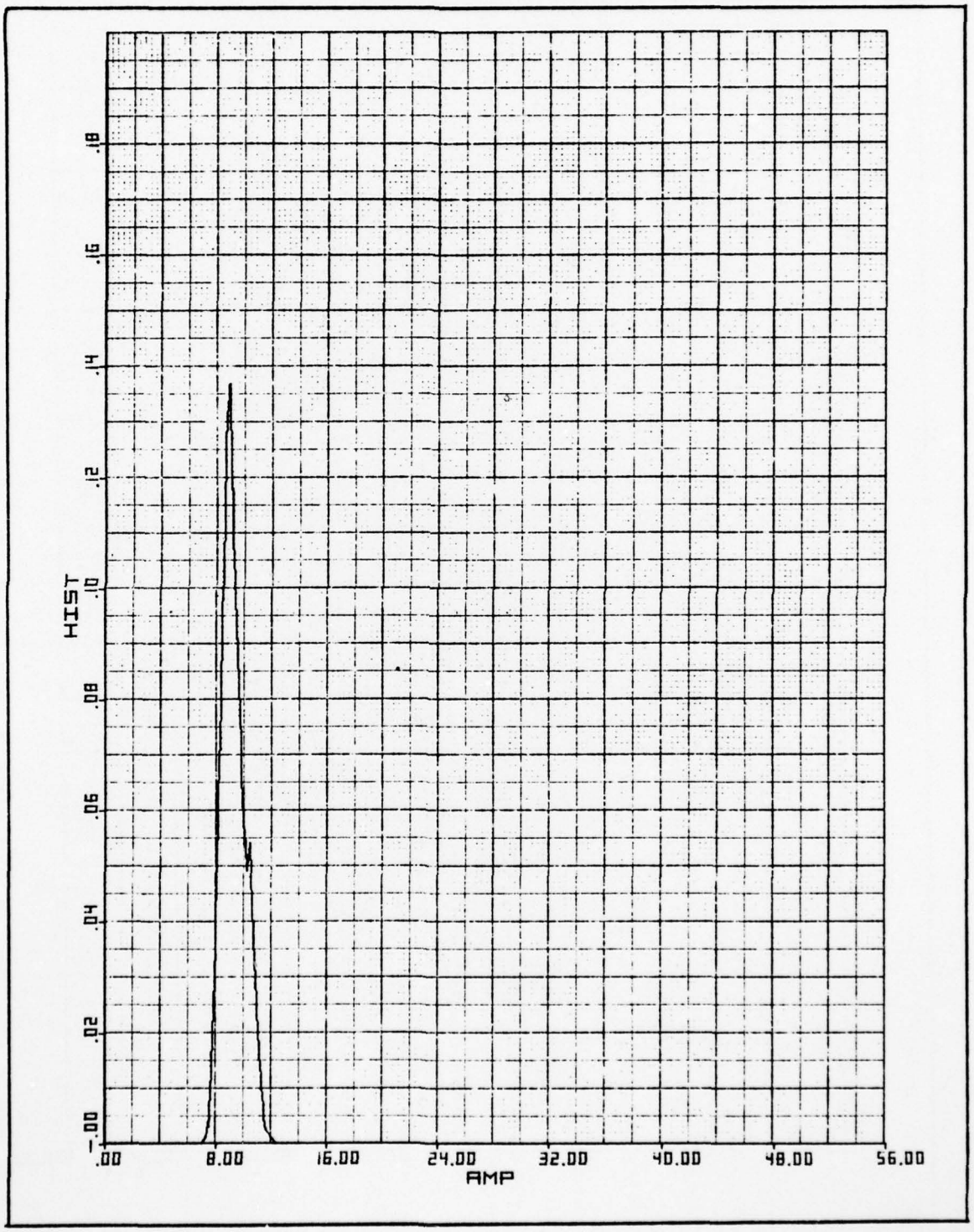

Figure 10-5 The Probability Density Function of the Map Mean

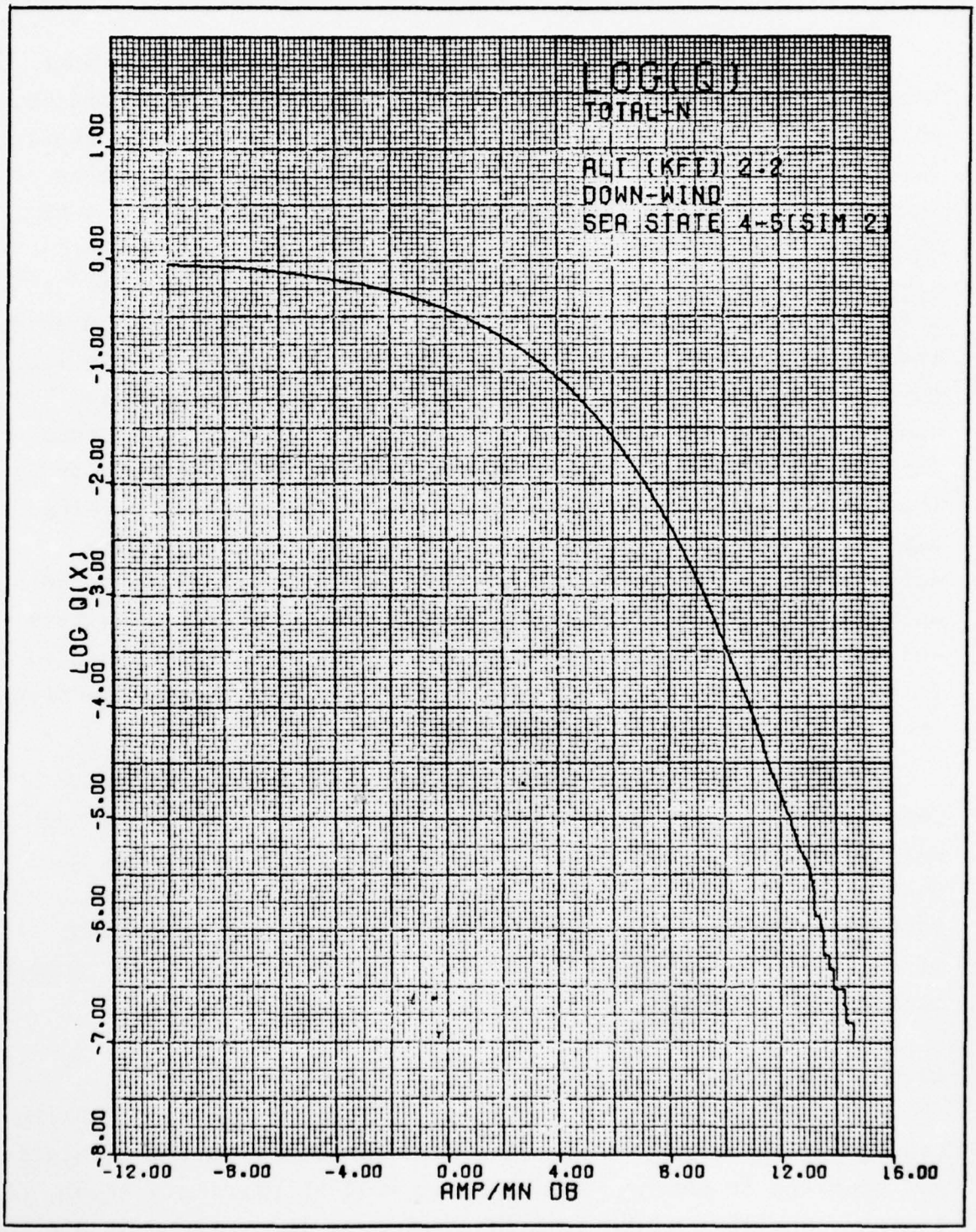

Figure 10-6 Log Q (χ) Simulated

In examining the autocorrelation of the mean, we note that the early portion of the curve looks somewhat exponential, while the later portion does some substantial meandering about 0.0. The first 50 cells (which is 500 FFTs) was least means squared fit to sn exponential resulting in a time constant of 291 FFTs. As shown earlier, $W_{3dB} = \frac{1}{\tau}$, so that $f_{3dB} = \frac{1}{2\pi\tau} = \frac{1}{1830 \text{ FFTs}}$. In the development of the autocorrelation, a total of 10,240 FFTs were processed. To illustrate the number of independent samples of the mean over this interval, if the low pass filter had a square cornor at f_{3dB}, one would need to sample at twice the rate to be able to reproduce this process. This would indicate a sample every 915 FFTs (about 8.2 seconds). Thus there are roughly 11 independent samples used to develop the autocorrelation function. To determine if the "sample" autocorrelation function so developed would have sample noise as high as 0.30 or so, a short timesharing program was written and various noise sequences were used. The conclusion reached is that the latter part of the autocorrelation function developed lies within the sample noise.

Examining the distribution of the mean, we note that a mean value of 9.3 with a standard deviation of 11% of the mean was experienced. In the modeling of the prf of the mean, an average value of 10.0 with a standard deviation of 7.9% of this value was intended, and with so few independent samples of the mean contained in Figure 10-5, the achieved result appears reasonable.

10.6 Validation and Results

The validation of the simulation was achieved by taking the equations and to model the random process from the simulation and checking it out on timeshare, as well as placing a known density (Rayleigh power distribution) into the simulation and processing the results through standard data reduction software.

Those items that were checked on timeshare include the pdf and autocorrelation of the mean, and the exponential least mean squared fit to the autocorrelation function. When the Rayleigh (exponential) power density was fed into the simulation, with no variation of the mean with time, the output tape was processed by the hit map software to produce Figure 10-7. As this figure indicates, the number of hits per unit time stayed approximately constant, and the number of hits per range gate increased slightly with range gate number. Examining this effect more carefully, a slight gain increase (3%) from first to last range gate was observed (primarily due to antenna pattern variation).

In Figure 10-8 to 10-10, the autocorrelation and P_{df} of the mean and pdf are shown for the actual data of Flight 605. Comparing these to the simulation outputs, we note that the autocorrelation and $Q(\chi)$ are quite good while the mean and standard deviation of the data are both roughly 1.4 times that of the simulation. In the simulation, only the correct form of the pdf of the mean was modeled -- a scale factor of 1.40 could have been used to obtain a closer correpsondence, but as no other statistical measures were affected, it was deemed not necessary. Of particular interest in Figures 10-10 and 10-6 is the close agreement in the tails and to the 10^{-5} and 10^{-6} points which itself provides a strong validation key to both the simulation and the data reduction software.

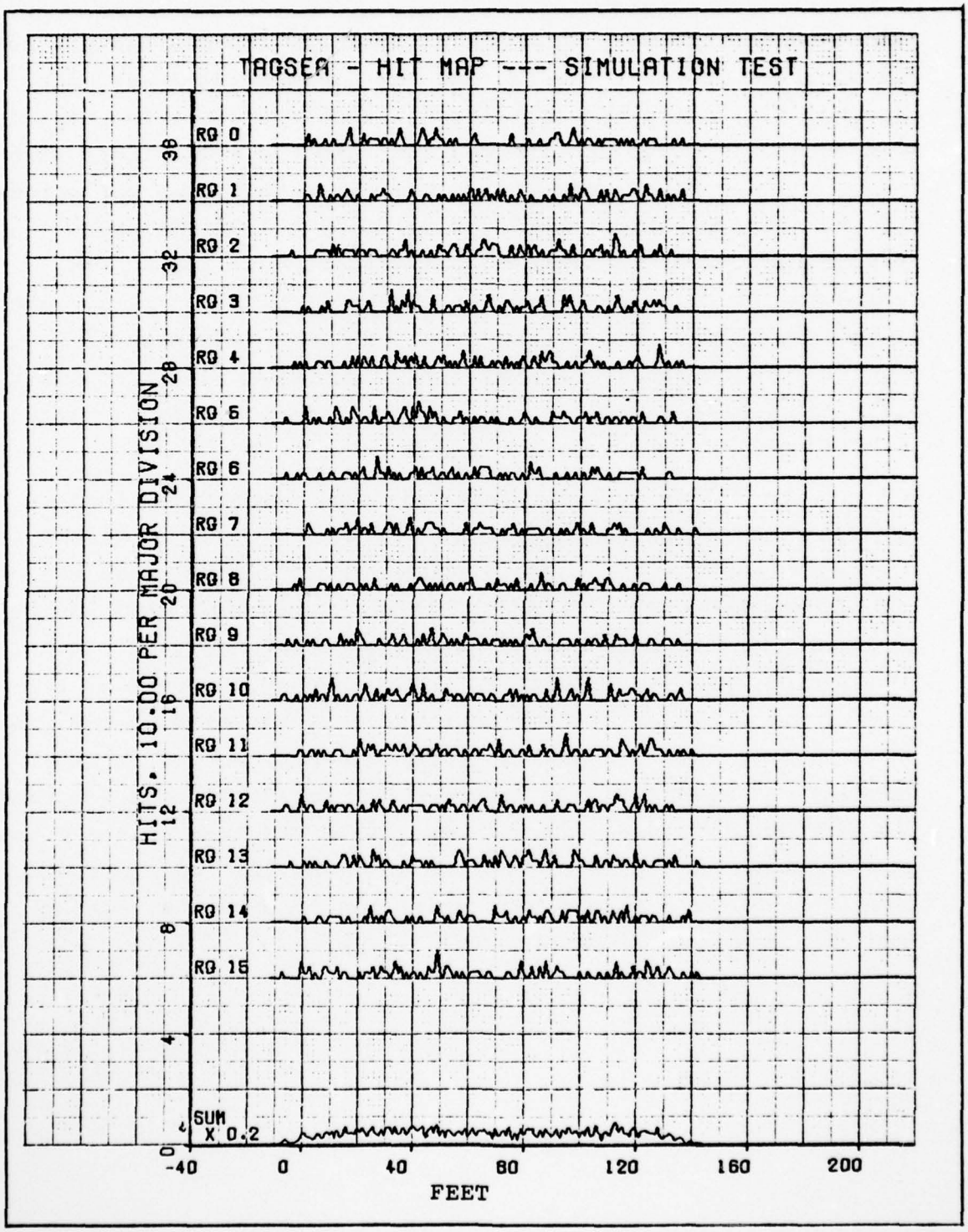

Figure 10-7 Hit Map - Simulation Test

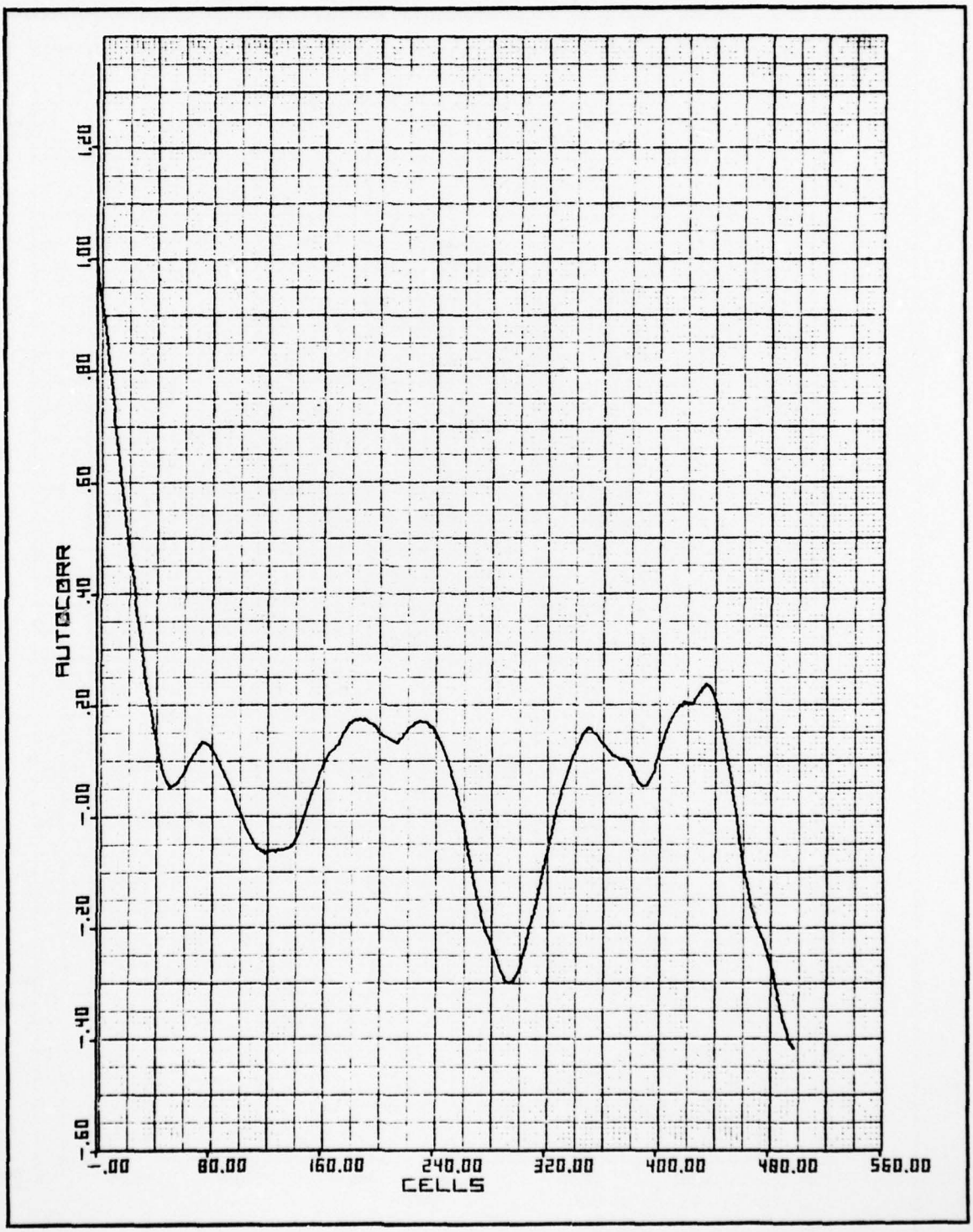

Figure 10-8 Autocorrelation Function of the Mean for Run 605

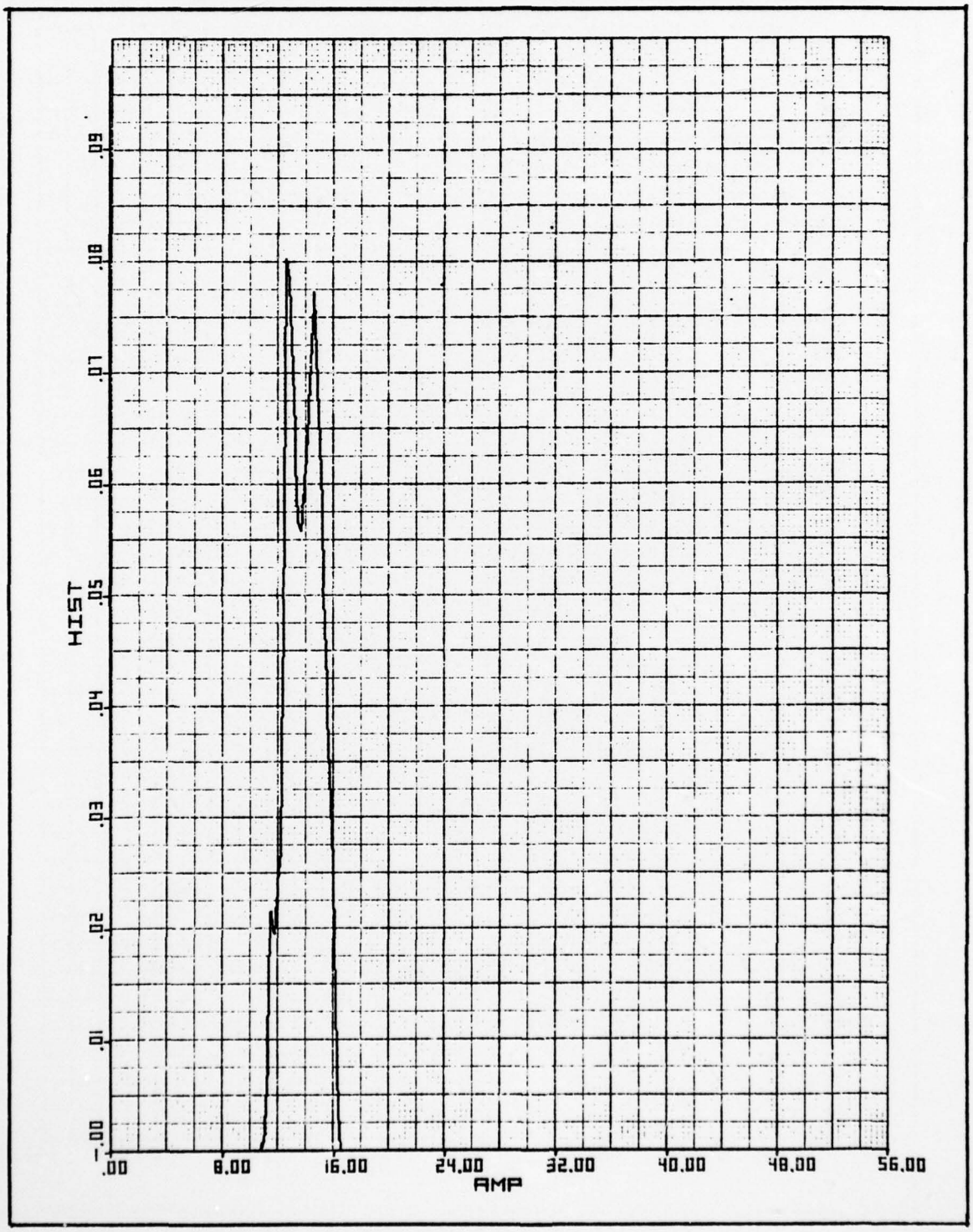

Figure 10-9 Probability Density Function of the Mean for Run 605

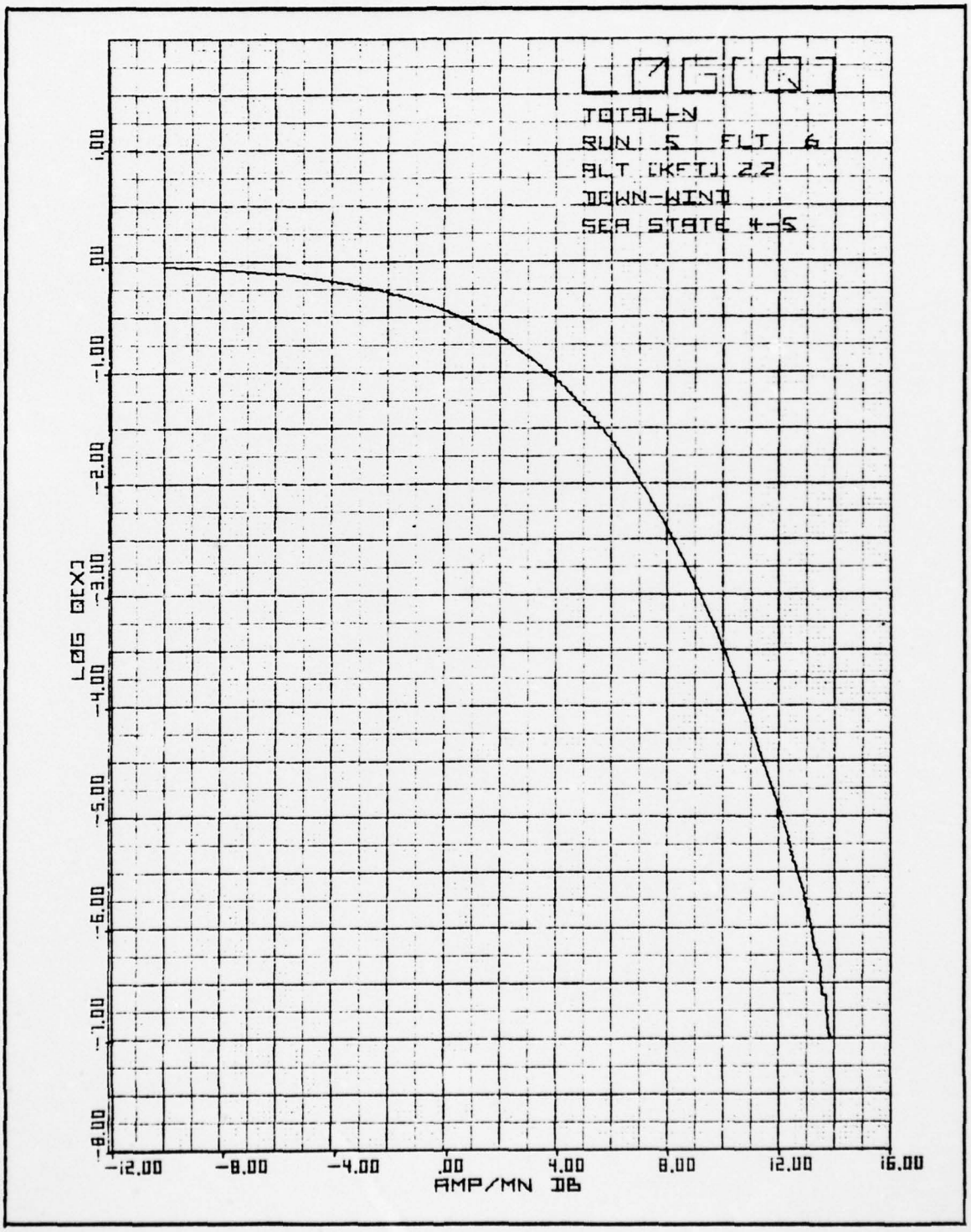

Figure 10-10 Log (Q) Data